

APPENDIX S



**Design Memorandum, Miner Flat Dam,
February 1987**

**MORRISON-MAIERLE, INC.,
VOLUMES I THRU V OF VI**

FEBRUARY 2007

017962-0002

DESIGN MEMORANDUM

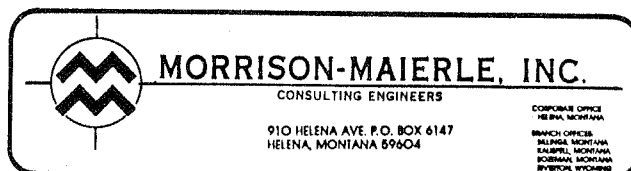
MINER FLAT DAM

DECEMBER, 1986

(REVISED FEBRUARY 1987)

WHITE MOUNTAIN APACHE TRIBE
WHITERIVER, ARIZONA

VOLUME 2 OF 6



MINER FLAT DAM
DESIGN MEMORANDUM

INDEX

| <u>Column</u> | <u>Section</u> | <u>Subject</u> | <u>Page</u> | |
|---------------|----------------------------|---------------------------------------------------------------|-----------------------------|-----------|
| One | AA. | Introduction | AA - 1 | |
| | A. | General Map | AB - 1 | |
| | B. | General Description of Local Conditions | AB - 1 | |
| | Drawings | | General Map A | Sht A1 |
| | | | General Map B | Sht A2 |
| | | | Surface Data - Topog. Map A | Sht C1 |
| | | | Surface Data - Topog. Map B | Sht C2 |
| | | | Surface Data - Topog. Map C | Sht C3 |
| | C. | Surface Data by Geodetic Research, Inc. | | |
| | ===== | | | |
| Two | D. | Foundation Data | | |
| | | D.1 - Geologic Data | | |
| | | D.2 - Foundation Stability Studies | | |
| | | D.3 - Seepage Model | | |
| | Photos | | Right Abutment | Fig D.1.1 |
| | | | Left Abutment | Fig D.1.2 |
| | | | Downstream View | Fig D.1.3 |
| | | | Upstream View | Fig D.1.4 |
| | Drawings | | Foundation Data A | Sht D1 |
| | | | Foundation Data B | Sht D1A |
| | | Bore Logs | Sht D2 | |
| | | Bore Logs | Sht D3 | |
| | | Bore Logs | Sht D4 | |
| | | Bore Logs | Sht D5 | |
| | | Bore Logs | Sht D6 | |
| E. | Construction Material Data | | | |
| ===== | | | | |
| Three | D. | Foundation Data by Mineral Systems, Inc. (Vol. 1 and 2) | | |
| ===== | | | | |
| Four | F. | Water for Construction Purposes | F - 1 | |
| | G. | Hydrologic Analysis | 1 | |
| | H. | Reservoir Data | 21 | |
| | I. | Spillway and Outlet Works Operation | 24 | |
| ===== | | | | |

MINER FLAT DAM
DESIGN MEMORANDUM

INDEX

| <u>Volumn</u> | <u>Section</u> | <u>Subject</u> | <u>Page</u> |
|---------------|----------------|-------------------------------------------|-------------|
| Five | J. | Miscellaneous Data | |
| | J.1 | Dam Design - General | J - 1 |
| | J.2 | Dam Design and Stability Analysis | J - 3 |
| | J.3 | Dam Thermal Stress Studies | J - 13 |
| | J.4 | Dam Aggregate and Mix Design | J - 18 |
| | J.5 | RCC Dam Construction - Spillway Facing | J - 20 |
| | J.6 | RCC Dam Construction - Schedule | J - 21 |
| | J.7 | Dam Cost Estimates | J - 28 |
| | J.8 | RCC Dam Specifications | J - 34 |
| | J.9 | Dam access Roads | J - 156 |
| | J.10 | Recreation Facilities | J - 157 |
| | J.11 | Public Safety and Visitor Facilities | J - 159 |
| | J.12 | Reservoir Clearing | J - 159 |
| | J.13 | Hydropower Facility | J - 159 |
| | J.14 | Construction Cost Estimate Summary | J - 161 |
| | J.15 | Drawings: | |
| | | RCC Dam - Plan | Sht J1 |
| | | RCC Dam - Section | Sht J2 |
| | | RCC Dam - Elevation | Sht J2A |
| | | Conventional Concrete Dam-Plan | Sht J3 |
| | | Conventional Concrete Dam- Section | Sht J4 |
| | | Power House Access Road - Plan/Profile | Sht J5 |
| | | Eastside Access Road | Sht J6 |
| | | Eastside Access Road | Sht J7 |

=====

| | |
|-----|----------------------------------------------------|
| Six | 1986 Environmental Assessment by Joe C. Elliott |
|-----|----------------------------------------------------|

=====

DESIGN MEMORANDUM

SECTION D

D.1 GEOLOGIC DATA

Geologic and engineering geologic field investigations have been conducted in the dam and reservoir area since February of 1982, principally by Mineral Systems, Inc. (MSI). The investigations included initial site mapping, geologic mapping, and preliminary core hole drilling in 1982. Site mapping, joint surveys, geophysical surveys, core drilling, in-situ permeability testing, and piezometer installation continued in 1983. Additional investigations including core drilling, in-situ permeability tests, piezometer installation, in-situ borehole deformation testing, and laboratory tests of materials strengths and properties were accomplished in 1985 and 1986. The information and data base resulting from the field investigations of the Miner Flat dam site are provided by three reports which are included by reference in this Design Memorandum. The three reports are:

1. "Engineering Geology and Mapping, Miner Flat Damsite and Reservoir, White Mountain Apache Tribe, Preliminary Report", Mineral Systems, Inc., August 1982.
2. "Preliminary Report, Engineering Geology, Miner Flat Dam Site, White Mountain Apache Reservation", Mineral Systems, Inc., November 1983.
3. "Preliminary Report, Engineering Geology, Miner Flat Dam Site, White Mountain Apache Reservation", Vols. I and II, Mineral Systems, Inc., July 1986.

The latter MSI report, dated July 1986, presents the most recent field investigations including information developed in response to the "Review and Evaluation of Dam Site Investigations" prepared by Harza Engineering Company. The earlier MSI reports prepared in 1982 and 1983 are included by reference because they include borehole logs, packer test results, and other data not reproduced in the 1986 MSI report.

Previous geologic investigations of the Miner Flat damsite and reservoir area consisted of a generalized regional geologic map of Navajo and Apache Counties, Arizona. The previous investigations did not present site specific data for the damsite and reservoir area. The 1986 MSI report provides geologic maps of the reservoir and damsite. The locations of foundation and abutment exploration drill holes and the locations of other types of geological and geophysical investigations of the dam site and reservoir area are shown on the geological maps. The 1986 MSI report also provides geologic cross sections through the dam site.

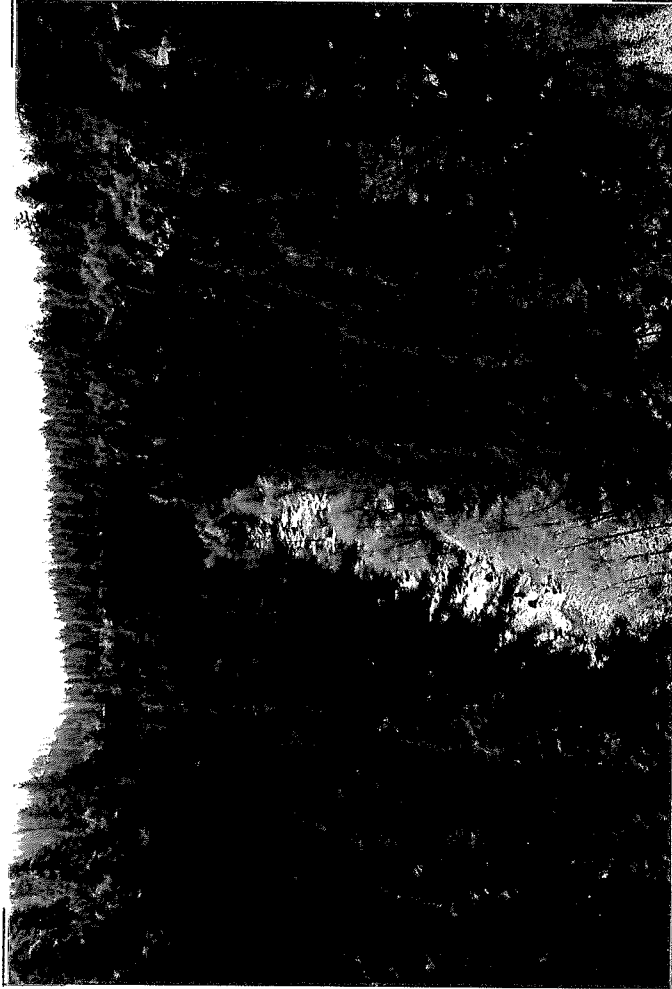
A series of color photographs are provided on Figures D.1.1 through D.1.4 to show the abutments at the damsite, the aggregate source area immediately upstream from the damsite, and the area immediately downstream from the damsite. Likewise, the drawings on Sheets D1 through D6 are presented to summarize herein the foundation geology, testing and sample locations, and drill hole logs.



FIGURE D.1.1 - RIGHT ABUTMENT



FIGURE D.1.2 - LEFT ABUTMENT



RIGHT

LEFT

FLOW

FIGURE D.1.3 - DOWNSTREAM

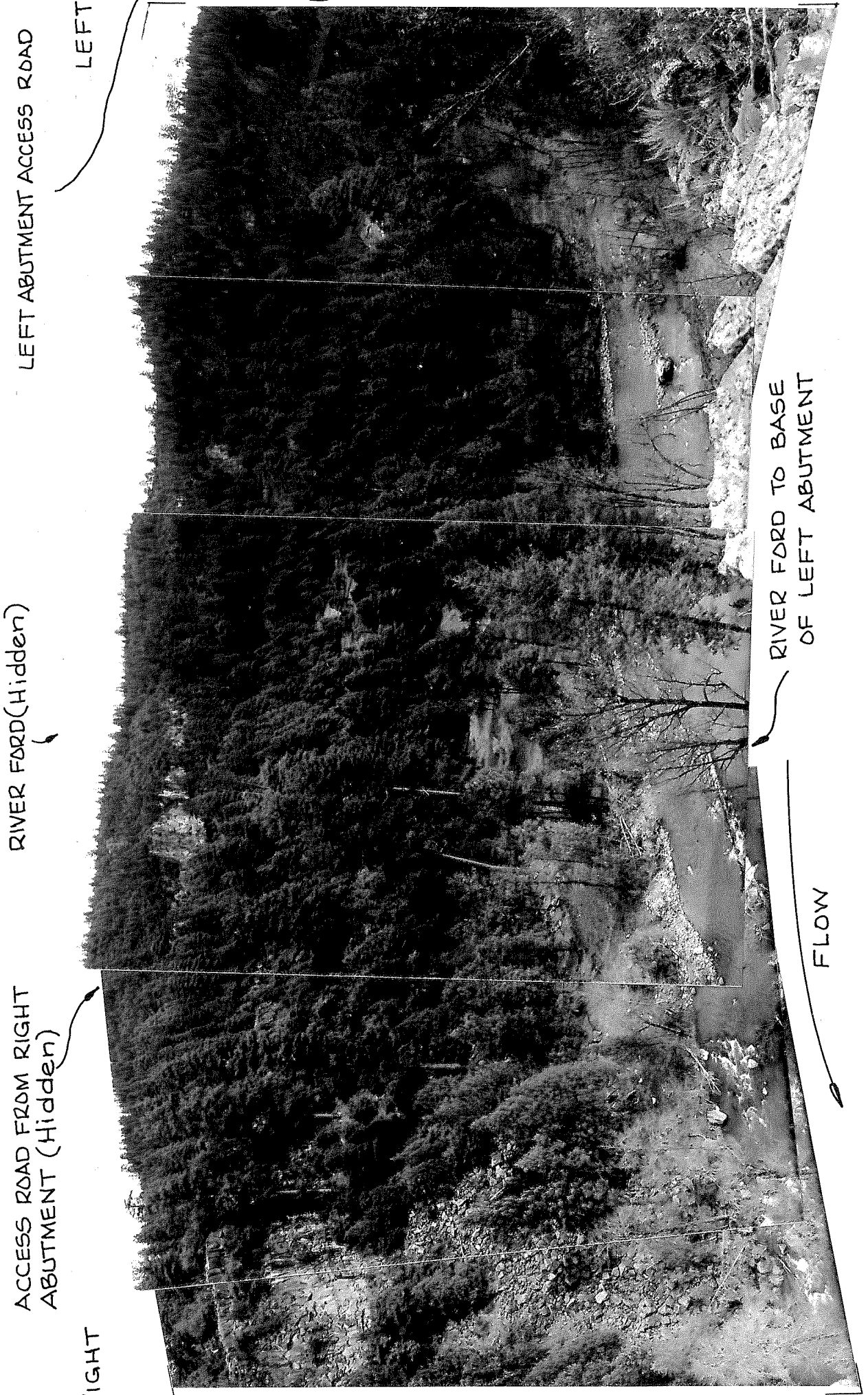


FIGURE D.1.4 - UPSTREAM (Aggregate Borrow/Rock Disposal Area)

EXPLANATION

Artificial fill
[Symbol]

ALLUVIAL DEPOSITS

ALLUVIUM
[Symbol] Qal
Boulders, cobbles, gravel, sand and silt along present stream channels.

TERRACES
[Symbol] Qtz
(Alluvium of boulders, cobbles, gravel, sand and silt; subscript relative age, 1 being the oldest.)

COLLUVIAL DEPOSITS

COLLUVIUM
[Symbol] Qc
(Derived from weathering of bedrock; letter symbols in parentheses are symbols for bedrock units from which colluvium derived.)

TALUS
[Symbol] Qta
(Letter symbols in parentheses are symbols for bedrock units from which talus derived.)

BEDROCK

QUATERNARY-TERTIARY GRAVEL
[Symbol] Qtg
(No outcrop)

BASALT
[Symbol] P1
(Massive to vesicular and scoriaceous basalt)

SUPAI FORMATION

(Sandstone, fine-grained rounded, well sorted, cross-stratified, massive bedded; Lower part interbedded with siltstone)

Contact, showing dip
(Dashed where approximately located)

Strike and dip of beds
[Symbol]

Strike and dip of joints
[Symbol]

Strike of vertical joint
[Symbol]

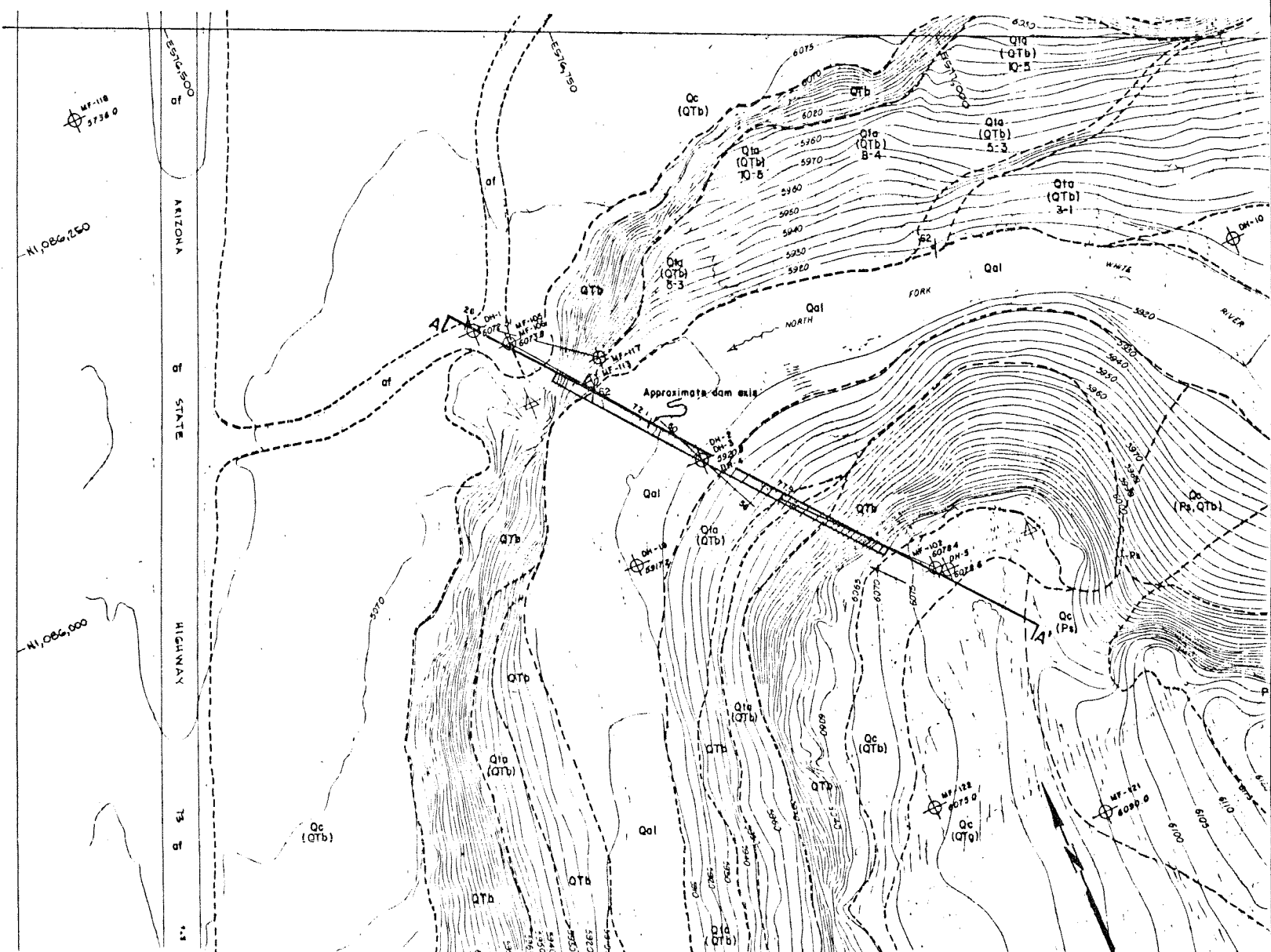
Drill Hole
[Symbol] MF-105
Surface drill hole with inclination

Line of detail survey
[Symbol] A-A'

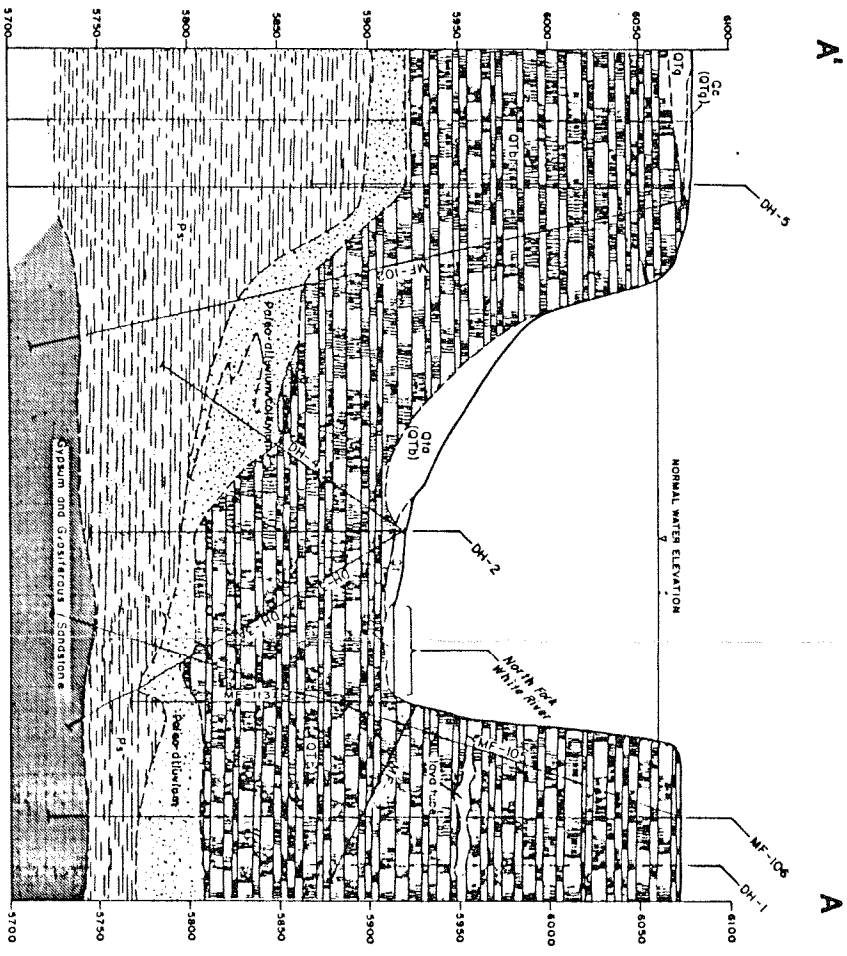
Geology by Charles S. Robinson



Golden, Colorado, June 1983



GEOLOGIC PLAN VIEW



GEOLOGIC SECTION A-A'

EXPLANATION

ALLUVIUM
[Symbol] Qal

TERRACES
[Symbol] Qtz

COLLUVIUM
[Symbol] Qc

TALUS
[Symbol] Qta

QUATERNARY-TERTIARY GRAVEL
[Symbol] Qtg

BASALT
[Symbol] P1

SUPAI FORMATION
(Showing sparsely units)

Contact

Drill Hole
[Symbol] MF-105

| NO. | DESCRIPTION | DATE | BY |
|-----|-------------|------|----|
| | | | |
| | | | |
| | | | |

REVISIONS

SCALE: 1"=50'

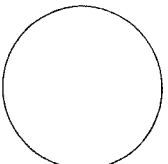
FOUNDATION DATA "A"

SHEET TITLE

MINER FLAT DAM
WHITE MOUNTAIN APACHE RESERVATION
NAVAJO COUNTY, ARIZONA

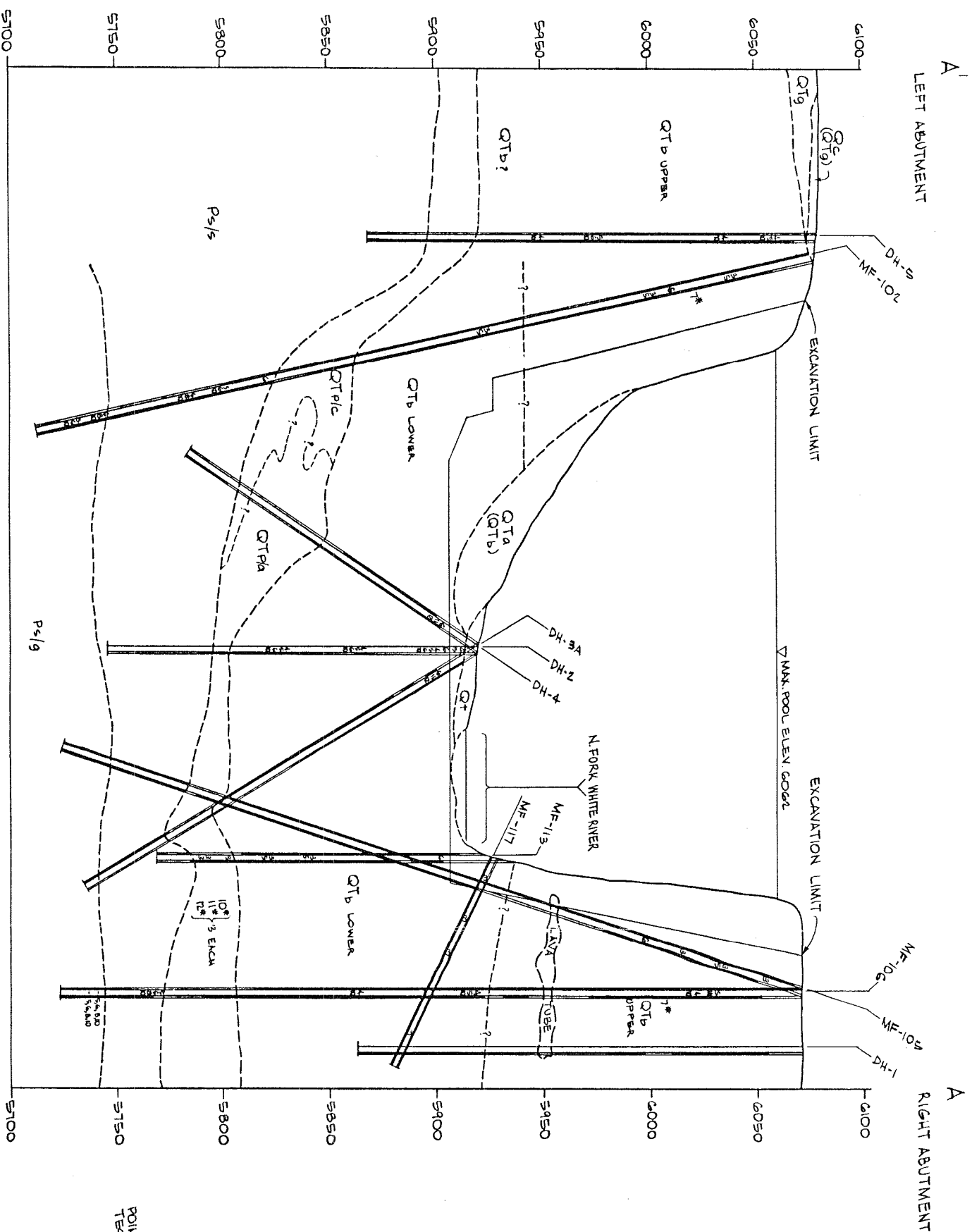
DRAWN BY: CJA
CHKD. BY: DD
APPR BY: CNK
DATE: 12-10-86
QA
PEER REVIEW

MORRISON-MAIERLE, INC.
CONSULTING ENGINEERS
910 HELENA AVE. P.O. BOX 6147
HELENA, MONTANA 59604



| NO. | DESCRIPTION | DATE | BY |
|-----|-------------|------|----|
| | | | |
| | | | |
| | | | |

PROJECT NUMBER
1780-14-Q2(GA)
SHEET NUMBER
D1



GEOLOGIC SECTION A-A

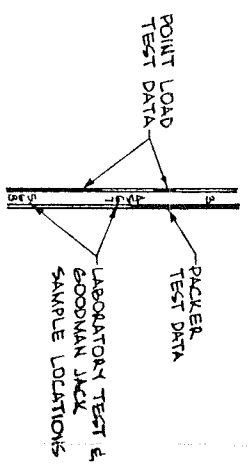
NOTE:
 1*, REMOVED DIRECT SHEAR ON COMPOSITE SAMPLE OF FLOW BOUNDARY MATERIAL FROM HOLES MF-102, 105, 4, 106. 10*, 11*, 4, 12*, DENSITY, GRADATION & LIMITS ON NEARBY OUTCROP SAMPLE OF PALEO ALLUVIUM/ COLLUVIUM.

EXPLANATION

- QT+ TERRACE
- QC COLLUVIUM (BEDROCK SOURCE SHOWN BY SYMBOL FOR ROCK UNIT)
- QTa TALUS (BEDROCK SOURCE SHOWN BY SYMBOL FOR ROCK UNIT)
- QTg QUATERNARY-TEXTURED CANEEL
- QTb BASALT UPPER-ANGULAR, COLLESCING VESICULAR & MASSIVE FLOWS LOWER-SINGLE MASSIVE FLOW
- Ps/s PALEO COLLUVIUM/ALLUVIUM 1c - PALEO COLLUVIUM 1a - PALEO ALLUVIUM
- Ps/l SUPAI FORMATION 1s - SANDSTONE/SILTSTONE 1g - Gypsiferous sandstone/gypsum

TEST LOCATION CODING

- FIELD TESTS
- 1. POINT LOAD
 - 2. PACKER TEST DATA
 - 3. GOODMAN JACK
- LABORATORY TEST (IN CORE)
- 4. UNIAXIAL w/o ELASTIC PROPERTIES
 - 5. UNIAXIAL w/ ELASTIC PROPERTIES
 - 6. DIRECT SHEAR (CORES)
 - 7. DIRECT SHEAR (REMOVED)
 - 8. TRIAXIAL (CORE)
 - 9. TRIAXIAL (REMOVED)
 - 10. DENSITY
 - 11. GRADATION
 - 12. ATTERBERG LIMITS



SCALE: 1"=30'

FOUNDATION DATA "B"

| NO. | DESCRIPTION | DATE | BY |
|-----|-------------|------|----|
| | | | |
| | | | |
| | | | |

MORRISON-MAIERLE, INC.
 CONSULTING ENGINEERS
 910 HELENA AVE. P.O. BOX 6147
 HELENA, MONTANA 59604

MINER FLAT DAM
 WHITE MOUNTAIN APACHE RESERVATION
 NAVAJO COUNTY, ARIZONA

PROJECT NUMBER
 1780-14-02(34)
D 1A
 SHEET NUMBER

DRAWN BY: **GA**
 CHECKED BY: **GA**
 APPR. BY: **GA**
 DATE: **12-10-86**
 GA
 PEER REVIEW

MINER FLAT

Drilled by: **Western Technologists**
 Logged by: **Charles H. Robinson**
 Elevation: **4673'**
 Bearing: **9°**
 Date Started: **1/29/82**
 Date Completed: **1/26/82**

| Depth (feet) | Lithologic Log | Description |
|--------------|----------------|---------------------------------------------------------------------------------------------------------------------------------------------------|
| 0 | | Basalt, massive, very fine-grained, aphanitic, porphyritic, few vesicles, iron and clay stained fractures. |
| 30 | | Basalt, vesicular, very fine-grained to aphanitic, vesicles filled with clay, iron and clay stained fractures. |
| 50 | | Basalt, massive to slightly vesicular. |
| 70 | | Basalt, vesicular, very fine-grained, aphanitic, porphyritic, with olivine. |
| 90 | | Basalt, massive very fine-grained, aphanitic-porphyrific w/ olivine, hard to very hard. |
| 110 | | Layer tube |
| 130 | | Basalt, vesicular, very fine-grained, vesicles filled with silica, fractures stained with clay. |
| 150 | | |
| 170 | | Basalt, massive, very fine-grained, aphanitic-porphyrific with olivine phenocrysts. Locally fractured with silica filling and some clay staining. |
| 210 | | |
| 212.0 | | EOH |

MINER FLAT

Drilled by: **Western Technologists**
 Logged by: **Charles H. Robinson**
 Elevation: **5922'**
 Bearing: **9°**
 Date Started: **2/6/82**
 Date Completed: **2/19/82**

| Depth (feet) | Lithologic Log | Description |
|--------------|----------------|------------------------------------------------------------------------------------------------------------------------------------------------------------------|
| 0 | | Silty sand. Alluvial terrace. |
| 30 | | Basalt, massive, medium gray, very fine-grained, aphanitic-porphyrific with phenocrysts of olivine, very hard, slightly fractured, fractures with stain of clay. |
| 70 | | |
| 90 | | |
| 100.5 | | |

MINER FLAT

Drilled by: **Boyles Bros.**
 Logged by: **Charles H. Robinson**
 Elevation: **5922'**
 Bearing: **9°**
 Date Started: **8/2/83**
 Date Completed: **8/6/83**

| Depth (feet) | Lithologic Log | Description |
|--------------|----------------|-------------------------------------------------------------------------------------------------------------------------------------------|
| 0 | | Basalt, massive, medium gray, very fine-grained, very hard, vesicular, scoriaceous, aphanitic, with incorporated sandstone and siltstone. |
| 30 | | Paleo-alluvium cobbles and gravel in silty sand. Clasts of basalt, sandstone, siltstone. |
| 130 | | Sandstone, reddish brown to pale yellowish green, silty, very fine to fine-grained, slightly calcareous, soft. |
| 170 | | |
| 178.3 | | EOH |

MINER FLAT

Drilled by: **Western Technologists**
 Logged by: **Charles H. Robinson**
 Elevation: **5922'**
 Bearing: **135°**
 Date Started: **2/19/82**
 Date Completed: **2/21/82**

| Depth (feet) | Lithologic Log | Description |
|--------------|----------------|-------------------------------------------------------------------------------------------------------------------------------------------------------------------|
| 0 | | Silty sand. Alluvial terrace. |
| 30 | | Basalt, massive, medium gray, very fine-grained, aphanitic-porphyrific, with olivine phenocrysts, very hard, slightly fractured, few fractures stained with clay. |
| 44.5 | | EOH |

MINER FLAT

Drilled by: **Boyles Bros.**
 Logged by: **Charles H. Robinson**
 Elevation: **6922'**
 Bearing: **135°**
 Date Started: **8/7/83**
 Date Completed: **8/9/83**

| Depth (feet) | Lithologic Log | Description |
|--------------|----------------|------------------------------------------------------------------------------------------------------------------------------------------------------------------------------|
| 0 | | colluvium, boulder and gravel with silty clayey sand. |
| 30 | | Basalt, massive, very fine-grained, aphanitic-porphyrific with olivine phenocrysts, very hard, slightly fractured with fractures stained with clay, some filled with silica. |
| 50 | | Basalt, vesicular, scoriaceous or flow breccia. |
| 70 | | |
| 90 | | Basalt, vesicular, scoriaceous or flow breccia. |
| 110 | | Paleo-colluvium, sandstone gravel and cobbles in a sandy matrix. |
| 130 | | Sandstone, reddish brown, fine- to very fine-grained, silty, slightly calcareous. |
| 161.5 | | EOH |

MINER FLAT

Drilled by: **Boyles Bros.**
 Logged by: **Pat Wiegand**
 Elevation: **6079'**
 Bearing: **9°**
 Date Started: **7/9/83**
 Date Completed: **7/12/89**

| Depth (feet) | Lithologic Log | Description |
|--------------|----------------|----------------------------------------------------------------------------------------------------------------------------|
| 0 | | Basalt, massive, very fine-grained, aphanitic-porphyrific, fractures are stained with clay. |
| 30 | | Basalt, vesicular, very fine-grained to aphanitic-porphyrific with olivine phenocrysts, clay in vesicles and on fractures. |
| 32.8, 39.2 | | Basalt, vesicular, scoriaceous basalt at flow boundaries 21.8, 29.2, clay filled vesicles. |
| 50 | | Basalt, massive clay stained fractures. |
| 70 | | Basalt, vesicular, clay filled fractures. |
| 90 | | Basalt, massive, dark gray, very fine-grained, porphyritic |
| 110 | | Basalt, vesicular, highly fractured, clay filled fractures and vesicles. |
| 130 | | Basalt, scoriaceous. |
| 150 | | Basalt, massive, very fine-grained, aphanitic-porphyrific with olivine phenocrysts. |
| 170 | | Basalt, massive. |
| 190 | | Basalt, flow breccia, scoriaceous. |
| 209.2 | | Basalt, vesicular, very fine-grained, aphanitic-porphyrific with olivine phenocrysts, clay filled fractures. |
| 210 | | Basalt, massive, very fine-grained, aphanitic-porphyrific with olivine phenocrysts. |
| 230 | | Paleo-colluvium, sandstone cobbles and gravel in a fine-grained sand matrix. |
| 250 | | Sandstone, reddish brown, very fine-grained, silty, calcareous. |
| 269.2 | | EOH |

| NO. | DESCRIPTION | DATE | BY. |
|-----|-------------|------|-----|
| | | | |
| | | | |
| | | | |

MORRISON-MAIERLE, INC.
 CONSULTING ENGINEERS
 910 HELENA AVE. P.O. BOX 6147
 HELENA, MONTANA 59604

DRAWN BY: **CJA**
 CHKD. BY: **DO**
 APR. BY: **CWK**
 DATE: **12-10-89**

MINER FLAT DAM
 WHITE MOUNTAIN APACHE RESERVATION
 NAVAJO COUNTY, ARIZONA

PROJECT NUMBER: **1780-14-02(34)**
 SHEET NUMBER: **D2**

SHEET TITLE: **FOUNDATION DATA "C"**

MINER FLAT

DRILL HOLE NO. DE-14
 Elevation: 6096'
 Bearing: #
 Date Started: 7/14/83

Drilled by: Boylan Bros.
 Logged by: Pat Wiegand
 Inclination: 30°
 Date Completed: 7/21/83

| Depth (Feet) | Lithologic Log | Description |
|--------------|----------------|----------------------------------------------------------------------------------------------------------------------------------------|
| 0 | | Quaternary-Tertiary gravel, cobbles and gravel in clayey, silty sand matrix. |
| 30 | | Basalt, massive, very fine-grained, aphanitic-porphyrific with olivine phenocrysts, fractures healed with silica or stained with clay. |
| 50 | | Basalt, vesicular to scoriaceous, very fine-grained, aphanitic-porphyrific, fractures stained and filled with clay. |
| 70 | | Basalt, massive, very fine-grained, aphanitic-porphyrific with olivine phenocrysts, fractures stained with clay. |
| 90 | | Paleo-alluvium, cobbles and gravel of basalt, quartzite, volcanic and intrusive rocks in a silty sand matrix. |
| 110 | | Sandstone, reddish brown to medium brown, very fine-grained to fine-grained, silty, slightly calcareous. |
| 130 | | |
| 150 | | |
| 170 | | |
| 180 | | EO.H. |

MINER FLAT

DRILL HOLE NO. DE-13
 Elevation: 5913'
 Bearing: #
 Date Started: 7/13/83

Drilled by: Boylan Bros.
 Logged by: Pat Wiegand and
 Inclination: 30°
 Date Completed: 7/24/83

| Depth (Feet) | Lithologic Log | Description |
|--------------|----------------|--------------------------------------------------------------------------------------------------------------------------------------|
| 0 | | Colluvium-Alluvium sand and gravel with cobbles of sandstone and basalt. |
| 30 | | Basalt, massive, moderate to dark gray, very fine-grained, aphanitic-porphyrific with olivine phenocrysts, very hard, see fractures. |
| 50 | | Basalt, scoriaceous, flow breccia, aphanitic-porphyrific. |
| 70 | | Paleo-alluvium, cobbles and gravel of quartzite, basalt, limestone, sandstone and igneous rocks in a sand matrix. |
| 90 | | Sandstone, reddish brown, very fine-grained, silty, slightly calcareous. |
| 110 | | Gypsum, white to grayish brown. |
| 130 | | Sandstone breccia, silty, gypsiferous. |
| 150 | | |
| 170 | | |
| 181.5 | | EO.H. |

FOUNDATION DATA 'D'

MINER FLAT DAM
 WHITE MOUNTAIN APACHE RESERVATION
 NAVAJO COUNTY, ARIZONA

DRAWN BY: CJA
 CHKD. BY: DO
 APPR. BY: CWK
 DATE: 12-10-86
 GA
 PEAR REVIEW

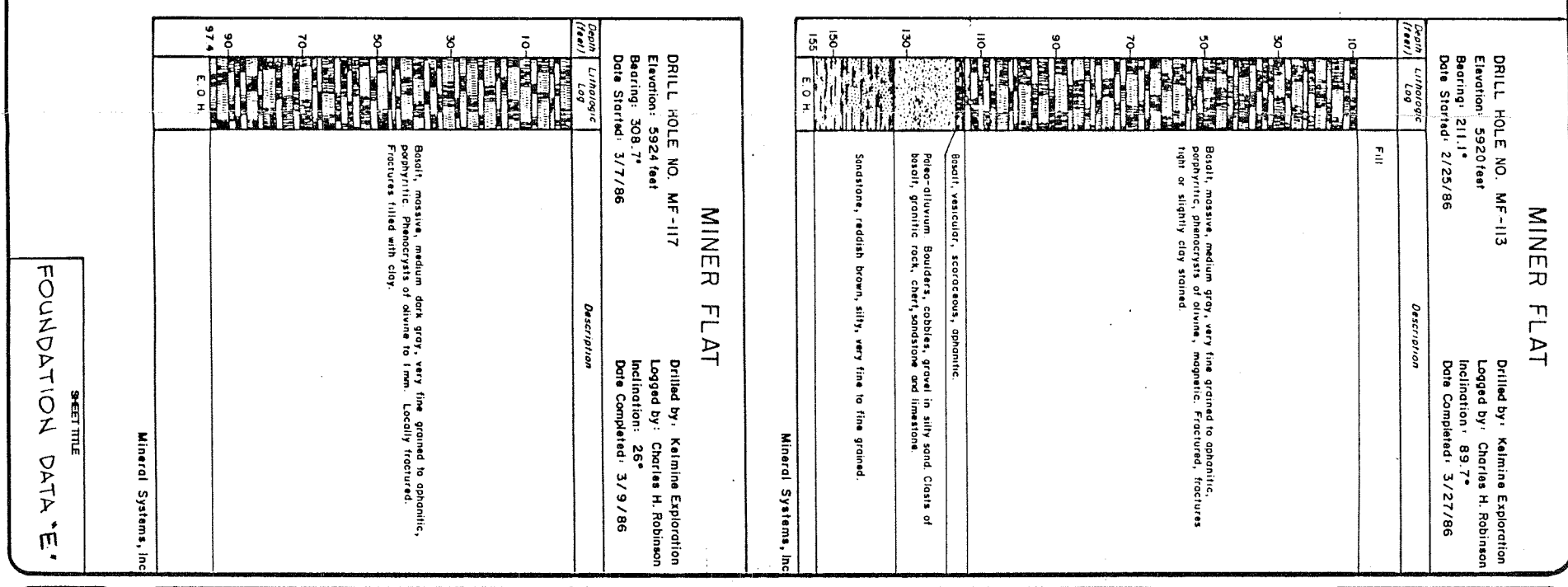
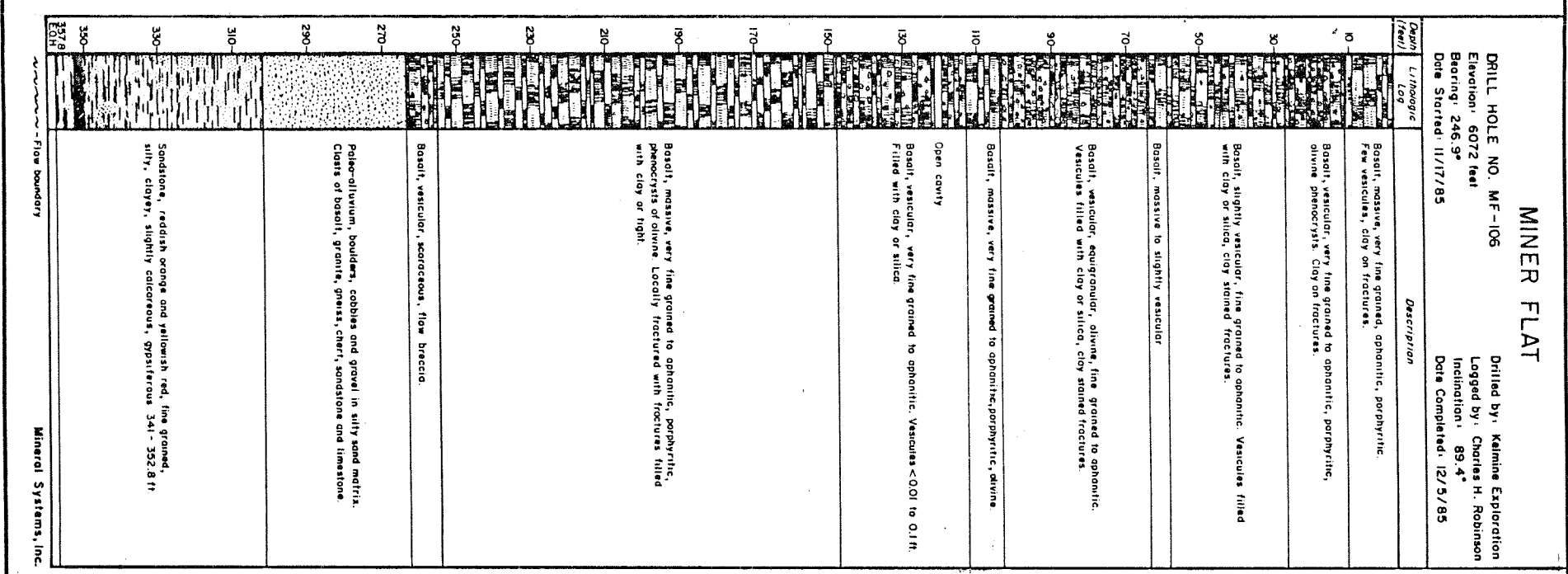
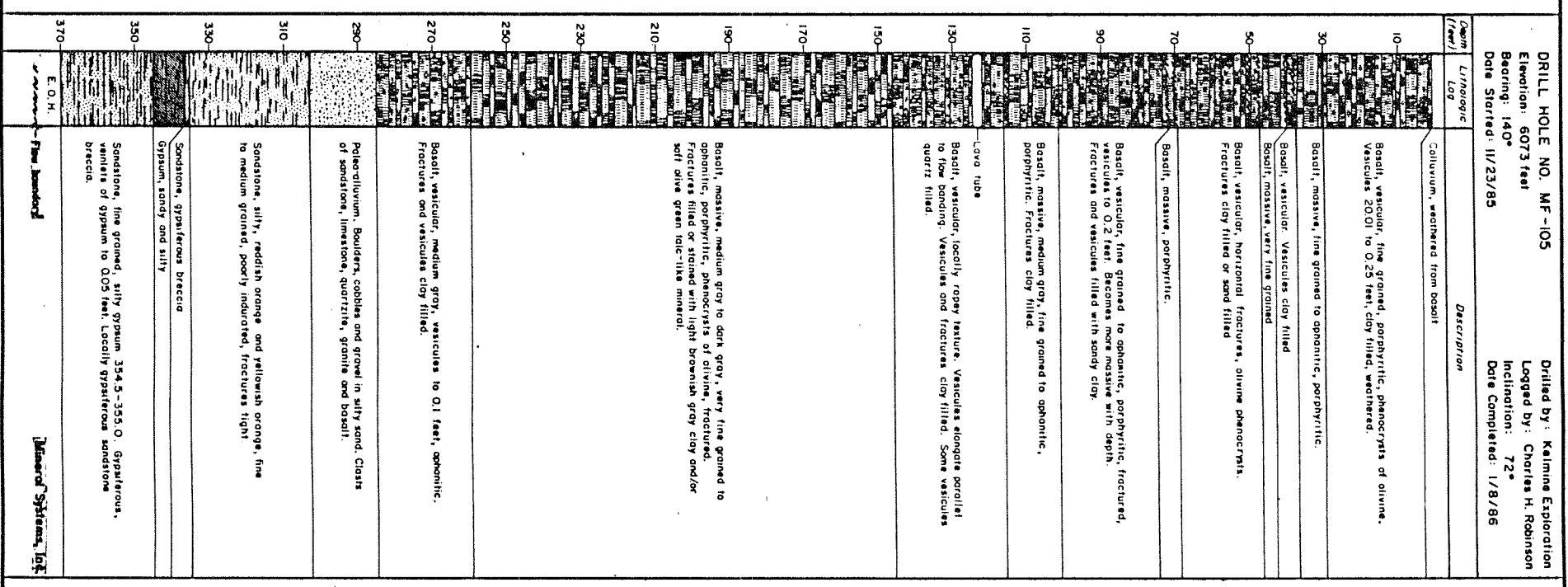
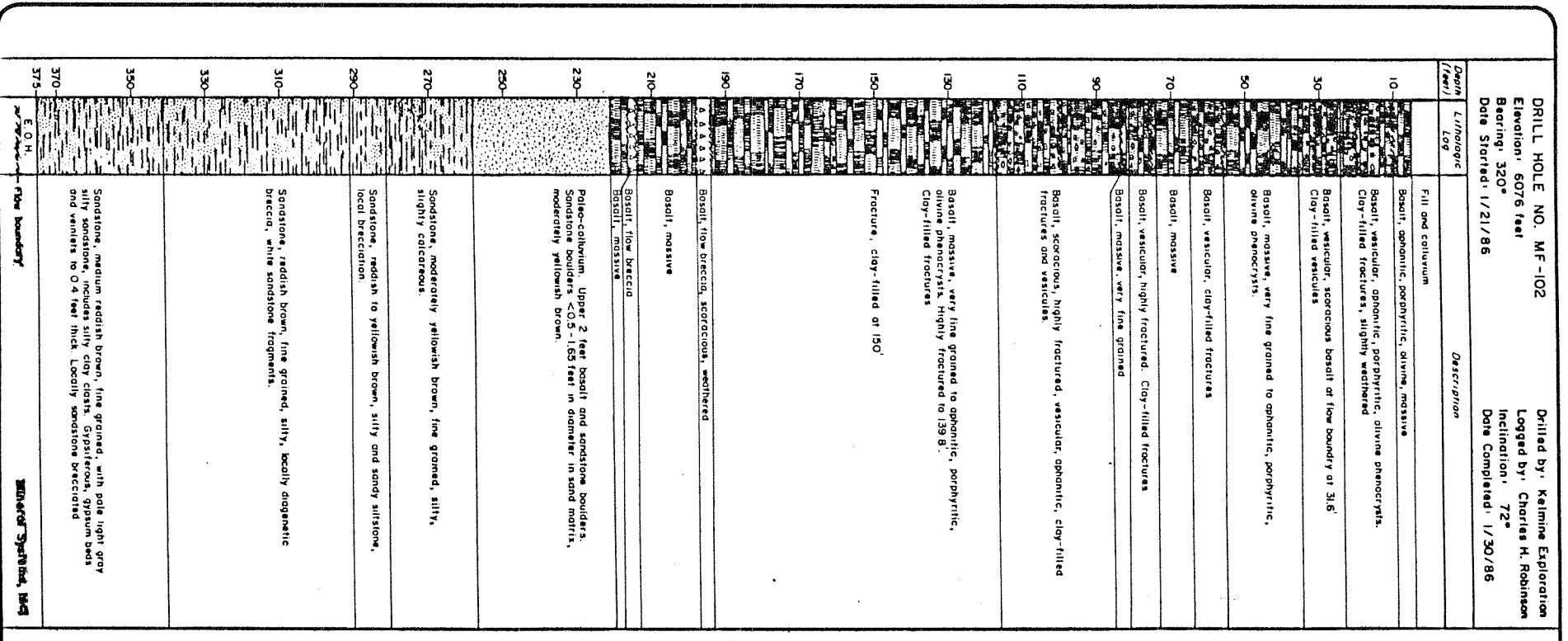
MORRISON-MAIERLE, INC.
 CONSULTING ENGINEERS
 910 HELENA AVE. P.O. BOX 6147
 HELENA, MONTANA 59604

COMPANY OFFICE
 HELENA, MONTANA
 BRANCH OFFICES
 BILLINGS, MONTANA
 BUTTE, MONTANA
 BOZEMAN, MONTANA
 SPOKANE, MONTANA

| NO. | DESCRIPTION | DATE | BY |
|-----|-------------|------|----|
| | | | |
| | | | |
| | | | |
| | | | |

REVISIONS

PROJECT NUMBER
 1780-14-02(34)
 SHEET NUMBER
D3



MINER FLAT

Drilled by: Kelmine Exploration
 Logged by: Charles H. Robinson
 Elevation: 5924 feet
 Bearing: 308.7°
 Date Started: 3/7/86
 Date Completed: 3/9/86

MINER FLAT

Drilled by: Kelmine Exploration
 Logged by: Charles H. Robinson
 Elevation: 5920 feet
 Bearing: 211.1°
 Date Started: 2/25/86
 Date Completed: 3/27/86

MINER FLAT

Drilled by: Kelmine Exploration
 Logged by: Charles H. Robinson
 Elevation: 6072 feet
 Bearing: 140°
 Date Started: 11/23/85
 Date Completed: 1/8/86

MINER FLAT

Drilled by: Kelmine Exploration
 Logged by: Charles H. Robinson
 Elevation: 6076 feet
 Bearing: 320°
 Date Started: 1/21/86
 Date Completed: 1/30/86

MINER FLAT

Drilled by: Kelmine Exploration
 Logged by: Charles H. Robinson
 Elevation: 6073 feet
 Bearing: 140°
 Date Started: 11/23/85
 Date Completed: 1/8/86

MINER FLAT

Drilled by: Kelmine Exploration
 Logged by: Charles H. Robinson
 Elevation: 2469 feet
 Bearing: 6072 feet
 Date Started: 11/17/85
 Date Completed: 12/5/85

MINER FLAT

Drilled by: Kelmine Exploration
 Logged by: Charles H. Robinson
 Elevation: 5924 feet
 Bearing: 308.7°
 Date Started: 3/7/86
 Date Completed: 3/9/86

MINER FLAT

Drilled by: Kelmine Exploration
 Logged by: Charles H. Robinson
 Elevation: 5920 feet
 Bearing: 211.1°
 Date Started: 2/25/86
 Date Completed: 3/27/86

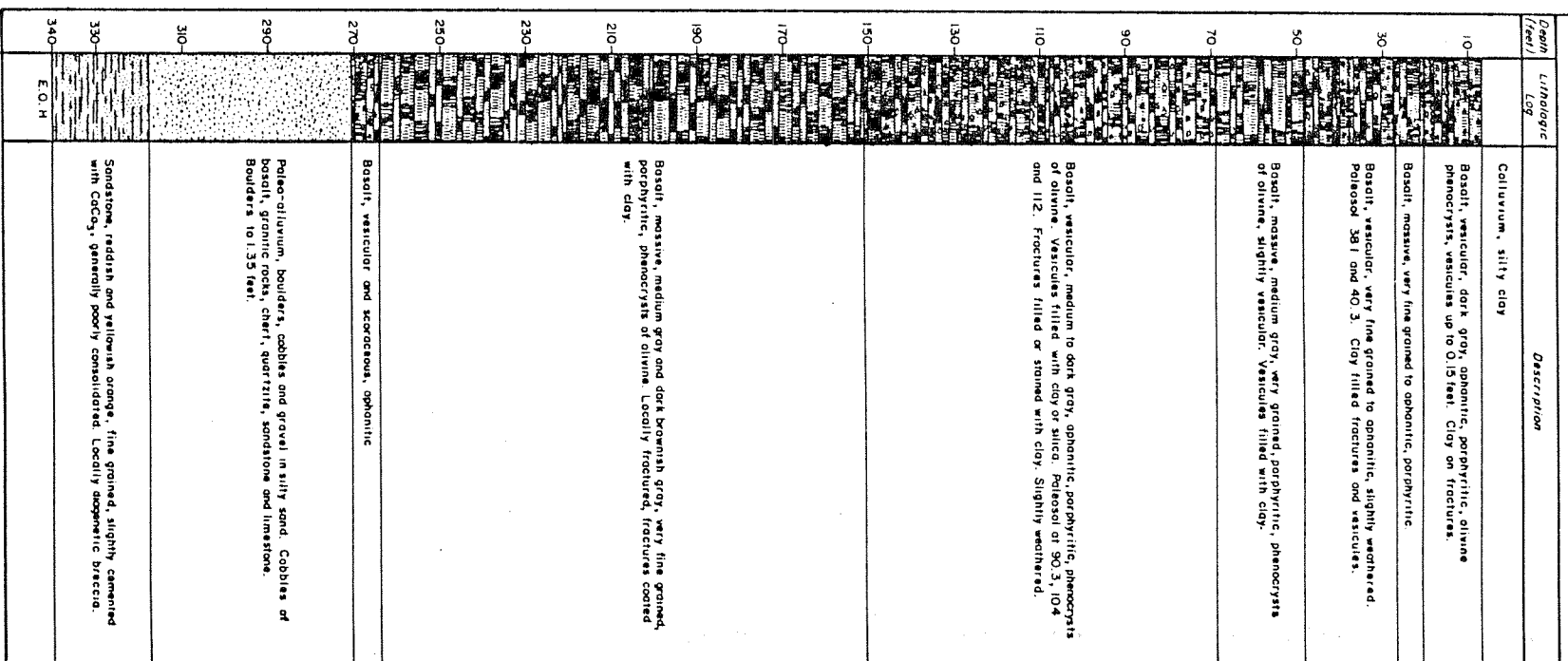
MINER FLAT

Drilled by: Kelmine Exploration
 Logged by: Charles H. Robinson
 Elevation: 6072 feet
 Bearing: 140°
 Date Started: 11/23/85
 Date Completed: 1/8/86

MINER FLAT

DRILL HOLE NO. MF-118
 Elevation: 6077 feet
 Bearing: 243.8°
 Date Started: 1/11/86

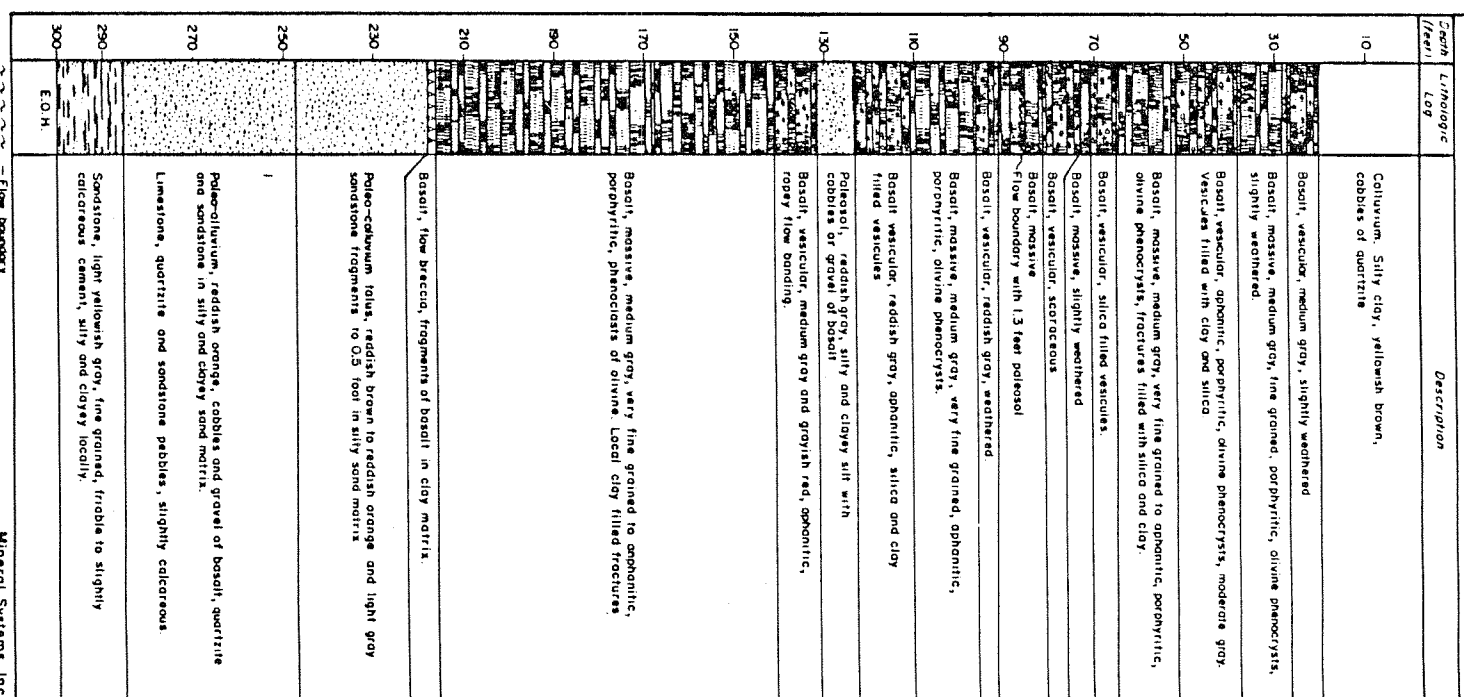
Drilled by: Kelmire Exploration
 Logged by: Charles H. Robinson
 Inclination: 89.5°
 Date Completed: 1/15/86



MINER FLAT

DRILL HOLE NO. MF-119
 Elevation: 6094 feet
 Bearing: 231.9°
 Date Started: 4/8/86

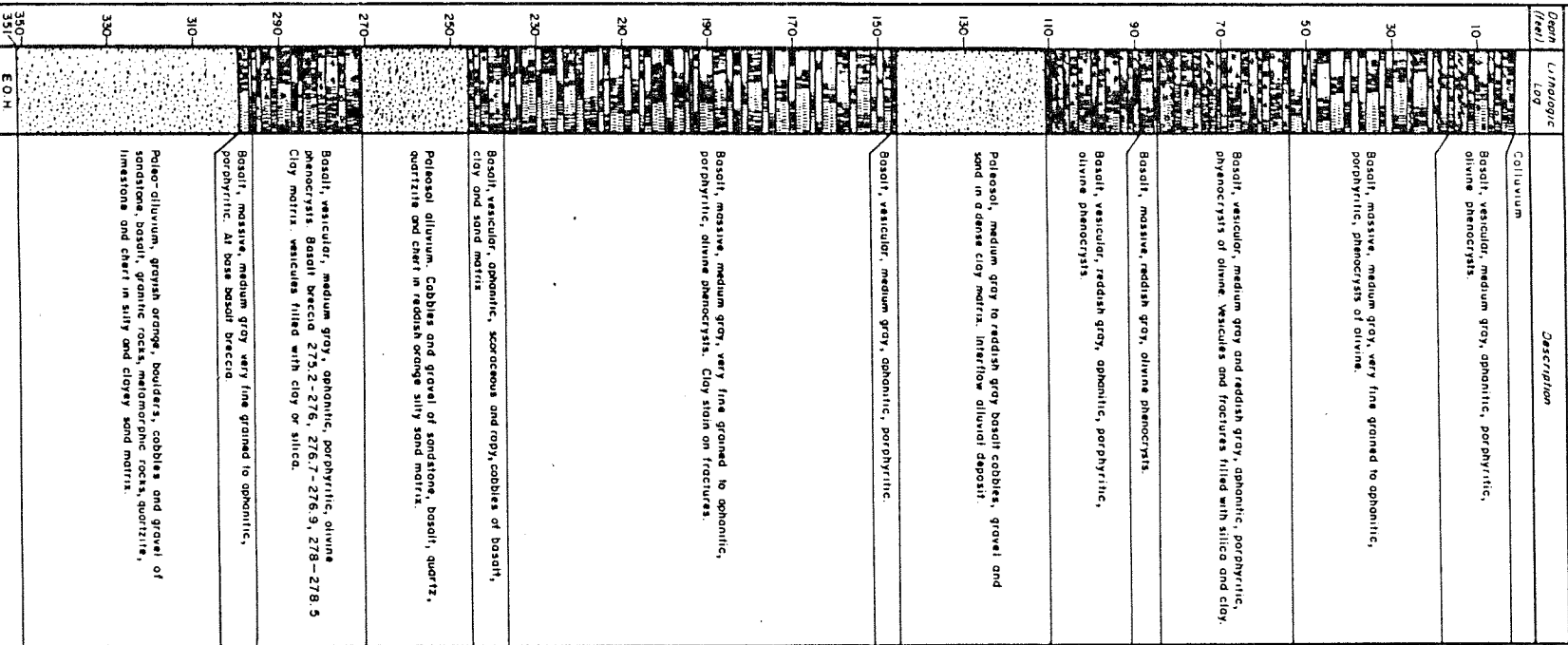
Drilled by: Kelmire Exploration
 Logged by: Charles H. Robinson
 Inclination: 89.9°
 Date Completed: 4/16/86



MINER FLAT

DRILL HOLE NO. MF-120A
 Elevation: 6082 feet
 Bearing: 248°
 Date Started: 4/18/86

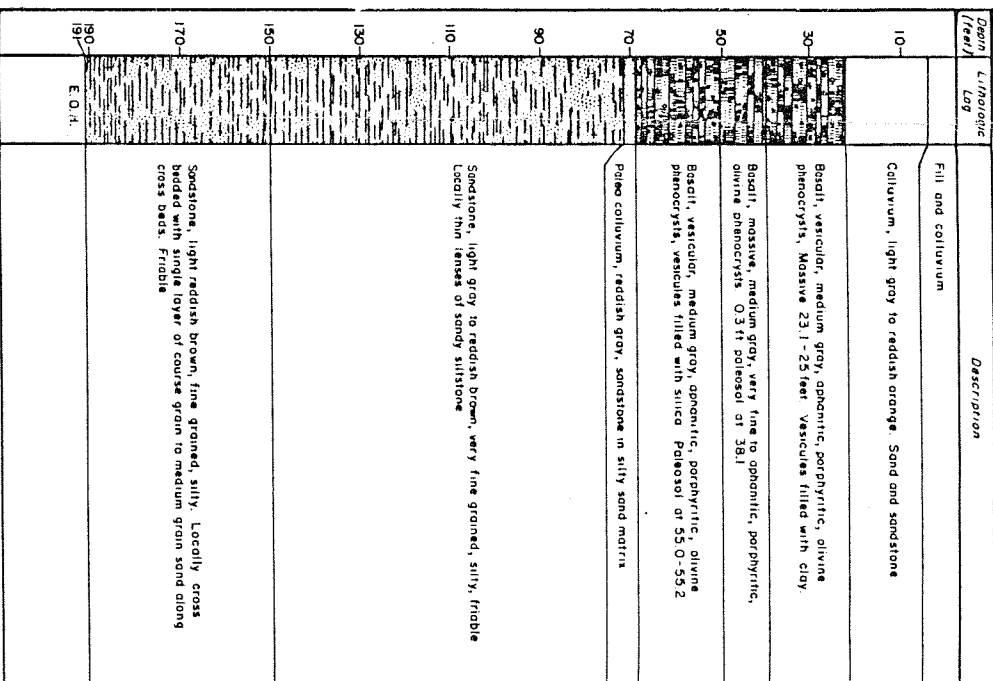
Drilled by: Kelmire Exploration
 Logged by: Charles H. Robinson
 Inclination: 89.5°
 Date Completed: 4/21/86



MINER FLAT

DRILL HOLE NO. MF-121
 Elevation: 6090 feet
 Bearing: 271°
 Date Started: 2/10/86

Drilled by: Kelmire Exploration
 Logged by: Charles H. Robinson
 Inclination: 89.8°
 Date Completed: 2/28/86



FOUNDATION DATA "F"

Mineral Systems, Inc.

| NO. | DESCRIPTION | DATE | BY |
|-----|-------------|------|----|
| | | | |
| | | | |
| | | | |
| | | | |

MORRISON-MAIERLE, INC.
 CONSULTING ENGINEERS
 910 HELENA AVE. P.O. BOX 6147
 HELENA, MONTANA 59604

DRAWN BY: CJA
 CK'D BY: DO
 APPR BY: CWK
 DATE: 12-10-86
 QA
 PER REVIEW

MINER FLAT DAM
 WHITE MOUNTAIN APACHE RESERVATION
 NAVAJO COUNTY, ARIZONA

PROJECT NUMBER: 1780-14-02(G4)
 SHEET NUMBER: D5

MINER FLAT

DRILL HOLE NO. MF-122
 Elevation: 6064 feet
 Bearing: 278.5°
 Date Started: 2/5/86

Drilled by: Kaimine Exploration
 Logged by: Charles H. Robinson
 Inclination: 89.9°
 Date Completed: 2/8/86

| Depth (feet) | Lithologic Log | Description |
|--------------|----------------|-------------------------------------------------------------------------------------------------------------------------------------------------------------------------------------|
| 10- | | Colluvium, clayey sand |
| 30- | | Basalt, vesicular, medium gray, aphanitic, porphyritic, olivine phenocrysts. Silica and clay filled vesicles and fractures. Specular hematite? |
| 50- | | Basalt, massive, medium gray, very fine grained, porphyritic, olivine phenocrysts |
| 70- | | Basalt, vesicular, medium gray, weathers reddish brown, aphanitic, porphyritic, olivine phenocrysts. Vesicles and veins filled with coarse basalt sand and clay. |
| 90- | | Basalt, massive, medium gray, very fine grained, porphyritic, olivine phenocrysts. Vesicles filled with clay at 65 ft. |
| 110- | | Basalt, massive, medium gray, very fine grained to aphanitic, porphyritic. Flow fractures. |
| 130- | | Basalt, vesicular and scoriaceous, medium gray, aphanitic, porphyritic, olivine phenocrysts. Sand size rock fragments between blocks of scoriaceous basalt up to 1.5 ft long. |
| 150- | | Sandstone, light reddish brown to medium brown, fine grained. Contact of basalt and sandstone sharp at 150.3 ft. Less than 0.03 ft. of paleo-colluvium. Sandstone silty and friable |
| 170- | | E.O.H. |
| 175- | | |

Mineral Systems, Inc.

MINER FLAT

DRILL HOLE NO. MF-123
 Elevation: 6113 feet
 Bearing: 90°
 Date Started: 3/13/86

Drilled by: Kaimine Exploration
 Logged by: Charles H. Robinson
 Inclination: 90°
 Date Completed: 3/25/86

| Depth (feet) | Lithologic Log | Description |
|--------------|----------------|------------------------------------------------------------------------------------------------------------------------------------------------------------------------------------------------|
| 10- | | Quaternary - Tertiary gravel. Cobbles and gravel in clayey, silty sand. At 43 ft. 2-3 ft. dark carbonaceous sandstone. From 51 ft., cobbles, gravel and sand of white, fine grained sandstone. |
| 30- | | |
| 50- | | |
| 70- | | Sandstone, light gray to pinkish gray, light pinkish orange, fine grained, silty, moderately indurated. Sandstone breccia at 74-76 ft. |
| 90- | | |
| 110- | | Sandstone, light gray to light pinkish gray, fine grained, silty, poorly indurated. Below 113 ft. interbedded reddish brown silty and clayey fine grained sandstone. |
| 130- | | Sandstone, medium reddish brown, fine to medium grained, silty, some clay, poorly indurated. |
| 150- | | Sandstone, light reddish to light yellowish brown, fine grained to very fine grained, silty, locally clayey, poorly indurated. |
| 170- | | |
| 207.5- | | |

Flow boundary

Mineral Systems, Inc.

MINER FLAT

DRILL HOLE NO. MF-124
 Elevation: 6081 feet
 Bearing: 90°
 Date Started: 3/1/86

Drilled by: Kaimine Exploration
 Logged by: Charles H. Robinson
 Inclination: 90°
 Date Completed: 3/4/86

| Depth (feet) | Lithologic Log | Description |
|--------------|----------------|---------------------------------------------------------------------------------------------------------------------------------------|
| 10- | | Quaternary - Tertiary gravel. Cobbles, gravel, sand and silt. |
| 30- | | Basalt, vesicular, medium gray, aphanitic, porphyritic, olivine phenocrysts. Vesicles filled with silty clay. |
| 50- | | Vesicular, clay filled flow boundary |
| 70- | | Basalt, massive, medium gray, very fine grained, porphyritic, olivine phenocrysts. Vertical fractures, clay filling. |
| 90- | | Basalt, vesicular, medium gray, aphanitic, porphyritic, olivine phenocrysts. Vesicular clay. |
| 110- | | |
| 130- | | Sandstone, light reddish orange, very fine grained, very friable. 99.4 - 101.3 only 2 pieces of sandstone recovered. Paleo-colluvium? |
| 180- | | |

Flow boundary

Mineral Systems, Inc.

MINER FLAT

DRILL HOLE NO. MF-125A
 Elevation: 189.9°
 Bearing: 189.9°
 Date Started: 3/5/86

Drilled by: Kaimine Exploration
 Logged by: Charles H. Robinson
 Inclination: 89.9°
 Date Completed: 3/7/86

| Depth (feet) | Lithologic Log | Description |
|--------------|----------------|----------------------------------------------------------------------------------------------------------------------------------------------------------|
| 10- | | Quaternary - Tertiary gravel |
| 30- | | Basalt, vesicular, medium gray, aphanitic, porphyritic, olivine phenocrysts |
| 50- | | Basalt, massive, medium gray, very fine grained, porphyritic |
| 70- | | Basalt, vesicular, medium gray, very fine grained to aphanitic, porphyritic, olivine phenocrysts, slightly magnetic. Clay filled vesicles and fractures. |
| 90- | | Basalt, massive, medium gray, very fine grained to aphanitic, porphyritic, olivine phenocrysts, slightly magnetic. Fractures vertical, stained with clay |
| 110- | | Basalt, vesicular, very fine grained to aphanitic, porphyritic. Vesicles filled with clay. |
| 130- | | Basalt, massive, medium gray, very fine grained to aphanitic, porphyritic, olivine phenocrysts, slightly magnetic. |
| 170- | | Basalt, vesicular, medium gray, aphanitic |

Flow boundary

Mineral Systems, Inc.

FOUNDATION DATA 'G'

SHEET TITLE

MINER FLAT DAM
 WHITE MOUNTAIN APACHE RESERVATION
 NAVAJO COUNTY, ARIZONA

DRAWN BY: CJA
 CHK'D BY: CWK
 APPR BY: CWK
 DATE: 12-10-86
 QA
 PEER REVIEW



MORRISON-MAIERLE, INC.
 CONSULTING ENGINEERS

910 HELENA AVE. P.O. BOX 6147
 HELENA, MONTANA 59604

COMPANY OFFICE
 HELENA, MONTANA
 BRANCH OFFICES
 BILLINGS, MONTANA
 BUTTE, MONTANA
 CALDWELL, MONTANA
 GREAT FALLS, MONTANA
 MISSOULA, MONTANA
 SPOKANE, MONTANA

| NO. | DESCRIPTION | DATE | BY |
|-----|-------------|------|----|
| | | | |
| | | | |
| | | | |

D6

PROJECT NUMBER
 1780-14-Q(34)
 SHEET NUMBER



Golder Associates

CONSULTING GEOTECHNICAL AND MINING ENGINEERS

REPORT
TO
MORRISON - MAIERLE INC
ON
STABILITY ANALYSIS OF THE
MINER FLAT DAM FOUNDATIONS
NAVAJO COUNTY, ARIZONA

DISTRIBUTION:

- 25 copies - Morrison - Maierle Inc.
Helena, Montana
- 1 copy - Mineral Systems Inc.
Golden, Colorado
- 2 copies - Golder Associates
Vancouver, B.C.

February, 1987

862-1622

TABLE OF CONTENTS

| | <u>PAGE</u> |
|------------------------------------------------------|-------------|
| 1.0 INTRODUCTION | 1 |
| 2.0 STATEMENT OF PROBLEM | 1 |
| 2.1 Foundation Stability Against Sliding | 2 |
| 2.2 Foundation Stresses and Deformation | 2 |
| 2.3 Stability of Cut Slopes | 3 |
| 2.4 Objectives | 3 |
| 3.0 DATA BASE | 3 |
| 3.1 Dam Layout and Loading | 4 |
| 3.2 Previous Reports | 5 |
| 3.3 Geologic Profiles | 6 |
| 3.4 Field Testing | 7 |
| 3.4.1 Point Load Testing | 7 |
| 3.4.2 Packer Testing | 8 |
| 3.4.3 Goodman Jack Testing | 8 |
| 3.5 Laboratory Testing | 8 |
| 3.5.1 Uniaxial Compressive Testing | 9 |
| 3.5.2 Direct Shear Testing | 9 |
| 3.5.3 RCC Dam Material | 10 |
| 4.0 MATERIAL PROPERTIES | 11 |
| 4.1 Summary of Geologic Conditions | 11 |
| 4.2 General Approach to Parameter Selection | 13 |
| 4.2.1 Parameters for Stability Analysis | 13 |
| 4.2.2 Parameters for Stress and Deformation Analysis | 14 |
| 4.3 Rock Mass Classification | 14 |
| 4.3.1 Classification Systems | 14 |
| 4.3.2 Classification of Rock Units | 15 |
| a. Basalt | 15 |
| b. Sandstone | 16 |
| 4.4 Strength Parameters | 16 |
| 4.4.1 Rock Mass | 16 |
| 4.4.2 Paleo-Soil | 17 |
| 4.4.3 Discontinuities and Flow Boundaries | 19 |
| 4.4.4 Dam/Bedrock Contact | 20 |
| 4.5 Deformation Parameters | 23 |
| 4.5.1 Rock Mass | 23 |
| 4.5.2 Paleo-Soil | 25 |
| 4.6 Summary | 27 |
| 5.0 ANALYSIS | 27 |
| 5.1 Methods | 27 |
| 5.1.1 Limit Equilibrium Solution | 28 |
| 5.1.2 Numerical Modelling | 29 |
| 5.1.3 Analytical Solutions | 31 |

TABLE OF CONTENTS
(Cont'd)

| | <u>PAGE</u> |
|-------------------------------------|-------------|
| 5.0 ANALYSIS (Cont'd) | |
| 5.2 Limit Equilibrium | 31 |
| 5.2.1 Dam Foundation Stability | 31 |
| 5.2.2 Stability of Excavated Slopes | 33 |
| 5.3 Finite Element Modelling | 35 |
| 5.3.1 Description of Model | 35 |
| 5.3.2 Deformation | 38 |
| 5.3.3 Stresses | 38 |
| 5.4 Analytical Solutions | 40 |
| 6.0 DESIGN | 41 |
| 6.1 Dam Stability | 41 |
| 6.1.1 Zone of Low RQD | 42 |
| 6.1.2 Paleo-Soil | 43 |
| 6.1.3 Dam-Foundation Contact | 44 |
| 6.2 Dam Settlement | 44 |
| 6.3 Slope Stability | 46 |
| 7.0 CONCLUSIONS AND RECOMMENDATIONS | 47 |
| 7.1 Conclusions | 47 |
| 7.2 Recommendations | 49 |
| 8.0 REFERENCES | 50 |

LIST OF FIGURES

- Figure 1 Site Location Plan
- Figure 2 Potential Foundation Problems
- Figure 3 Proposed Dam Layout
- Figure 4 Boundary Loading Conditions
- Figure 5a Geologic Section with Histograms of Core Recovery
- Figure 5b Geologic Section with Histograms of Rock Quality Designation (RQD)
- Figure 5c Geologic Section with Histograms of Fracture Index
- Figure 5d Geologic Section with Histograms of Clay Filled Fracture Occurrence
- Figure 5e Geologic Section with Histograms of Uniaxial Compressive Strength
- Figure 5f Geologic Section with Histograms of Permeability
- Figure 6 Plan of Typical Foundation Profiles
- Figure 7a Typical Foundation Profile AA-AA'
- Figure 7b Typical Foundation Profile BB-BB'
- Figure 7c Typical Foundation Profile CC-CC'
- Figure 8 Equal Area (Lower Hemisphere) Plot of Discontinuities (Joints) in Basalt
- Figure 9 Geologic Section with Histograms of Rock Mass Rating
- Figure 10 Empirical Rock Mass Failure Criterion
- Figure 11 Rock Mass Strength Parameters
- Figure 12 Paleo-Soil Strength Parameters
- Figure 13 Rock Mass Deformation Parameters
- Figure 14 Sarma Analysis of Dam Foundation Stability
- Figure 15 Sarma Analysis of Excavated Slope Stability
- Figure 16 Linear Finite Element Mesh and Boundary Load Conditions
- Figure 17a Results of Finite Element Analysis Showing Deformations - Case 1
- Figure 17b Results of Finite Element Analysis Showing Deformations - Case 2

LIST OF FIGURES
(Cont'd)

- Figure 17c Results of Finite Element Analysis Showing Deformations - Case 3
- Figure 17d Results of Finite Element Analysis Showing Deformations - Case 4
- Figure 17e Results of Finite Element Analysis Showing Deformations - Case 5
- Figure 17f Results of Finite Element Analysis Showing Deformations - Case 6
- Figure 17g Results of Finite Element Analysis Showing Deformations - Case 7
-
- Figure 18a Results of Finite Element Analysis Showing Total Principal Stresses - Case 1
- Figure 18b Results of Finite Element Analysis Showing Total Principal Stresses - Case 2
- Figure 18c Results of Finite Element Analysis Showing Total Principal Stresses - Case 3
- Figure 18d Results of Finite Element Analysis Showing Total Principal Stresses - Case 4
- Figure 18e Results of Finite Element Analysis Showing Total Principal Stresses - Case 5
- Figure 18f Results of Finite Element Analysis Showing Total Principal Stresses - Case 6
- Figure 18g Results of Finite Element Analysis Showing Total Principal Stresses - Case 7
-
- Figure 19 Stress Conditions Paleo-Soil Layer A
- Figure 20 Approximate Distribution of Settlement

LIST OF TABLES

- Table 1 List of Morrison - Maierle Inc. Drawings of Proposed Miner Flat Dam Site Layout
- Table 2 List of Reports By Mineral Systems Inc. on Engineering Geology of Miner Flat Dam Site.
- Table 3 Summary of Results of Point Load Tests from Mineral Systems Inc. Investigation of Miner Flat Dam Site
- Table 4 Summary of Results of Packer Tests from Mineral Systems Inc. Investigation of Miner Flat Dam Site

LIST OF TABLES
(Cont'd)

| | |
|----------|----------------------------------------------------------------------------------------------|
| Table 5 | Results of Goodman Jack Tests from Mineral Systems Inc. Investigation of Miner Flat Dam Site |
| Table 6 | Results of Uniaxial Compressive Testing Program Undertaken by Morrison-Maierle Inc. |
| Table 7 | Results of Direct Shear Testing Program Undertaken by Morrison-Maierle Inc. |
| Table 8 | Properties of RCC Dam Material Provided by Morrison-Maierle Inc. |
| Table 9 | Rock Mass Rating Chart |
| Table 10 | Range of Material Properties |
| Table 11 | Sarma Limit Equilibrium Stability Analysis of Potential Sliding Failure in Dam Foundation |
| Table 12 | Sarma Limit Equilibrium Stability Analysis of Sliding Failure in Abutment Slopes |
| Table 13 | Summary of Finite Element Analysis Runs |
| Table 14 | Summary of Calculated Vertical Displacements Along Base of Dam |

1.0 INTRODUCTION

Golder Associates has been retained by Morrison-Maierle Inc. of Helena, Montana to carry out a preliminary foundation stability analysis for the proposed Miner Flat Dam on the White Mountain Apache Reservation in Arizona. Authorization to proceed was received in a letter from Morrison-Maierle Inc. dated November 24, 1986. The project is in the preliminary engineering design phase and the foundation analysis is needed to complement similar studies on the dam structure being carried out by Morrison-Maierle Inc.

The proposed dam is located on the North Fork of the White River at Miner Flat, east of State Highway 73, about eight miles south of McNary, to the northeast of Pheonix, Arizona (Figure 1). The river valley at this location is steep-sided and formed by near vertically jointed columnar basalt. The proposed dam will consist of a 160 foot high Roller Compacted Concrete (RCC) gravity structure founded on the basalt. The basalt is separated from the underlying sandstone of the Supai Formation by up to 40 feet of paleo-soil which lies some 30 to 100 feet below the base of the valley at the dam site.

This report describes analyses carried out. Potential foundation stability problems are outlined, the basis of the geomechanical model is presented, and the selection of input parameters is discussed. The methods of analyses, the results and recommendations for further investigation, testing, and analyses to refine or clarify the conclusions of this study are also included.

2.0 STATEMENT OF PROBLEM

The proposed Miner Flat Dam is to be located in a steep canyon in the North Fork River. The walls and floor of the canyon consist of a

series of basalt flows. Site investigations have identified that between the basalts and the underlying sandstones is a paleo-soil layer. This layer is a mixture of boulders, gravels, sands and silts.

Review of this basic geologic model of the dam site has indicated that two potential foundation problems exist, as illustrated in Figure 2. These are sliding or shear failure along various planes of weakness within the foundation rocks or abutment slopes and excessive settlements along the base of the dam due to consolidation of the underlying paleo-soil.

2.1 Foundation Stability Against Sliding

Available geologic information indicated that three potential sliding surfaces might exist in the dam foundation, these being:

- o sliding along the dam/basalt contact;
- o sliding through a zone of low quality basalt, identified from the drillhole logs, that may contain adversely oriented joints or planes; and
- o sliding through the paleo-soil layer with breakout through the basalt.

2.2 Foundation Stresses and Deformations

The paleo-soil layer varies in thickness in both the upstream/downstream direction and along the dam axis. Due to this variation, uneven consolidation and compaction of the paleo-soil under dam loads may occur leading to differential settlement both between the toe and heel of the dam and from one abutment to the other along the dam axis. Depending on the magnitude, such differential settlements could lead to the development of excessive stress in the dam, the underlying basalt and the paleo-soil.

2.3 Stability of Cut Slopes

The proposed construction methods indicate that relatively steep slopes will be excavated to prepare both dam abutments. Some of these slopes will be open only during construction, while others will be permanent. The presence of any adversely oriented planes of weakness and the development of high water pressures in these slopes after reservoir filling may cause slope instability.

2.4 Objectives

The objectives of the study have therefore been to assess the likely occurrence of the specific stability problems outlined above; that is to assess;

- o the potential for sliding or shear failure in the foundation rocks;
- o the deformation of the foundation rocks under dam and reservoir loading; and
- o the stability of the proposed abutment excavations.

At this stage no consideration has been given to stability aspects of canyon walls either upstream or downstream of the dam, nor has consideration been given to other aspects of dam stability, such as resistance to overturning. These are addressed elsewhere.

3.0 DATA BASE

The engineering geology of the Miner Flat Dam site was previously investigated by Mineral Systems Inc. (MSI) who also carried out exploratory drilling, geologic mapping and preliminary field testing. The results of their work has been documented in various reports, as

discussed below. Subsequently, laboratory testing on selected core samples from the drilling program was undertaken by Morrison-Maierle Inc. (MMI).

Details of the topography, dam layout and proposed construction were provided to Golder Associates by MSI and MMI. Golder Associates assembled, reviewed and evaluated this data, and then constructed a geomechanical model of the site. Because some of the geotechnical parameters required as input to the analyses were poorly defined, it was necessary to use a range of values and assess the sensitivity of the dam stability to variations in those parameters.

3.1 Dam Layout and Loading

Details of the site topography and dam layout as summarized in Figure 3, were produced by MMI. A list of drawings supplied is given in Table 1.

TABLE 1

LIST OF MORRISON-MAIERLE INC. DRAWINGS OF PROPOSED
MINER FLAT DAM SITE LAYOUT

| TITLE | SCALE | NUMBER | DATE |
|-----------------------------------------------|------------|------------|----------|
| 1. Plan - R.C.C. Gravity Dam | 1" to 20' | Unnumbered | Undated |
| 2. Section - R.C.C. Gravity Dam | 1" to 20' | Unnumbered | Undated |
| 3. Upstream Elevation - R.C.C. Gravity Dam | 1" to 20' | Unnumbered | Undated |
| 4. General Map "B" | 1" to 400' | A2 | 12-10-86 |
| 5. Surface Data - Topographic Map ""B" | 1" to 400' | C2 | 12-10-86 |
| 6. Surface Data - Topographic Map "C" | 1" to 400' | C3 | 12-10-86 |
| 7. Foundation Data "B" (Section A'-A) | 1" to 30' | Unnumbered | Undated |
| a. Untitled SECTION A | 1" to 30' | Unnumbered | Undated |
| b. Untitled SECTION B | 1" to 30' | Unnumbered | Undated |
| c. Untitled SECTION C | 1" to 30' | Unnumbered | Undated |

The details of external loads on the dam, shown in Figure 4, were provided in a memorandum from Morrison-Maierle dated 10 December, 1986.

3.2 Previous Reports

The results of the engineering geology investigation carried out by MSI are documented in the reports listed in Table 2.

These reports contain descriptions of general site conditions, geology and structure. The results of geologic mapping, line surveys, geophysical investigations and drilling and field testing programs are also provided. Preliminary assessments of engineering rock mass parameters to be used in analysis were discussed. Appendices attached to

these reports provided both the descriptive borehole logs and the engineering geology logs.

TABLE 2

LIST OF REPORTS BY MINERAL SYSTEMS INC. ON
ENGINEERING GEOLOGY OF MINER FLAT DAM SITE

| <u>Title</u> | <u>Date</u> |
|---------------------------------------------------------------------------------------------------------------------------------------------------------------|----------------|
| 1. <u>Preliminary Report</u> Engineering Geology Miner Flat Damsite and Reservoir White Mountain Apache Reservation Arizona. | July, 1982 |
| 2. <u>Preliminary Report</u> Engineering Geology Miner Flat Dam Site White Mountain Apache Indian Reservation Arizona. | November, 1983 |
| 3. <u>Preliminary Report</u> Engineering Geology Miner Flat Dam Site White Mountain Apache Reservation Navajo County, Arizona Volume I and Volume II | July, 1986 |

No core photographs were available from the original core logging program carried out by MSI.

In December, 1986 MMI undertook selective relogging of the core and obtained core photographs. These photographs were forwarded to Golder Associates in a memorandum dated 8 January, 1987.

3.3 Geologic Profiles

Data from the engineering geology logs provided by MSI were used to construct a series of engineering geologic sections along the dam centre line, showing histograms of:

- o core recovery
- o rock quality designation (RQD)

- o fracture index
- o clay filled fracture occurrence
- o uniaxial compressive strength
- o permeability

These sections are given in Figures 5a through 5f, respectively.

Three typical foundation profiles showing geologic conditions beneath the dam were prepared by MSI. These profiles, oriented perpendicular to the dam axis, are referenced in plan on Figure 6 and are given in Figures 7a, 7b and 7c.

Geologic fabric of the basalt in the vicinity of the dam as determined from data collected from detailed line surveys is shown in Figure 8.

3.4 Field Testing

Preliminary field testing carried out by MSI consisted of point load testing on intact core specimens, in situ packer testing, and down-hole Goodman Jack testing. The results of this testing were given in the MSI reports listed in Table 3.

3.4.1 Point Load Testing

Selected pieces of core from the drilling investigation were broken using point load testing equipment. Using the point load strength indices obtained, equivalent uniaxial compressive strengths were calculated. The results are summarized in Table 3 and plotted as a series of borehole histograms in Figure 5e.

TABLE 3

SUMMARY OF RESULTS OF POINT LOAD TESTS
 FROM MINERAL SYSTEMS INC. INVESTIGATION OF MINER FLAT DAM SITE

| | Basalt | | | Paleo-Soil | | Sandstone | Gypsiferous Sandstone | |
|--------------------------|----------------|-------------|-----------------|----------------|-------------|----------------|-----------------------|-------------|
| | Vertical Holes | Angle Holes | Low-Angle Holes | Vertical Holes | Angle Holes | Vertical Holes | Vertical Holes | Angle Holes |
| Maximum | 42,109 | 36,547 | 36,547 | 957 | 10 | 13,983 | 8,263 | 6,594 |
| Minimum | 957 | 3,851 | 25,424 | 10 | 10 | 10 | 1,351 | 1,510 |
| Average | 23,780 | 22,863 | 32,308 | 35 | 10 | 2,654 | 4,018 | 3,284 |
| Number of Samples Tested | 255 | 58 | 17 | 64 | 10 | 60 | 7 | 12 |

* Equivalent Uniaxial Compressive Strength (psi)

3.4.2 Packer Testing

Packer tests were carried out to determine the hydraulic conductivity or permeability of the rock and paleo-soil formations. These tests were carried out at a constant head. Flow was measured at 5, 10 and 15 or 20 minute intervals.

The results of packer testing are plotted as histograms in Figure 5f and summarized in Table 4.

3.4.3 Goodman Jack Testing

A Goodman Jack was used to measure borehole wall deformation as a function of applied load. These measurements were used to calculate the in situ elastic deformation moduli (Young's Modulus, E) of both the basalt and paleo-soil.

The results of Goodman Jack testing are reproduced Table 5.

3.5 Laboratory Testing

Data from the results of the laboratory testing undertaken by MMI was reported to Golder Associates by memorandum. This data included:

- o the results of uniaxial compressive strength testing (memorandum dated 17 December 1986); and
- o the results of direct shear testing on saw cut samples of the basalt core and on a sample of flow boundary material (memorandum dated 16 January 1987).

Data on the strength and deformation properties of the Roller Compacted Concrete dam construction material were provided through MMI

TABLE 4

SUMMARY OF RESULTS OF PACKER TESTS
 FROM MINERAL SYSTEMS INC. INVESTIGATION OF MINER FLAT DAM SITE

| | Basalt | | | Paleo-Soil | | Sandstone | Gypsiferous Sandstone | |
|-----------------|-----------------------|-----------------------|-----------------------|-----------------------|-----------------------|-----------------------|-----------------------|-----------------------|
| | Vertical Holes | Angle Holes | Low-Angle Holes | Vertical Holes | Angle Holes | Vertical Holes | Vertical Holes | Angle Holes |
| Maximum | 1.17×10^{-4} | 5.71×10^{-4} | 1.15×10^{-4} | 3.54×10^{-4} | 3.85×10^{-4} | 1.73×10^{-3} | 2.40×10^{-6} | 8.72×10^{-5} |
| Minimum | 5.20×10^{-8} | 8.26×10^{-7} | 7.47×10^{-5} | 9.56×10^{-6} | 1.06×10^{-4} | 2.08×10^{-5} | 1.55×10^{-6} | 4.33×10^{-5} |
| Average | 1.99×10^{-6} | 5.11×10^{-5} | 9.37×10^{-5} | 5.92×10^{-5} | 1.76×10^{-4} | 2.87×10^{-4} | 2.12×10^{-6} | 6.55×10^{-5} |
| Number of Tests | 13 | 18 | 3 | 8 | 3 | 10 | 2 | 3 |

* Hydraulic Conductivity of Boreholes (cm/sec)

TABLE 5

RESULTS OF GOODMAN JACK TEST FROM
MINERAL SYSTEMS INC. INVESTIGATION OF MINER FLAT DAM SITE

| Hole Number | Rock Type | Top of Interval Tested (Feet) | Young Modulus (psi x 10 ⁶) | | Refract | |
|----------------|--------------------|----------------------------------------|-------------------------------------------|--------|---------|--------|
| | | | Extend E(near) | E(far) | E(near) | E(far) |
| MF-102 | Basalt | 40.5 | 0.68 | 0.59 | 1.02 | 0.81 |
| MF-102 | Basalt | 80.5 | 0.42 | 0.34 | 0.85 | 0.70 |
| MF-102 | Basalt | 160.5 | 1.32 | 1.31 | 2.06 | 1.96 |
| MF-105 | Basalt | 18.8 | 0.45 | 0.29 | -- | -- |
| MF-105 | Basalt | 39.1 | 0.87 | 0.58 | 1.51 | 1.29 |
| MF-105 | Basalt | 59.6 | 0.78 | 0.036 | -- | -- |
| MF-113 | Basalt | 80.8 | 2.46 | 1.66 | 2.21 | 1.48 |
| MF-113 | Basalt | 101.5 | 2.58 | 2.22 | 2.76 | 2.46 |
| MF-113 | Paleo- alluvium | 121.5 | 0.16 | 0.07 | 0.46 | ERR |
| MF-113 | Paleo- alluvium | 130.6 | 53.91 | 15.58 | -- | -- |
| MF-113 | Paleo- alluvium | 133.0 | 0.03 | 0.35 | -- | -- |
| MF-117 | Basalt | 10.0 | 0.94 | 0.57 | 0.93 | 0.87 |
| MF-117 | Basalt | 30.0 | 1.49 | 0.72 | 1.51 | 1.06 |
| MF-117 | Basalt | 50.0 | 0.99 | 1.02 | 1.39 | 1.12 |
| MF-117 | Basalt | 90.2 | 1.13 | 0.74 | 1.62 | 1.86 |

by an independent consultant, E.K. Schrader, in a note dated Nov. 5/6/7, 1986.

3.5.1 Uniaxial Compressive Testing

The uniaxial compressive testing program was undertaken by the University of Arizona on behalf of MMI. This testing program was used to determine uniaxial compressive strength, density, elastic moduli and Poisson's ratio, for each of the samples tested. The test data are reproduced in Table 6. The uniaxial compressive strength data are also plotted as points on the dam axis section in Figure 5e.

3.5.2 Direct Shear Testing

A number of direct shear tests were done on saw cut surfaces from NX core samples of the basalt. In addition, a direct shear test was carried out on a composite sample of clay and basalt flow boundary material recovered from a number of drill holes. Each of the samples were tested at normal stresses of 50, 100, 150 and 200 psi. The saw cut tests were used to determine the base friction angle of the basalt. The composite sample was used to determine the residual friction angle of the flow boundary material.

The results of Direct Shear Testing are reproduced in Table 7.

TABLE 6

RESULTS OF UNIAXIAL COMPRESSIVE TESTING PROGRAM
UNDERTAKEN BY MORRISON-MAIERLE INC.

| Sample | Rock Type | Drill Hole | Depth (ft) | Uniaxial | | Density (lbs/cu ft) | Elastic Constants | |
|--------|------------|------------|---------------|-------------------------|----------|------------------------|----------------------|------------------|
| | | | | Compressive Strength | Strength | | Elastic Mod (psi) | Poisson Ratio |
| U-2A | MAS BASALT | DH-2 | 16.8 - 26.1 | 15,737 | | 178 | 4,501,078 | .27 |
| U-13A | MAS BASALT | DH-106 | 155.0 - 155.7 | 16,837 | | 173 | 2,554,148 | .19 |
| U-1A | MAS BASALT | DH-2 | 6.9 - 16.8 | 50,400 | | 178 | 5,533,514 | .25 |
| U-3A | MAS BASALT | DH-2 | 54.5 - 62.4 | 32,943 | | 178 | 8,044,664 | .42 |
| U-15A | MAS BASALT | DH-106 | 158.9 - 159.7 | 18,962 | | 176 | 4,324,483 | .29 |
| U-4A | MAS BASALT | DH-2 | 90.2 - 100.5 | 15,064 | | 177 | 8,705,493 | .40 |
| U-14A | MAS BASALT | DH-106 | 156.2 - 157.4 | 18,104 | | 174 | 4,036,184 | .21 |
| U-2B | MAS BASALT | DH-2 | 16.8 - 26.1 | 21,963 | | 177 | --- | --- |
| U-3B | MAS BASALT | DH-2 | 54.5 - 62.4 | 31,845 | | 178 | --- | --- |
| U-13B | MAS BASALT | DH-106 | 155.0 - 155.7 | 25,746 | | 173 | --- | --- |
| U-15B | MAS BASALT | DH-106 | 158.9 - 159.7 | 18,512 | | 176 | --- | --- |
| U-16 | MAS BASALT | DH-106 | 215.0 - 218.9 | 22,450 | | 181 | --- | --- |
| U-7 | MAS BASALT | DH-5 | 45.3 - 47.2 | 11,143 | | 166 | --- | --- |
| U-14B | MAS BASALT | DH-106 | 156.2 - 157.4 | 27,195 | | 175 | --- | --- |
| U-18 | MAS BASALT | DH-2 | 6.9 - 16.8 | 45,075 | | 178 | --- | --- |
| U-10 | VES BASALT | DH-106 | 41.1 - 43.0 | 10,569 | | 149 | 7,002,875 | .29 |
| U-5 | VES BASALT | DH-5 | 19.5 - 21.0 | 11,095 | | 161 | 4,254,604 | .30 |
| U-11 | VES BASALT | DH-106 | 50.6 - 52.5 | 15,133 | | 171 | --- | --- |
| U-12 | VES BASALT | DH-106 | 118.4 - 120.2 | 6,833 | | 134 | --- | --- |
| U-8 | VES BASALT | DH-5 | 104.7 - 106.2 | 6,494 | | 125 | --- | --- |
| U-9 | VES BASALT | DH-5 | 132.0 - 132.9 | 6,530 | | 143 | --- | --- |
| U-6 | VES BASALT | DH-5 | 23.5 - 24.4 | 3,218 | | 132 | --- | --- |
| U-17 | SILTY SS | DH-106 | 306.8 - 309.8 | 1,588 | | 151 | 521,081 | .27 |
| U-20 | GYP SIL SS | DH-106 | 337.1 - 338.7 | 3,105 | | 148 | 1,080,152 | .13 |
| U-22 | GYP SS | DH-102 | 358.5 - 360.5 | 1,882 | | 142 | 1,291,449 | .07 |
| U-18 | GYP SS | DH-106 | 332.2 - 333.7 | 3,101 | | 144 | 3,039,394 | .16 |
| U-19 | GYP SIL SS | DH-106 | 336.8 - 336.8 | 2,715 | | 153 | 765,127 | .24 |

Notes:

MAS - massive
VES - vesicular
SS - sandstone
GYP - gypsiferous
SIL - silty

TABLE 7

RESULTS OF DIRECT SHEAR TESTS FROM
TESTING PROGRAM UNDERTAKEN BY MORRISON-MAIERLE INC.

| SAMPLE | FRICION ANGLE (degrees) |
|----------------------|-------------------------|
| S1B - Saw Cut Basalt | 36* |
| S2A - Saw Cut Basalt | 35 |
| S2B - Saw Cut Basalt | 38* |
| S3A - Saw Cut Basalt | 40 |
| S3B - Saw Cut Basalt | 33 |
| S4A - Saw Cut Basalt | 40* |
| S4B - Saw Cut Basalt | 28 |
| Upper Basalt | 39.5** |
| Flow Boundary | 23 |

* Base Friction Angle

** Residual Friction Angle

As part of the direct shear test program, Atterberg Limits were determined from small sample of clay joint infilling from the Upper Basalt flow boundaries. The results of this testing were,

liquid limit 65%

plastic limit 29%

3.5.3 RCC Dam Material

The strength and deformation properties of the RCC dam material provided by MMI, are reproduced in Table 8.

TABLE 8

PROPERTIES OF RCC DAM MATERIAL PROVIDED BY MORRISON-MAIERLE INC.

| PROPERTY | Cohesion (psi) | Friction Angle (degrees) | Density lb/ft ³ | Deformation Modulus (psi) |
|------------------|-------------------|--------------------------------|-------------------------------|---------------------------------|
| usual - 6 month | 100 | 45 | - | - |
| usual - 1 year | - | - | 153 | 2.0 x 10 ⁶ |
| unusual - 1 year | 115 | 50 | - | - |
| extreme - 1 year | 155 | 55 | - | - |

4.0 MATERIAL PROPERTIES

To develop a model of the dam foundation it was necessary to assign realistic geotechnical properties to each of the rock units and to the paleo-soil. Of particular importance was the determination of rock and paleo-soil strength and deformation parameters. The necessary parameters have been inferred from available geologic data, laboratory test results and from published data.

4.1 Summary of Geologic Conditions

The available data, indicates that for purposes of engineering analysis the foundation of the proposed Miner Flat Dam can be divided into three geologic units, a surface basalt layer, an underlying paleo-soil layer, and a basement consisting of sandstone and gypsiferous sandstone. The distribution of these units is shown on geologic cross-sections, Figure 7a) to 7c).

The ancestral valley of the North Fork of the White River was carved into sandstones of the Permian Age Supai Formation. These sandstones are pale reddish brown to yellowish brown, fine grained and well sorted. Beds within the sandstone range in thickness from less than an

inch to 15 feet. The thickest beds are massive and conspicuously cross bedded. The beds of the Supai Formation strike northeast to northwest and dip about 3 to 7 degrees to the east. Joints are spaced at intervals of 0.5 to 3 feet and typically strike at right angles or parallel to the strike of the beds. The sandstone joints dip at 60 to 90 degrees. At depth the sandstone becomes gypsiferous. The gypsiferous member and the sandstone above are considered as one unit for analysis purposes.

Along the walls of the ancestral valley, weathering products of the sandstones accumulated as colluvium, and flooding in the valley bottom deposited alluvium derived from erosion upstream. Subsequently basalt flowed down the ancestral valley pushing the colluvium and alluvium aside or sandwiching it against the surface of the underlying sandstone. The result of the basalt flow was the development of a paleo-soil which, in the vicinity of the dam foundation, ranges in thickness from less than an inch to as much as 40 feet.

The paleo-colluvium is thought to consist of weathered angular blocks of talus sandstone, or pieces of sandstone bound in matrix of silt and clay derived from slope wash deposits. The paleo-alluvium is thought to consist of clay, silt and sand, and gravel cobbles and boulders composed of igneous metamorphic or sedimentary rock. Since core recovery was very low in this material and the range of material types and possible grain size distribution may be variable, the paleo-colluvium and paleo-alluvium have been considered as one unit for analysis purposes. Observations of the paleo-soil in limited outcrop indicates that the material may stand in vertical cuts up to 30 feet high. The paleo-soil is believed to be dense. Hydraulic conductivities of 10^{-4} to 10^{-5} cm/sec were measured in packer tests.

The basalt, which will form the immediate foundation and both abutments of the dam, consists of a series of flows and is very dark grey to black, weathering medium to dark grey. It is fine grained to aphanitic and locally porphoritic and contains vesicules of less than 0.05 in to 0.15 in. The vesicules occur in bands of 1 inch to 1 foot wide. Individual flows range from about 20 to 80 feet in thickness and there is typically a thin clay seam of 0.1 to 4 inches between flows.

Discontinuities in the basalt are related to flow banding and joints are the result of basalt cooling. These joints have an average spacing of 1.8 feet and an average length of 3.9 feet. The jointing pattern is columnar, as shown in Figure 8, with predominantly horizontal and near vertical orientation. Generally the basalt is considered to be of good to very good quality.

4.2 General Approach to Parameter Selection

4.2.1 Parameters for Stability Analysis

The necessary input parameters for the analysis of the foundation stability against sliding are γ , the material unit weight, c , the cohesion and ϕ , the friction angle. Laboratory results were available from which base frictional strength of the basalts and the residual strength of the flow boundaries could be estimated. No direct data was available on the in situ strength of the basalt or sandstone rock masses. The paleo-soils were particularly difficult to describe in geotechnical terms. This was a result of poor recoveries and difficulties experienced in sampling. No paleo-soil material was therefore available for testing.

To estimate the in situ strength of the rock it was necessary to utilize the geologic data to rate the rock mass according to its quality and from this rating assess a range of rock mass strength parameters.

For the paleo-soils it was necessary to rely on available published data, and this resulted in selection of lower bound strength envelopes for analysis. For the RCC dam material, both the data supplied by MMI and data published in the proceedings of the the ASCE Symposium on Roller Compacted Concrete (Denver, Colorado, May, 1985) were utilized.

4.2.2 Parameters for Stress and Deformation Analysis

The necessary input parameters for the analysis of foundation stresses and deformations are Young's modulus of deformation, E , Poisson Ratio, ν , as well the c , ϕ , and γ , the strength and density parameters discussed in the previous subsection.

Some laboratory data for E and ν , for the intact basalt and sandstone were provided as were typical data for the RCC dam material. Little data however was available to determine the deformation parameters of the paleo-soil.

In order to arrive at values of deformation parameters for the rock mass, a rock mass classification method was used in conjunction with the results of the laboratory and in situ Goodman Jack testing.

Deformation parameters for the paleo soil were determined primarily from published data. This resulted in a wide range of values being considered.

4.3 Rock Mass Classification

4.3.1 Classification Systems

In recent years rock mass classification systems have been developed to make use of measurable parameters in an attempt to minimize judgemental bias and to permit a quantifiable rock mass rating. Two

widely used rock mass classification systems are the Q System (Barton et al, 1974) and the Rock Mass Rating System (Bieniawski, 1974, 1976). Bieniawski's CSIR RMR method was used for this study. The parameters required for input to determine an RMR value are;

- o strength of the intact rock material
- o drill core quality (RQD)
- o spacing of joints
- o condition of joints
- o groundwater condition

Each of these five input parameters is assigned a rating based on the descriptions given in Table 9. The RMR value is determined by summing these assigned ratings.

4.3.2 Classification of Rock Units

The RMR classification values for the rock mass in the vicinity of the dam are plotted as histograms on the Geologic Section in Figure 9. These values were determined by assigning ratings from Table 9, to each of the core run intervals. The RQD, uniaxial compressive strength and fracture index parameters were obtained from the data plotted on Figures 5a to 5c. Generalized factors were assigned for joint and ground water conditions.

- o Basalt

Based on the description of the joints provided in the MSI reports a joint condition rating of 20 and a ground water rating of 7 was assumed. The resulting RMR value for the basalt rock mass ranged from 50 to 90, though most values fell in the range 55 to 75. An average value of 65 was selected for analysis purposes.

ROCK MASS RATING CHART

TABLE 9

CSIR GEOMECHANICS CLASSIFICATION OF JOINTED ROCK MASSES CLASSIFICATION PARAMETERS AND THEIR RATINGS

| PARAMETER | | RANGES OF VALUES | | | | | | | |
|-----------|----------------------------------|---------------------------------------------------------------------------|---------------------------------------------------------------------------------------|-------------------------------------------------------------------------------|------------------------------------------------------------------------------|-----------------------------------------------------------------------------------------------------------|----------------------------------------------------------------------|---------|----------|
| 1 | Strength of intact rock material | Rock strength rating | R5 | R4 | R3 | R2 | R1 For this low range - uniaxial compressive test is preferred | | |
| | | Uniaxial compressive strength | >29 ksi | 14.5 - 29 ksi | 7.25 - 14.5 ksi | 3.6 - 7.25 ksi | 1.5-3.6 ksi | 0.5 ksi | <0.5 ksi |
| | Rating | | 15 | 12 | 7 | 4 | 2 | 1 | 0 |
| 2 | Drill core quality RQD | | 90% - 100% | 75% - 90% | 50% - 75% | 25% - 50% | < 25% | | |
| | Rating | | 20 | 17 | 13 | 8 | 3 | | |
| 3 | Fracture index frac./ft. | | <0.1 | 0.1 - 0.3 | 0.3 - 1.0 | 1.0 - 6.0 | >6.0 | | |
| | Rating | | 30 | 25 | 20 | 10 | 5 | | |
| 4 | Condition of joints | | >10 Very rough surfaces Not continuous No separation Hard joint wall rock | 6 - 10 Slightly rough surfaces Separation <1 mm Hard joint wall rock | 2 - 6 Slightly rough surfaces Separation <1 mm Soft joint wall rock | 0 - 2 Slickensided surfaces or Gauge <5 mm thick or Joints open 1-5mm Continuous joints | Soft gouge >5mm thick or Joints open >5mm Continuous joints | | |
| | Rating | | 25 | 20 | 12 | 6 | 0 | | |
| 5 | Ground water | Inflow per 10m borehole length | None | | <25 litres/min. | 25 - 125 litres/min. | >125 litres/min. | | |
| | | Ratio $\frac{\text{joint water pressure}}{\text{major principal stress}}$ | OR | | OR | OR | OR | | |
| | General conditions | 0 | | 0.0 - 0.2 | 0.2 - 0.5 | >0.5 | | | |
| | Rating | OR | | OR | OR | OR | | | |
| | | Completely dry | Moist only (interstitial water) | | Water under moderate pressure | Severe water problems | | | |
| Rating | | 10 | | 7 | 4 | 0 | | | |

ROCK MASS CLASSES DETERMINED FROM TOTAL RATINGS

| Rating | 100 - 81 | 80 - 61 | 60 - 41 | 40 - 21 | < 20 |
|-------------|----------------|-----------|-----------|-----------|----------------|
| Class No. | I | II | III | IV | V |
| Description | Very good rock | Good rock | Fair rock | Poor rock | Very poor rock |

Modified from Bieniaski.

PROJECT NO.
 DRAWN
 REVIEWED
 DATE

o Sandstone

Based on the description of joints provided, a joint condition rating of 12 and a ground water rating of 7 was assumed. The resulting RMR values for the sandstone rock mass ranged between 40 and 70, though most values fell between 45 and 65. An average value of 55 was selected for analysis purposes.

4.4 Strength Parameters

The dam and foundation can be regarded as a discontinuum consisting of a series of blocks of intact rock and roller compacted concrete separated by various planes of weakness. The behaviour of this system will be controlled by both the strength of the intact materials and the strength along planes of weakness (e.g. joints, flow boundaries, and contacts).

4.4.1 Rock Mass

An empirical rock mass failure criterion, developed by Hoek and Brown (1980), has been used to predict rock mass strength of the basalt and sandstone. The criterion consists of a number of empirical equations which allow strength envelopes to be constructed for different rock types and qualities. The empirical failure criterion, illustrated on Figure 10, is defined using the constants m and s according to the equation:

$$\sigma_1' = \sigma_3' + (m \sigma_c \sigma_3' + s \sigma_c^2)^{1/2}$$

where σ_1' and σ_3' are major and minor principal effective stress and σ_c is the uniaxial compressive strength of the rock.

The constants m and s can be determined using the equation

$$\begin{aligned}m/m_i &= \exp (RMR-100)/14 \\s &= \exp (RMR-100)/6\end{aligned}$$

where RMR is the rock mass rating and m_i is the value of m for intact rock as described in Figure 10.

The basalt at the Miner Flats has been classified as a "good quality mass" of "fine grained polyminerallic igneous crystalline rock." The sandstone at the site has been classified as a "fair to good quality mass" of "arenaceous rock with strong crystals and poorly developed crystal cleavage."

Estimated strength envelopes for the basalt and sandstone are shown on Figure 11 for a range of RMR and UCS values. These envelopes represent peak strength conditions of in-place rock masses and assume that the rock mass is homogeneous and isotropic. Mid range values of c and ϕ , selected for analysis from these envelopes, are $c = 140$ psi, $\phi = 55^\circ$ for the basalt, and $c = 70$ psi, $\phi = 40^\circ$ for the sandstone. Field experience has shown that rock mass strengths calculated using m and s parameters defined by this failure criterion are conservative.

4.4.2 Paleo-Soil

Poor core recovery in the paleo-soil and the difficulty associated with sampling and testing materials of this type resulted in very little field data, and no laboratory data. The shear strength of the paleo-soil was therefore determined primarily from published data on the strength of compacted rockfill. As the paleo-soil consists of a broad range of particle sizes from boulders and cobbles to silt and clay, the rockfill analogy is considered a reasonable approximation.

It has been assumed that the paleo-soil consists predominantly of detrital material from the sandstone rock which existed at the surface prior to the basalt flows. The shear strength of compacted sandstone rockfill has been measured by Charles and Watt (1980). Their findings are reproduced in Figure 12a. From this graph an average value of $\phi = 35^\circ$ and $c = 14$ psi is indicated for the range of stresses likely to develop within the paleo-soil zones. Other laboratory test data on the shear strength of rockfill has been published by Barton and Kjaernsli (1981). This data relates the effects of particle size, compressive strength of the intact rockfill material (σ_c), the in situ confining pressure (σ_n') and the particle roughness (R) to the friction angle ϕ using the formula:

$$\phi = R \log \left(\frac{s}{\sigma_n'} \right) + \phi_b$$

The factor s is an empirically determined equivalent strength parameter and is a function of average particle size and the unconfined compressive strength of the particle. Based on data presented by Barton and Kjaernsli for rockfill under confinement a value of $s = 0.25$ was selected.

Using a base friction angle of 30° for sandstone, and a uniaxial compressive strengths ranging between 1000 and 2500 psi and, an equivalent roughness of about 8 (which corresponds to rough, subangular to angular colluvium material), a friction angle of approximately 35° is indicated within the range of normal stresses likely to develop within the sandstone. A probable range of friction angles for the paleo-soil, predicted by the above criterion, is plotted in Figure 12b.

4.4.3 Discontinuities and Flow Boundaries

The shear strength of uncemented discontinuities in rock is a result of two components. The first of these is termed the base friction angle, ϕ_b and refers to the frictional strength of a smooth surface. The base friction angle is inherent to the rock type and represents the minimum or residual strength for a discontinuity in that rock. The value of ϕ_b is not dependent on the scale of the test sample and the stress level in the direction normal to the surface.

The second component of the shear strength is the roughness caused by asperities along the discontinuity surface. At low normal stresses the effect of roughness is to cause dilation of the discontinuity during shear displacement, thereby increasing the angle of friction. At higher normal stresses, the mechanism of shear changes from dilation to shearing through the asperities. The failure envelope is curved and the total frictional strength is dependent on a third parameter, the stress level.

Barton and Choubey (1977) have proposed the following empirical relationship between the above three parameters and peak friction angle (ϕ_p along a discontinuity):

$$\phi_p = JRC \cdot \text{Log}_{10}(JCS / \sigma_n') + \phi_b,$$

where,

σ_n' = the normal stress acting across the joint

ϕ_b = the base friction angle for rock

JRC = the joint roughness coefficient

JCS = the uniaxial strength of the joint wall

From the results of laboratory testing, core logging and detailed line surveys, the following values were selected:

Base friction of basalt (ϕ_b) = 35° (see results of direct shear tests, Figure 9)

Joint roughness coefficient (JRC) = 7

Joint compressive strength = 15000 psi

At a normal stress across the joint of 50 psi, the estimate peak friction angle would be 52° ; at 100 psi the peak friction angle would be 50° . Since the discontinuities are uncemented, a conservative value of $c = 0$, $\phi_p = 50^\circ$ was used for analyses. These strength parameters ignore any intact ridges which may occur along any potential failure surface or any steps in that surface.

Peak shear strength along flow boundaries was estimated at $c = 0$, $\phi = 40^\circ$ based on the results of direct shear testing given in Table 7 and observed asperities and undulations along these surfaces.

4.4.4 Dam/Bedrock Contact

Shear strength along the dam/bedrock contact is a result of three components,

- rock/concrete friction properties
- rock/concrete adhesion value

- roughness and size of asperities along the rock surface

The first of these can be expressed as the base rock/concrete friction angle ϕ_{bc} which is similar to the base friction angle for uncemented discontinuities described in the previous subsection.

The second component of shear strength, the rock/concrete adhesion, can only be considered if cementing develops between the concrete and the rock. Since no test data is available to assign such a value, a conservative approach was taken and a value of zero was assumed.

The third component of the shear strength can be expressed as the roughness and asperity angle (i). Patton (1966) has demonstrated that the roughness and asperity angle (i) can be combined with the base friction angle (ϕ_{bc}) of the dam/bedrock contact to obtain an estimate of the peak frictional strength available along the contact.

Observations of the drill core, at the dam alignment and in the channel of the river made by MSI indicate that at least three orders of roughness and asperities exist. The first order asperities are on the scale of the drill core and have been termed the joint roughness effect. The second and third order asperities are of a scale greater than the drill core diameter and are inferred from observations in the river channel and on the erosion surface of the basalt flows. The second order asperities have been termed the waviness effect and the third asperities have been termed the step effect.

For failure to occur along the dam/bedrock interface the frictional properties between the concrete and rock must be exceeded and there must be shear through, or dilation over, the first order asperities (joint roughness), second order asperities (waviness) and third order asperi-

ties (steps) The roughness angle along the contact (i) is therefore a function of:

$$i = \text{fn} (\phi_j, \phi_w, \phi_s)$$

where ϕ_j is the effect of joint roughness, ϕ_w is the effect of waviness and ϕ_s is the effect of the steps.

The base friction angle ϕ_{bc} for the dam/bedrock contact has been estimated at 35° based on previous work by Robinson et al (1986). This work indicated that the value of ϕ_{bc} was approximately equal to the base friction angle ϕ_b of saw cut samples.

As discussed in the previous section, the joint roughness effect ϕ_j can be evaluated using the empirical relationship prepared by Barton and Choubey (1977 where

$$\phi_j = \text{JRC} \log_{10} (\text{JCS} / \sigma'_n)$$

As discussed previously the JRC is considered to be approximately 7 based on the reported results of detailed line survey and core logging data. The average uniaxial compressive strength of intact basalt is reported as 15,000 psi and the strength of the roller compacted concrete is estimated at 1,700 psi. Using a normal stress range of 50 to 100 psi and a JCS value of 1,700 psi, the joint roughness effect ϕ_j calculated from the above equation is approximately 9° to 11° .

The waviness and step effects have been estimated from MSI's field observations of the dam/bedrock contact angle. The reported observations indicate that the contact angle varies from horizontal to at least 80° . Since the proposed foundation excavation profile slopes downstream the step effect has been significantly reduced. A conservative estimate of the mean contact angle based on the MSI observations and the proposed

excavation profile, is 10° . Together these figures ($\phi_j + \phi_w + \phi_s$) give a roughness angle (i) of about 20° and result in a probable peak friction angle, ϕ_p , of 55° .

During excavation, an evaluation of the size of joint blocks along the foundation should be carried out. Since any potential slip surface must either pass through the rock mass or dilate over the ridges formed by intact blocks, the step effect of intact joint blocks will, significantly increase the peak friction angle over the conservative estimate used here.

4.5 Deformation Parameters

4.5.1 Rock Mass

Rock mass deformation is influenced by both the deformation characteristics of intact rock and the deformation characteristics of discontinuities within the rock mass. The approach used to determine the modulus of deformation for the sandstone and basalt rock masses involved combining data from three separate sources. These were:

- o measurement of deformation moduli from laboratory testing of intact rock samples;
- o measurements of in-situ moduli using borehole Goodman Jack tests; and
- o evaluation of in-situ moduli from empirical relationships between rock mass quality and published deformation moduli data.

Laboratory measurements of Young's Modulus and Poisson's Ratio have been carried out. The results of these measurements were given in Table 6. The measured deformation moduli for the basalt samples ranged between 2.55×10^6 psi and 8.71×10^6 psi and the measured Poisson Ratios ranged between 0.19 and 0.40. The average values for the basalt samples were 5.44×10^6 psi and 0.29 for the deformation modulus and

Poisson's Ratio respectively. The measured deformation modulus for the sandstone samples ranged between 0.52×10^6 psi and 3.04×10^6 psi with an average value of 1.34×10^6 psi, and the measured Poisson Ratio ranged between 0.07 and 0.27 with an average value of 0.17.

The results of borehole Goodman Jack Testing were reproduced in Table 5. The Goodman Jack Tests gave two sets of moduli, a loading stage (Extend) moduli and a rebound (Retract) moduli. A wide range of values were measured in the Basalt. Loading moduli ranging from 0.29×10^6 psi up to 2.58×10^6 psi were measured, while rebound moduli ranged from 0.7×10^6 psi up to 2.76×10^6 psi. The average moduli values for loading was 1.44×10^6 psi, and for rebound was 1.47×10^6 psi. Goodman Jack tests were not carried out in the sandstone.

The results of Goodman Jack testing in the basalt indicate values consistently lower than the laboratory test values. The construction of the Goodman Jack is such that when in a very hard material, such as the basalt, the stiff cylinders of the jack tend to generate line loads rather than full circumference loading which would occur in softer materials. This effect is difficult to quantify and therefore the jack results must be considered, at the least, to be approximate.

Empirical relationships between rock mass rating and in situ modulus for deformation have been presented by Bieniawski, (1978) and Serafim and Pereira (1983). These relationships are shown in Figure 13. The two charts shown, indicate that based on the RMR values calculated in Section 3, the in situ deformation modulus for the sandstone could range between 0.74×10^6 psi and 2×10^6 psi, while the in situ deformation modulus for the basalt could range between 2.9×10^6 psi and 4.35×10^6 psi.

The value of deformation modulus selected for the sandstone rock mass was 0.7×10^6 psi, which is the lower bound of the empirical range and approximately half the average laboratory measured value for intact specimens. A Poisson ratio of 0.25 was selected, corresponding approximately with the measured ratio in the laboratory.

The value of deformation modulus selected for the basalt rock mass was 3.6×10^6 psi which is about mid range for values determined empirically, slightly more than half the average laboratory measured value, and is slightly more than twice the values measured in situ with the Goodman Jack. A Poisson ratio of 0.25 was selected which corresponds approximately with measured ratios in the laboratory.

4.5.2 Paleo-Soil

Deformation of a material such as the paleo-soil is influenced by the in situ density of the material, the distribution of particle sizes within the material, the shape of those particles, and the deformation characteristics of the material constituting the larger particles. The amount of data available on these fundamental properties for the paleo-soil was very limited. For this reason it was necessary to rely almost entirely on published data on the deformability of rock fill. Consequently a wide range of possible deformation moduli values were considered.

Some of the most extensive testing of the deformability of soils of this type is that reported by Marsal (1973). Though the materials Marsal was working with may not be the same as those of which the paleo-soil consists, the values indicate a lower range of possible moduli for use in a sensitivity analysis. Marsal's data indicates that under initial loading conditions a reasonable lower bound deformation moduli for rockfill may be in the range of 7000 psi. This could be considered

an absolute lower bound value for the paleo-soil since it has subjected to a considerable initial load (pre-load) from the weight of overlying basalt. Marsal's data indicates that under reloading conditions a reasonable deformation moduli for rockfill may be in the range of 35,000 psi. In order to arrive at an absolute upper bound value for deformation moduli for the paleo-soil, the material could be considered as a very poor quality rock mass. Based on the work by Serafim and Pereira illustrated on Figure 13, a deformation modulus in the order of 0.8×10^6 psi would be reasonable for such a material.

The resulting values of deformation moduli used for the paleo-soil in the analyses are:

- 7,000 psi - lower bound
- 35,000 psi - mid range
- 800,000 psi - upper bound
- 3,600,000 psi - equivalent to basalt

A Poisson ratio value of 0.35 was selected for the paleo-soil.

A limited number of in situ borehole Goodman Jack tests were carried out in the paleo-soil as recorded in Table 6. Values of deformation modulus ranged widely from 0.07×10^6 psi to 53.9×10^6 psi. The limited number of these tests and the scattered results are inconclusive. Due to the lack of homogeneity in the paleo-soil, uniform deformation of the borehole during a test and, test repeatability is unlikely. The deformation moduli interpreted from these tests have therefore not been used in selecting representative values.

4.6 Summary

Table 10 summarizes the estimated range of values for material properties.

5.0 ANALYSIS

Construction of the Miner Flats dam together with the impounding of the associated reservoir will result in a change in the state of stress within the foundation. Depending on the strength and deformation characteristics of the various foundation materials, these stress changes could result in a number of problems, including:

- o excessive shear stresses along adversely oriented discontinuities; such as joint surfaces or geologic contacts and;
- o generation of excessive differential settlements along the dam base.

It has been assumed that due to the high strength of basalts on which the dam will be founded that bearing capacity failure in the soil mechanics sense is not a problem. Specific analyses to calculate the factor of safety against such a mechanism have therefore not been carried out. In addition excavation of rock to develop the abutment walls could potentially give rise to slope stability problems.

The following methods have been used to evaluate these potential problems:

- o limit equilibrium solutions based on rigid block mechanics;
- o analytical solutions based on elastic theory; and
- o numerical solutions based on elastic theory.

TABLE 10
RANGE OF MATERIAL PROPERTIES

| | | Sandstone Rockmass | Basalt Rockmass | RC Concrete Dam | Paleo-Soil |
|----------------------------|------|-----------------------|--------------------|--------------------|------------|
| c (Cohesion) psi | high | 100 | 200 | 175 | 14 |
| | mid | 70 | 140 | 100 | 0 |
| | low | 20 | 70 | 35 | 0 |
| ∅ (Friction) degrees | high | 45 | 65 | 55 | 38 |
| | mid | 40 | 55 | 45 | 35 |
| | low | 35 | 45 | 40 | 32 |
| (Unit Weight) pcf | high | 150 | 175 | - | 145 |
| | mid | 145 | 165 | 153 | 140 |
| | low | 140 | 160 | - | 135 |
| E (Modulus) psi | high | 2.1E6 | 4.5E6 | 2.0E6 | 80.0E4 |
| | mid | 0.7E6 | 3.6E6 | 0.8E6 | 3.4E4 |
| | low | 0.5E6 | 2.8E6 | 0.5E6 | 0.7E4 |
| (Poisson Ratio) | high | 0.30 | 0.30 | - | 0.50 |
| | mid | 0.25 | 0.25 | 0.20 | 0.35 |
| | low | 0.20 | 0.20 | - | 0.20 |

5.1 Methods

5.1.1 Limit Equilibrium Solutions

This type of analysis is based on rigid block mechanics and is ideally suited for evaluating the stability of rock slopes and the dam foundation against potential sliding failure.

The method of analysis used for both the dam foundation and the rock slopes was a two-dimensional, general failure surface, non-vertical slice technique developed by Sarma (1979). In this method the geometry of the sliding mass is defined by the co-ordinates of the corners of a number of three- or four-sided elements, while the phreatic surface is defined by the co-ordinates of its intersections with the slice sides. A closed form solution is then used to calculate the critical horizontal acceleration K_c required to induce a state of limiting equilibrium in the slope. The static factor of safety of the slope is then found by reducing the values of $\tan \phi$ and c , the cohesion to $\tan \phi/F$ and c/F (where F is the factor of safety) until $K_c=0$.

In order to determine whether the analysis is acceptable, a final check is carried out to assess whether all the effective normal stresses acting across the bases and sides of the slices are positive. If negative stresses are found, the slice geometry must be varied until these negative stresses are eliminated.

The Sarma analysis allows different shear strengths (defined by cohesion and angle of friction) to be specified for each slice base and side. In the analyses carried out at Miner Flats the interslice boundaries were assigned zero shear strength. These conditions were chosen to coincide with the standard method of analysis used by the U.S. Army Corps of Engineers (CEM 1110-2-2200, Gravity Dam Design). Water pressures acting on the sides and base of each slice were included in

the analysis. External forces due to water pressure in tension cracks or behind the dam were also incorporated.

5.1.2 Numerical Modelling

To model more precisely the foundation behaviour and, in particular the response of the paleo-soil horizon, finite element modelling has been used. In recent years, this method has become an increasingly powerful technique used in investigations of soil and rock mechanics problems. Its importance lies in its ability to solve statically indeterminate problems, principally the redistribution of stress in rock or soil mass, arising from deformations that take place due to excavation, or application of load.

Though it is realized that behaviour of the dam and foundation rocks is a three dimensional problem it was considered that for preliminary design purposes the problem could be simplified to two dimensions based on the assumption of plane strain. The plane strain condition specifies that strain in the Z-direction, ϵ_z , is zero. It follows from this assumption that the shear stress components τ_{zy} and τ_{xy} are also zero. From Hooke's Law:

$$\epsilon_z = \frac{1}{E} \{ \sigma_z - \nu (\sigma_x + \sigma_y) \}$$

since $\epsilon_z = 0$

$$\sigma_z = \nu (\sigma_x + \sigma_y)$$

where E is the Young's Modulus and ν is the Poisson's Ratio.

The stress field, therefore, comprises the independent stress components σ_x , σ_y and τ_{xy} .

It is considered that the above assumption is valid for preliminary modelling the Miner Flats Dam and its underlying foundations. The z-axis of the model, equivalent to the length of the dam is greater than the x-axis or y-axis. The x-axis, equivalent to dam width, and the y-axis, equivalent to dam height, are approximately equal.

For the purposes of computation, the dam cross section is divided into a number of discrete elements. These elements are tied together at their corners and are constrained in deformation such that the joint between any two elements remains closed without contact stresses actually developing between them.

It can be shown that the force/displacement response of this mosaic of elements is identical to that of an elastic continuum provided that the elements are small relative to the stress gradient across them. It follows that the size of element is immaterial in a uniformly stressed region. Large elements are sufficient where the variation in stress and displacement are gradual, that is, in locations remote from the excavation boundaries. In regions where the stress gradients are steep, the elements should be sufficiently small for the stress or displacement differences across them to be negligible.

Each element is subjected at its nodes to forces and displacements that are related to each other by the stress-strain characteristics of the element. At any one node, the sum of the individual element forces is equal to the external forces applied to the node, as a result of which the nodal displacements may be expressed in terms of the external nodal forces.

Since the nodal displacements and the external nodal forces can each be divided into two independent components, two such expressions can be found for each node. A set of simultaneous equations equal to

double the number of nodes and containing the same number of unknown components of displacement can, therefore, be set up.

Three of these equations are dependent, which correspond to the three rigid body degrees of freedom. Consequently, three components of displacement at selected nodes are to be equated to zero and the number of equations reduced by three. A solution of the remaining set of equations will yield the unknown components of nodal displacement whence the corresponding forces and stresses can be calculated.

5.1.3 Analytical Solutions

This type of analysis is based on closed form standard analytical elastic solutions such as those developed by Boussinesq and presented by Poulos and Davis (1978). The analysis procedure was used as a first approximation of potential foundation problems and as a check of the results from the finite element analyses.

5.2 Limit Equilibrium Analysis

5.2.1 Dam Foundation Stability

As discussed previously, three possible slip surfaces have been identified in the dam foundation. These slip surfaces are shown on Figure 14 and are identified as follows:

- o slip surface 1 - along the dam/bedrock contact, from the heel to the toe of the dam;
- o slip surface 2 - along a vertical tension crack at the upstream heel of the dam through a zone of potentially fractured basalt (defined by measured low RQDs) beneath the dam;
- o slip surface 3 - through the paleo-soil layer which outcrops upstream of the dam, with breakout through intact basalt downstream of the dam toe.

Loading conditions for each slip surface are shown in Figure 14 and ranges for strength parameters used in the analyses of each slip surface are summarized in Table 11. Each analyses was carried out using a F.S.L. water elevation of 6082 feet, horizontal ice load of 5000 lbs per lineal foot and an effective horizontal silt load. Two different foundation drainage conditions were analyzed:

1. a uplift pressure varying linearly from F.S.L. at the heel of the dam to tailwater level at the toe of the dam, for the case where foundation drainage is inoperative.
2. an uplift pressure varying linearly from a value at the heel of the dam equal to 1/3 of the head difference (reservoir head minus tailwater head) to the tailwater value, for the case where a grout curtain and drainage system near the upstream heel of the dam is fully operative.

Each failure surface was also analyzed under a pseudo-static earthquake loading of 0.1 g horizontal and 0.05 g vertical. The hydrodynamic effect of the reservoir was modelled by increasing the water density. The earthquake loading analysis assumed that the foundation drainage and grouting measures were fully operative.

The results of the various analyses are given on Table 11. These results indicate that along the dam/foundation contact (slip surface 1), using estimated mid range values for strength (expected condition) along the contact of $c = 0$ psi and $\phi = 55^\circ$, the factor of safety against sliding failure is 2.20 for the condition with drains operable; 1.50 for the condition with drain inoperable; and, 1.65 under earthquake loading, assuming operable drains. The results also indicate that the factor of safety can be rapidly increased by increasing cohesion along the slip surface. This could be achieved by physically constructing a shear key or making due allowance for a cohesive bond between the dam and the foundation rocks.

TABLE 11

SARMA LIMIT EQUILIBRIUM STABILITY ANALYSIS OF
POTENTIAL SLIDING FAILURE IN DAM FOUNDATION

| ANALYSIS | STRENGTH PARAMETERS | | | | | | F.O.S. | | |
|------------------------|---------------------|---------------------------|----------------|---------------------------|-----------|---------|-------------|--|--|
| | Basalt | | Paleo-Soil | | Undrained | Drained | Earthquake* | | |
| | Cohesion (psi) | Friction ϕ (degrees) | Cohesion (psi) | Friction ϕ (degrees) | | | | | |
| Slip Surface 1 | 0 | 40 | - | - | 0.90 | 1.40 | 1.05 | | |
| Dam/Foundation Contact | 70 | 40 | - | - | 2.15 | 2.55 | 1.95 | | |
| | 0 | 55 | - | - | 1.50 | 2.20 | 1.65 | | |
| | 70 | 55 | - | - | 2.76 | 3.44 | 2.60 | | |
| | 0 | 65 | - | - | 2.30 | 3.30 | 2.50 | | |
| | 70 | 65 | - | - | 3.50 | 4.47 | 3.40 | | |
| Slip Surface 2 | | | | | | | | | |
| Low RQD Zone | 0 | 40 | - | - | 1.05 | 1.44 | 1.04 | | |
| | 140 | 40 | - | - | 3.57 | 3.97 | 2.99 | | |
| | 0 | 55 | - | - | 1.79 | 2.46 | 1.76 | | |
| | 140 | 55 | - | - | 4.32 | 4.98 | 3.72 | | |
| | 0 | 65 | - | - | 2.68 | 3.68 | 2.65 | | |
| | 140 | 65 | - | - | 5.19 | 6.21 | 4.62 | | |
| Slip Surface 3 | | | | | | | | | |
| Paleo-Soil | 0 | 40 | 0 | 35 | 1.03 | 1.19 | 0.89 | | |
| | 140 | 40 | 0 | 35 | 2.30 | 2.45 | 1.95 | | |
| | 0 | 55 | 0 | 35 | 1.34 | 1.46 | 1.18 | | |
| | 140 | 55 | 0 | 35 | 2.62 | 2.76 | 2.25 | | |
| | 0 | 55 | 0 | 40 | 1.45 | 1.61 | 1.26 | | |
| | 140 | 55 | 0 | 40 | 2.76 | 2.93 | 2.30 | | |

* Note: Combined With Drained Conditions

Analyses of slip through a potentially fractured zone below the dam (slip surface 2), using estimated lower bound strength values (expected worst case) of $c = 0$ and $\phi = 40^\circ$, indicate that the structure could be marginally stable under conditions where the drains became inoperative, or under earthquake loading. Using mid range strength values (expected condition) for the basalt of $\phi = 55^\circ$, $c = 140$ psi, the factor of safety against failure is 4.98 under the conditions where drainage is operative, 4.32 under condition of inoperative drains and approximately 3.72 under earthquake loading.

An analysis of a potential slip surface through the paleo-soil zone, with breakout through intact basalt (slip surface 3), was done using lower bound strength values (expected worst case) for the paleo-soil of zero cohesion and $\phi = 35^\circ$ and estimated average strength values (expected condition) for the basalt of $\phi = 55^\circ$, $c = 140$ psi. The calculated factors of safety range from approximately 2.76 for the condition with fully operative drains, to 2.62 for the condition with inoperative drains, down to 2.25 under earthquake loading condition. The introduction of some cohesion and an increase in the friction angle of the paleo-soil will increase factors of safety; however additional sampling and testing of the paleosoil will be required to justify increasing these strength parameters.

5.2.2 Stability of Excavated Slopes

The left and right abutments of the dam will be excavated prior to construction of the dam. The proposed excavation line will result in the development of faces as steep as 80° . The basalts in the existing valley wall stand near vertical along the right abutment but are much flatter on the left abutment.

A study of the kinematics of failure of the left and right abutment slopes was carried out with the aid of the stereoplot shown on Figure 8. Though it was found that the majority of joints mapped dipped at angles steeper than the proposed slope angles, a number of potential failure geometries were identified. These included planar, wedge and toppling modes. Due to the steep dips, however, and the expected size of joints, such failures are anticipated to be of limited size.

In order to examine a possible worst case condition it was assumed that potential slip surfaces might develop from the crest of the abutments along steeply dipping cooling joints, through intact basalt to daylight along the zone of flow boundary material, identified during the drilling investigation. The geometry of these surfaces are shown in Figure 15.

Each abutment was analyzed using a range of strength parameters. Two different ground water conditions were assumed, namely:

- o a fully drained condition with the piezometric surface at, or near, the elevation indicated during the field investigation.
- o a condition of moderate water pressure under an artificially high piezometric surface.

The results of the limit equilibrium analyses of the excavated slopes are similar for both the right and left abutments and are given in Table 12. These results indicate that with the use of mid range strength parameters (expected condition) along the potential slip surface (ϕ flow boundary = 40° , zero cohesion; ϕ cooling joint = 40° , zero cohesion, and ϕ intact basalt = 55° , cohesion = 140 psi) the factor of safety is approximately 2.0 under fully drained conditions. An increase in piezometric level reduces the factor of safety to 1.40.

TABLE 12

SARMA LIMIT EQUILIBRIUM STABILITY ANALYSIS OF
POTENTIAL SLIDING FAILURE IN ABUTMENT SLOPES

| Location | Friction Angle Flow Boundary (degrees) | Friction Angle (degrees) | | Cohesion Intact Basalt (psi) | Friction Angle Joints (degrees) | F.O.S. | |
|----------------|----------------------------------------|--------------------------|---------------|------------------------------|---------------------------------|---------|-----------|
| | | Intact Basalt | Intact Basalt | | | Drained | Undrained |
| Left Abutment | 40 | 40 | 40 | 0 | 40 | 1.02 | 0.75 |
| | 40 | 55 | 55 | 0 | 40 | 1.25 | 0.91 |
| | 40 | 55 | 55 | 140 | 40 | 2.01 | 1.65 |
| | 40 | 55 | 55 | 0 | 55 | 1.44 | 1.01 |
| | 40 | 55 | 55 | 140 | 55 | 2.41 | 1.85 |
| Right Abutment | 40 | 40 | 40 | 0 | 40 | 1.04 | 0.62 |
| | 40 | 55 | 55 | 0 | 40 | 1.29 | 0.75 |
| | 40 | 55 | 55 | 140 | 40 | 2.00 | 1.40 |
| | 40 | 55 | 55 | 0 | 55 | 1.48 | 0.83 |
| | 40 | 55 | 55 | 140 | 55 | 2.37 | 1.59 |

Minor slope stability problems such as individual block toppling or sliding may occur during slope excavation. The blocks of ground involved are expected to be small and are best stabilized during construction on an as need basis by measures such as rock bolting and meshing.

5.3 Finite Element Modelling

5.3.1 Description of Model

o Geometry and Mesh

The dam and foundation was modelled with the aid of a two dimensional finite element computer program (FES2D). This program used linear elastic plane strain quadrilateral and triangular elements. The finite element mesh consisted of 687 nodal points and 743 elements.

Boundary conditions, external loadings, and the general layout of the mesh are shown in the inset of Figure 16. A detailed mesh "window" showing the dam and the foundation in the immediate vicinity of the dam is included on the figure with node and element numbers. The table in the top right hand corner of Figure 16 identifies nodes and elements which are referenced in the discussion of results. The mesh was drawn to allow for the analysis of three different sets of geologic foundation conditions, corresponding with those shown in profiles AA-AA', BB-BB' and CC-CC' on Figures 7a, 7b and 7c, respectively.

Within this overall model a number of different cases were examined. Changes were made in applied loads, and paleo-soil properties. Table 13 summarizes the parameters investigated in the individual cases. With one exception, all analyses were carried out on what was considered to be the most critical foundation geometry, that is a

TABLE 13
SUMMARY OF FINITE ELEMENT ANALYSIS RUNS

| Case | Loads | | | | Young's Modulus Paleo-Soil (psi) | Remarks |
|------|---------|-------|------|-----|----------------------------------------|---------------------------------------------------------------------------------|
| | Gravity | Water | Silt | Ice | | |
| 1 | X | X | X | X | 3.6×10^6 | Full reservoir loads with paleo-soil Layer A at stiffness same as basalt. |
| 2 | X | X | X | X | 8.0×10^5 | Full reservoir loads with paleo-soil Layer A at upperbound stiffness. |
| 3 | X | X | X | X | 3.5×10^4 | Full reservoir loads with paleo-soil Layer A at mid range stiffness. |
| 4 | X | X | X | X | 7.0×10^3 | Full reservoir loads with paleo-soil Layer A at lower bound stiffness. |
| 5 | X | - | - | - | 3.5×10^4 | End of construction condition with paleo-soil Layer A at mid range stiffness. |
| 6 | X | - | - | - | 7.0×10^3 | End of construction condition with paleo-soil Layer A at lower bound stiffness. |
| 7 | X | X | X | X | 3.5×10^4 | Full reservoir loads with paleo-soil Layer B at mid range stiffness. |

shallow, thick paleo-soil profile as represented by Profile A, Figure 16.

A single analysis was done using Profile B, Figure 16, in which the paleo-soil was both thinner and deeper. This profile is considered to represent the typical geologic conditions beneath the dam.

o Loading and Boundary Conditions

The loading and boundary conditions applied to the dam and rock mass are illustrated in Figure 16. Water loads were applied to the ground surface, upstream of the dam and to the upstream face of the dam. The elevation heads for these loads were 6082 ft for cases 1, 2, 3, 4 and 7. For cases 5 and 6 no water loads were incorporated, representing conditions at end of construction. In addition to water loads, an ice loading of 5000 lbs/ft was applied at the 6082 ft elevation and an effective silt loading was applied vertically to the ground surface, and horizontally against the dam.

It was assumed that residual tectonic forces existed within the foundation rock, a result of the depositional and erosional history of the area. Tectonic forces were therefore applied to the model in a horizontal direction and were assumed to be equivalent to the overburden load. In terms of stress that is:

$$\sigma_H = \sigma_V = \rho \cdot g \cdot h$$

where σ_H is the horizontal stress, σ_V is the vertical stress, g is the acceleration applied to the rock mass due to gravity, ρ the density of the rock and h the depth below ground surface.

The depth h was measured from the dam base. No account was therefore taken of the horizontal toe stresses that exist due to the proximity of the steep valley walls. This assumption is considered to give conservative results

No uplift water pressures were modelled beneath the dam. All the finite element analyses considered total, and not effective stresses. The influence of pore water pressure was incorporated in a subsequent manual calculations and analysis of the stress results in Section 5.3.3.

Boundary conditions imposed in the model, see Figure 16, are summarized as follows:

- o no vertical movement along the horizontal boundary at the base of the model was permitted. The bottom corners of the model were rigidly fixed;
- o no horizontal movement along the vertical boundaries at the upstream and downstream sides of the model were permitted; and
- o nodes and elements within the rest of the model were permitted freedom to move in any direction under response to stress conditions.

The application of external loads on the foundation in each analysis (water, silt, ice, and the dam) occurred simultaneously and instantaneously. It is observed in the results that the dam material undergoes deformation due to self weight. These deformations would occur during construction as a matter of course but for purposes of simplifying the analysis this method was considered acceptable.

5.3.2 Deformation

Displacements along the base of the dam are largely dependent on the thickness, depth, and modulus of deformation selected for the paleo-soil layer. Plots showing the deformed shape of the dam as predicted by the modelling are provided in Figures 17a through 17g. These figures also give the calculated displacements for each of the cases analyzed. Table 14 provides a summary of displacement at the heel and toe of the dam. Shown on this table are total and differential settlements determined for the end of construction conditions, Layer A geometry; the full reservoir conditions using four different values of the deformation modulus in paleo-soil Layer A; and, for full reservoir conditions, Layer B.

The modelling results indicate that the construction of the dam over a soft paleo-soil layer of variable thickness (lower bound $E = 7 \times 10^3$ psi) could result in end of construction settlements at the base of the dam approaching one inch and end of construction differential settlements along the base of the dam approaching 1/2 inch. The effect of water, silt and ice loads (reservoir full condition) could cause an additional settlement at the heel of the dam of up to 3/4 inch and additional differential settlement along the base of the dam approaching 1/2 inch. The result is a net settlement of more than 2 inches and a differential settlement of more than 1 inch.

5.3.3 Stresses

The dam and reservoir system will impose stresses on the foundation rock and the paleo-soil layer. The distribution of stresses within the foundation will depend on the relative stiffness of the foundation materials and the magnitudes of the external loads imposed. The finite element analyses were carried out as total stress analyses and the

TABLE 14
SUMMARY OF CALCULATED VERTICAL DISPLACEMENTS
ALONG BASE OF DAM

| CASE | Modulus of Deformation of: | | | | |
|------------------------------------------------|----------------------------------------|----------------------------------------|----------------------------------------|----------------------------------------|----------------------------------------|
| | paleosoil A 3.0x10 ⁶ psi | paleosoil A 8 x 10 ⁵ psi | paleosoil A 3.5x10 ⁴ psi | paleosoil A 7 x 10 ³ psi | paleosoil B 3.5x10 ⁴ psi |
| | Inches | Inches | Inches | Inches | Inches |
| Settlement during construction at heel of dam. | 0.15 (est) | 0.19 (est) | 0.48 | 1.41 | 0.23 (est) |
| Settlement during construction at toe of dam. | 0.09 (est) | 0.09 (est) | 0.17 | 0.52 | 0.15 (est) |
| Differential settlement due to construction. | 0.06 | 0.10 | 0.31 | 0.89 | 0.07 |
| Settlement due to water loading heel of dam. | 0.16 | 0.19 | 0.57 | 0.70 | 0.20 |
| Settlement due to water loading toe of dam. | 0.10 | 0.09 | 0.14 | 0.29 | 0.13 |
| Differential settlement due to water loading. | 0.07 | 0.10 | 0.43 | 0.41 | 0.08 |
| Net settlement at heel of dam. | 0.31 | 0.38 | 1.05 | 2.12 | 0.43 |
| Net settlement at toe of dam. | 0.19 | 0.18 | 0.31 | 0.81 | 0.28 |
| Net differential settlement. | 0.13 | 0.20 | 0.74 | 1.31 | 0.15 |

magnitude and orientation of maximum total principal stresses for each of the cases analyzed are shown on Figures 18a to 18g. The total principal stresses for each of the reference elements are also shown on the figures.

The main reason for evaluating stresses distributions within the foundation was to assess the effects of the dam and reservoir loadings on the paleo-soil layer. A review of the stress tensors shown on Figures 18a through 18g indicate that the paleo-soil is well confined and that the magnitude of shear stresses developed within the paleo-soil are small.

The total stresses calculated in the finite element analysis have been used to determine factors of safety against failure of the paleo-soil. For the seven cases analyzed, the calculated factor of safety was 4 or greater for paleo-soil elements beneath the toe and heel of the dam.

Evaluation of effective stresses in the paleo-soil requires knowledge of the pore pressure distribution within the paleo-soil. Since data on anticipated pore pressure distributions after reservoir filling were not available, conservative estimates were made. It was assumed that at the end of construction the pore pressure in the paleo-soil Layer A would therefore be approximately 25 psi at element 495 beneath the heel of the dam, and that the pore pressure would drop to 20 psi at element 470 beneath the toe of the dam. Under reservoir full conditions it was estimated that the pore pressure in the paleo-soil layer would be approximately 60 psi at element 495 beneath the heel of the dam and that the pore pressure would drop to 45 psi at element 470 beneath the toe of the dam.

In Figure 19, Mohr circles, showing total and effective stresses for elements 495 and 470 beneath the heel and toe of the dam respectively, are plotted for both end of construction and reservoir full conditions. The circles lie well below the estimated strength envelope for the paleo-soil (see Section 4.4.2). Since it is anticipated that pore pressures in the paleo-soil will be lower than the values discussed above, the margin of safety against shear failure in the paleo-soil will be higher than shown on Figure 19.

5.4 Analytical Solutions

As a first approximation of possible stress distributions beneath the dam, a number of closed form analytical solutions were used. These assume that the foundation behaves as an isotropic homogenous mass.

The first case analyzed was at the end of construction condition with full dam weight on the foundation, but without reservoir loading (analogous to finite element cases 5 and 6). The dam was modelled as an infinite strip subjected to triangular loading. The resulting distribution of vertical stresses at the depth of the paleo-soil layer was very similar to that calculated by the finite element analyses.

The second case analyzed was also at the end of construction condition but this time the dam was modelled as a rectangular area subjected to triangular loading. At the center of the dam the elastic total vertical stress distribution was little changed from the case of the infinite strip. However, beneath the ends of the rectangle significantly lower total vertical stresses were calculated. At the depth of the paleo-soil layer total vertical stresses were approximately half those determined in the case of the infinite strip. End effects, which are not taken into account in the two-dimensional finite element analysis, are therefore significant.

The third case analyzed was intended to estimate the magnitude of stresses locked into the dam foundation as the result of downcutting of the river valley. The dam site was modelled as a homogeneous isotropic infinite mass subjected to a uniform geostatic load beneath a ground surface level coincident with the tops of the present valley walls. Downcutting of the valley and the resulting stress relief was modelled by removing a rectangularly loaded infinite strip from the valley floor. The results of the analysis indicate that for the steep walled, narrow valley modelled, stresses locked in beneath the edges of the valley floor are of similar magnitude to the anticipated stresses to be imposed by the proposed dam.

The results of these analytical solutions indicate that the assumptions made for the finite element analyses concerning geostatic stress level in the dam foundation and the assumed triangular loaded infinite strip configurations are conservative.

The three-dimensional effects of the river valley at the site will result in reduced stresses in the paleo-soil and consequently deformations of the paleo-soil and dam foundation will also be reduced.

6.0 DESIGN

6.1 Dam Stability

The various site investigation studies carried out at Miner Flats Dam have identified two zones in the foundation along which sliding or shear failure may be kinematically possible. These are:

- 1) a zone of low measured RQD within the basalt
- 2) the paleo-soil

In addition a third potential plane of weakness is represented by the contact between the foundation rocks and the dam itself.

6.1.1 Zone of Low RQD

A number of holes drilled on the right abutment and at the dam mid point encountered low values of RQD. When the results obtained were plotted on a geologic section (see Figure 5b) it was possible to correlate the occurrence of these low RQD values between holes. This correlation was only possible however between holes on the right abutment and those at mid point. No correlation could be extended to the left abutment.

Downstream only a single borehole was available for correlation. Unfortunately due to the natural fall in rockhead, extrapolation resulted in the low RQD zone daylighting above this hole.

Several explanations exist for the low RQD's these include:

- o poor drilling practice resulting in drilling induced fractures;
- o the low RQD values are a result of near vertical fractures and therefore should not be correlated laterally; and
- o the presence of a low angle fracture zone.

A conservative approach has been adopted. It was assumed that that the low RQD's were due to the presence of low angle fracture zone. In addition it was assumed that this fracture zone extended over the entire footprint area of the dam and that a vertical release surface was available upstream. The resulting geometry was then analyzed.

The results (presented in Section 5.2.1) indicated that only under the most severe assumptions, of lower bound values for strength and a non-functioning drain system or earthquake loading, did the calculated factor of safety approach unity. On the basis of a more detailed examination of drill core carried by MMI subsequent to the analysis it would appear that the low RQD's were a result of poor drilling practice (as evidenced by grinding of core) and the presence of near vertical fractures. It would therefore appear that the lateral correlation of the low RQD's may not be justified.

Based therefore, on the results of a 'worst case' analysis and the findings of detailed core logging it is concluded that sliding or shear failure through a low RQD zone in the basalt has a sufficiently high factor of safety.

6.1.2 Paleo-Soil

The paleo-soil extends from sub-crop immediately upstream of the dam heel, and under the entire dam footprint. It is extremely variable, both in its depth beneath foundation level, its thickness and its consistency. Towards the left abutment the paleo-soil is approximately 35 ft thick and is some 40 ft below foundation level; 80 ft below foundation level and approximately 10 ft thick at dam mid point; and 60 ft below foundation level and approximately 20 ft thick toward the right abutment.

The soil profile found toward the left abutment was used for analysis; again, adopting a 'worse case' approach. In order to make a slip surface through the paleo-soil kinematically feasible, a downstream 'break-out' surface through the basalts had to be assumed. From an examination of rock fabric (see Figure 8) no joint surfaces with the required orientation have been encountered. The assumed 'break-through' surface will therefore be stepped, partially along existing joints and

partially through intact rock. This results in a high shear strength zone which will resist any down dip movement in the paleo-soil.

The results of the limit equilibrium analyses (see Section 5.2.1) and the finite element modelling (see Section 5.3) indicate that, even under extreme loading conditions, the calculated factor of safety is approximately 2 or greater. It is believed that this represents an adequate factor of safety, particularly as it is a result of analyzing 'worse case' geometry.

6.1.3 Dam-Foundation Contact

The contact between the dam and the rock foundation represents a surface along which sliding or shear failure may occur. Factors of safety were calculated using a range of strengths for the dam-foundation interface and using different loading conditions. The results indicate that based on the estimated strength along this contact the calculated factor of safety is in excess of 1.4 under extreme loading conditions (i.e. drains inoperative or earthquake loading) and in excess of 2.2 under normal operating conditions. It should be noted that the strength estimates were based on the assumption that the dam base had a relatively smooth profile and that no cohesion was developed. If the profile was more stepped, thus allowing for a greater degree of interlocking, the calculated factors of safety would be substantially increased. Similarly, if cohesion was developed along the contact, as has been demonstrated in recent testing carried by the U.S. Corps of Engineers at Willowdale Dam, the calculated factors of safety would be substantially increased.

6.2 Dam Settlement

The prediction of settlement along the base of the dam has been carried out with the aid of results obtained from two dimensional finite element modelling. Two foundation geometries were modelled. The first geometry (based on the geologic section given in Figure 7c) considered a paleo-soil layer approximately 10 ft thick and located some 80 ft below foundation level and is believed to represent the average or typical foundation geology. The second geometry modelled was based on the geologic section given in Figure 7a. It comprised a paleo-soil layer approximately 40 ft thick and was located some 35 ft beneath foundation level. This second profile is considered to represent a 'worse case' foundation geometry. Based on the results of the modelling (see Table 17) the predicted differential settlement between the toe and heel of the dam ranged between approximately 0.13 inches and 1.3 inches. The magnitude of the predicted settlement is substantially a function of the value assumed for the deformation modulus of the paleo-soil.

As a base case it was assumed that the paleo-soil had a deformation modulus equivalent to that of the basalt. Under this assumption the net differential settlement predicted was 0.13 inches. This value was similar to the predicated settlement for the deep thin paleo-soil geometry. It can be implied from this similarity that over the majority of the dam base where the paleo-soil is relatively deep and thin that differential settlements will be largely controlled by the dam geometry and the properties of the overlying basalt and should therefore be relatively small. Towards the left abutment, where the paleo-soil layer is thick and shallow, the properties of the layer will be the major influence on settlement. Under assumed 'worse case' conditions, that the paleo-soil is very soft, the predicted differential settlement between the heel and toe of the dam is approximately 1.3 inches. Under, however, the

assumed expected condition, the predicted differential settlements are approximately 0.75 inches.

To assist in planning construction procedures and to delineate areas that may require more investigation during detailed engineering, the area beneath the dam has been zoned, Figure 20. Each zone represents a particular settlement pattern and, as such, offers an approximate guide to the distribution of differential settlements across the dam base. Zone boundaries are based on the estimated depth to the paleo-soil from foundation level; while, settlement patterns within the zones are based on the results of the 2-D numerical modelling.

Settlements within Zones 1 and 2 (see Figure 20), where the paleo-soil is at depth, will be largely controlled by the properties of the basalt founding rocks. By contrast, settlement in Zone 4, where the paleo-soil is shallow, will be strongly influenced by the properties of the paleo-soil itself. Zone 3 represents a transition between Zone 2 and Zone 4.

Zone 1 coincides with the left and right abutments where the paleo-soil is generally in excess of 100 ft. below the dam/rock contact. Differential settlements are expected to be small (~ 0.1 inch).

Within Zone 2, the modelling results indicate that total settlements of up to 0.45 inch may occur along the dam heel, while up to 0.30 inch may occur along the dam toe; thus indicating a differential settlements of up to 0.15 inch between the heel and toe. Though, as yet, no modelling has been carried out parallel to the dam axis, little lateral differential settlement is expected within Zone 2 or between Zone 1 and Zone 2.

Calculated total settlements in Zone 4, (using expected values for paleo-soil properties) were 1.05 inch along the dam heel and 0.30 inch along the dam toe; resulting in a possible differential settlement between heel and toe of 0.75 inch. Zone 4 is located immediately adjacent to the left abutment. As settlement within Zone 4 takes place, it is believed that some stress transfer will take place from the "softer" Zone 4 foundation to the "stiffer" abutment foundation. Such a stress transfer will result in reduced total settlements and hence a decrease in differential settlement. However, as a result of the juxtaposition of "softer" and "stiffer" zones lateral differential settlements is expected to occur. Using the results of the numerical modelling (which because of 2-D nature are believed to represent a "worst" case) lateral differential settlements of up to 0.6 inch may occur between Zone 2 and Zone 4.

To enable more accurate predictions of differential settlements between the heels and toe of the dam and laterally more information is required on the geometry and properties of the paleo-soil underlying Zone 4. This should be addressed during the final detailed engineering studies.

It is believed that the very nature of the two-dimensional modeling has resulted in conservative predictions of values for settlement. This conservativeness is a result of the following:

- o stress transfer along the contact between the dam and its abutments. This will reduce the load on the dam foundation;
- o the effect of horizontal stress concentration (notch effect) at the base of the valley. This results in an additional clamping force across the dam foundation; and
- o the assumption that the dam and the foundation rock are intimately connected (i.e. the assumption that the dam and foundation are a continuum).

These three factors would all tend to reduce the amount of settlement and hence the differential settlements that will occur over the dam base.

6.3 Slope Stability

The rocks that will be exposed during the excavation of left and right abutment slopes exhibit brittle rock characteristics. The stability in these rocks will therefore be controlled, by and large, by the orientation, spacing and size of discontinuities that exist within the rock mass.

The stability analyses has indicated that the calculated factors of safety against overall slope failure is adequate. However minor stability problems comprising sliding or toppling of small blocks are expected to occur on both abutment slopes. Due to the height of the slopes dislodgement of such blocks present a substantial hazard to men and equipment working below. Remedial measures must, therefore, be considered. These may include rock or cable bolting, mesh or the provision of catch benches. The use of smooth wall blasting techniques such as pre-split or cushion blasting will greatly assist in the control of local stability problems.

It is believed that the design of appropriate remedial measures is best accomplished during construction when the exposed rock mass can be fully inspected.

7.0 CONCLUSIONS AND RECOMMENATIONS

7.1 Conclusions

Aspects of foundation and abutment stability of the proposed Miner Flats Dam have been investigated with the aid of limit equilibrium

analyses and numerical modelling. Prior, however, to conducting these analyses appropriate input parameters had to be selected based on the results of the various site investigations and of laboratory testing.

The paleo-soil unit presented a particular problem. Due to sampling and testing difficulties little direct information was available for this unit. Published data had to be relied upon. Uncertainties associated with this approach therefore required that sensitivity analyses be conducted in order that the range of probable values for the input be investigated. Based on the results of these analyses the following conclusions were reached;

- A) Sliding or Shear Failure
 - o Along Dam-Foundation Contact: Using mid range values for strength (the expected case) and normal loading conditions, the calculated factor of safety was 2.20; under assumed 'worst' case loading conditions the calculated factor of safety was 1.50. It is believed that these calculated factors of safety could be greatly increased by ensuring that a cohesive bond between the dam and the foundation rocks is developed, or, by providing a more irregular foundation profile, thus allowing substantial interlocking between the dam and the foundation rocks.
 - o Along Low RQD Zone: Based upon the results of a 'worst' case analysis and the findings of detailed core logging it is believed that a sufficient strength can be mobilized through the low RQD to essentially preclude a slip type of failure.
 - o Along/Through Paleo-soil: Based upon 'worst' case analyses, in terms of both assumed strength values and possible failure

geometries, it is believed that sufficient strength can be mobilized through the paleo-soil and the basalt to essentially preclude a slip type of failure. Inherent in this conclusion, however, is the assumption that the potential slip surface passes through the basalt mass and not along an existing plane of weakness.

B) Abutment Slopes

Planar, wedge, and toppling style failures are kinematically possible in both abutment slopes. Due to the attitude and size of joint surfaces, individual failures are expected to be of limited extent. Remedial measures will be necessary to ensure the safety of men and equipment working below these slopes.

c) Deformation of Dam Foundation

The results of the finite element modelling indicate the following foundation behaviour:

- o The deformation of the dam foundation is sensitive to the depth, thickness and deformation modulus of the paleo-soil layer.
- o The weight of the dam at end of construction causes settlement at the upstream heel of the dam, and rotation in the upstream direction.
- o The weight of water within the reservoir depresses the base of the reservoir but the water pressure also causes rotation of the dam in the downstream direction.
- o The paleo-soil is confined and is not subject to the development of excessive stress at either the end of the construction condition or their reservoir full condition.

- o Predicted differential settlements along the dam base ranged from approximately 0.1 inch to 1.3 inches, depending on loading conditions and the assumed value for the deformation modulus for the paleo-soil. It is believed that these predictions are conservative due to the inherent limitations of the two-dimensional model used.
- o Settlements are a function of dam geometry and paleo-soil thickness, depth and modulus. From available data these would appear to change gradually and therefore no sudden change in settlement is expected.

7.2 Recommendations

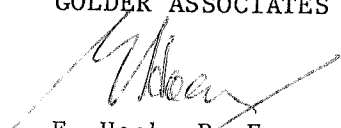
In deriving the above conclusions a number of assumptions were made, particularly with regard to paleo-soil properties and to foundation and abutment geology. The following recommendations therefore follow:

- o little geologic information is available in the vicinity of the dam toe. Before construction at least three exploratory drill holes should be put down in this area to confirm or otherwise the predicted geology;
- o the assumed deformation modulus for the paleo-soil is based on published data. An attempt should be made to more fully characterize this material in order to obtain better estimates of its properties;
- o Smooth wall blasting methods should be used to excavate the abutment slopes in order to minimize vibration damage. As localized wedge and block failures are anticipated some form of remedial measure should be implemented; and

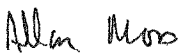
- o As more detailed information becomes available the present geomechanical model should be up-dated and review analysis conducted.


Yours very truly,

GOLDER ASSOCIATES



E. Hoek, P. Eng.


A. Moss


A. Rice, P. Eng.

EH/AM/AR/gg
862-1622

8.0 REFERENCES

Bieniawski, Z.T. Determining rock mass deformability: experience from case histories. Intl. J. Rock Mechanics and Mining Sciences, Vol. 15, 1978, pages 237-247.

Bieniawski, Z.T. Geomechanics classification of rock masses and its application in tunnelling. Proc. Third International Congress on Rock Mechanics, ISRM, Denver, Volume 11A, 1974, pages 27-32.

Bieniawski, Z.T. Rock mass classification in rock engineering, Proc. Symposium on Exploration for Rock Engineering, Johannesburg, Volume 1, 1976, pages 97-106.

Serafim, J.L. and Pereira, J.P. Consideration of the Geomechanics Classification of Bieniawski. Proc. Intl. Symp. on Engng. Geol. and Underground Construction. Lisbon, Portugal, 1983, pages 1133-44.

Hoek, E. and Brown, E.T. 1980, Underground Excavations in Rock, Institute of Mining and Metallurgy, London.

Hoek, E. Strength of Jointed Rock Masses. Geotechnique 33, No. 3, 1983, pages 187-223.

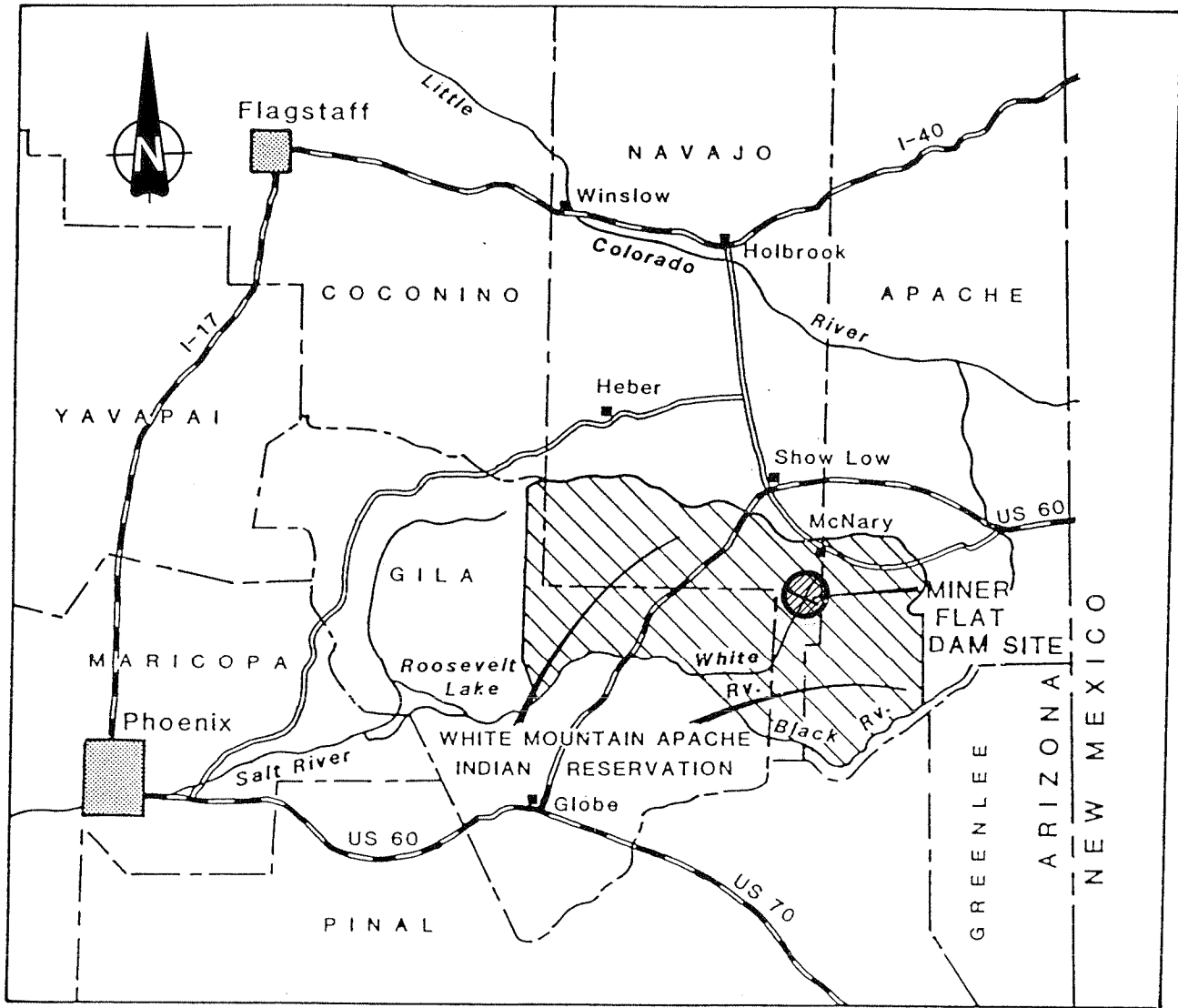
Charles, J.A. and Watt, K.S. The Influence of Confining Pressure on Shear Strength of Compacted Rockfill. Geotechnique 30, No. 4, 1980, pages 353-367.

Barton, N. and Kjaernsli, B. 1981 "Shear Strength of Rockfill". Journal of the Geotechnical Engineering Division, Proceedings, American Society of Civil Engineers, Vol. 107, G77, July 1981, pages 873-891.

Sarma, S.K. Stability Analysis of Embankments and Slopes. J. Geotechnical Engineering Division, Proceedings, American Society of Civil Engineers Vol. 105, G712, 1979, pages 1511-1524.

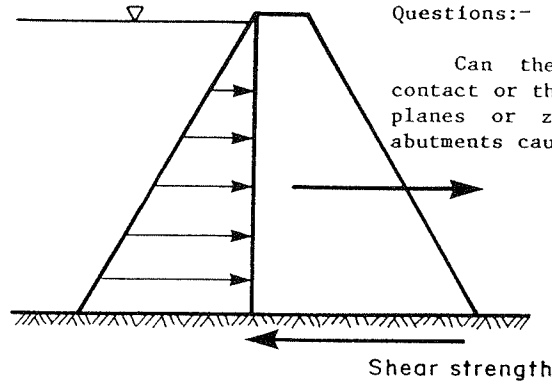
SITE LOCATION PLAN

Figure 1



PROJECT NO. 862-1622 DRAWN
REVIEWED DATE JAN. 1987

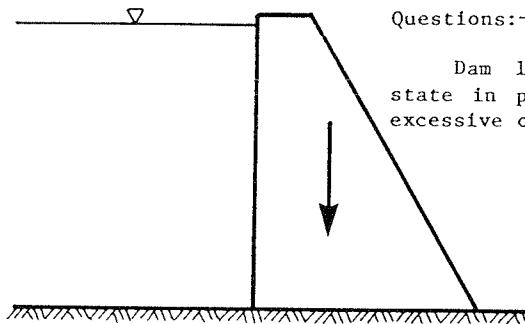
a) Stability



Questions:-

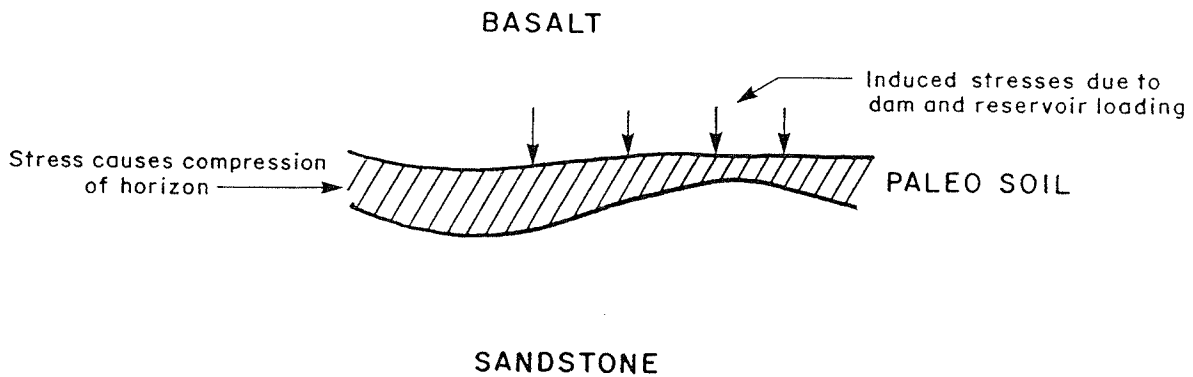
Can the strength along the dam/rock contact or the presence of adversely oriented planes or zones within the foundation or abutments cause instability?

b) Settlement



Questions:-

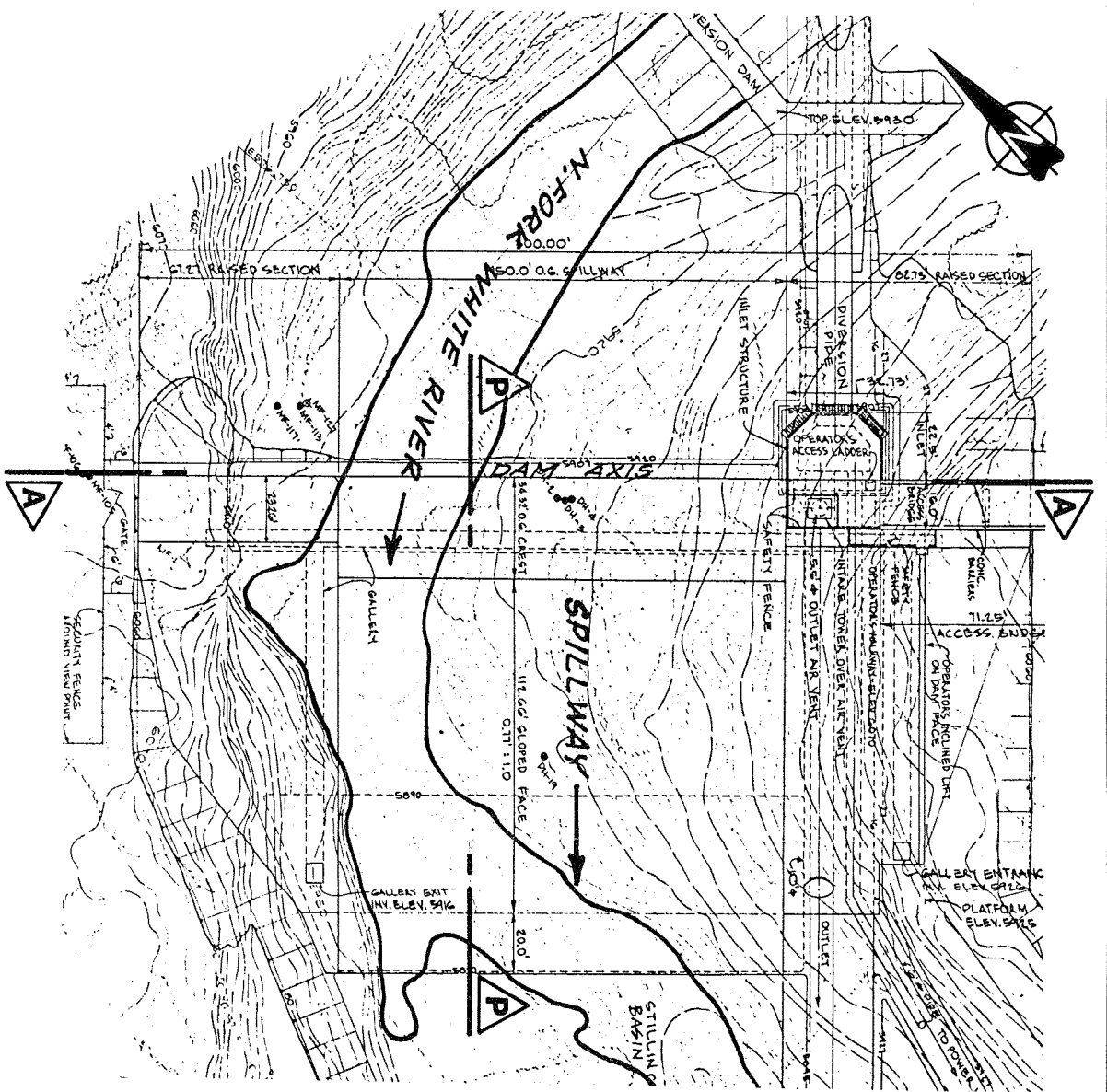
Dam load results in change of stress state in paleosoil. Can this give rise to excessive or differential settlement?



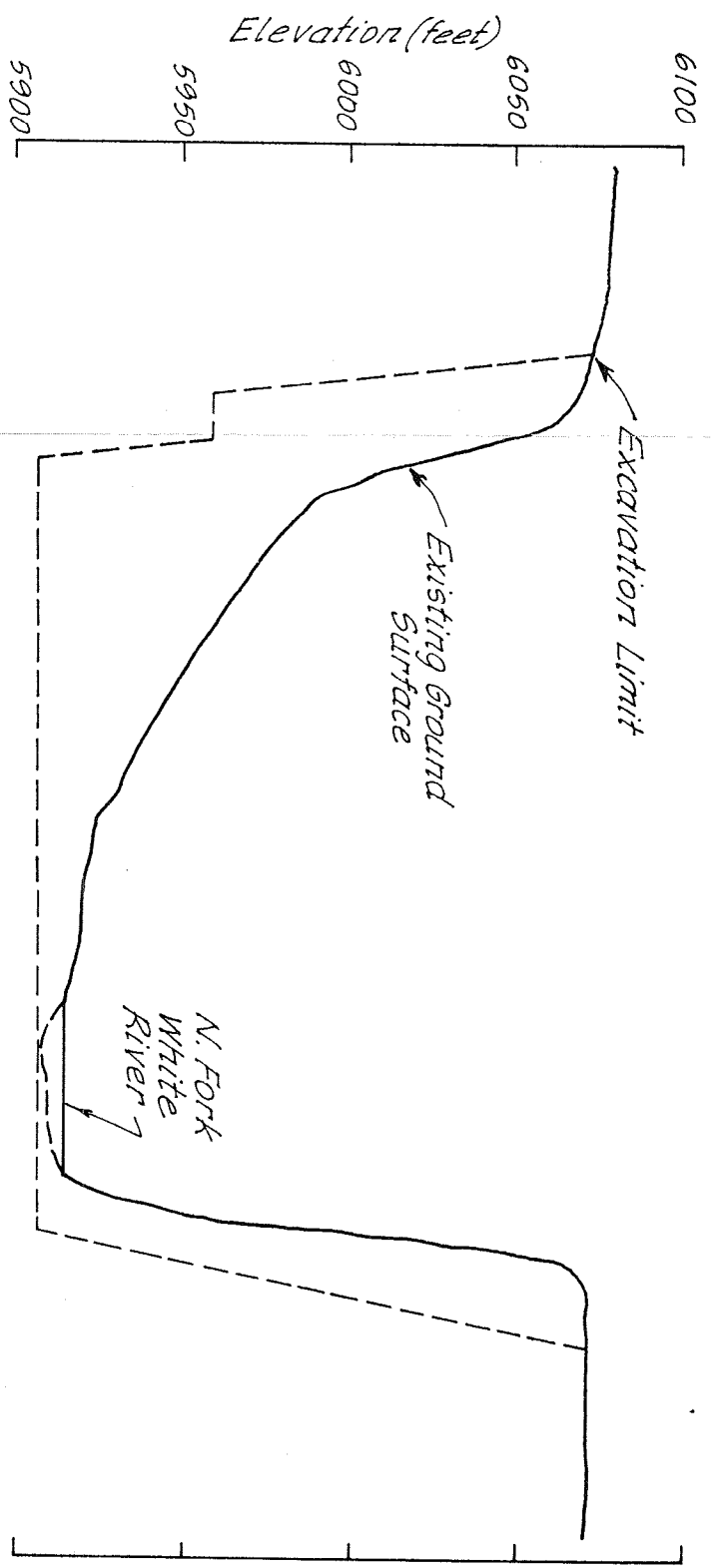
PROJECT NO. 862-1622
DRAWN
REVIEWED
DATE Jan. 187

PROPOSED DAM LAYOUT

Figure 3

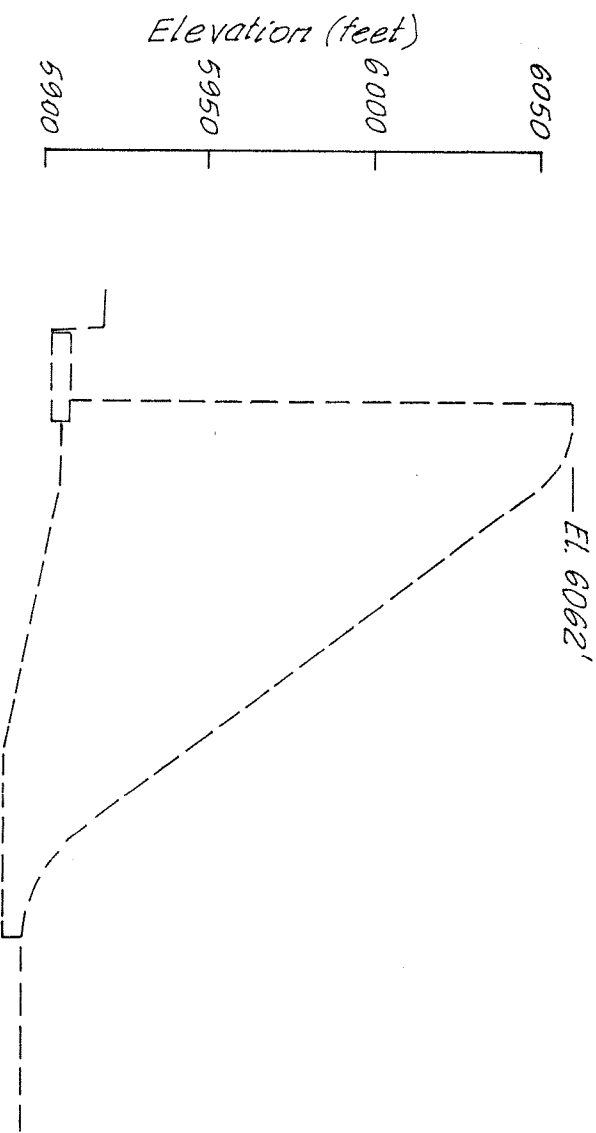


PLAN



SECTION A - A'

Note: Geometric layout of proposed dam provided by Morrison-Maierle Inc. or drawings referenced in the text.



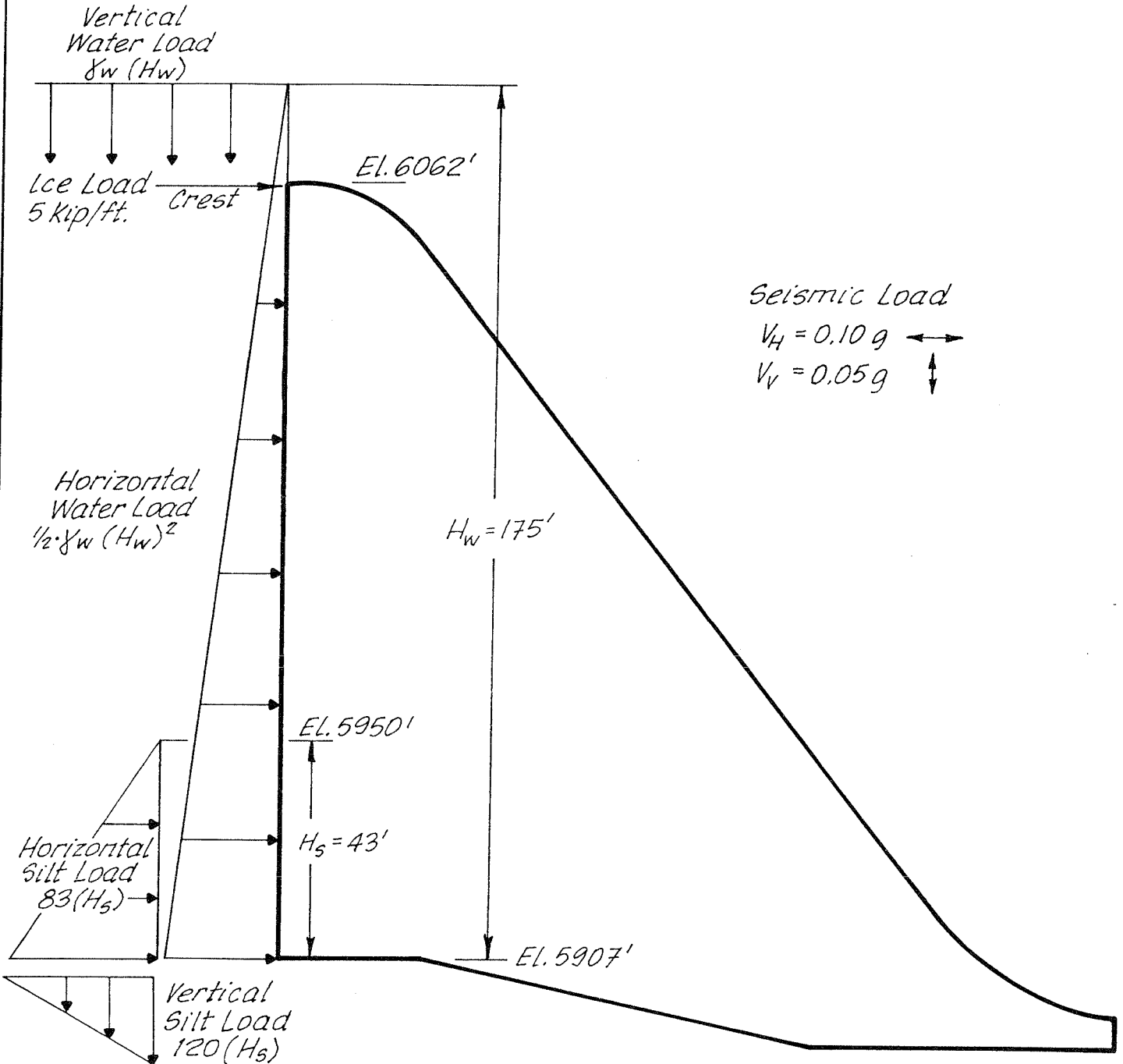
DAM PROFILE P - P'

Goldier Associates

Scale: 1/4 inch to 60 feet.

BOUNDARY LOADING CONDITIONS

Figure **4**



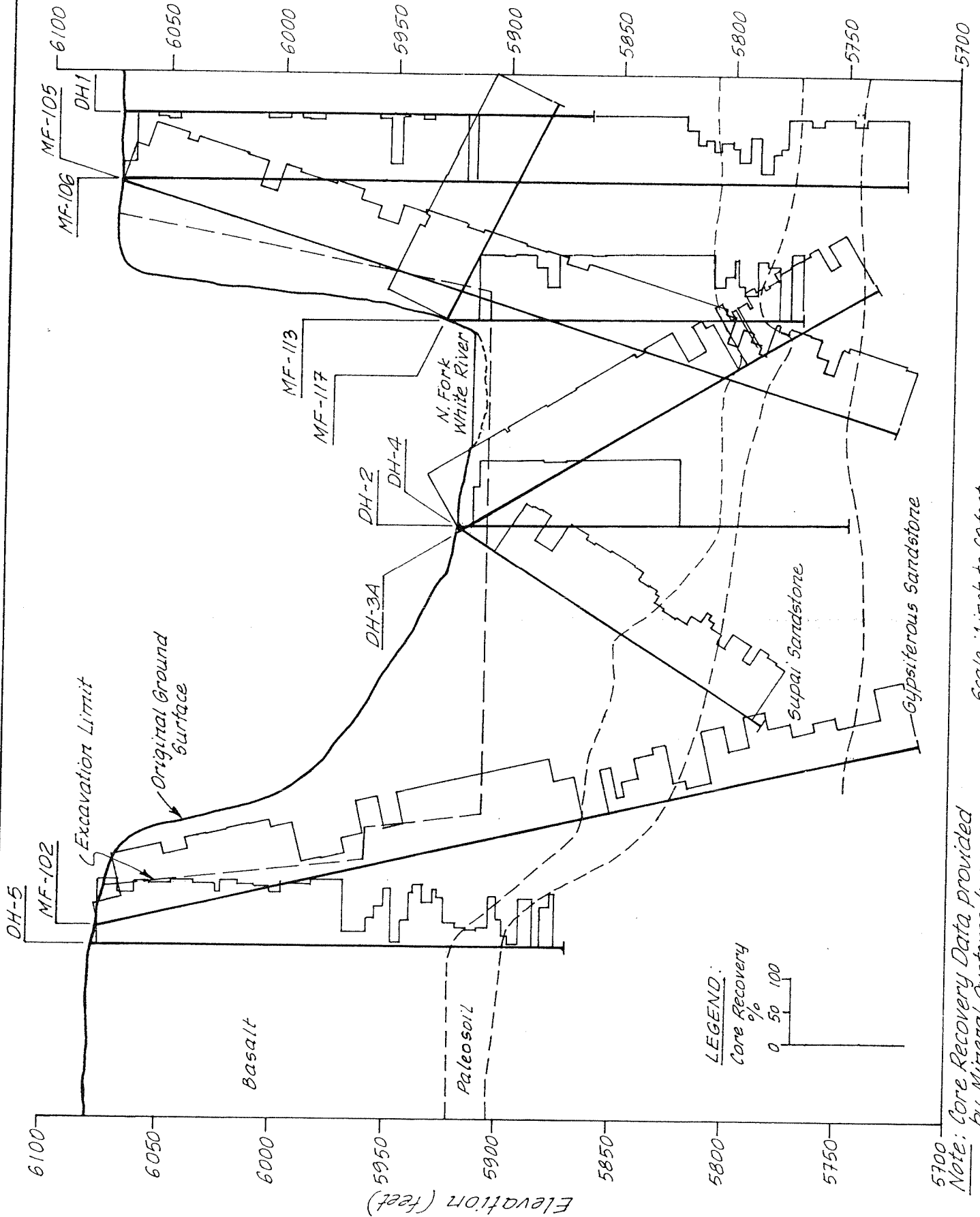
Note: Boundary loading conditions provided by Morrison & Maierle Inc.

Scale: 1 inch to 30 feet

PROJECT NO. 862-1622
 DRAWN BY
 REVIEWED
 DATE var. '87

GEOLOGIC SECTION WITH HISTOGRAMS OF CORE RECOVERY

Figure **5a**

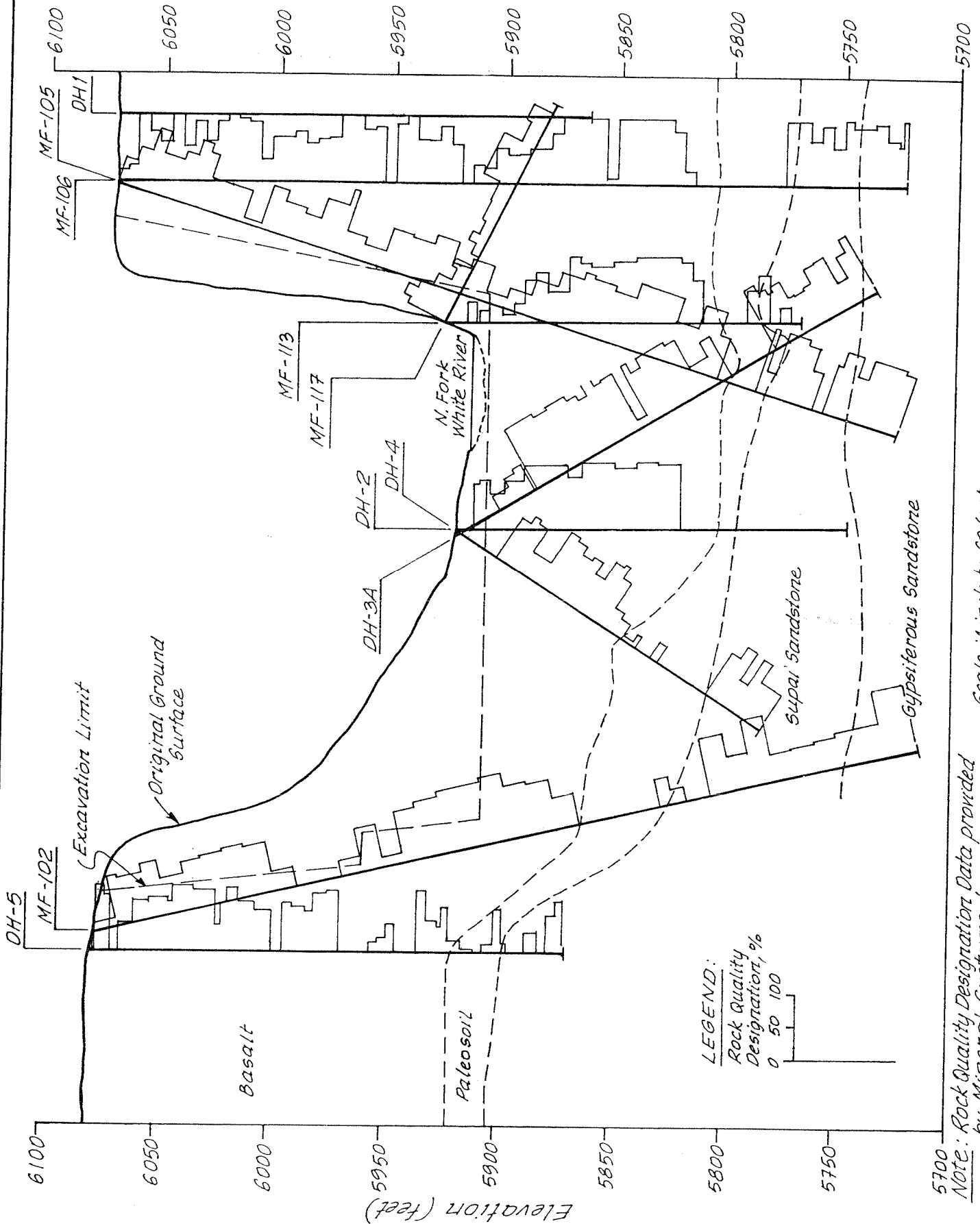


Scale: 1 inch to 60 feet.

PROJECT NO. 862-1622 DRAWN BY [Signature] REVIEWED DATE Jan. 1987

GEOLOGIC SECTION WITH HISTOGRAMS OF ROCK QUALITY DESIGNATION (RQD)

Figure **5b**



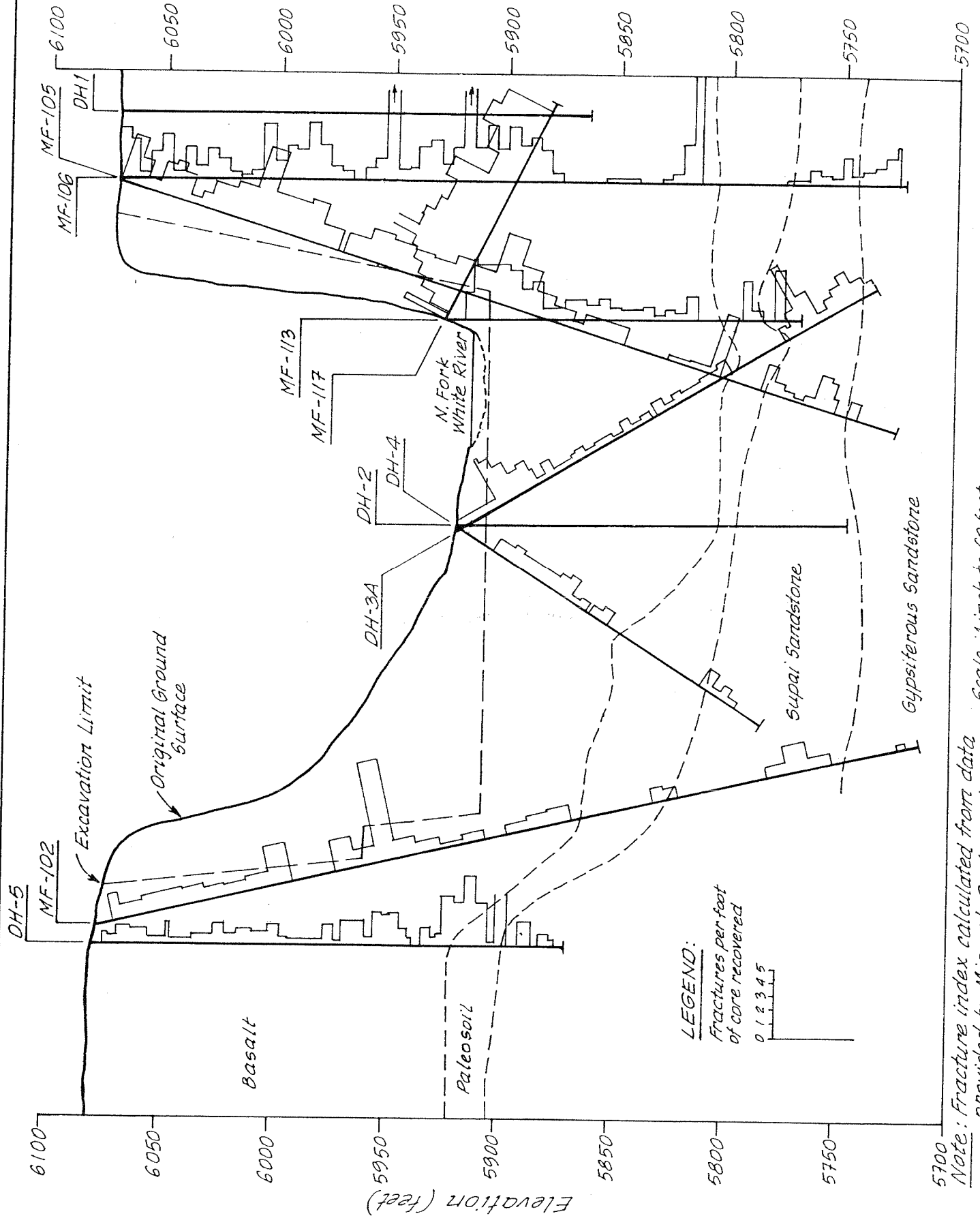
PROJECT NO. 862-1622 DRAWN & REVIEWED DATE Jan. 187

Note: Rock Quality Designation Data provided by Mineral Systems Inc.

Scale: 1 inch to 60 feet.

GEOLOGIC SECTION WITH HISTOGRAMS OF FRACTURE INDEX

Figure **5c**

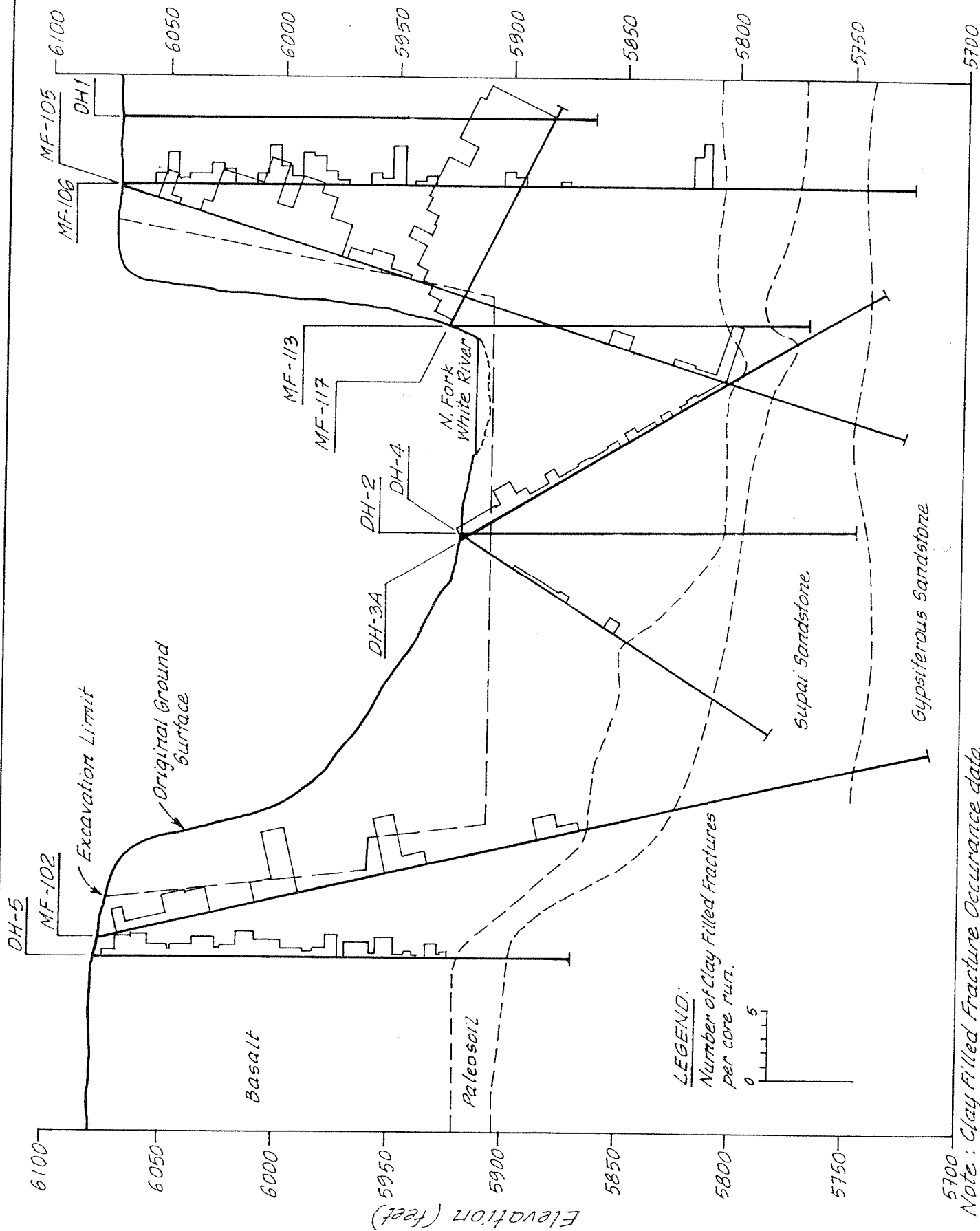


PROJECT NO. 861-1622 DRAWN S. REVIEWED DATE Jan. 1987

Note: Fracture index calculated from data provided by Mineral Systems Inc. Scale: 1 inch to 60 feet.

GEOLOGIC SECTION WITH HISTOGRAMS OF CLAY FILLED FRACTURE OCCURANCE

Figure **5d**



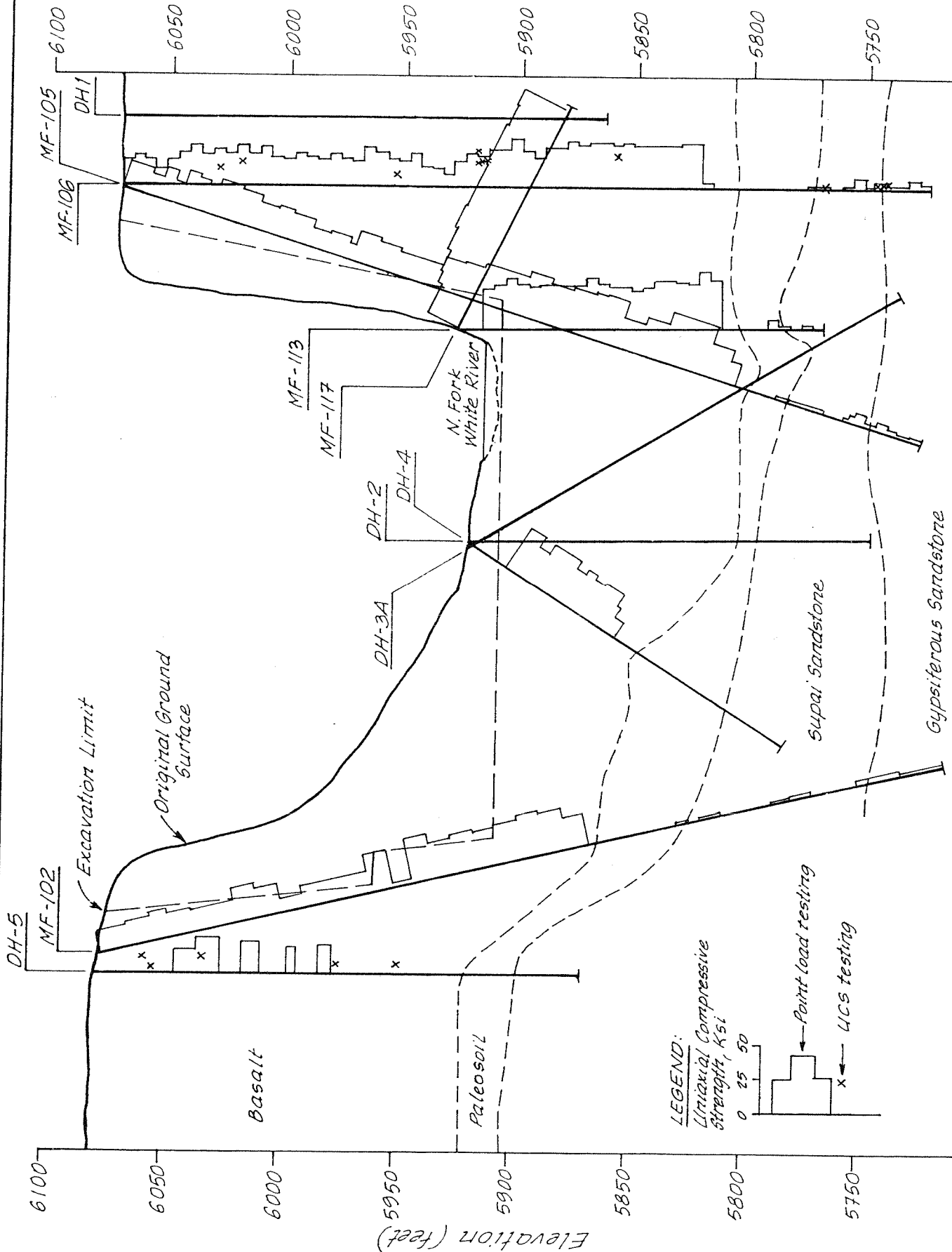
Note: Clay Filled Fracture Occurrence data provided by Mineral Systems Inc.

Scale: 1 inch to 60 feet

PROJECT NO. 862-1622 DRAWN S. REVIEWED DATE Jan. 187

GEOLOGIC SECTION WITH HISTOGRAMS OF UNIAXIAL COMPRESSIVE STRENGTH

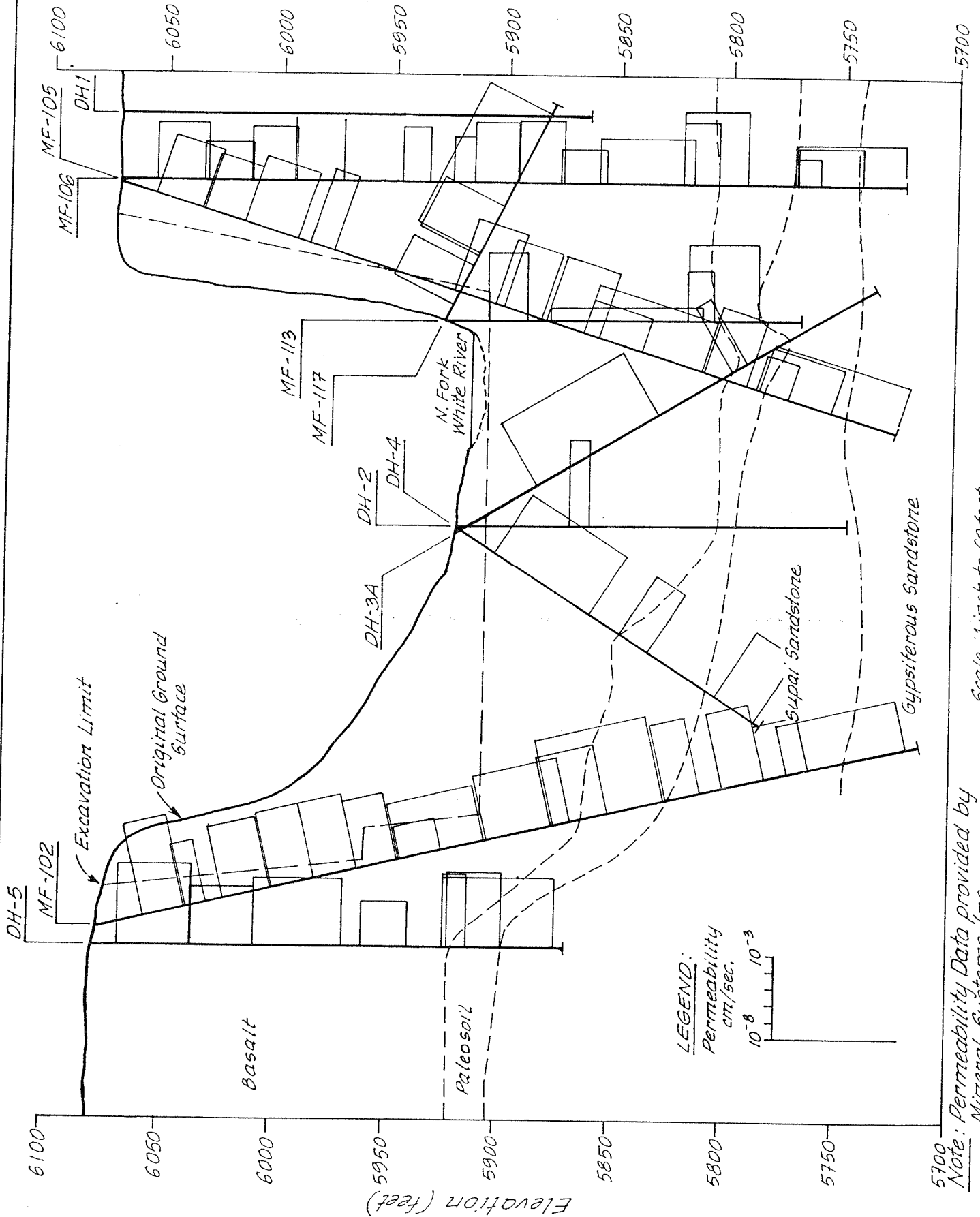
Figure **5e**



PROJECT NO. 862-1622 DRAWN BY DATE Jan. 1987 REVIEWED

GEOLOGIC SECTION WITH HISTOGRAMS OF PERMEABILITY

Figure **5f**

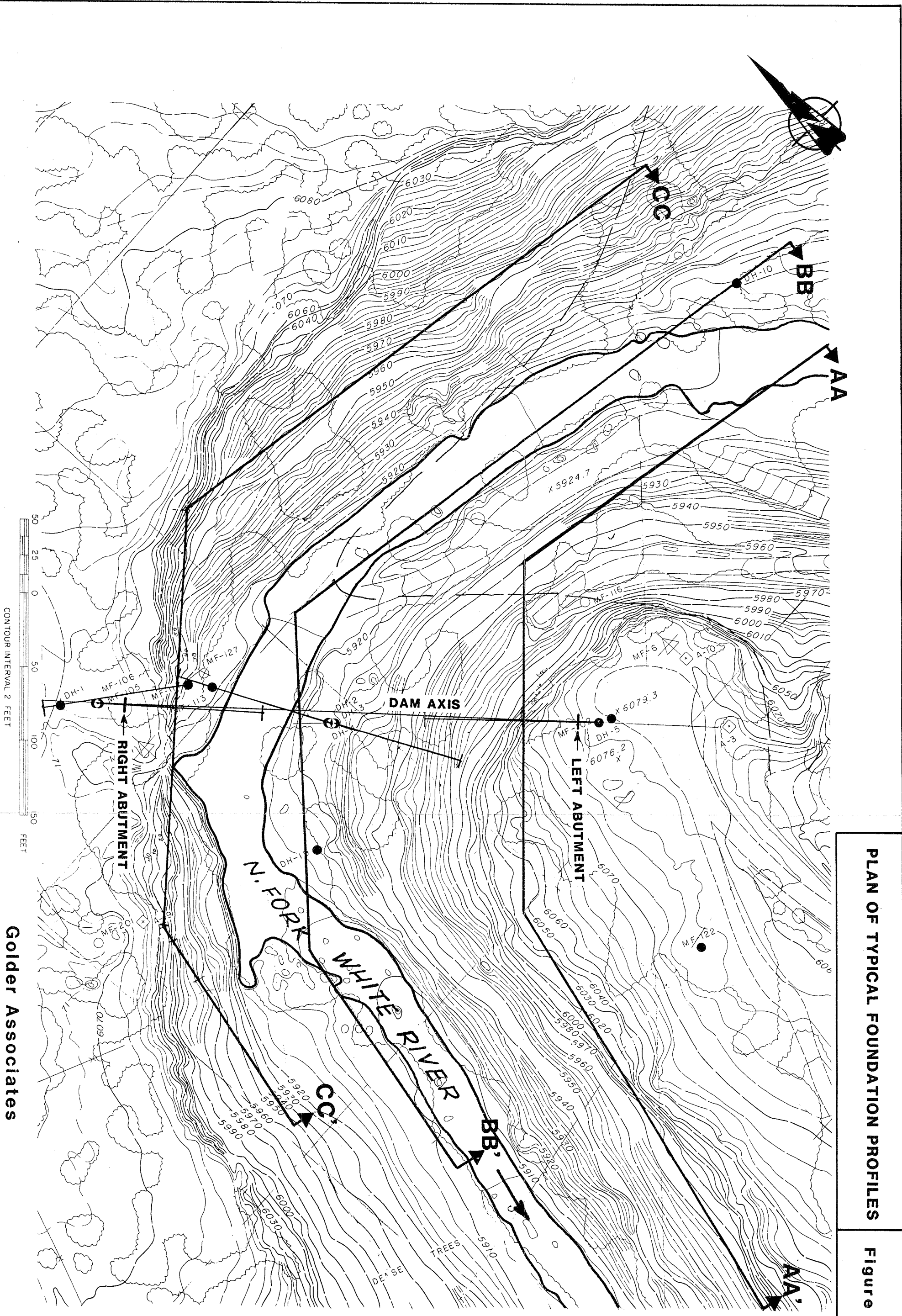


Scale: 1 inch to 60 feet.

Note: Permeability Data provided by
Miteral Systems Inc.

PLAN OF TYPICAL FOUNDATION PROFILES

Figure 6



Golden Associates

Elevation (feet)
6100
6050
6000
5950
5900
5850
5800
5750
5700



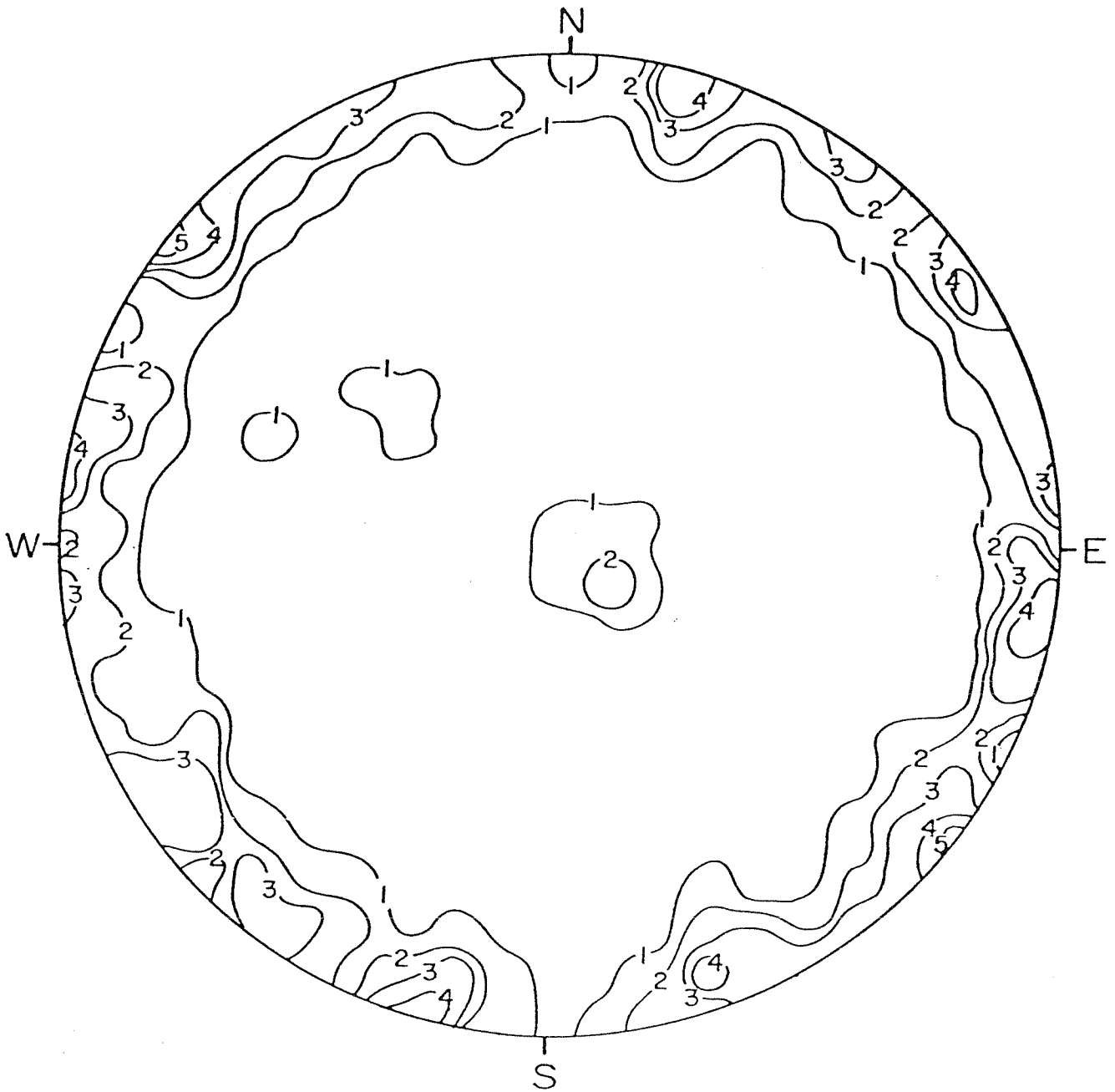
Note : Typical foundation profile prepared by Mineral Systems Incorporated.

Scale : 1 inch to 60 feet

Golder Associates

**EQUAL AREA (LOWER HEMISPHERE)
PLOT OF DISCONTINUITIES (JOINTS) IN BASALT**

Figure **8**

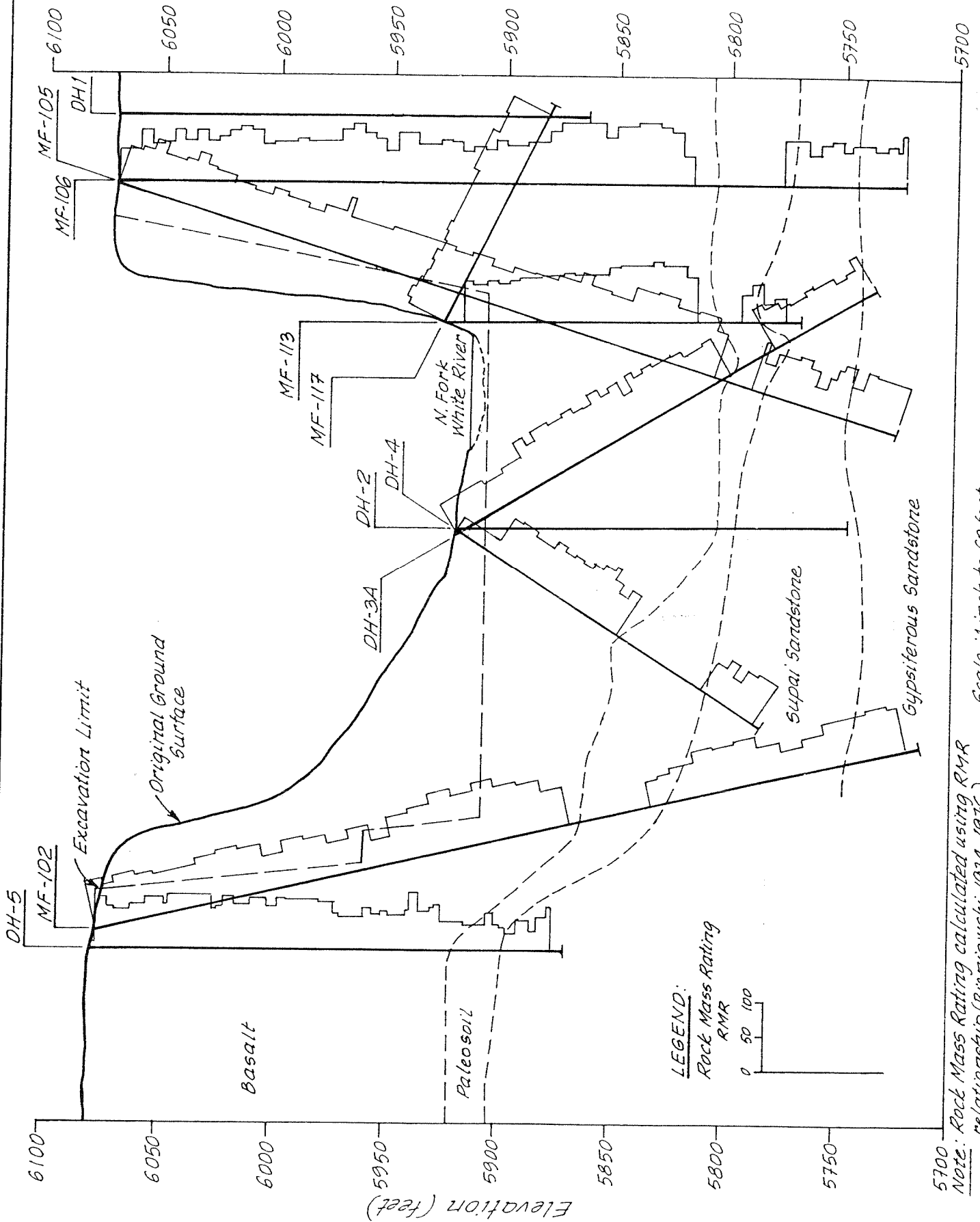


222 poles, Contour Interval 1 percent

Note: Discontinuity data obtained from detailed line surveys in the vicinity of the dam site by Mineral Systems Inc. (1983).

GEOLOGIC SECTION WITH HISTOGRAMS OF ROCK MASS RATING (RMR)

Figure 9

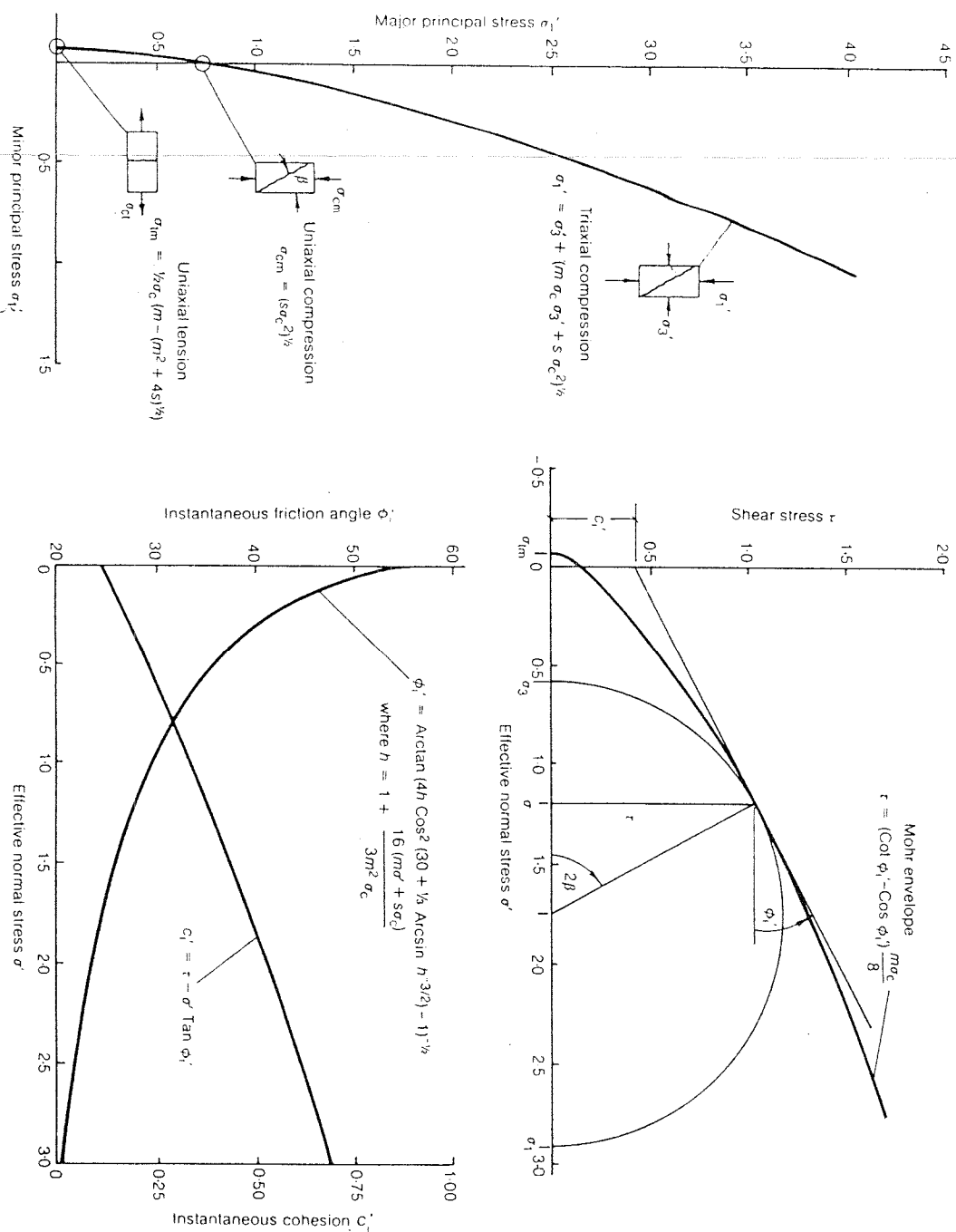


PROJECT NO. 862-1622 DRAWN & REVIEWED DATE 4/27/87

Note: Rock Mass Rating calculated using RMR relationship (Bieriaowski, 1974, 1976).

Scale: 1 inch to 60 feet.

| APPROXIMATE RELATIONSHIP BETWEEN ROCK MASS QUALITY AND MATERIAL CONSTANTS | | Disturbed rock mass m & s values | | Undisturbed rock mass m & s values | |
|---------------------------------------------------------------------------------------------------------------------------------------------------------------------------------------------------------------------------------------------------------------------------------------------------------------------------------------------------------------------|------------------------------------------------------------------------|-----------------------------------------------------------------------------------------------|--------------------------------------------------------|---------------------------------------------------------------------------------------------------------------|---------------------------------------------------------------------------------------------------------------------------------------------------|
| <p><i>Empirical failure criterion</i></p> $\sigma_1 = \sigma_3 + (m\sigma_c\sigma_3 + s\sigma_c^2)^{1/2}$ <p> σ_1 = major principal stress σ_3 = minor principal stress σ_c = uniaxial compressive strength of intact rock, and m, s are empirical constants </p> | INTACT ROCK SAMPLES | LABORATORY SIZE SPECIMENS FREE FROM DISCONTINUITIES | CSIR rating RMR = 100 NGI rating Q = 500 | CSIR rating RMR = 85 NGI rating Q = 100 | VERY GOOD QUALITY ROCK MASS |
| | VERY GOOD QUALITY ROCK MASS | Tightly interlocking undisturbed rock with unweathered joints at 1 to 3m. | m = 2.40 s = 0.082 m = 4.10 s = 0.189 | m = 0.821 s = 0.00293 m = 2.865 s = 0.0205 | GOOD QUALITY ROCK MASS |
| | GOOD QUALITY ROCK MASS | Fresh to slightly weathered rock, slightly disturbed with joints at 1 to 3 m. | m = 0.575 s = 0.00293 m = 2.006 s = 0.0205 | m = 0.128 s = 0.00009 m = 0.947 s = 0.00198 | FAIR QUALITY ROCK MASS |
| | FAIR QUALITY ROCK MASS | Several sets of moderately weathered joints spaced at 0.3 to 1 m. | m = 0.128 s = 0.00009 m = 0.947 s = 0.00198 | m = 0.029 s = 0.000003 m = 0.447 s = 0.00019 | POOR QUALITY ROCK MASS |
| | POOR QUALITY ROCK MASS | Numerous weathered joints at 30 to 500mm with some gouge. Clean compacted waste rock. | m = 0.029 s = 0.000003 m = 0.447 s = 0.00019 | m = 0.007 s = 0.0000001 m = 0.219 s = 0.00002 | VERY POOR QUALITY ROCK MASS |
| | VERY POOR QUALITY ROCK MASS | Numerous heavily weathered joints spaced at less than 50mm with gouge. Waste rock with fines. | m = 0.007 s = 0.0000001 m = 0.219 s = 0.00002 | ARENACEOUS ROCKS WITH STRONG CRYSTALS AND POORLY DEVELOPED CRYSTAL CLEAVAGE <i>sandstone and quartzite</i> | LITHIFIED ARGILLACEOUS ROCKS <i>mudstone, siltstone, shale and slate (normal to cleavage)</i> |
| ARENACEOUS ROCKS WITH STRONG CRYSTALS AND POORLY DEVELOPED CRYSTAL CLEAVAGE | <i>sandstone and quartzite</i> | m = 15.00 s = 1.00 m = 15.00 s = 1.00 | m = 0.183 s = 0.00009 m = 1.353 s = 0.00198 | FINE GRAINED POLYMINERALLIC IGNEOUS CRYSTALLINE ROCKS <i>andesite, dolerite, diabase and rhyolite</i> | COARSE GRAINED POLYMINERALLIC IGNEOUS AND METAMORPHIC CRYSTALLINE ROCKS <i>amphibolite, gabbro, gneiss, granite, norite and quartz-diorite</i> |
| FINE GRAINED POLYMINERALLIC IGNEOUS CRYSTALLINE ROCKS | <i>andesite, dolerite, diabase and rhyolite</i> | m = 17.00 s = 1.00 m = 17.00 s = 1.00 | m = 0.061 s = 0.000003 m = 0.959 s = 0.00019 | VERY POOR QUALITY ROCK MASS | |
| COARSE GRAINED POLYMINERALLIC IGNEOUS AND METAMORPHIC CRYSTALLINE ROCKS | <i>amphibolite, gabbro, gneiss, granite, norite and quartz-diorite</i> | m = 25.00 s = 1.00 m = 25.00 s = 1.00 | m = 0.015 s = 0.000001 m = 0.469 s = 0.00002 | | |



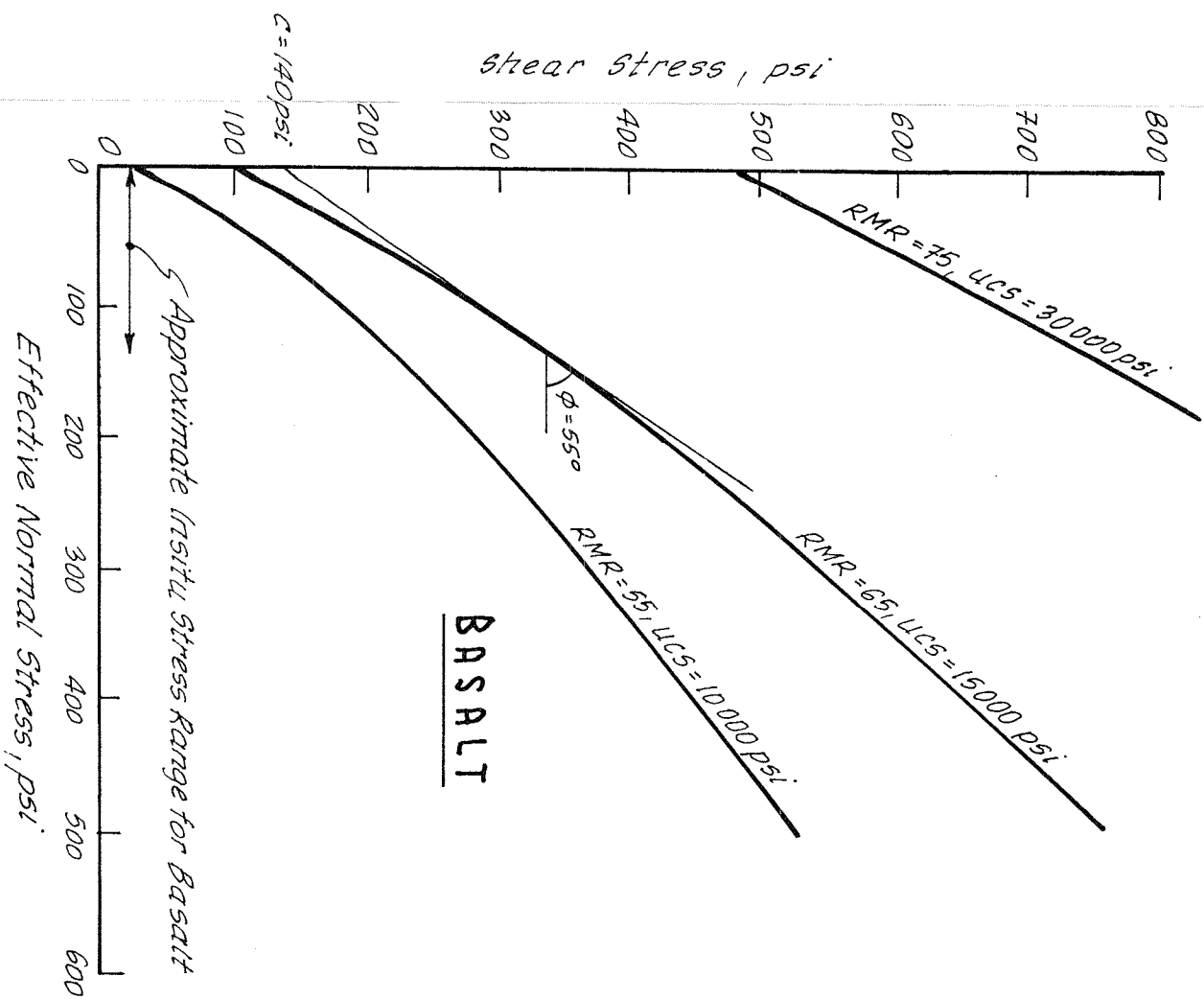
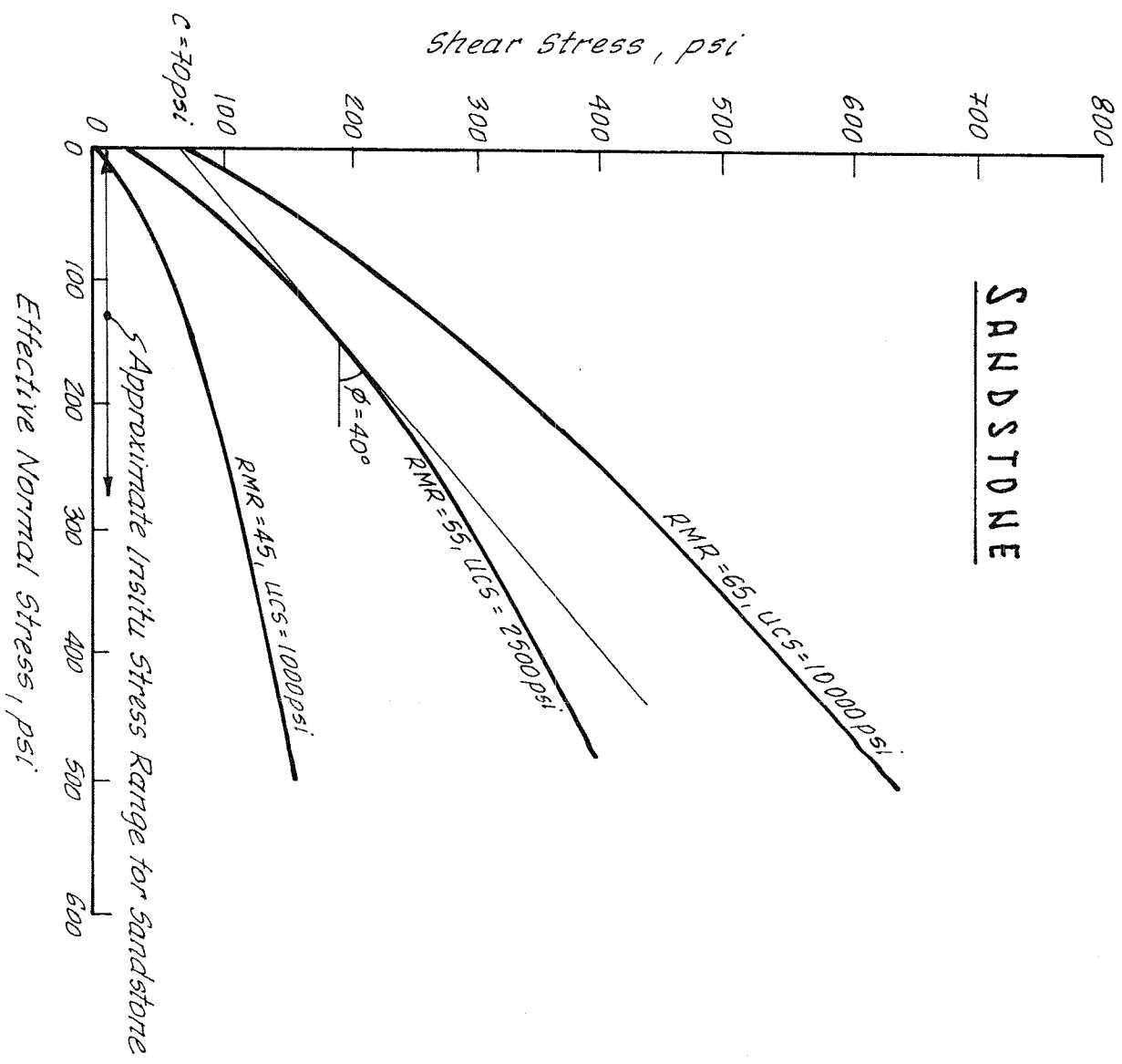
$$m/s = \exp[(RMR - 100)/4]$$

$$s = \exp[(RMR - 100)/6]$$

Note: Method of determining rock mass strength parameters using m and s values, proposed by Hoek and Brown (1980).

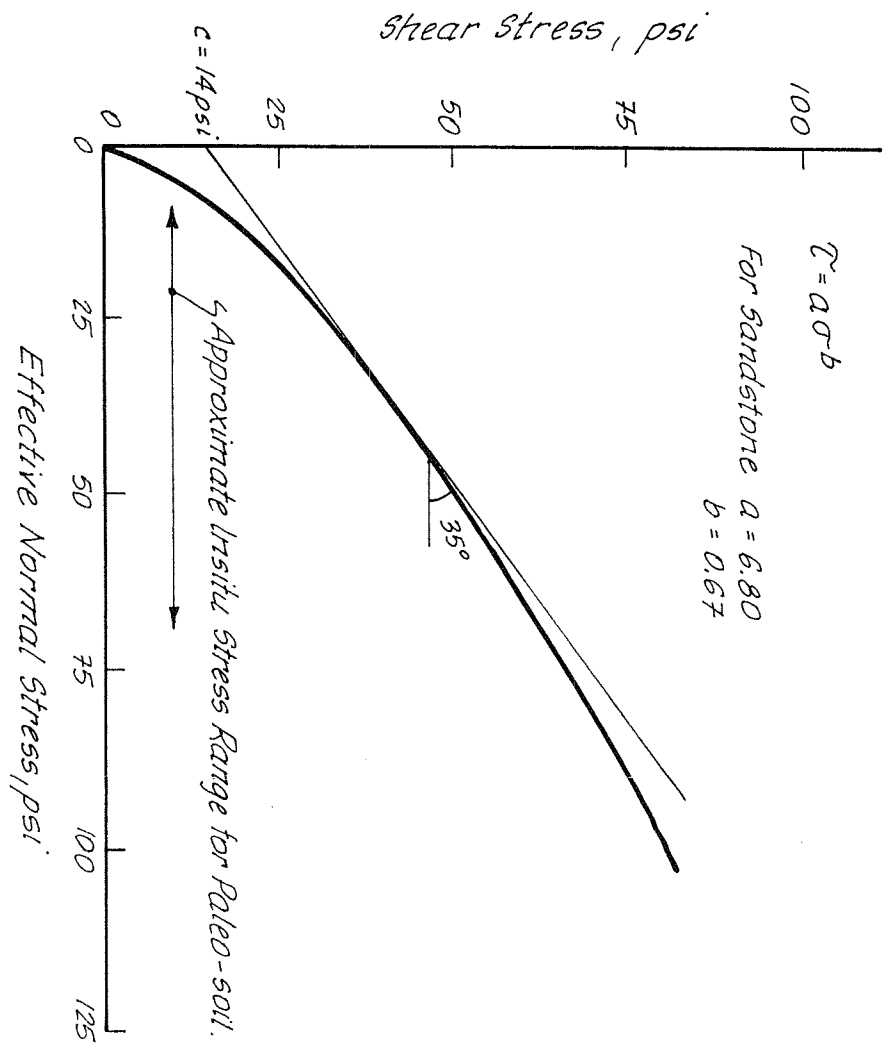
EMPIRICAL ROCK MASS FAILURE CRITERION

Figure 10

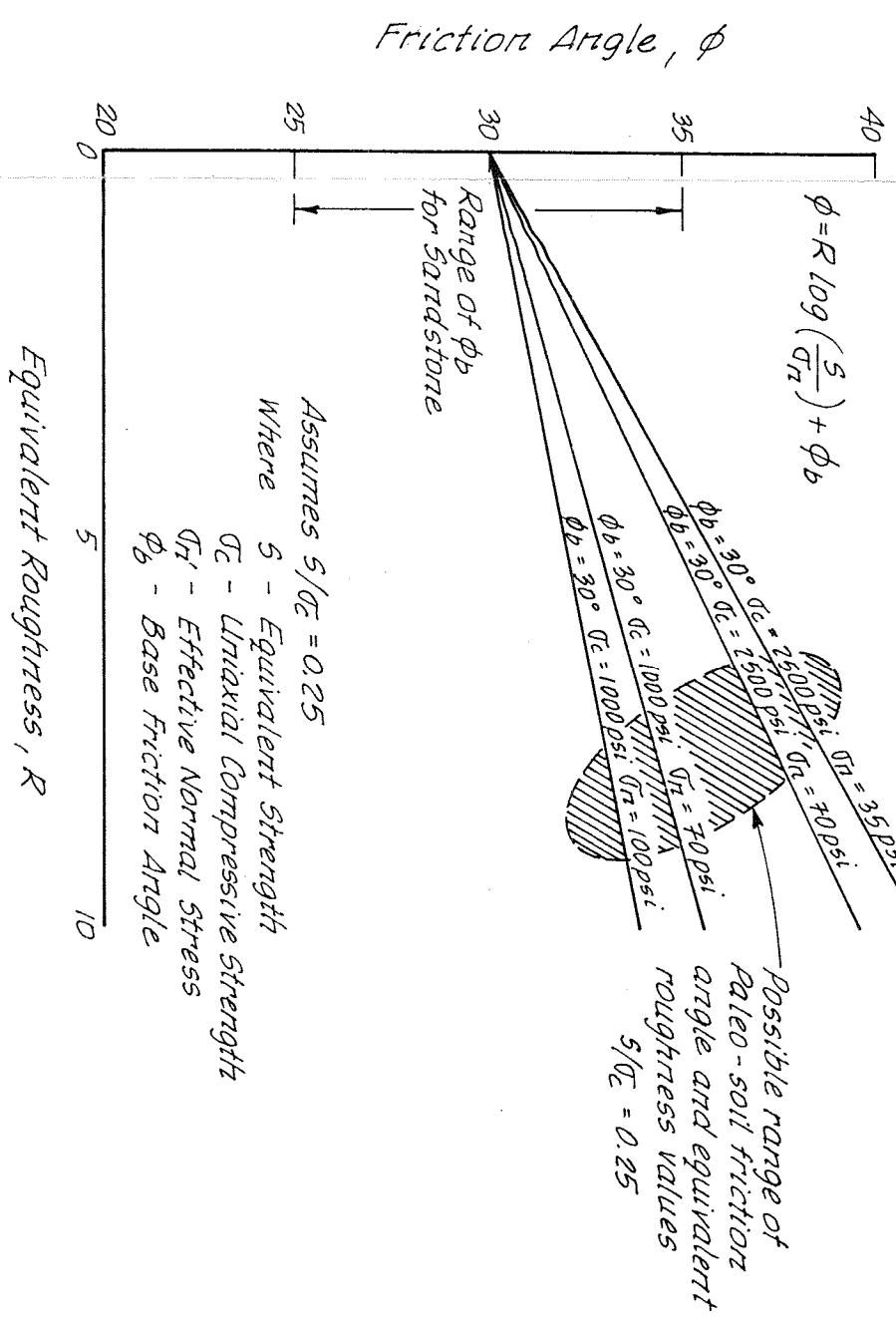


ROCK MASS STRENGTH PARAMETERS

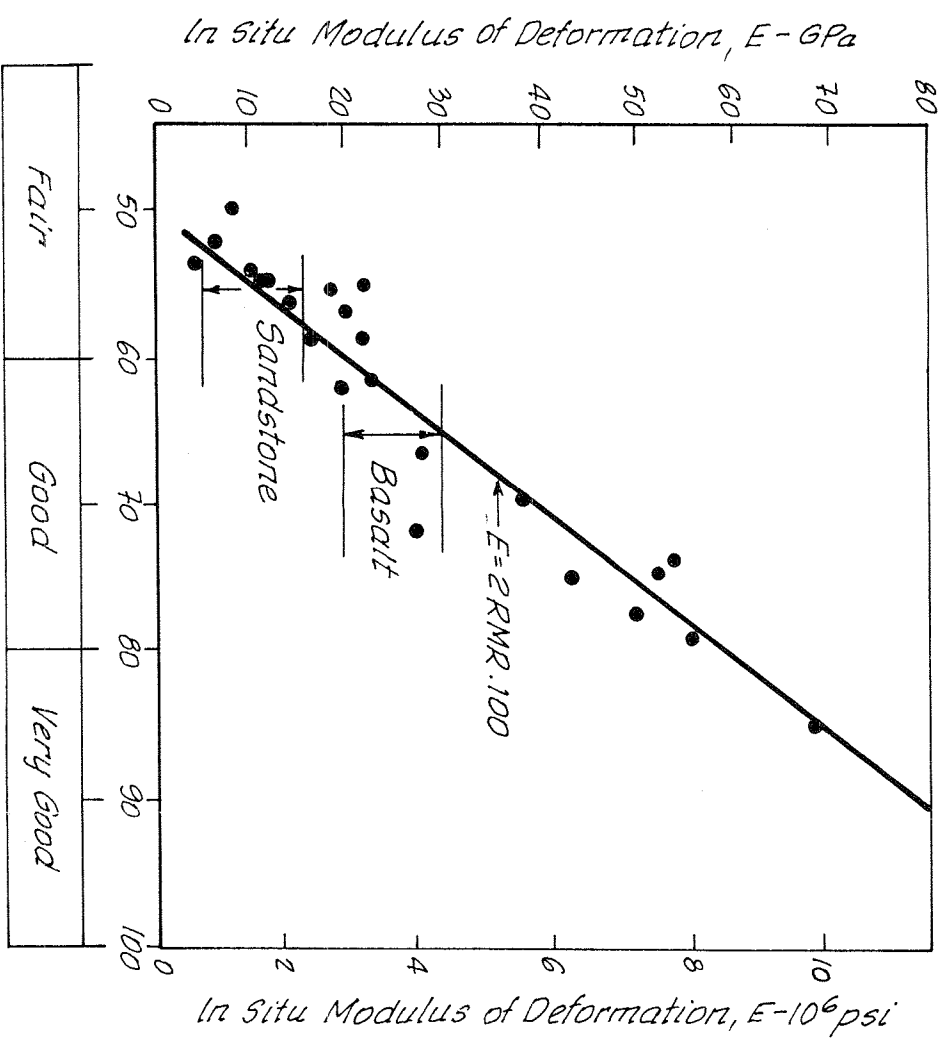
Figure 11



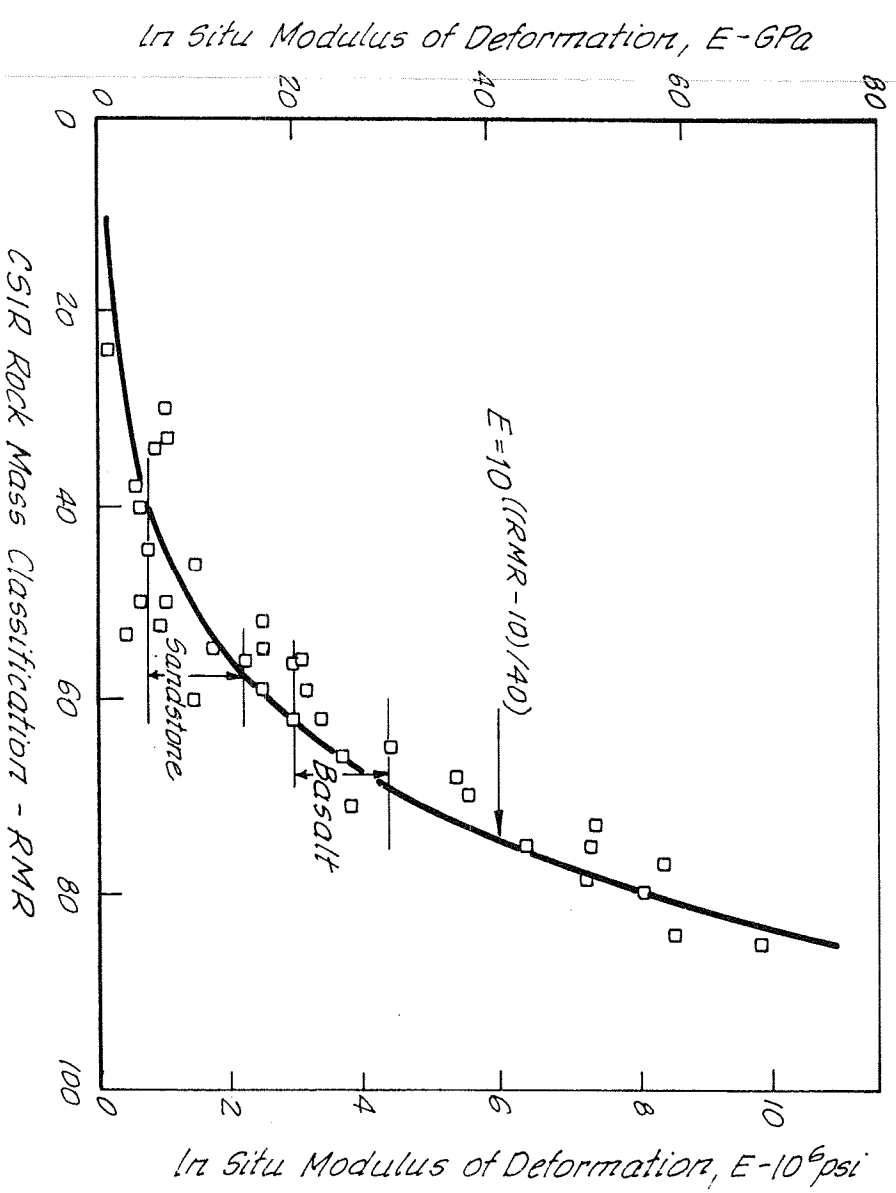
a) Shear strength of compacted Sandstone Rockfill after Charles and Watt (1980).



b) Shear strength of Rockfill after Barton and Kjarnesli (1981).



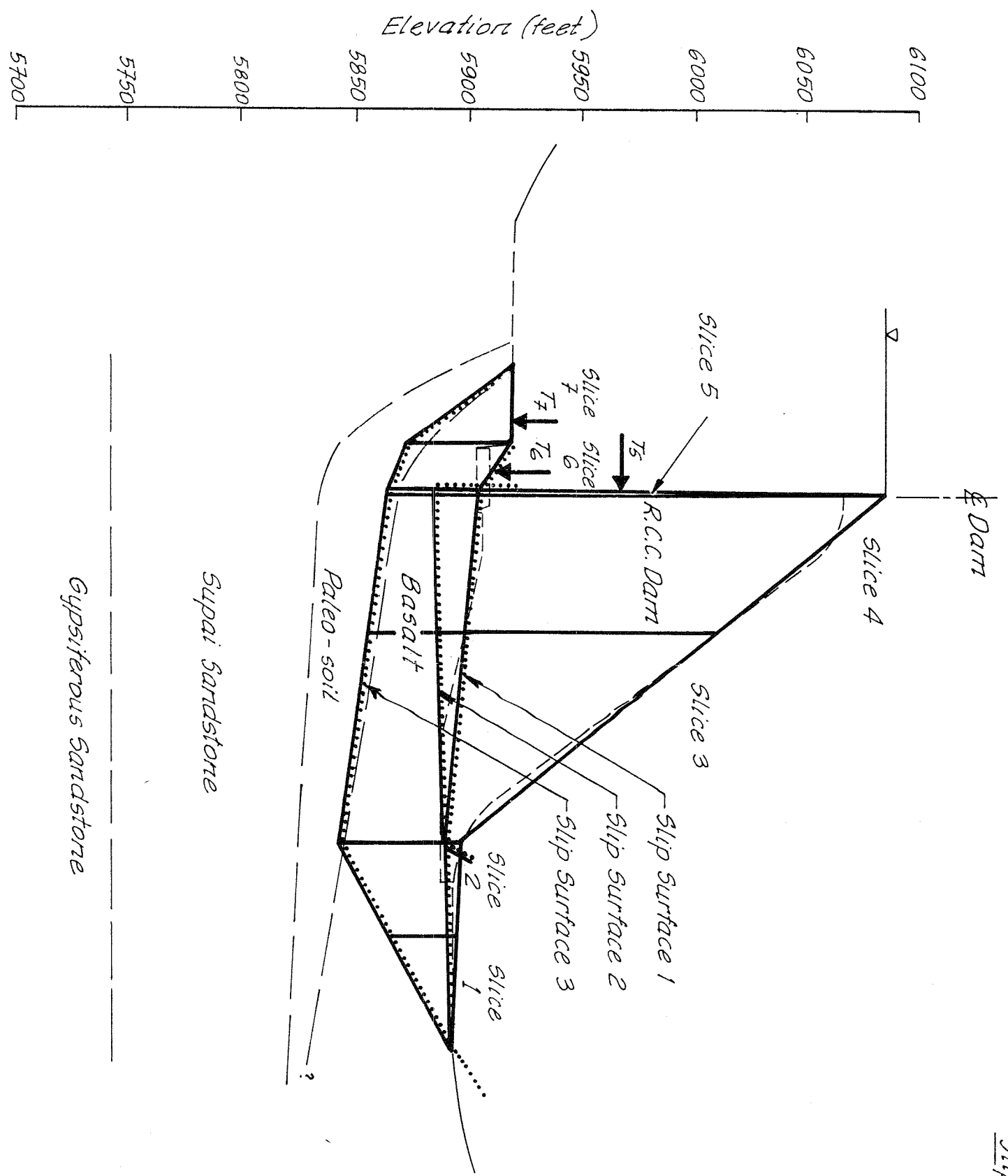
a) Relationship between rock mass quality and in situ modulus of deformation after Bieniawski (1978).



b) Relationship between rock mass quality and in situ modulus of deformation after Serafim and Pereira (1983).

SARMA ANALYSIS OF DAM FOUNDATION STABILITY

Figure 14

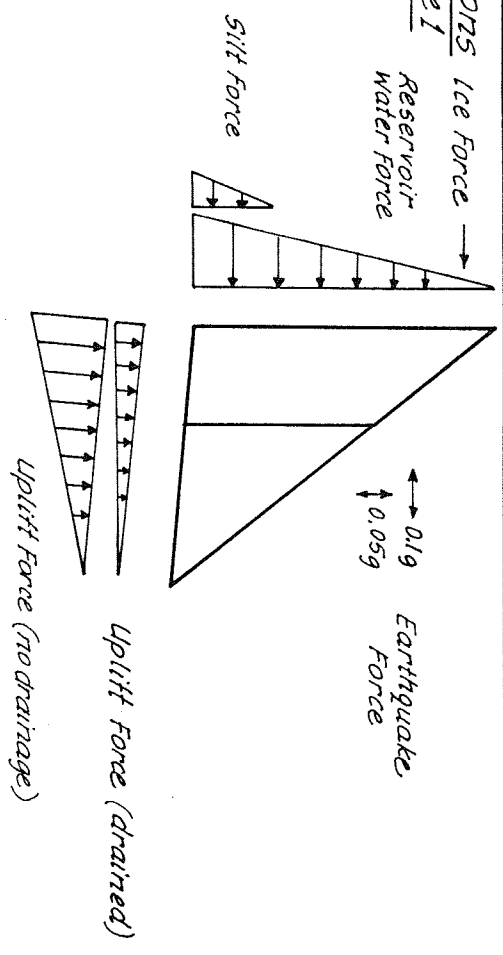


Notes:

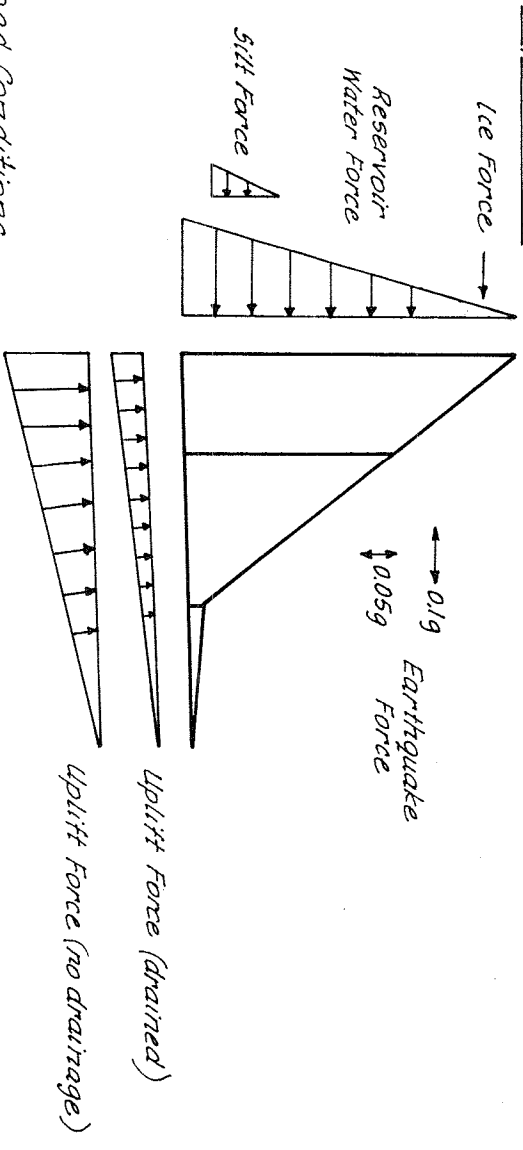
- T_5 - Horizontal silt and ice load
- T_6 - Vertical water and silt load
- T_7 - Vertical water and silt load

Scale: 1 inch to 60 feet

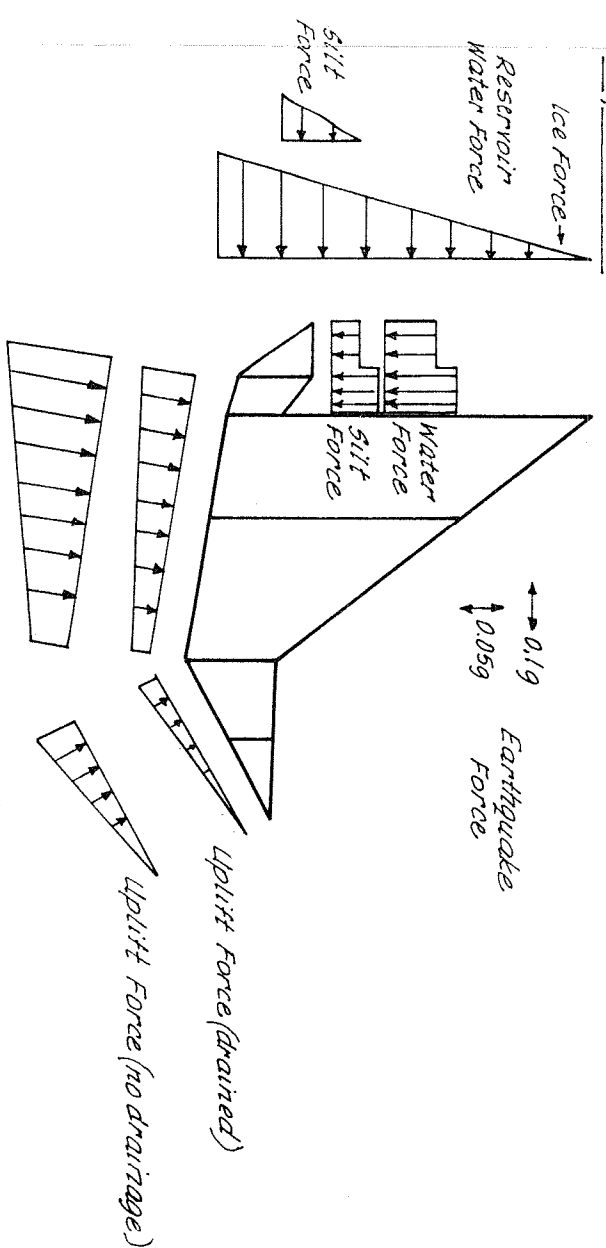
Load Conditions
Slip Surface 1



Load Conditions
Slip Surface 2



Load Conditions
Slip Surface 3

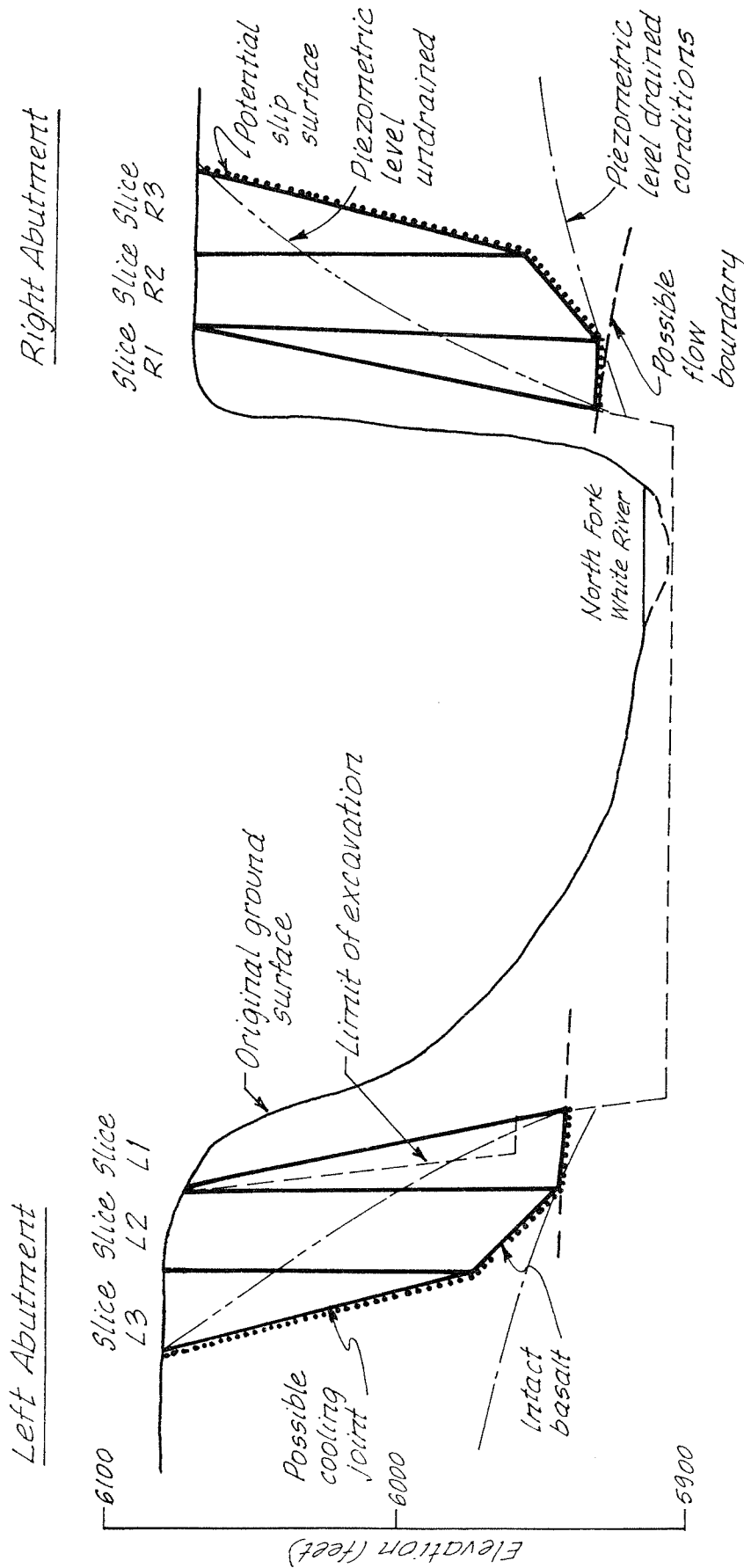


Golden Associates

Note: Force Diagrams Not to Scale.

SARMA ANALYSIS OF EXCAVATED SLOPE STABILITY

Figure **15**

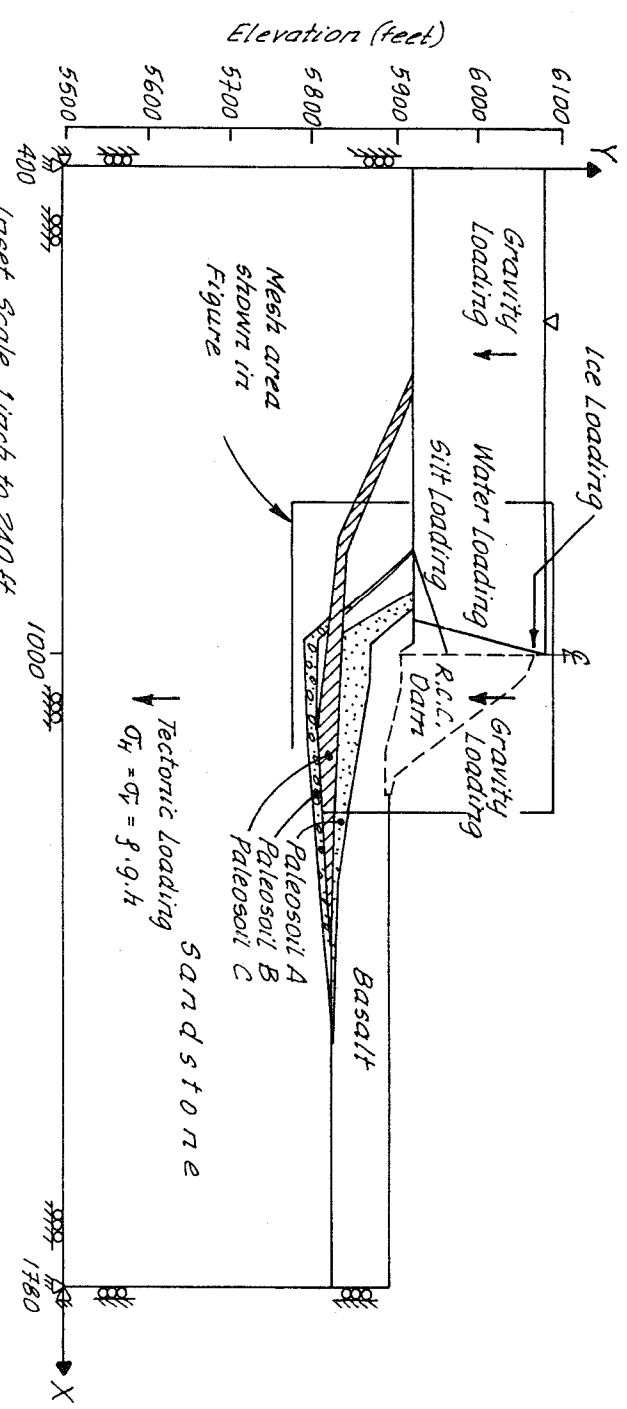


Scale: 1 inch to 60 feet.

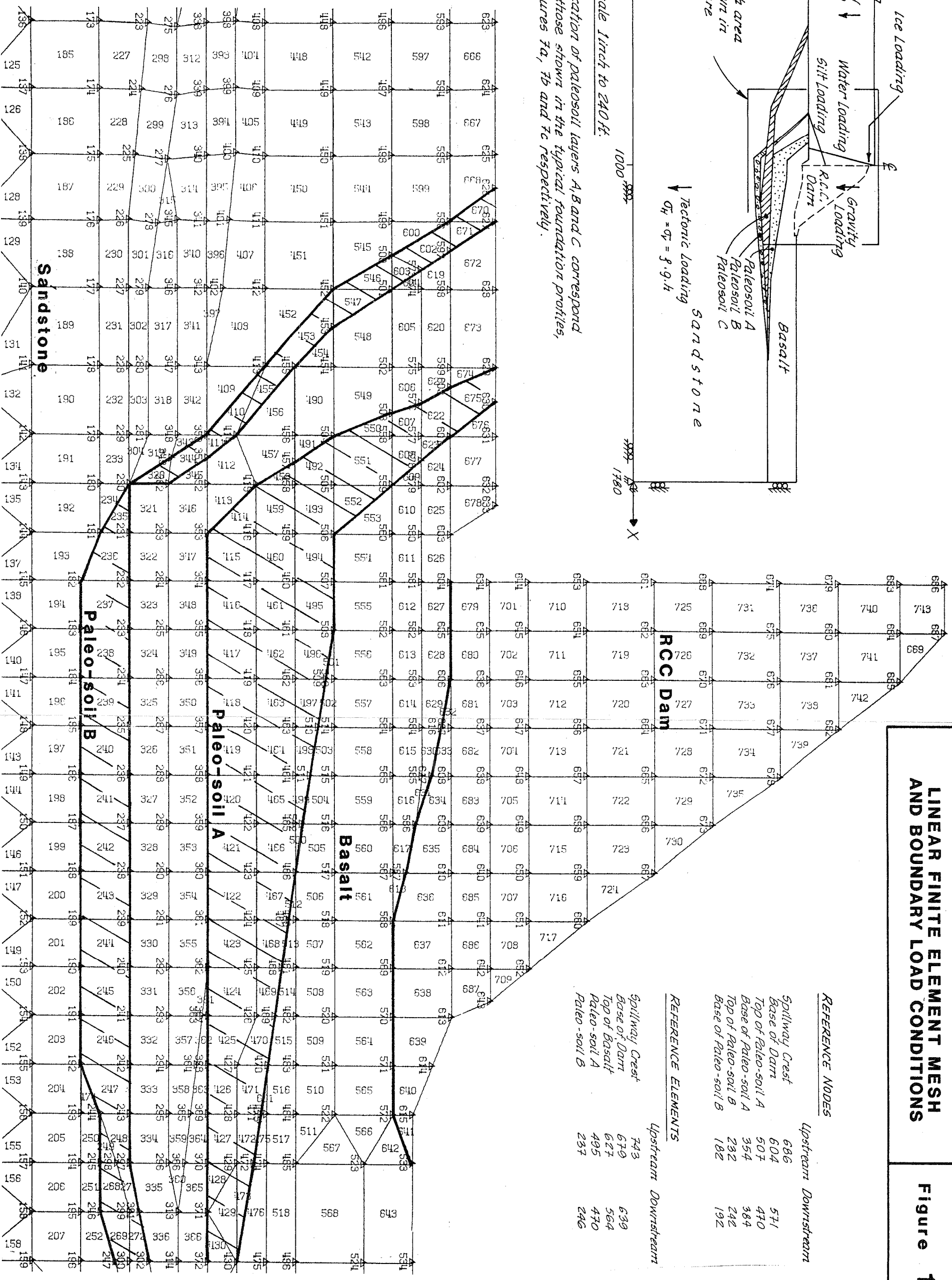
PROJECT NO. _____ DRAWN _____ REVIEWED _____ DATE _____

LINEAR FINITE ELEMENT MESH AND BOUNDARY LOAD CONDITIONS

Figure 16



Note: Location of paleosol layers A, B and C correspond to those shown in the typical foundation profiles, Figures 7a, 7b and 7c respectively.



REFERENCE NODES

- | | | | |
|----------------------|-----|----------------------|-----|
| Spillway Crest | 686 | Lipstream Downstream | 571 |
| Base of Dam | 604 | | 470 |
| Top of Paleo-soil A | 507 | | 384 |
| Base of Paleo-soil A | 354 | | 242 |
| Top of Paleo-soil B | 232 | | 192 |
| Base of Paleo-soil B | 182 | | |

REFERENCE ELEMENTS

- | | | | |
|----------------|-----|----------------------|-----|
| Spillway Crest | 743 | Lipstream Downstream | 639 |
| Base of Dam | 679 | | 564 |
| Top of Basalt | 627 | | 470 |
| Paleo-soil A | 495 | | 246 |
| Paleo-soil B | 237 | | |

Scale: 1 inch to 30 feet

Golden Associates

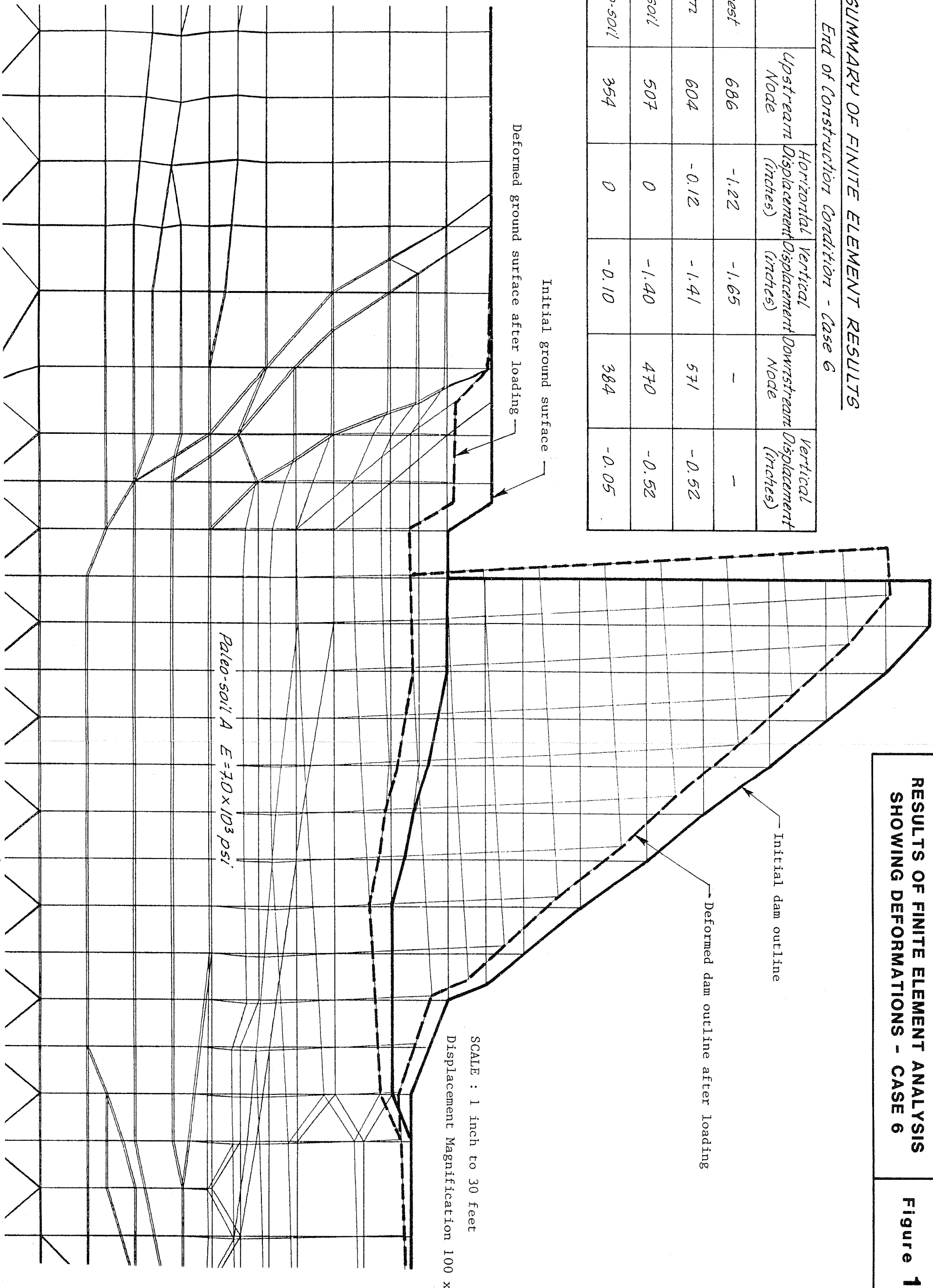
SUMMARY OF FINITE ELEMENT RESULTS

End of Construction Condition - Case 6

| Location | Upstream Node | Horizontal Displacement (inches) | Vertical Displacement (inches) | Downstream Node | Vertical Displacement (inches) |
|--------------------|---------------|----------------------------------|--------------------------------|-----------------|--------------------------------|
| Spillway Crest | 686 | -1.22 | -1.65 | - | - |
| Base of Dam | 604 | -0.12 | -1.41 | 571 | -0.52 |
| Top of Paleo-soil | 507 | 0 | -1.40 | 470 | -0.52 |
| Base of Paleo-soil | 354 | 0 | -0.10 | 384 | -0.05 |

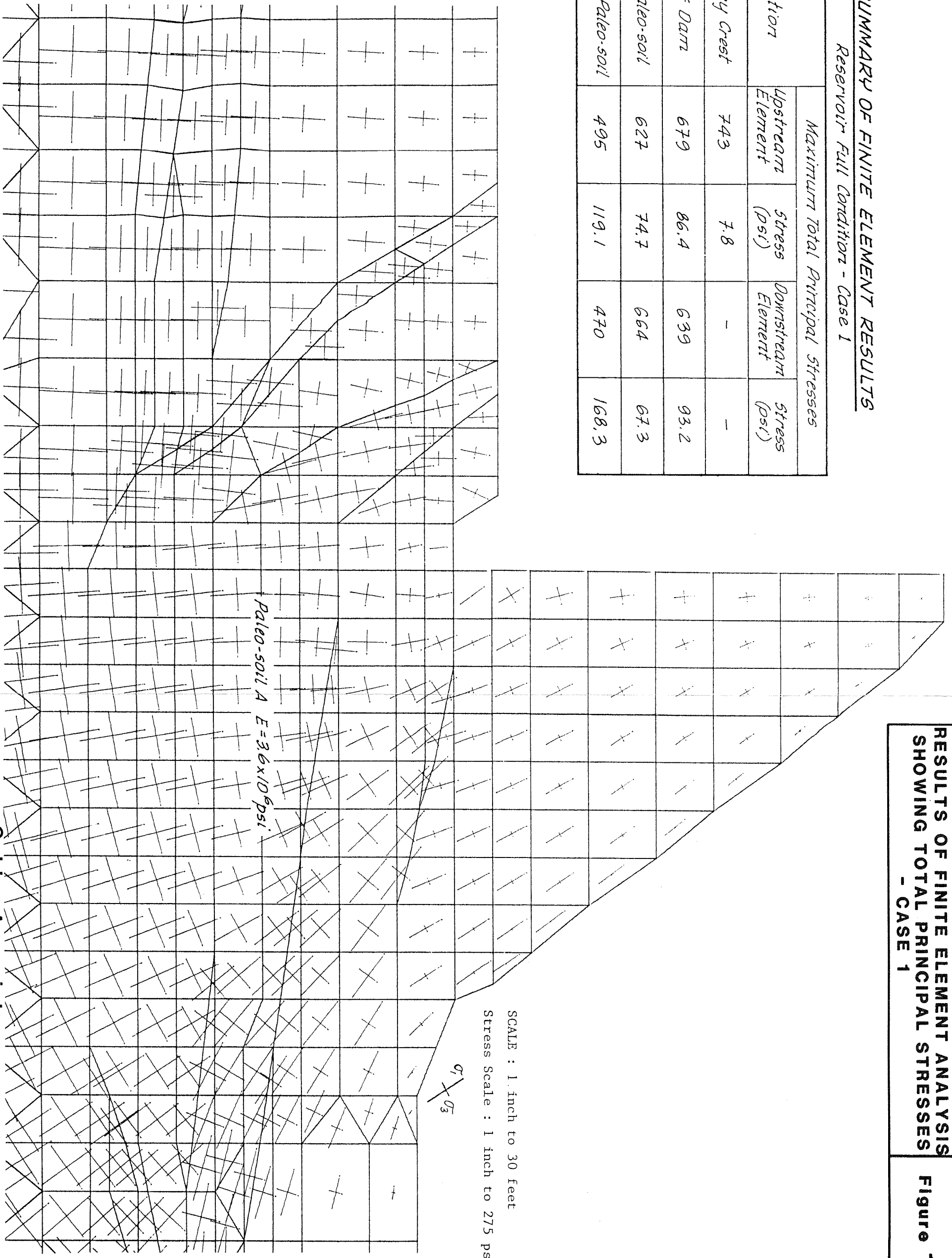
**RESULTS OF FINITE ELEMENT ANALYSIS
SHOWING DEFORMATIONS - CASE 6**

Figure 17f



SUMMARY OF FINITE ELEMENT RESULTS
 Reservoir Full Condition - Case 1

| Location | Maximum Total Principal Stresses | | | |
|--------------------|----------------------------------|--------------|--------------------|--------------|
| | Upstream Element | Stress (psi) | Downstream Element | Stress (psi) |
| Spillway Crest | 743 | 7.8 | - | - |
| Base of Dam | 679 | 86.4 | 639 | 93.2 |
| Top of Paleo-soil | 627 | 74.7 | 664 | 67.3 |
| Base of Paleo-soil | 495 | 119.1 | 470 | 168.3 |

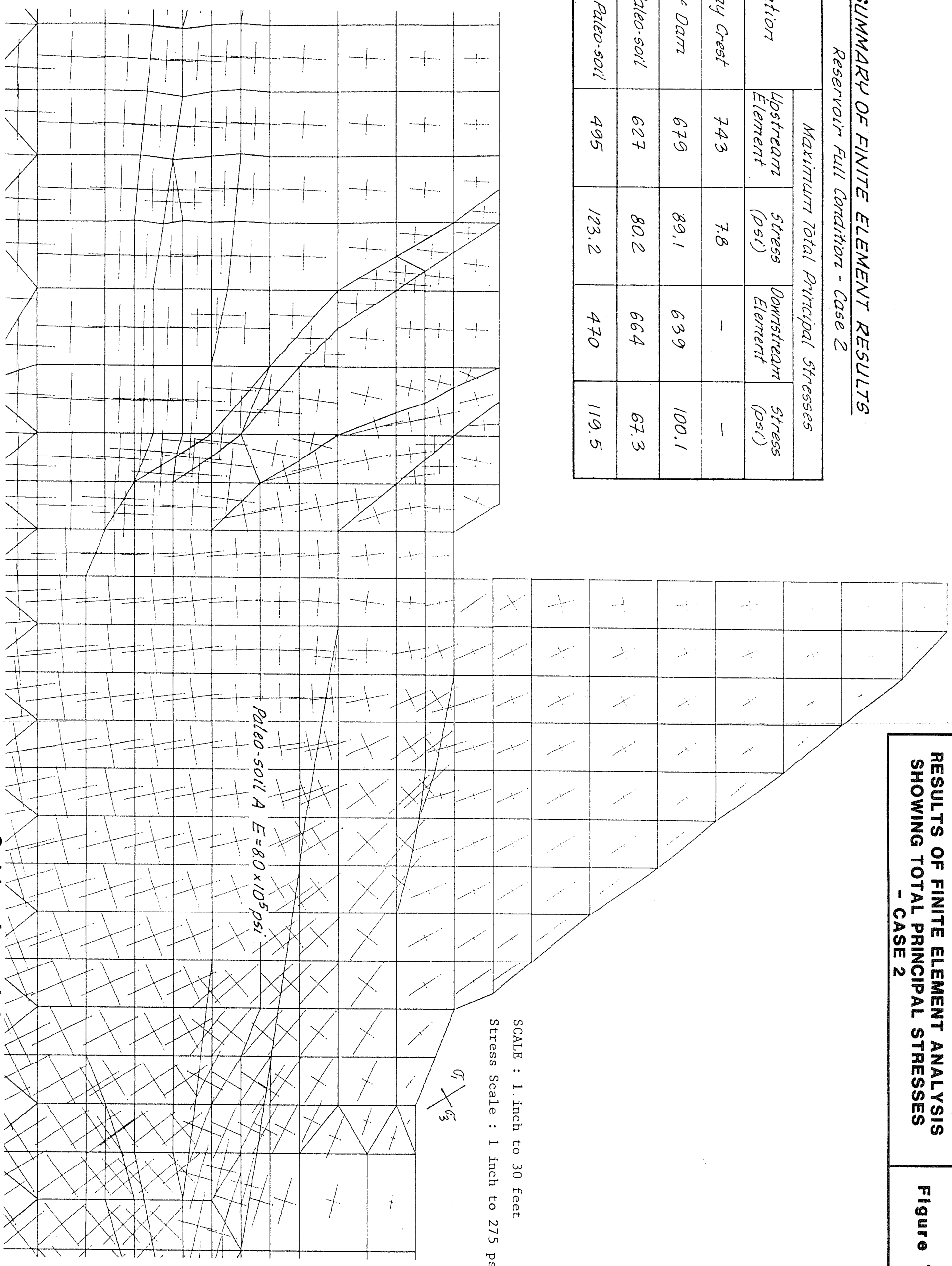


RESULTS OF FINITE ELEMENT ANALYSIS
 SHOWING TOTAL PRINCIPAL STRESSES
 - CASE 1
Figure 18a

Golden Associates

SUMMARY OF FINITE ELEMENT RESULTS
Reservoir Full Condition - Case 2

| Location | Maximum Total Principal Stresses | | | |
|--------------------|----------------------------------|--------------|--------------------|--------------|
| | Upstream Element | Stress (psi) | Downstream Element | Stress (psi) |
| Spillway Crest | 743 | 7.8 | - | - |
| Base of Dam | 679 | 89.1 | 639 | 100.1 |
| Top of Paleo-soil | 627 | 80.2 | 664 | 67.3 |
| Base of Paleo-soil | 495 | 123.2 | 470 | 119.5 |



**RESULTS OF FINITE ELEMENT ANALYSIS
 SHOWING TOTAL PRINCIPAL STRESSES
 - CASE 2**

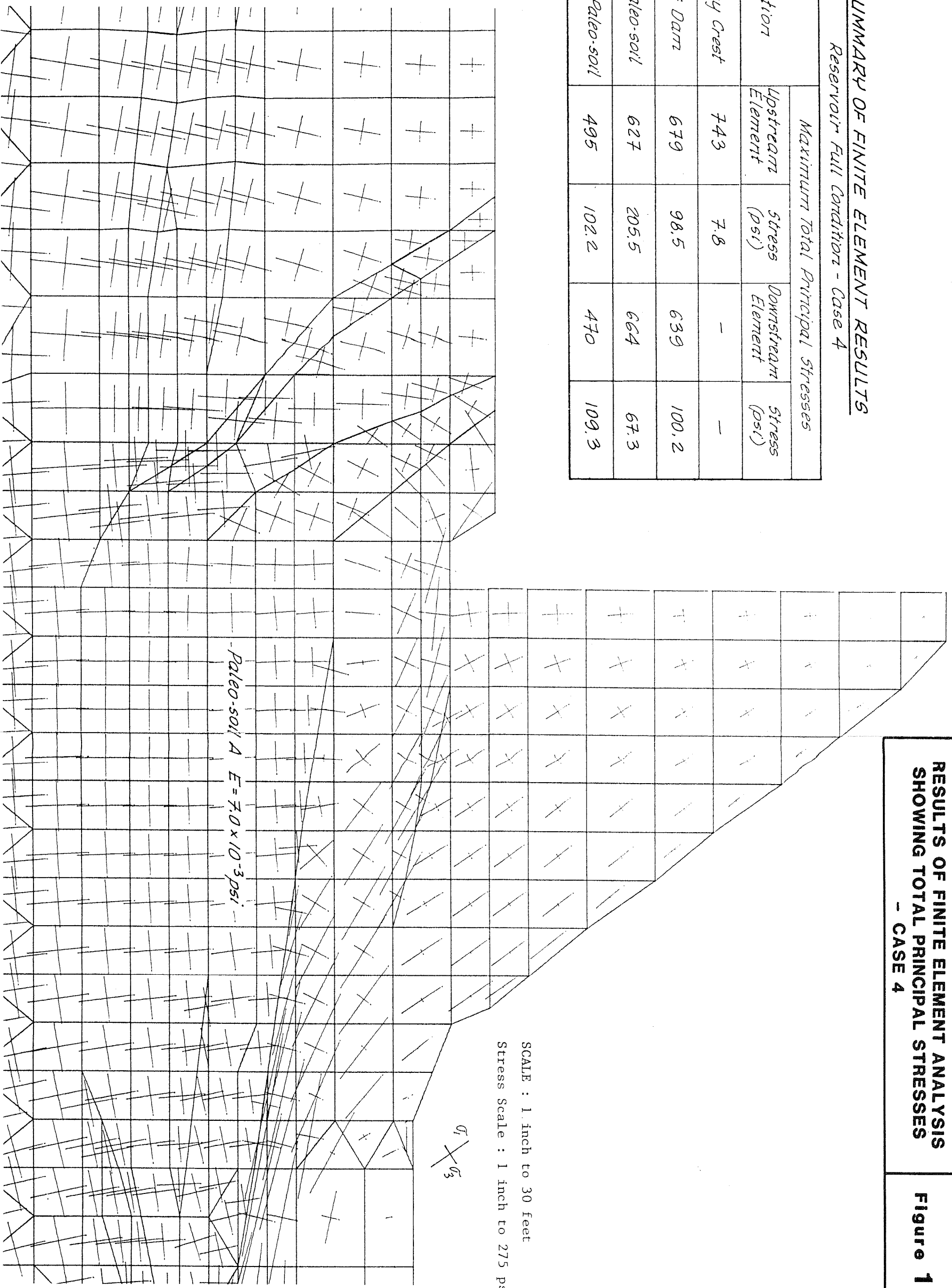
Figure 18b

SUMMARY OF FINITE ELEMENT RESULTS
 Reservoir Full Condition - Case 4

| Location | Maximum Total Principal Stresses | | | |
|--------------------|----------------------------------|--------------|--------------------|--------------|
| | Upstream Element | Stress (psi) | Downstream Element | Stress (psi) |
| Spillway Crest | 743 | 7.8 | - | - |
| Base of Dam | 679 | 98.5 | 639 | 100.2 |
| Top of Paleo-soil | 627 | 205.5 | 664 | 67.3 |
| Base of Paleo-soil | 495 | 102.2 | 470 | 109.3 |

RESULTS OF FINITE ELEMENT ANALYSIS
 SHOWING TOTAL PRINCIPAL STRESSES
 - CASE 4

Figure 18d

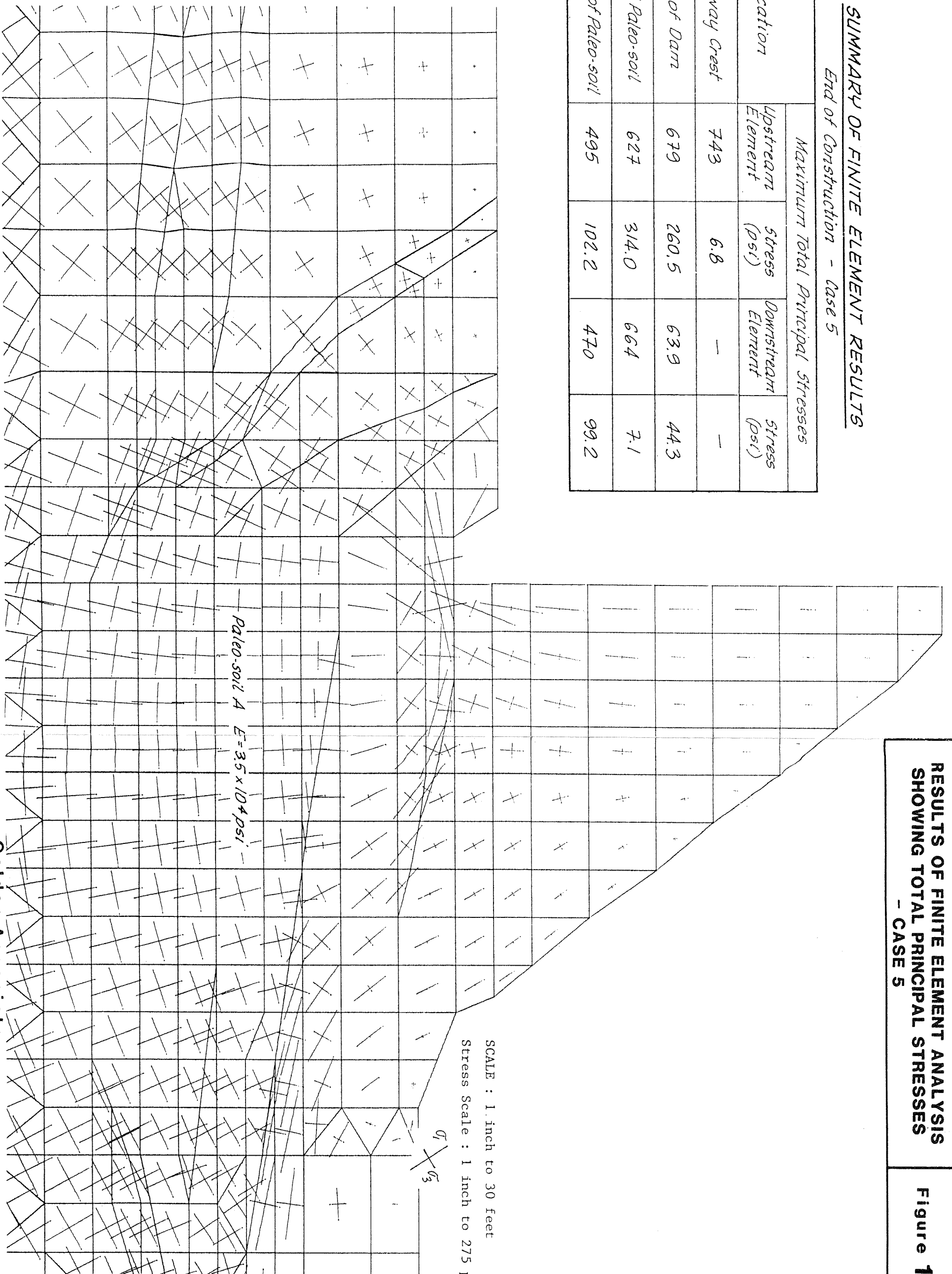


Golder Associates

SUMMARY OF FINITE ELEMENT RESULTS

End of Construction - Case 5

| Location | Maximum Total Principal Stresses | | | |
|--------------------|----------------------------------|--------------|--------------------|--------------|
| | Upstream Element | Stress (psi) | Downstream Element | Stress (psi) |
| Spillway Crest | 743 | 6.8 | - | - |
| Base of Dam | 679 | 260.5 | 63.9 | 44.3 |
| Top of Paleo-soil | 627 | 314.0 | 664 | 7.1 |
| Base of Paleo-soil | 495 | 102.2 | 470 | 99.2 |

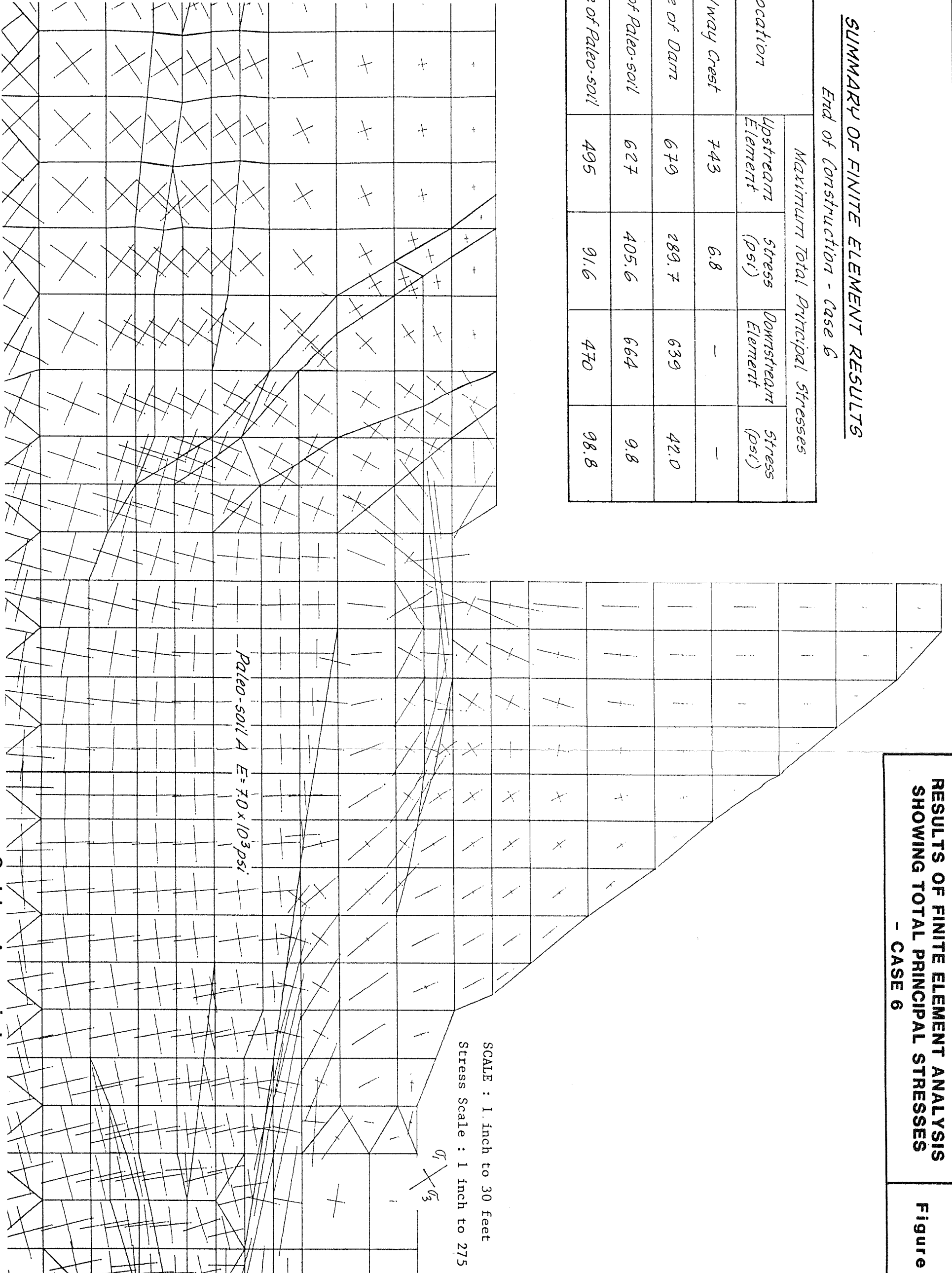


**RESULTS OF FINITE ELEMENT ANALYSIS
SHOWING TOTAL PRINCIPAL STRESSES
- CASE 5**

Figure 18e

SUMMARY OF FINITE ELEMENT RESULTS
End of Construction - Case 6

| Location | Maximum Total Principal Stresses | | | |
|--------------------|----------------------------------|--------------|--------------------|--------------|
| | Upstream Element | Stress (psi) | Downstream Element | Stress (psi) |
| Spillway Crest | 743 | 6.8 | - | - |
| Base of Dam | 679 | 289.7 | 639 | 42.0 |
| Top of Paleo-soil | 627 | 405.6 | 664 | 9.8 |
| Base of Paleo-soil | 495 | 91.6 | 470 | 98.8 |



SCALE : 1 inch to 30 feet
 Stress Scale : 1 inch to 275 psi

Goldier Associates

**RESULTS OF FINITE ELEMENT ANALYSIS
 SHOWING TOTAL PRINCIPAL STRESSES
 - CASE 6**

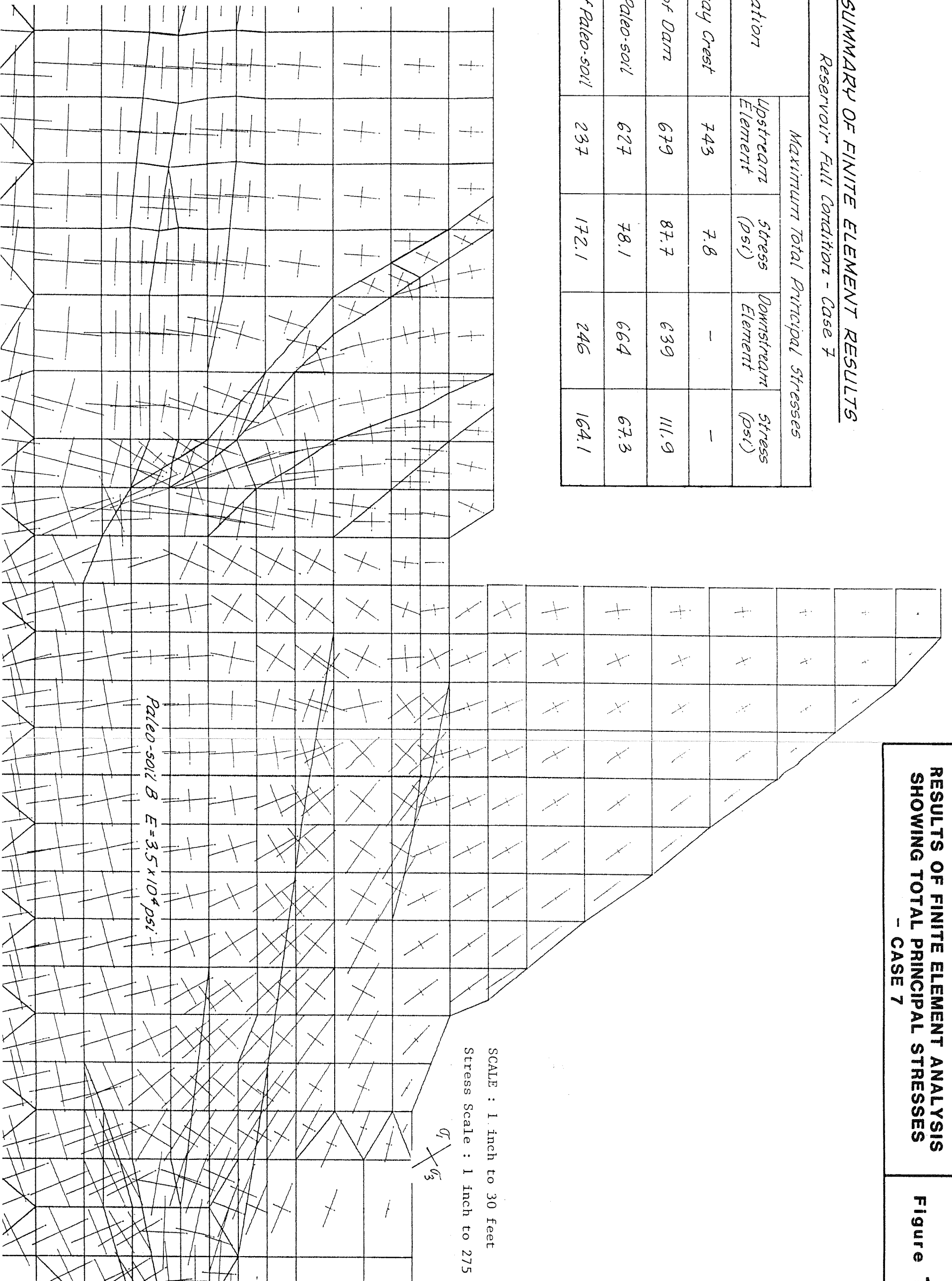
Figure 18f

SUMMARY OF FINITE ELEMENT RESULTS
 Reservoir Full Condition - Case 7

| Location | Maximum Total Principal Stresses | | | |
|--------------------|----------------------------------|--------------|--------------------|--------------|
| | Upstream Element | Stress (psi) | Downstream Element | Stress (psi) |
| Spillway Crest | 743 | 7.8 | - | - |
| Base of Dam | 679 | 87.7 | 639 | 111.9 |
| Top of Paleo-soil | 627 | 78.1 | 664 | 67.3 |
| Base of Paleo-soil | 237 | 172.1 | 246 | 164.1 |

RESULTS OF FINITE ELEMENT ANALYSIS
 SHOWING TOTAL PRINCIPAL STRESSES
 - CASE 7

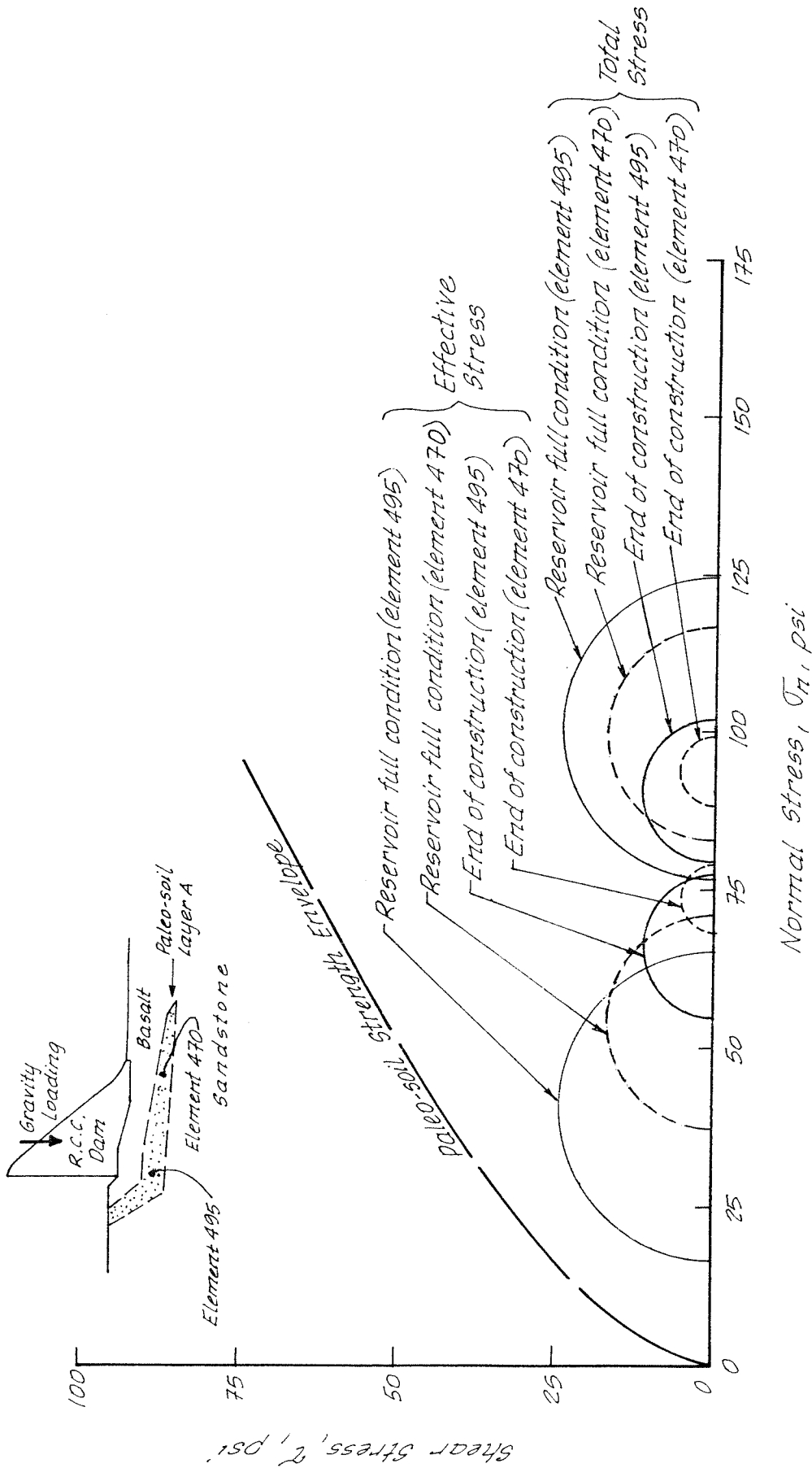
Figure 18g



Goldier Associates

STRESS CONDITIONS IN PALEO-SOIL LAYER A

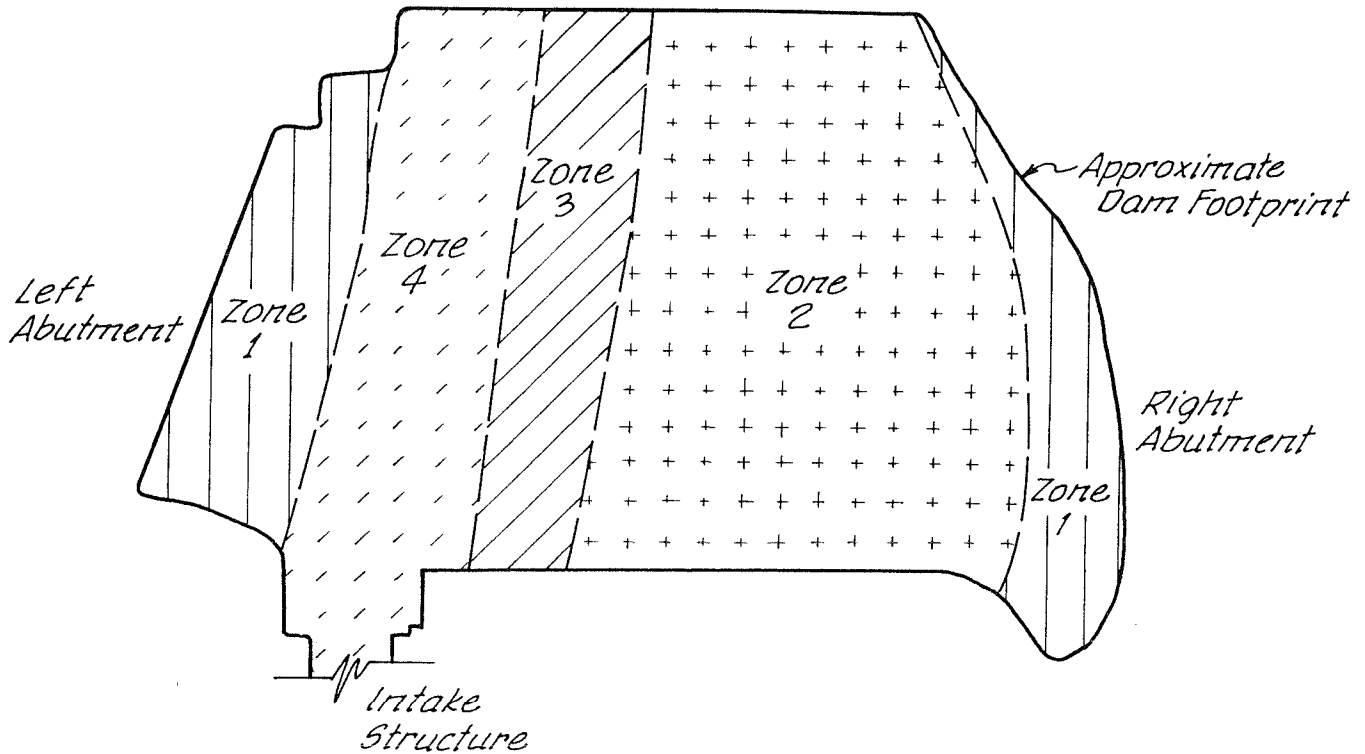
Figure 19



Normal stress, σ , psi

Note: Effective stress conditions calculated from results of Finite Element Analysis with paleo-soil layer A $E = 3.5 \times 10^4$ psi (cases 3 and 5) using estimated pore pressures.

PROJECT NO. DRAWN REVIEWED DATE



- Zone 1 - Paleo-soil >100 ft. deep;
Predicted Differential Settlement heel to toe ~0.1 inch (estimate)
- Zone 2 - Paleo-soil 80 to 100 ft. deep;
Predicted Differential Settlement heel to toe ~0.15 inch (from modelling)
- Zone 3 - Paleo-soil 60 to 80 ft. deep;
Predicted Differential Settlement heel to toe ~0.40 inch (estimate)
- Zone 4 - Paleo-soil 30 to 60 ft. deep;
Predicted Differential Settlement heel to toe ~0.75 inch (from modelling)

Not to Scale.

PROJECT NO. DATE REVIEWED DRAWN

The damsite is located on bedrock in an area of low seismic activity and is not considered to be subject to significant seismic loading. The detailed site mapping indicates that faults are not present in the mapped area. The minimum seismic accelerations of 0.10g horizontal and 0.05g vertical as recommended by the U.S. Bureau of Reclamation are considered appropriate.

The geologic units involved in the dam foundation analysis and identifiable as having differing physical and engineering properties are:

Upper Basalt - A series of relatively thin (about 10 to 40 feet thick), subhorizontal, vesicular to massive, coalescing basalt flows form the abutments of the dam beginning at an elevation approximately 25 feet above foundation grade and extending to the top of the abutments. The flows exhibit typical, pervasive, subvertical thermal jointing and interflow boundaries with 0.1-4 inches of fine-grained, granular infilling. The Upper Basalt flows are relatively fresh with no indication of significant strength loss from weathering processes.

The Upper Basalt flows will not be significantly loaded by the dam but will form the abutments on either side of the structure. As such, their shear strength and permeability properties are required parameters for evaluation of abutment stability whereas the deformation properties are of lesser importance. Direct shear testing of sawn surfaces in the NX core was used to measure the shear strength of clean basalt discontinuities. Interflow boundaries were subjected to separate testing procedures. Ten uniaxial tests (including four with elastic properties) were used to provide information on intact rock strength and intact deformation characteristics in the Upper Basalt flows. Density values were obtained from the uniaxial samples for assessment of intact rock density. Five Goodman Jack tests were completed in the Upper Basalt and were compared to the uniaxial modulus data to help assess rock mass deformation characteristics.

Packer testing in the vertical and subvertical drill holes indicated generally low in-situ formation permeability. Occasional zones of circulation loss were encountered during drilling. The major one of these zones was interpreted as a lava tube encountered within the right abutment. Packer testing of the lava tube zone resulted in a minor "blow out" of water from the nearby cliff face before establishing any other significant flow. The lava tube is interpreted to be a blind cavity and is not considered indicative of a significant "plumbing system" within the Upper Basalt.

Abutment grouting or additional excavation may be required if significant open jointing and flow boundaries are encountered during foundation excavation. Present planning is for a minimum 20 feet of basalt to be excavated from the abutments. The 20 feet of rock removal is considered to be an appropriate depth of excavation to remove basalt significantly effected by weathering, by stress relief opening of columnar jointing, or by erosion along flow boundaries.

Abutment stability analysis assumes full reservoir head with linear pressure drop. The fracture orientation and fracture

spacing in the Upper Basalt flows indicates that subhorizontal gravity relief drains can be used successfully to control seepage pore pressures in the basalt abutments.

Other engineering and construction considerations presented by the abutment rocks include preparation of the abutment slopes. Controlled blasting will be essential to construction of the unbenched cut slopes of the foundation excavation in order to reduce blast damage to the abutment rock and to mitigate rockfall potential. Blasting will be evaluated on a performance basis with 85-90% of presplit barrels visible on the finished slope. Mitigation procedures to reduce rockfall hazard during construction include scaling, spot bolting and chain-link mesh.

Flow Boundaries - The flow boundaries between the basalt flows in the Upper Basalt present discontinuities important to the analysis of block sliding in the abutments and to the potential for piping of fines from the contact zones. Typically, the flow boundaries contain 0.1-4 inches of fine-grained, granular infilling. Although flow boundaries were detected in the Upper Basalt flows at some locations, flow boundary interbeds between the flows were not detected in the foundation and abutment area of the proposed dam.

The NX core drilling did not recover samples of interflow boundaries materials suitable for direct shear testing of intact core. Accordingly, a composite bulk sample of fines and basalt recovered from the flow boundaries in drill holes MF-102, MF-105, and MF-106 was remolded and consolidated in a shear box where it was subjected to direct shear testing in a saturated condition. The results of the direct shear tests of the bulk sample were used to conservatively approximate the shear strength along the interflow boundaries.

Atterberg Limits tests were performed on a composite sample of clay infilling recovered in NX core from flow boundaries. The results were used in the evaluation of the potential influence of this material on shear strength and its general susceptibility to piping. The location of the flow boundaries above the dam's foundation grade, the minimal thickness of the flow boundaries, and the lack of spatial continuity of the boundaries indicates that the potential for piping of interflow material is not a significant threat to the structural integrity of either the gravity dam or the abutments.

Lower Basalt - A single, subhorizontal, massive basalt flow forms the immediate foundation of the dam from approximately 25 feet above upstream foundation grade to a range of approximately 40 to 100 feet below the upstream foundation grade. The Lower Basalt is quite variable in thickness with a subhorizontal upper contact and a lower contact that follows the ancestral pre-basalt valley. The lower contact is characterized by a vesicular to scoriaceous flow breccia zone generally less than 10 feet thick.

The Lower Basalt is a single flow without significant subhorizontal discontinuities or evidence of weathering induced strength reduction. Structurally, it is dominated by the typical subvertical thermal jointing common to basalt flows. Packer testing, core logging and outcrop inspection indicate the subvertical joints are typically clean and tight at depth. The Lower Basalt

forms the immediate foundation of the dam. The compressive strength and deformation characteristics of the Lower Basalt are provided by point load and RQD data in conjunction with 21 uniaxial tests (13 with elastic properties), seven direct shear tests on saw cut surfaces, and seven in-situ Goodman Jack tests. Rock density values were obtained from the uniaxial test samples.

An anomalous zone of low RQD values with highly variable core recovery and high intact rock strength was encountered at a depth of approximately 20 feet immediately below the upstream foundation grade. As indicated on the engineering geologic logs of holes penetrating the zone, (Mineral Systems Inc., 1983; Mineral Systems Inc., 1986) the rock reportedly exhibits increased jointing subparallel to the core axis and joints contain "clay filling" & "clay staining".

Detailed re-examination of the rock core samples from the zone of low RQD's revealed the low RQD's are the result of the rock coring practices. Evidence of the effects of the coring procedures include grinding of the core samples, breakage of the core, and slipped samples. The core samples further indicate that the presence of subvertical fractures aligned generally parallel to the core significantly aggravated the difficulties of obtaining intact rock core. The effects of the drilling and coring in conjunction with the near vertical fractures clearly induced considerable fracturing and breakage of the core with the result that core recovery was variable and low RQD's were observed.

Accordingly, the low RQD's and variable core recovery observed in the zone are attributed to a combination of stress relieved vertical columnar joints and drilling induced fractures. Although the zone of low RQD in the lower basalt cannot be correlated laterally into the left abutment, the evidence suggests that the zone may be laterally continuous across the width of the valley floor cut into the stratified basalt sequence at the site. This conclusion is consistent with the interpretation that the fact the vertical fractures interfered with the coring process indicates stress release and enlargement of the fractures due to unloading caused by entrenchment of the valley into the basalts. Accordingly, the stability analysis presented in the following section of this design memorandum assumes a conservatively worst case for the zone of low RQD's in which it is analyzed as a low angle fracture zone extending over the entire footprint area of the dam. Under this worst case analysis it is demonstrated that an adequate factor of safety exists for sliding or shear failure through a low angle fracture zone of low RQD in the basalt foundation.

Paleo Colluvium/Alluvium - A layer of unconsolidated material is present between the Lower Basalt flow and the underlying Supai Formation bedrocks. The thickness of the basalt overlying the unconsolidated material ranges from about 40 feet near the left abutment to 80 feet near the dam mid point and about 60 feet near the right abutment. The thickness of the unconsolidated material ranges from about 35 feet near the left abutment to 10 feet at the dam mid point and 20 feet thick near the right abutment.

The unconsolidated material represents the surficial deposits which were present in the ancestral valley of the North Fork of the White River at the time basalt flows began to fill the ances-

tral valley. Accordingly, the unconsolidated materials buried by the basalts which filled the ancestral river valley include fluviially deposited silty sand and gravel deposited along the ancestral river channel and flood plain, fine-grained silt and sand deposits emplaced as colluvial foot slope deposits along the valley margins, and sandstone rock rubble in a fine-grained silty sand matrix deposited as talus at the base of cliffs on the ancestral valley walls. The unconsolidated deposits buried by the basalts are collectively referred to herein as Paleo Colluvium/Alluvium.

The NX core barrels used in the coring program did not recover intact samples of the Paleo Colluvium/Alluvium materials. The partial samples recovered and the response of the equipment during coring of the Paleo Colluvium/Alluvium interval indicate that the Paleo Colluvium/Alluvium consists of coarse gravel, cobbles, and boulders in a dense matrix of silty sand. Examination of outcrops of the Paleo Colluvium/Alluvium downstream from the proposed damsite support this interpretation. The only field data developed regarding the strength parameters of the Paleo Colluvium/Alluvium was completion of three Goodman Jack tests in drill hole MF-113. The results of the tests are not considered to be representative or reliable. Laboratory data regarding the materials properties of the Paleo Colluvium/Alluvium was not obtained due to the lack of samples for analysis.

Core holes reamed through the Paleo Colluvium/Alluvium indicated that although the materials are essentially unindurated, they stand well in the borehole walls, are slowly permeable, and are relatively dense and compact. The geologic conditions at the site indicate that the Paleo Colluvium/Alluvium was subjected to considerable preloading by from the weight of the basalt before the contemporary river valley was entrenched into the basalt. Thus the Paleo Colluvium/Alluvium materials under the dam foundation are anticipated to be preconsolidated. The in-situ permeability tests and the recovered material indicates the Paleo Colluvium/Alluvium is sandy in nature and apparently without significant clay or open work gravel components. As such, and considering it has already carried a load greater or equal to that from the dam, significant time-dependent settlement problems are considered highly unlikely. Compression of the unit is expected to occur during construction under elastic conditions rather than due to permeability controlled consolidation by release of pore pressure.

Based on the foregoing considerations plus the limited field data from the boreholes and from the examination of the Paleo Colluvium/Alluvium outcrops downstream from the damsite, the Paleo Colluvium/Alluvium is considered to be analogous to compacted rockfill material. Accordingly, a range of values for shear strength and deformation parameters was determined for the Paleo Colluvium/Alluvium principally from published data for compacted rockfill.

Because direct information for the materials properties of the Paleo Colluvium/Alluvium was not available, a wide range of presumptive values obtained from the published literature was used in the stability analysis to provide predictions based on the conservatively worst case conditions probable. The stability analysis presented in the following section of this memorandum

indicates a factor of safety of 2 or greater for a sliding or shear failure through the Paleo Colluvium/Alluvium under worst case conditions.

Analysis of total settlements using the range of published values assigned to the Paleo Colluvium/Alluvium indicates that under worst case conditions, lateral differential settlement related to the Paleo Colluvium/Alluvium in the foundation will be a design consideration. Clearly, more information on the geometry and material properties of the Paleo Colluvium/Alluvium underlying the foundation is required and will be obtained during the final engineering studies. If the final engineering studies indicate that a potential for excessive differential settlement actually exists due to the properties of the Paleo Colluvium/Alluvium, then remedial measures such as consolidation grouting or cast-in-place piles will be evaluated.

The Paleo Alluvium/Colluvium presents a potential path for seepage losses from the reservoir. The potential seepage paths include seepage under the dam through the buried sediments of the ancestral river valley as well as seepage through the left abutment through the buried sediments on the ancestral valley wall. Geologic relationships indicate that seepage through the left abutment Paleo Colluvium/Alluvium could daylight on the valley wall downstream from the dam whereas seepage through the main paleo channel would daylight approximately one mile downstream from the dam. The potential seepage losses and seepage pressures associated with the Paleo Colluvium/Alluvium are discussed in detail in Section D.3 herein. Finite difference modeling of seepage through the abutments and buried paleo channel under the basalt as presented in Section D.3 indicates that seepage losses will not be significant.

The outcrop of the Paleo Colluvium/Alluvium has not been mapped immediately downstream of the reservoir. However, it is presumed the unit conforms to the base of the basalt and daylights along the basal contact of the basalt. As such, the Paleo Alluvium/Colluvium is confined beneath basalt in the left abutment for at least 820 feet downstream from the dam where, buried beneath Supai talus, a "window" through the basalt may occur (Figure 3, Mineral Systems Inc., 1986). With the exception of the potential "window", the main channel of the buried Paleo Colluvium/Alluvium should not daylight for approximately a mile downstream from the dam (Mineral Systems Inc., 1986, p. 43). The seepage analysis presented in Section D.3 herein indicates that even if the Paleo Colluvium/Alluvium material is susceptible to piping, the hydraulic gradient of the phreatic seepage surfaces simulated by the digital seepage model is considerably less than the gradient generally associated with the onset of piping conditions. If subsequent studies or experience indicate a significant potential for piping, for example at the "window" through the basalt downstream from the left abutment, a series of filter protected gravity drain holes through the basalt or a filter blanket drain at the outcrop will mitigate the piping problem.

Supai Sandstone/Siltstone - The Supai Formation is the lowermost geologic unit mapped or penetrated by drill holes at the proposed damsite. The surface outcrops and uppermost part of the Supai Formation penetrated by the drill holes consists of interbedded fine-grained sandstone and siltstone. The sandstone and silt-

stone forms the ridge behind the left abutment and comprises approximately 30 to 90 feet of the thickness of the bedrocks investigated by coring beneath the axis of the damsite. The upper contact of the interbedded sandstone and siltstone is the erosional surface formed by the ancestral river valley, approximately 80 to 135 feet below the heel of the dam.

The interbedded sandstone and siltstone of the Supai Formation does not present any unusual or limiting design considerations for the foundation performance. The depth of the unit below foundation grade considered with the confined nature and history of loading of the unit indicate it will not negatively impact the project design or construction. Shear strength and deformation parameters of the interbedded sandstone and siltstone were determined by five direct shear tests (two on saw cut surfaces and three on intact samples), four uniaxial compressive tests (two with elastic properties), and four Goodman Jack tests in the sample intervals subjected to uniaxial testing.

Supai Gypsiferous Sandstone/Gypsum - The deepest unit investigated beneath the dam is a facies of the Supai Formation composed of fine-grained gypsiferous sandstone with lenses of gypsum. This unit has a gradational, subhorizontal upper contact approximately 160 feet below the heel of the dam.

For the same reasons given for the interbedded sandstone and siltstone facies above, the gypsum bearing facies is considered to not significantly impact the foundation performance. A general suite of tests consisting of seven uniaxial compression tests (four with elastic properties), four direct shear on core, and two direct shear tests on saw cut surfaces were completed on samples from the gypsiferous sandstone facies in the Supai Formation. All of the Supai Formation beneath the dam foundation is saturated and in-situ permeability tests of the gypsiferous sandstone facies indicate a low permeability (approximately 10^{-6} cm/sec). As such, the potential for dissolution of gypsum is considered to be insignificant.

D.2 FOUNDATION STABILITY STUDIES

The present design is based on a preliminary engineering geologic assessment of the site. The site geology does not present exceedingly difficult or unusual foundation problems and is well suited to a concrete gravity dam of either conventional concrete or roller compacted concrete construction.

A simple foundation shape is maintained in order to eliminate stress concentrations in the dam and allow efficient excavation. For the conventional concrete option it avoids narrow monoliths with small base areas, small areas of difficult concrete placement and torsion on monoliths. For the joint-free, roller compacted concrete option it avoids small areas of difficult placement.

The amount of dental concrete required is expected to be small. Controlled blasting procedures will be required to excavate the foundation with dental concrete used for voids that will not be filled during normal placement. For the roller compacted concrete option a high slump, bedding mix will be used at all interfaces between foundation rock and the dam. This technique, using procedures tested and proven on other projects, results in excellent dam to rock bonding.

Foundation and abutment stability studies were accomplished by Golder Associates and are presented in the report titled, "Report to Morrison-Maierle, Inc. on Stability Analysis of the Miner Flat Dam Foundations, Navajo County, Arizona", which is presented herein beginning on the following page. Data for the stability studies were provided from the Mineral Systems, Inc. field investigations and from independent laboratory tests of materials properties provided to Golder Associates by Morrison-Maierle, Inc. Summaries of the field and laboratory data are provided in the Golder Associates report with a narrative description of the stability problem, the analytical methods applied to the problem, and conclusions and recommendations.

DESIGN MEMORANDUM

SECTION D

TABLE OF CONTENTS

D.3 SEEPAGE MODELS.....D3-1
1.1. INTRODUCTION.....D3-1
1.2. MODELING METHODOLOGY.....D3-1
1.2.1. Input/Output Parameters.....D3-3
1.2.2. Boundary Conditions.....D3-4
1.3. BURIED PALEOALLUVIAL CHANNEL SEEPAGE MODEL.....D3-6
1.3.1. Input Variables.....D3-7
1.3.2. Simulation Concepts.....D3-8
1.3.3. Seepage Flow Simulations.....D3-12
1.3.4. Uplift Pressures.....D3-15
1.3.5. Conclusions.....D3-35
1.4. ABUTMENTS SEEPAGE MODEL.....D3-36
1.5. SUMMARY.....D3-42

L I S T O F F I G U R E S

1-1: Schematic of Seepage Flow Model.....D3-10
1-2: Paleoalluvial seepage losses at field permeability....D3-13
1-3: Paleoalluvial seepage losses at 100 X permeability....D3-14
1-4: Elevations on top of buried channel.....D3-16
1-5: Pore pressure elevation head after one year.....D3-17
1-6: Pore pressure elevation head after two years.....D3-18
1-7: Pore pressure elevation head after three years.....D3-19
1-8: Pore pressure elevation head after four years.....D3-20
1-9: Uplift pressure distribution (psi) after one year....D3-21
1-10: Uplift pressure distribution (psi) after two years...D3-22
1-11: Uplift pressure distribution (psi) after three years.D3-23
1-12: Uplift pressure distribution (psi) after four years..D3-24
1-13: Net pressure distribution profile at 200 PCF.....D3-27
1-14: Net pressure distribution profile at 130 PCF.....D3-31
1-15: Net pressure distribution profile at zero PCF.....D3-34
1-16: Abutment seepage surface.....D3-37
1-17: Seepage rate.....D3-40

L I S T O F T A B L E S

1-1: Net pressure distribution at 200 PCF basalt density...D3-26
1-2: Net pressure distribution at 130 PCF basalt density...D3-30
1-3: Net pressure distribution at zero PCF basalt density..D3-33
1-4: Abutments seepage model aquifer parameters.....D3-39
1-5: Abutment seepage rates.....D3-41

D.3 SEEPAGE MODELS

1.1. INTRODUCTION

Numerical simulation of seepage flows by means of digital modeling was used to evaluate potential seepage conditions in the foundation and abutments of the Miner Flat Dam site. The potential seepage path evaluated in the foundation of the dam was a buried paleoalluvial channel consisting of unconsolidated deposits of alluvium of the ancestral pre-basalt North Fork of the White River. Potential seepage paths evaluated in the abutments of the dam included fractured basalt in the right abutment; and basalt, paleocolluvium, and the Supai Formation in the left abutment.

1.2. MODELING METHODOLOGY

The modeling methodology selected to simulate seepage flows and pore pressures in the foundation and abutment materials at the Miner Flat Dam is a finite difference model. The model employs conventional iterative alternating implicit solution of simultaneous partial differential equations governing nonsteady state, two-dimensional groundwater flow between model nodes. The program code used for the Miner Flat Dam seepage simulations is a widely available groundwater flow simulation program referred to as the Prickett-Lonnquist Aquifer Simulation Model (PLASM). The mathematical model was initially prepared by the Illinois State Water Survey (Prickett and Lonquist, 1971). The original PLASM code of Prickett and Lonquist (1971) was retained in the Miner Flat Dam models and modified with a number of subroutines to facilitate input and output data management.

Other modifications to the PLASM code were limited to provisions to deal with dewatered nodes and nodes that were in an initially dewatered or dry condition. Aquifer transmissivities

in the model were based on the product of the permeability and the differential head along the permeability vectors. Because the differential head between dry nodes is zero, the transmissivity between dry nodes will always remain at zero under the original PLASM code. Consequently, dry nodes will always remain dry because water cannot flow into an area of zero transmissivity. Accordingly, minor reprogramming of the original PLASM code was required to revise this particular aspect of the original model.

Selection of a finite difference model for numerical simulation of seepage flow in the buried channel at the Miner Flat Dam was based on consideration of several factors:

1. Digital modeling provided considerable advantages over steady state and transient flow net analyses by responding to the complex three-dimensional distribution of boundary conditions at the site.
2. Laborious construction of transient flow nets was avoided by the application of digital modeling with the result that both transient and steady state seepage conditions were determined rapidly for a wide range of input parameters.
3. The model selected is well documented and easily acquired.
4. The model is a valid numerical model of proven credibility.
5. The model is easily adapted to most computers.
6. The model output may be modified to a number of easily used formats.
7. Input parameters required for the model are based on information that is normally provided by conventional field investigations and which does not require unusual or difficult field tests and measurements.
8. Input parameters may be readily modified over a range of values to test the sensitivity of the seepage analysis to the accuracy of the field measurements of aquifer permeability and to assumptions in extrapolation of data from drill hole locations to the rest of the model.

1.2.1. Input/Output Parameters

Input parameters for the Miner Flat Dam seepage models included 11 variables as follows:

1. X and Y coordinates defining the node positions and dimensions.
2. Permeability (hydraulic conductivity) in the X and Y direction (anisotropic as appropriate) based on packer tests of permeability conducted in boreholes in the field.
3. Transmissivity vectors in the X and Y directions to provide anisotropic transmissivity as required.
4. An unconfined aquifer storage coefficient.
5. A confined aquifer storage coefficient.
6. Initial head (pore pressure) in the aquifer.
7. The elevation of the bottom of the aquifer (bottom of the seepage zone).
8. The elevation of the top of the aquifer (top of the seepage zone, i.e., elevation of the base of the confining bed, if any).

Model output parameters consisted of pore pressure (head), rate of seepage flow, change in pore pressure, and an index map of node conditions (i.e., confined, unconfined, dry, sink, boundary, etc.).

The input variables for the seepage model of the buried paleoalluvial channel were based on a 12 by 24 or 288 node array for a total of 3,168 discrete input values. The overall grid dimensions were 2,018.75 feet wide by 16,477.35 feet long. Input variables defining the coordinates of the nodes in the model were based on a nonuniform grid spacing designed to include a reservoir area, the dam, and the area downstream from the dam. The nonuniform grid was designed specifically to provide reasonable definition of the controlling boundary conditions in the foundation, abutments, and downstream areas. Values for the input variables were defined by superimposing the model grid over the

geologic maps and cross sections prepared by Mineral Systems, Inc. as presented in "Preliminary Report - Engineering Geology Miner Flat Dam Site, White Mountain Apache Reservation".

The model of seepage through the abutments of the dam site utilized an 18 by 17 array consisting of 306 nodes for a total of 3,366 discrete input values. The overall dimensions of the abutment seepage model were 4,280 feet parallel to the axis of the proposed dam and 3,580 feet perpendicular the the alignment of the proposed dam axis. The arrays used to define the model nodes and boundary conditions for the model of the paleoalluvial channel are shown on Figure 1-1 and those for the model of seepage through the abutment rocks are shown on Figure 1-16. Geologic information provided by Mineral Systems Inc. was used in defining the input variables to the abutments seepage model.

1.2.2. Boundary Conditions

Geologic conditions identified by the geotechnical investigations of the site and presented in the Mineral Systems, Inc. report which were regarded as significant controlling factors in designing the modeling grids and establishing the boundary conditions in the two seepage models included geologic contacts between different materials, thicknesses of the various materials, elevations of geologic contacts, and field measurements of hydraulic conductivities of the various geologic materials. Terrain data provided by the 1 inch to 200 feet topographic maps with 5-foot contour intervals provided additional definition of boundary conditions influencing seepage paths and hydraulic gradients.

The thickness of the paleoalluvium penetrated by drill holes on a cross section along the dam axis was used to define the the seepage zone or aquifer thickness of the paleoalluvial buried

channel. Basalt overlying the buried channel and bedrocks bounding the bottom and sides of the buried channel were assumed to be impermeable boundaries to groundwater movement. Both the buried channel seepage model and the abutments seepage model included a vertical zone of unconfined permeable paleocolluvium in the left abutment of the damsite.

The unconfined paleocolluvium zone in the left abutment provided direct hydraulic communication between the reservoir area upstream from the dam and the river valley downstream from the dam so that a seepage path was present in the left abutment from the reservoir to the downstream area in the left abutment in both models. The seepage path was assumed to have a minimum thickness of 10 feet normal to the geologic contacts and was assigned the same permeability as the paleocolluvium in the buried channel model. In the abutments seepage model the paleocolluvial seepage path in the left abutment was assumed to be the entire width and thickness of the nodes defining the seepage path and therefore ranged in width from 150 to 270 feet or substantially thicker and wider than the actual field conditions. The paleocolluvial channel representations in the two seepage models was unconfined just as is the paleocolluvial interface between the basalt and Supai Formation in the left abutment shown on the Mineral Systems, Inc. cross sections.

In the buried channel seepage model, a wedge paleocolluvial material, assumed to be 10 feet thick normal to the geologic contacts, was projected into the Miner Flat Dam reservoir area from the buried paleoalluvial channel beneath the basalt. The paleocolluvial wedge provided a direct seepage path from the surface water reservoir into the buried paleocolluvial channel under the basalt foundation at the dam site. The buried channel

seepage model carried the buried paleoalluvial channel downstream from the Miner Flat Dam to a location identified by Mineral Systems, Inc. where the paleoalluvial channel daylights into the river valley and would therefore discharge seepage at the land surface downstream from the dam.

The wedge of paleocolluvial material, 10 feet thick normal to the geologic contacts, was used to provide hydraulic communication in the buried channel seepage model between the buried paleoalluvial channel and the wall or floor of the river channel downstream from the dam. Therefore, if the pore pressure head elevation in the paleoalluvium downstream from the dam increased above the elevation of the interface between the basalt and the underlying Supai Formation exposed in the valley wall downstream from the dam, the model allowed seepage water to flow from the buried channel into the North Fork of the White River.

1.3. BURIED PALEOALLUVIAL CHANNEL SEEPAGE MODEL

Design of the nonuniform grid for the buried channel seepage model was based on consideration of the previously described hydrogeologic boundary conditions that determine the potential gradients of seepage paths in the paleocolluvium and paleoalluvium at the Miner Flat Dam site, assuming that the stratified basalt and bedrocks act as essentially impervious strata confining significant seepage flows to the unconsolidated prebasalt colluvium and alluvium. Field measurements of average hydraulic conductivities in the materials indicated an average value of 5.11×10^{-5} cm/sec for the basalt, or an order of magnitude less permeability than the average value of 1.76×10^{-4} for the paleoalluvium. Grid spacings were selected to provide reasonable definition of the geohydrologic boundary conditions indicated by the Mineral Systems, Inc. geotechnical investigations and

resulted in the following coordinate spacings for the buried channel seepage model:

| Coordinate Interval | X Coordinate Spacings (feet) | Y Coordinate Spacings (feet) |
|---------------------|------------------------------|------------------------------|
| 1 - 2 | 506.25 | 3,844.34 |
| 2 - 3 | 337.50 | 3,844.34 |
| 3 - 4 | 225.00 | 2,562.89 |
| 4 - 5 | 150.00 | 1,708.59 |
| 5 - 6 | 100.00 | 1,139.06 |
| 6 - 7 | 100.00 | 759.38 |
| 7 - 8 | 100.00 | 506.25 |
| 8 - 9 | 100.00 | 337.50 |
| 9 -10 | 100.00 | 225.00 |
| 10 -11 | 100.00 | 150.00 |
| 11 -12 | 100.00 | 100.00 |
| 12 -13 (x-Bndy) | 100.00 | 100.00 |
| 13 -14 Total | 2,018.75 | 100.00 |
| 14 -15 | | 100.00 |
| 15 -16 | | 100.00 |
| 16 -17 | | 100.00 |
| 17 -18 | | 100.00 |
| 18 -19 | | 100.00 |
| 19 -20 | | 100.00 |
| 20 -21 | | 100.00 |
| 21 -22 | | 100.00 |
| 22 -23 | | 100.00 |
| 23 -24 | | 100.00 |
| 24 - y-Bndy | | 100.00 |
| | | Total 16,477.35 |

1.3.1. Input Variables

Transmissivity values used in the buried channel seepage flow simulations were based on the field measurements of an average value of hydraulic conductivity of 1.76×10^{-4} cm/sec as reported in the geotechnical report by Mineral Systems, Inc. The actual values of hydraulic conductivity used in the seepage flow simulations for the paleoalluvium ranged from 1.00×10^{-4} cm/sec to 1.00×10^{-2} cm/sec, i.e., the order of magnitude of the field measurements in one simulation and 100 times the order of magnitude of the field measurements in the second seepage flow simulation. The range of hydraulic conductivities used was employed to test the sensitivity of the model to the accuracy of the field measurements of hydraulic conductivity.

Transmissivity in the model is the product of the saturated

thickness times the permeability. The model automatically recalculated a new transmissivity for each node as water levels in the seepage zone changed. Thus, transmissivity values were continuously adjusted during the seepage flow simulations to reflect the ongoing changes in the pore pressure in the seepage zone.

An unconfined aquifer storage coefficient of 0.01 was used for the paleoalluvial material in the buried channel seepage model based on the assumption that the unconfined storativity of the seepage zone in the paleoalluvium was approximately equal to an assumed value of effective porosity of 1.0 percent in the paleoalluvial materials. Field measurements of the paleoalluvial material porosity were not available, however, sensitivity testing of the porosity assumption indicated that the assumption had little effect on the final seepage flows and pressures indicated by the model. Similar assumptions and sensitivity testing were used to arrive at a presumptive value of 10^{-4} for storativity for confined seepage flow conditions in the seepage zone. The model compared the pore pressure elevation to the elevation of the base of the confining layer for each node in order to assign an unconfined or confined storage coefficient value as appropriate during the seepage flow simulations.

1.3.2. Simulation Concepts

Initial pore pressures in the paleoalluvium seepage zone were established by setting the head elevations in the aquifer equal to the gradient of the North Fork of the White River. A series of transient flow simulations were then conducted to arrive at a simulation of steady state flow in the paleoalluvial aquifer without the presence of the dam and reservoir. The dam and reservoir were then superimposed instantaneously upon the steady state flow condition, with a full reservoir, and subse-

quent transient flow simulations were accomplished until seepage flow from the full reservoir reached steady state flow conditions as indicated by the absence of significant head change at nodes in the model. Steady state seepage flow from the full reservoir was used as a measure of potential seepage pore pressures.

The elevations of the top and bottom of the paleoalluvial seepage zone materials were obtained by superimposing the model grid over a series of geologic cross sections and profiles prepared from the Mineral Systems, Inc. geologic maps and cross section data combined with the topographic map contour elevation data for the study site. The top and bottom elevations define the thickness of the seepage flow path. Moreover, the relationship between the pore pressure head elevation and the elevation at the base of the confining layer, if any, determines if the model uses an unconfined or a confined aquifer storage coefficient. The topographic elevation of the surface outcrop of the paleocolluvial wedge in the left abutment and in the river valley downstream from the dam is the threshold elevation at which seepage pore pressure in the paleoalluvial seepage zone will cause seepage discharge from the valley walls into the White River downstream from the dam.

Figure 1-1 is a schematic of the seepage flow model at the end of one year of seepage flow simulation. The following designations are used on Figure 1-1 to show aquifer and boundary conditions in the model after one year of seepage flow from a full reservoir behind the Miner Flat Dam:

1. C = confined aquifer node - This symbol indicates that the pore pressure in the paleoalluvium/paleocolluvium is at an elevation head in excess of the basal elevation of the overlying basalt and seepage flow is occurring as confined groundwater flow which is exerting an uplift pressure on the overlying basalt and/or the dam.

MINER FLAT DAM WITH RESERVOIR, AFTER 4-YEARS SIMULATION

NODE DESIGNATIONS

CONFINED AQUIFER NODE = C, UNCONFINED AQUIFER NODE = U
 DEWATERED AQUIFER NODE = DRY, NON-AQUIFER NODE = ----

| # | 1 | 2 | 3 | 4 | 5 | 6 | 7 | 8 | 9 | 10 | 11 | 12 |
|----|------|--------|--------|--------|--------|--------|--------|--------|--------|------|------|------|
| 24 | ---- | SOURCE | SOURCE | SOURCE | SOURCE | SOURCE | SOURCE | SOURCE | SOURCE | ---- | ---- | ---- |
| 23 | ---- | C | C | C | C | C | C | C | SOURCE | ---- | ---- | ---- |
| 22 | ---- | C | C | C | C | C | C | C | SOURCE | ---- | ---- | ---- |
| 21 | ---- | C | C | C | C | C | C | C | SOURCE | ---- | ---- | ---- |
| 20 | ---- | C | C | C | C | C | C | C | SOURCE | ---- | ---- | ---- |
| 19 | ---- | C | C | C | C | C | C | C | SOURCE | ---- | ---- | ---- |
| 18 | ---- | C | C | C | C | C | C | C | C | ---- | ---- | ---- |
| 17 | ---- | C | C | C | C | C | C | C | C | C | ---- | ---- |
| 16 | ---- | C | C | C | C | C | C | C | C | C | ---- | ---- |
| 15 | ---- | C | C | C | C | C | C | C | C | C | C | ---- |
| 14 | ---- | C | C | C | C | C | C | C | C | C | C | ---- |
| 13 | ---- | C | C | C | C | C | C | C | C | C | C | ---- |
| 12 | ---- | C | C | C | C | C | C | C | C | C | C | SINK |
| 11 | ---- | C | C | C | C | C | C | C | C | C | C | SINK |
| 10 | ---- | C | C | C | C | C | C | C | C | C | C | SINK |
| 9 | ---- | C | C | C | C | C | C | C | C | C | C | SINK |
| 8 | ---- | C | C | C | C | C | C | C | C | C | C | SINK |
| 7 | ---- | C | C | C | C | C | C | C | C | C | C | SINK |
| 6 | ---- | C | C | C | C | C | C | C | C | C | C | SINK |
| 5 | ---- | C | C | C | C | C | C | C | C | C | U | SINK |
| 4 | ---- | U | C | C | C | C | C | C | C | C | U | SINK |
| 3 | ---- | U | C | C | C | C | C | C | C | C | U | SINK |
| 2 | ---- | U | C | U | U | U | U | U | U | U | U | SINK |
| 1 | ---- | SINK | SINK | SINK | SINK | SINK | SINK | SINK | SINK | SINK | SINK | SINK |

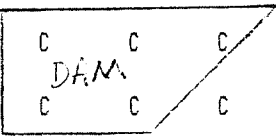


Fig. 1-1: Schematic of Seepage Flow Model

2. U = unconfined aquifer node - This symbol indicates that seepage flow is taking place in the paleoalluvium/paleocolluvium, however, the pore pressure has not caused the phreatic surface (potentiometric surface) to rise to the basal elevation of the overlying basalt and seepage flow is occurring without exerting an uplift pressure on the basalt and/or dam.
3. DRY = dewatered aquifer node - This symbol indicates a node in which the paleoalluvial/paleocolluvial material is entirely drained. This condition exists in the model only as an initial condition in the wedge of paleocolluvium between the buried paleoalluvium and the river valley and disappears during the flow simulations as the seepage pressure elevation rises in the buried paleoalluvial channel seepage path and seepage flows over the threshold through the paleocolluvium nodes and into the row of sinks representing the river valley.
4. --- = nonaquifer node - This symbol indicates a node with zero permeability and zero transmissivity, i.e., a no flow boundary within the model. No flow boundaries are used to represent the right side of the paleoalluvial channel and to represent the portion of the left reservoir bank and left abutment consisting of the Supai Formation.
5. SOURCE = reservoir or source - This symbol indicates the area within the model which supplies water to simulate either the steady state source of recharge to the paleoalluvial seepage path from the river during pre-dam conditions or the steady state source of recharge to the paleoalluvial seepage path from the Miner Flat reservoir. These nodes are assigned essentially infinite storativity values in the model.
6. SINK = discharge location - This symbol indicates the location of a node which has been assigned essentially infinite storativity in the model and which elevation is set low enough that seepage always flows from adjacent nodes into this type of node anytime there is water available in the adjacent nodes. The sink nodes are used to represent the White River valley downstream from the proposed dam in order to provide a place for seepage flow to discharge laterally from the paleoalluvial channel into the river valley when seepage pore pressures become sufficient to support such discharge. The sink nodes are also used across row 1 of the model to simulate the location at which the paleoalluvial channel is intersected by the river valley downstream from the damsite and to which confined or unconfined seepage flow in the paleoalluvial channel must discharge.

As shown on Figure 1-1, the five nodes in the model located within the foundation area of the proposed Miner Flat Dam are (6,17), (6,18), (7,17), (7,18), and (8,18). The grid spacing in the vicinity of the dam and reservoir is 100 by 100 feet, includ-

ing the nodes within the foundation area.

1.3.3. Seepage Flow Simulations

The number of time increments and the duration of each time increment required to reach steady state seepage flow from the continuously full surface water reservoir condition was established by trial and error transient seepage flow simulations. The transient seepage flow simulations indicated that when the order of magnitude of the average measured field hydraulic conductivity of 1.00×10^{-4} cm/sec was used as an input variable, essentially steady state seepage flow was established by the end of four years of seepage in the paleoalluvial materials.

As shown on Figure 1-2, seepage losses from the reservoir through the paleoalluvial materials were about seven gallons per minute. Seven gallons per minute amounts to about 11.3 acre-feet per year of seepage losses. The rate of seepage loss as determined by the model is related directly and linearly to the hydraulic conductivity of the seepage path materials. Accordingly, if it is assumed for the sake of sensitivity testing that the field measurement values of hydraulic conductivity for the paleoalluvial materials were increased of two orders of magnitude by a multiple of 100, the rate of seepage under steady state conditions would be about 700 gpm or 1129 acre-feet per year as shown on Figure 1-3. The estimated seepage losses shown on Figures 1-2 and 1-3 represent only the steady state seepage losses through the paleoalluvial materials and are not indicative of bank loss or bank storage rates for the entire reservoir.

Surface water hydrology analysis for the watershed indicates that an average of 50,000 to 60,000 acre-feet per year of water will be spilled over the dam annually. In view of this fact, it is concluded that annual seepage losses of 1,129 acre-feet to the

Miner Flat Dam Seepage Losses Through Buried Channel with Reservoir (Flows Based on Measured Permeability Values)

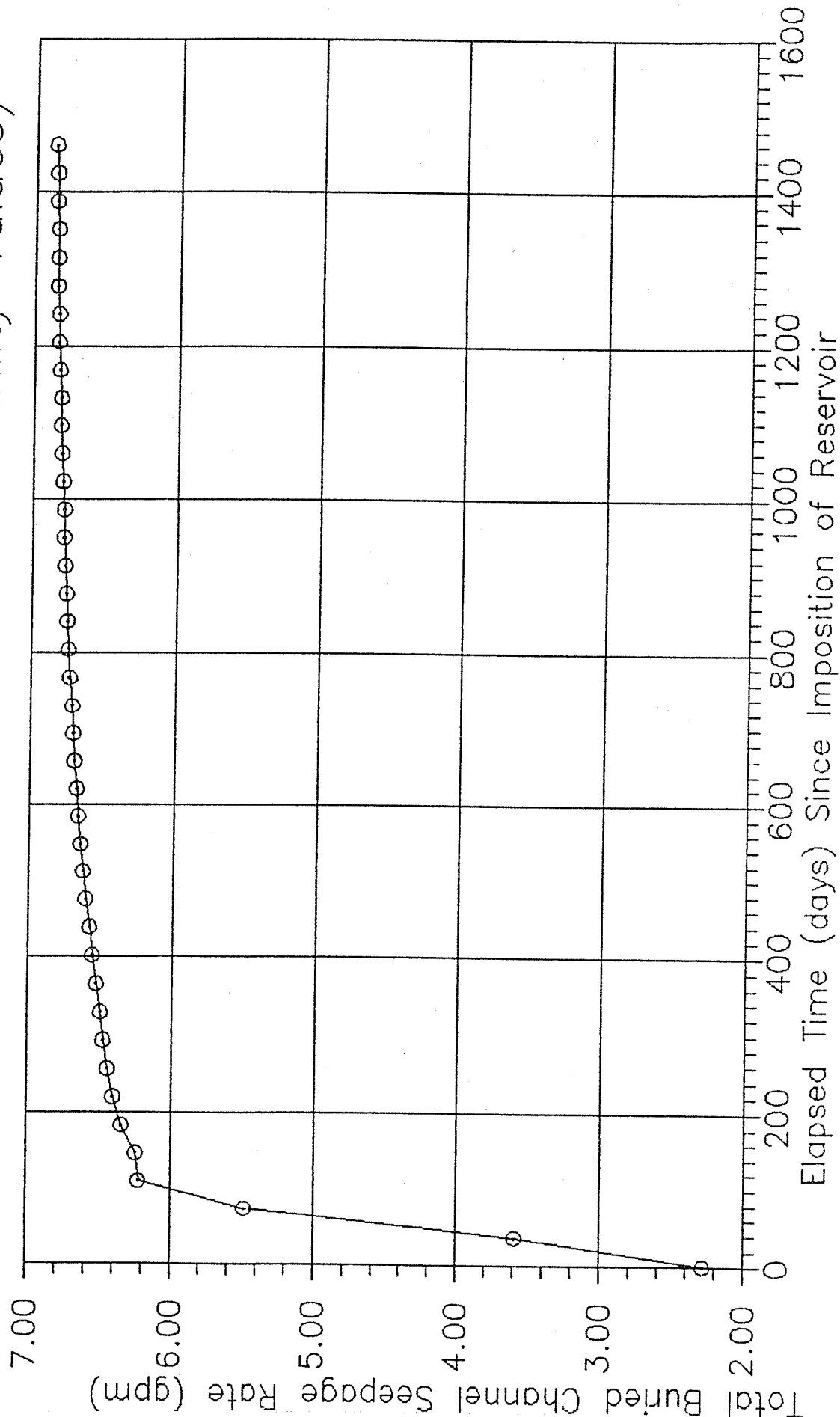


Fig. 1-2: Paleoalluvial seepage losses at field permeability.

Miner Flat Dam
 Seepage Losses Through Buried Channel, with Reservoir
 (Flows Based on Measured Permeability x 100)

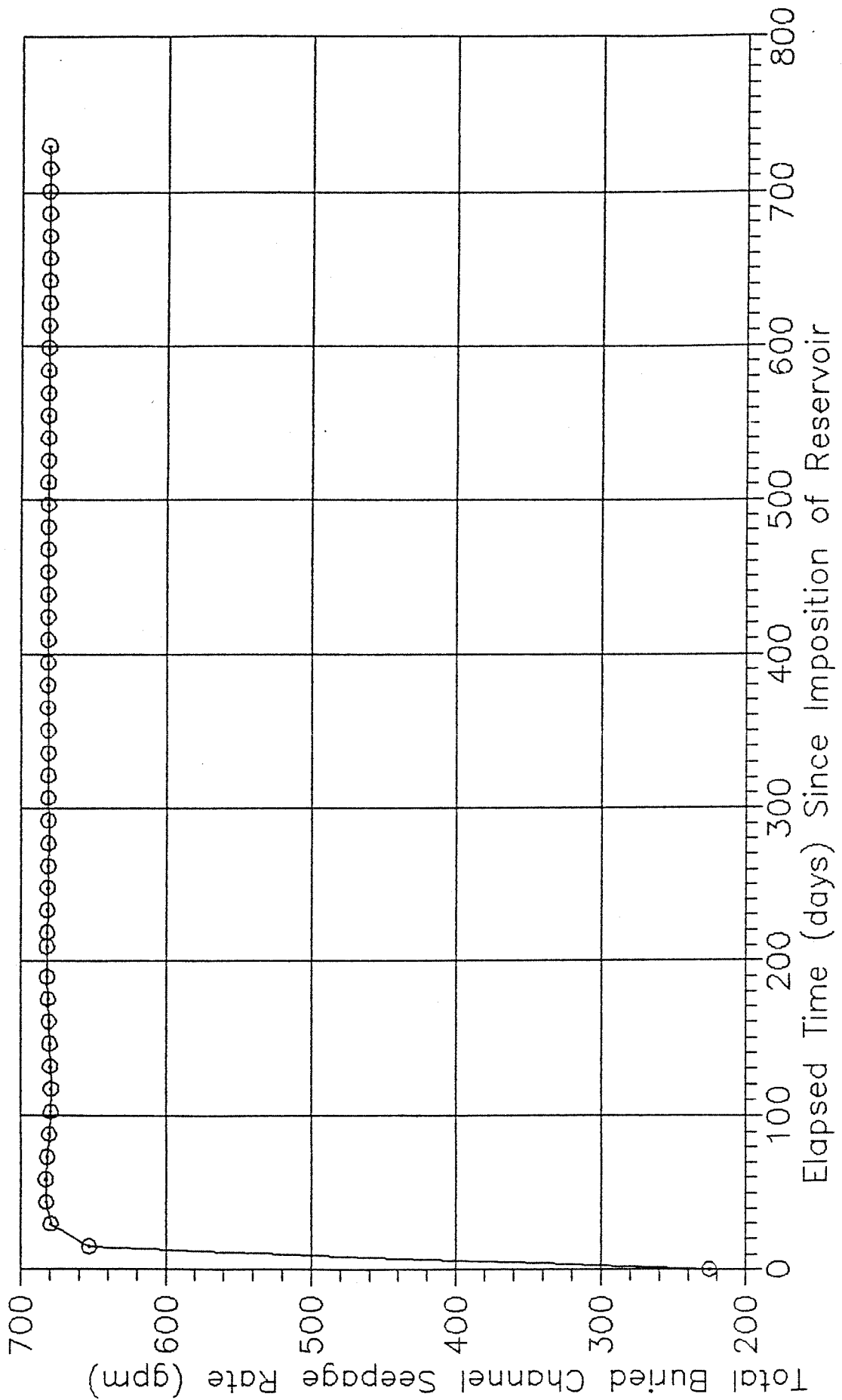


Fig. 1-3: Paleoalluvial seepage losses at 100 X permeability.

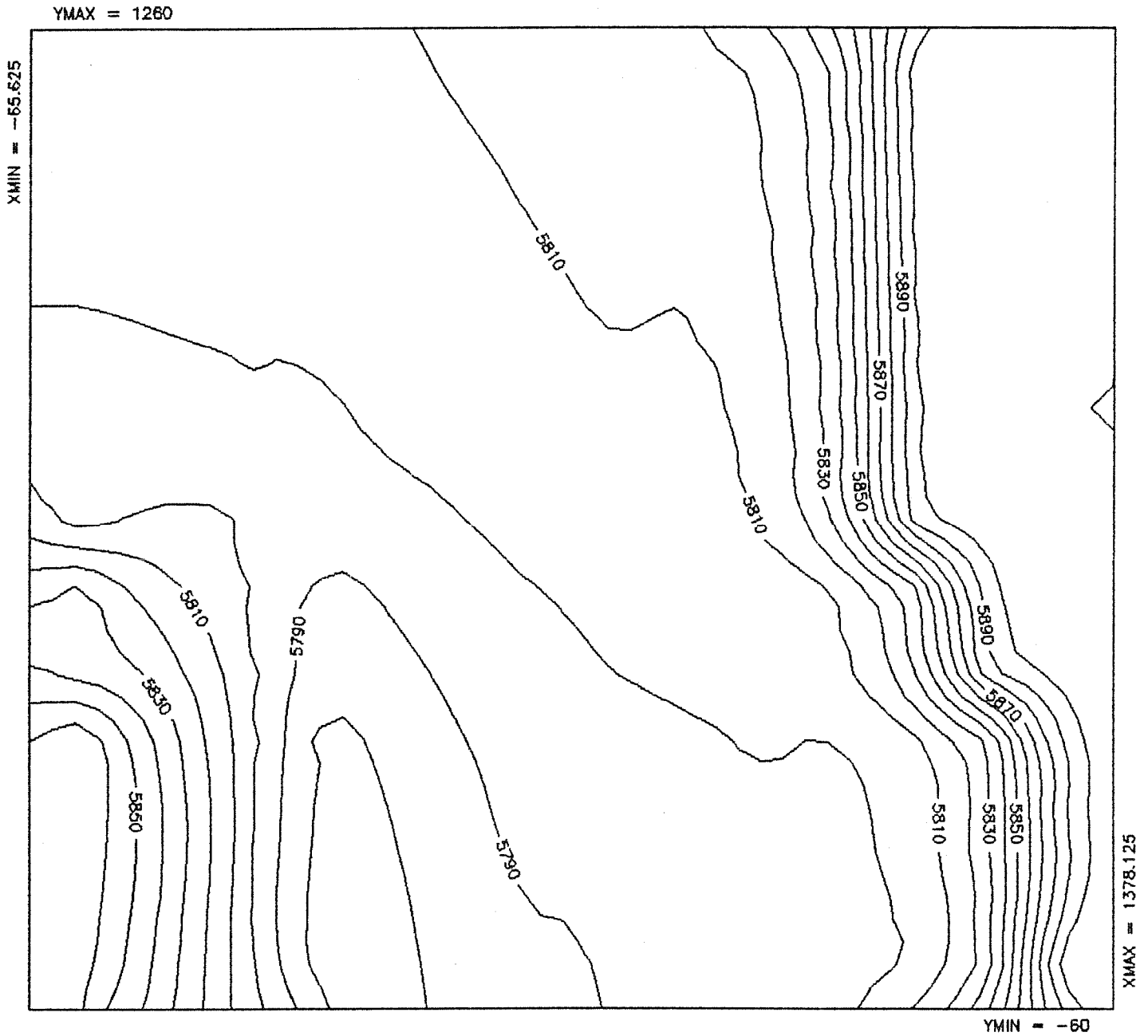
buried paleoalluvial channel will not be significant compared to the reservoir storage and the available water supply.

1.3.4. Uplift Pressures

The finite difference model used to simulate seepage flow through the paleoalluvial buried channel at the Miner Flat Dam provides the same information as provided by conventional flow net analysis. The model determines the pore pressure and seepage rates at known locations as a product of the permeability and the net head change from node to node in the model. Thus, the finite difference model was used as a flow net in the seepage analysis. However, whereas a conventional flow net analysis is conducted along a single vertical slice of the seepage flow path, the finite difference model provided an evaluation of the distribution of head and the associated seepage flow quantity on an areal basis taking into consideration the effects of boundary conditions which would not appear on a simplistic line of section flow net. Accordingly, the finite difference modeling methods used, provided a better evaluation of uplift pressure distribution and seepage flow quantities than would be obtained by conventional flow net analysis.

Output from the Miner Flat Dam seepage flow model was utilized as input for a series of computer generated contour maps of pore pressure distribution and uplift pressure distribution related to steady state seepage in the paleoalluvial buried channel. The elevations on the surface of the buried paleoalluvium (i.e., the elevation of the base of the overlying basalt layer where present) as used in the seepage model are shown on Figure 1-4.

Computer generated maps on Figures 1-5 through 1-8 show the phreatic surface (potentiometric surface) in the buried channel



Upper Surface Elevation of Buried Gravel Channel

Fig. 1-4: Elevations on top of buried channel.

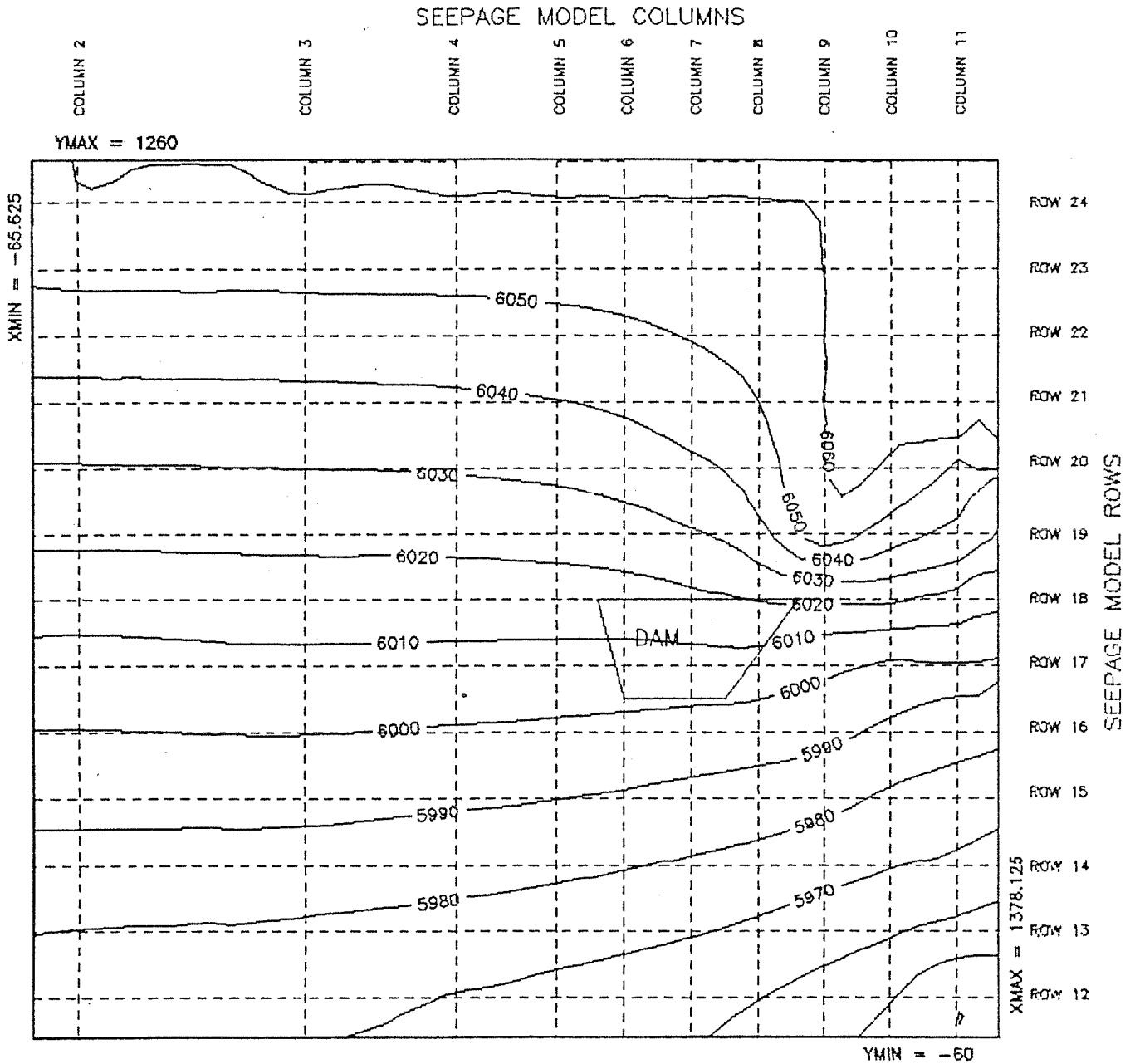


Fig. 5: Buried channel head (ft) at 1 year.

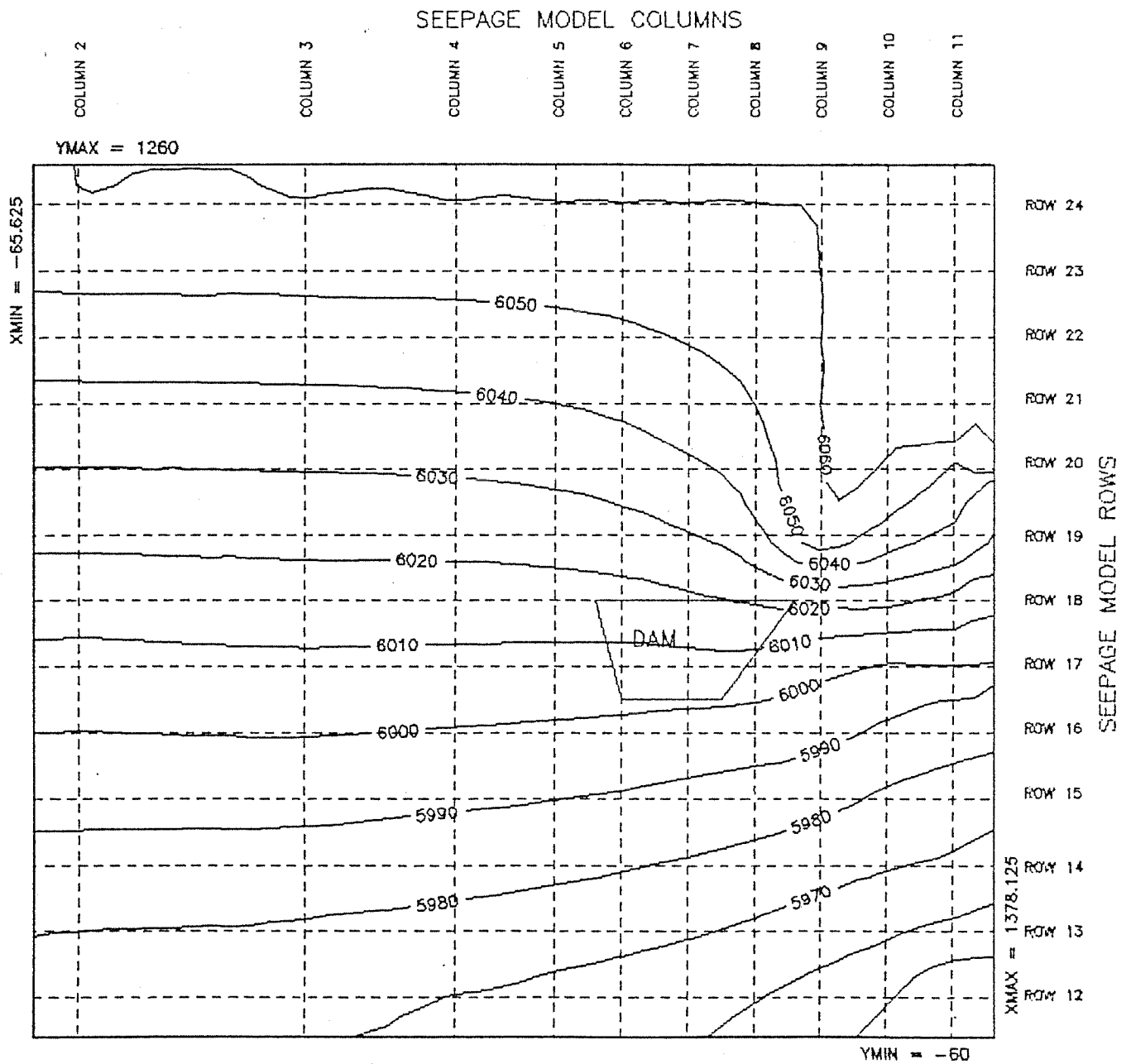


Fig. 6: Buried channel head (ft) at 2 years.

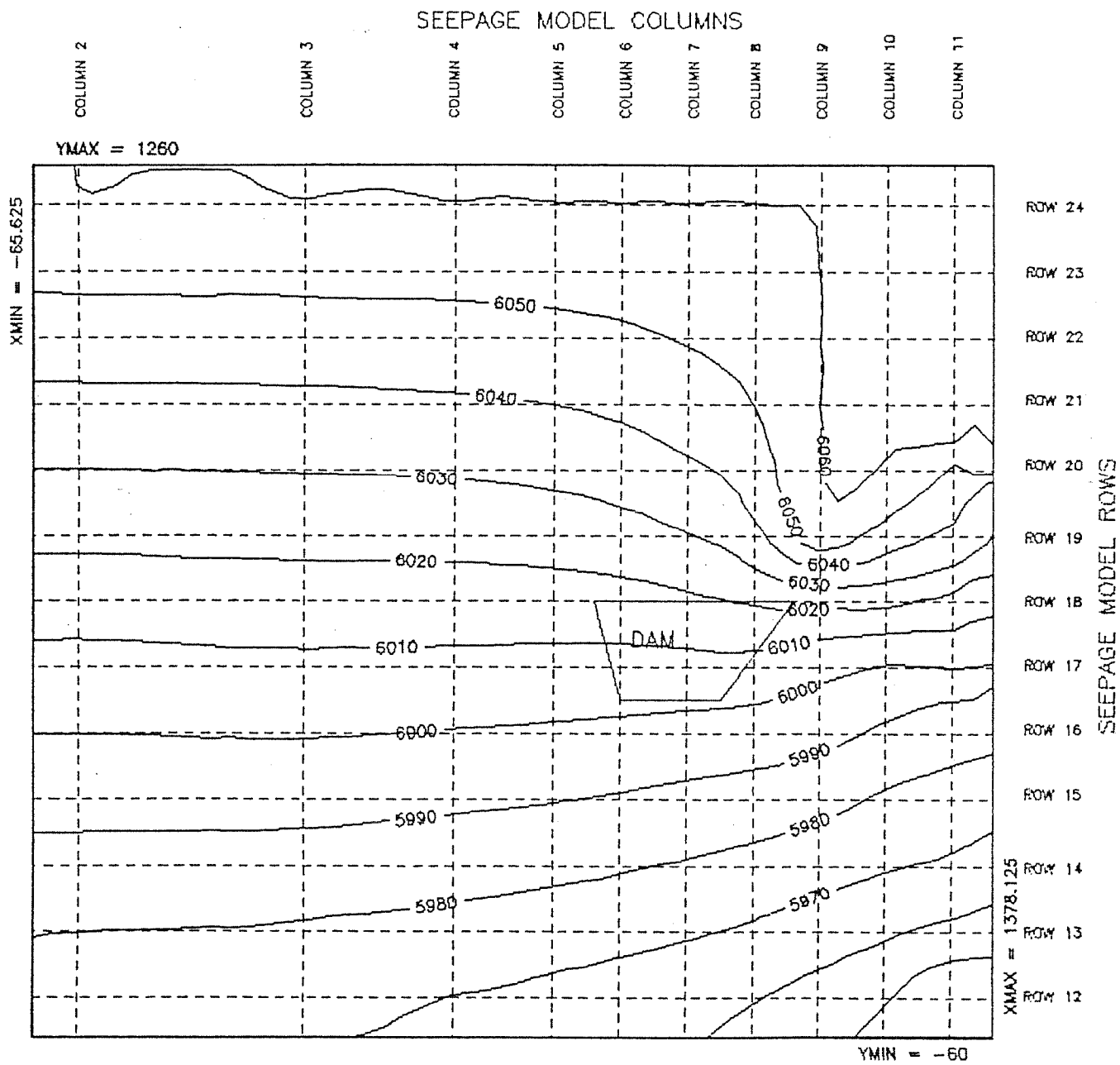


Fig. 7: Buried channel head (ft) at 3 years.

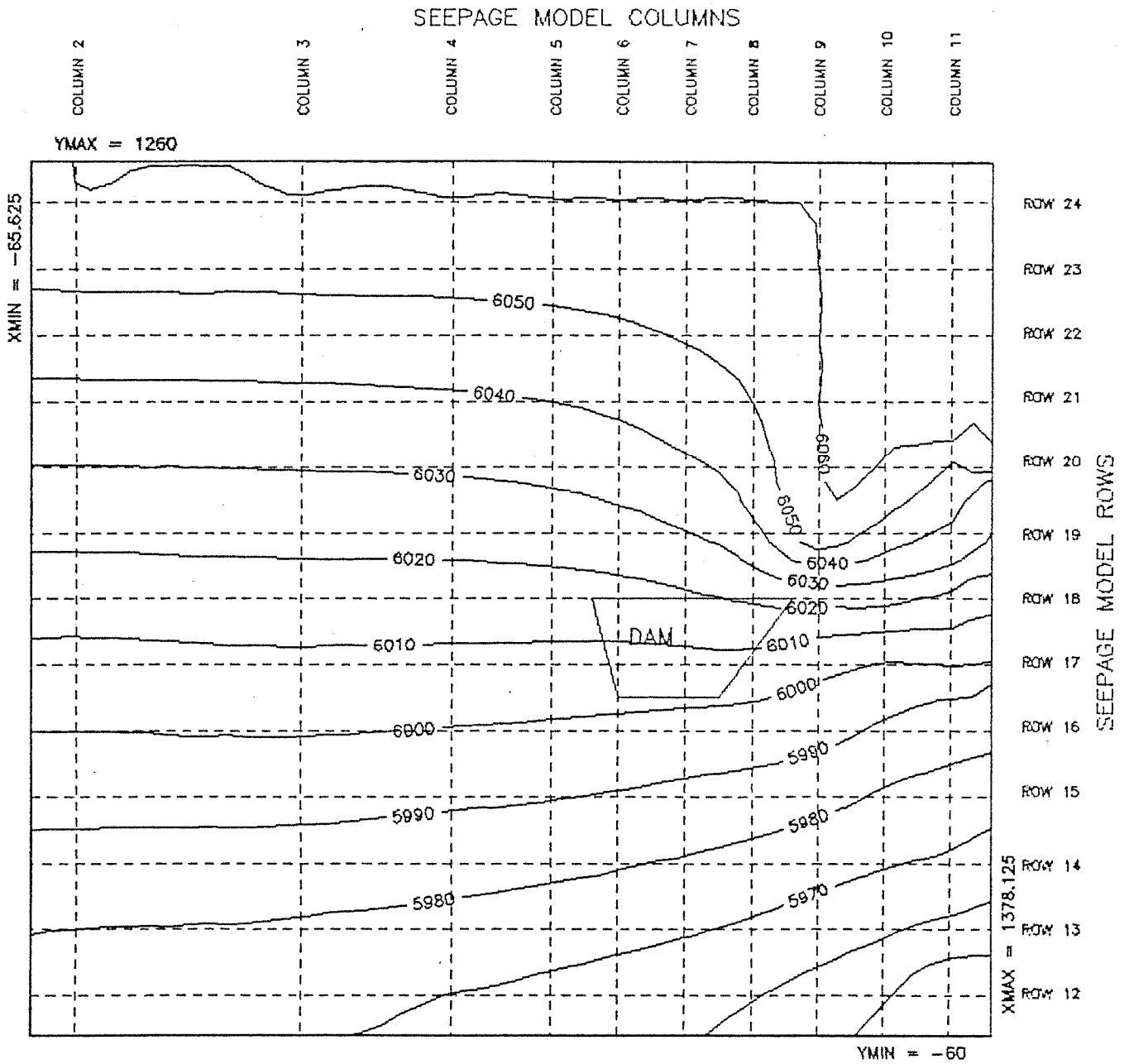


Fig. 8: Buried channel head (ft) at 4 years.

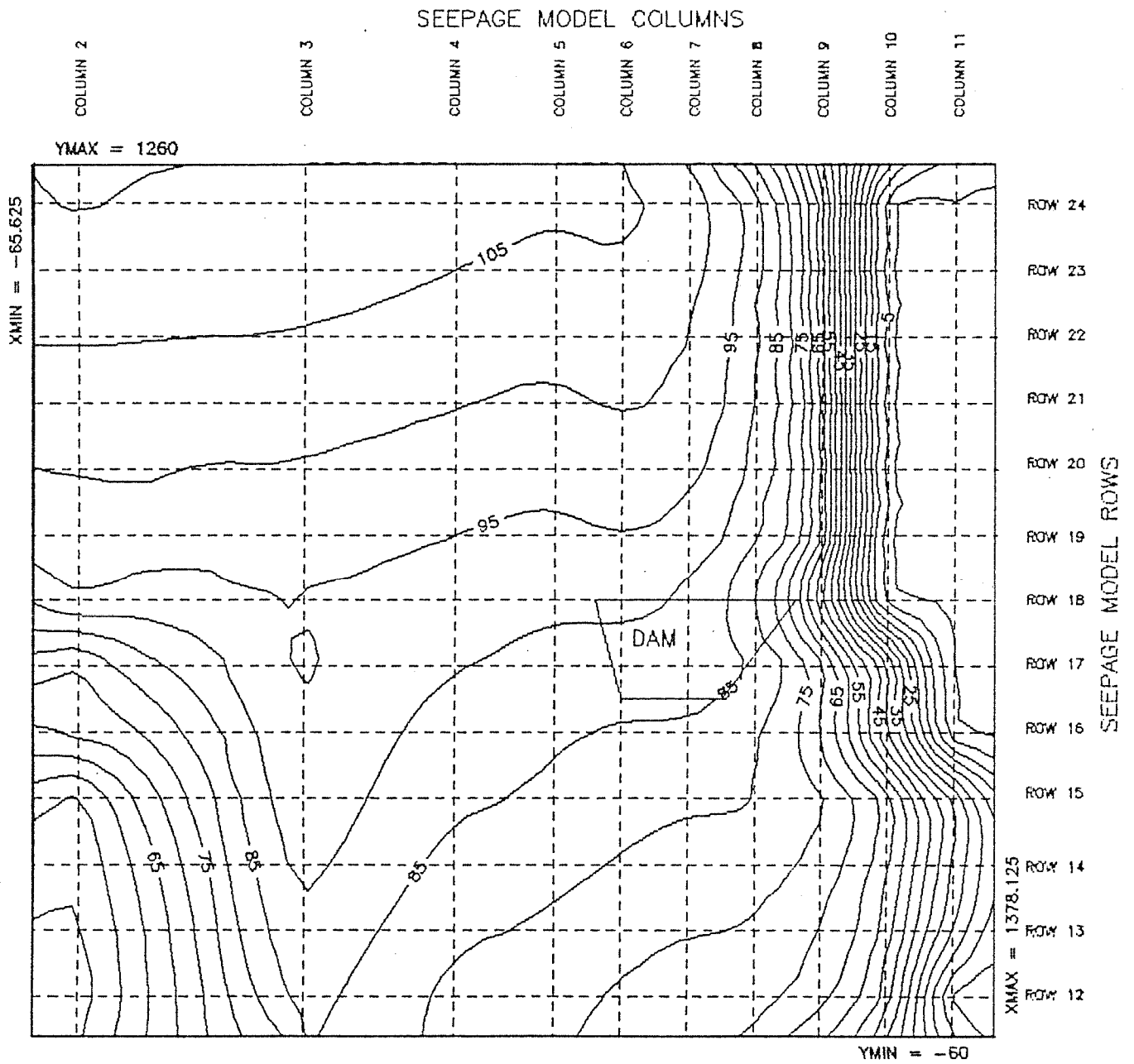
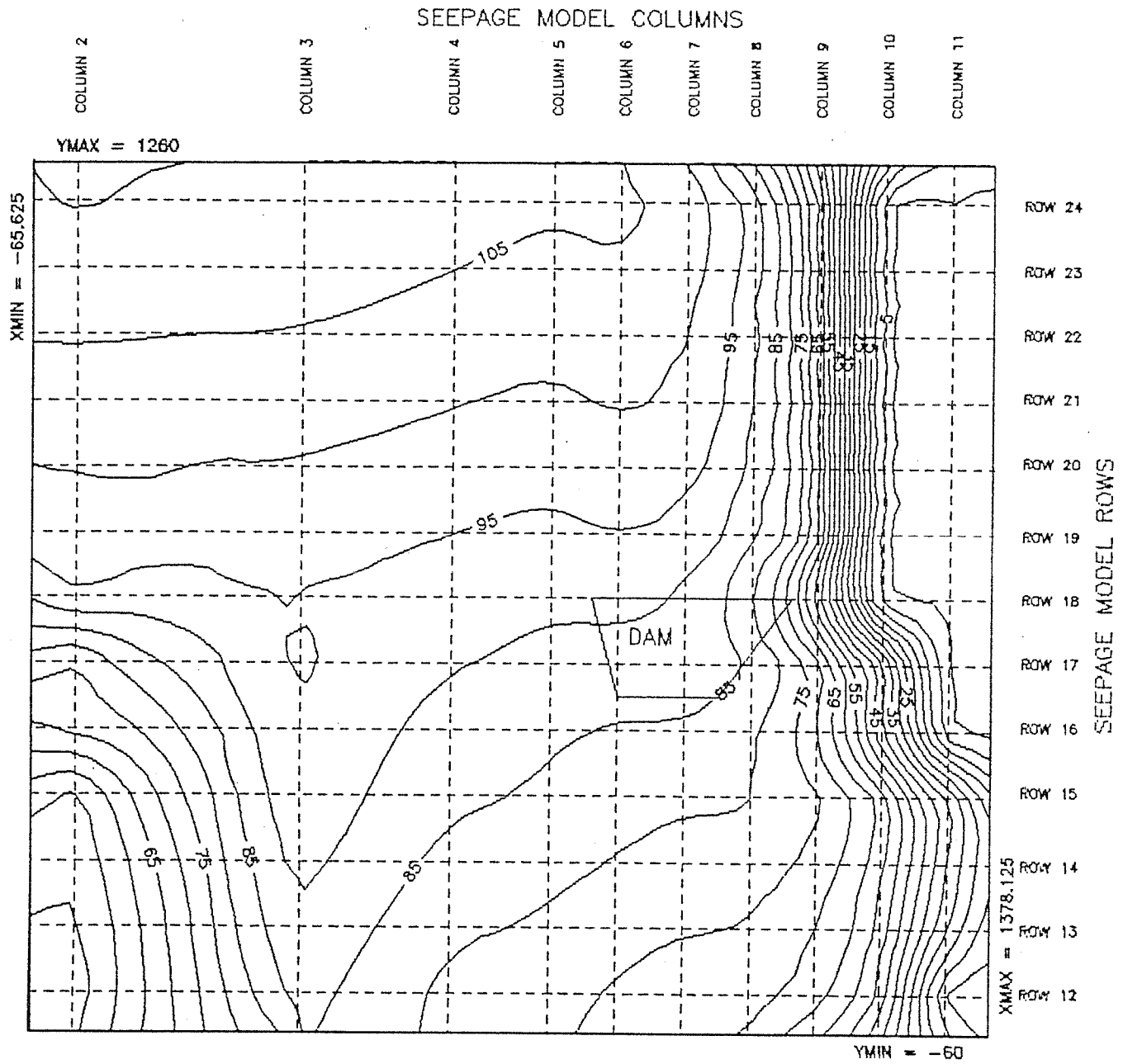


Fig. 9: Buried channel uplift pressure (psi) at 1 year.



g. 10: Buried channel uplift pressure (psi) at 2 years.

Fig. 1-10: Uplift pressure distribution (psi) after two years.

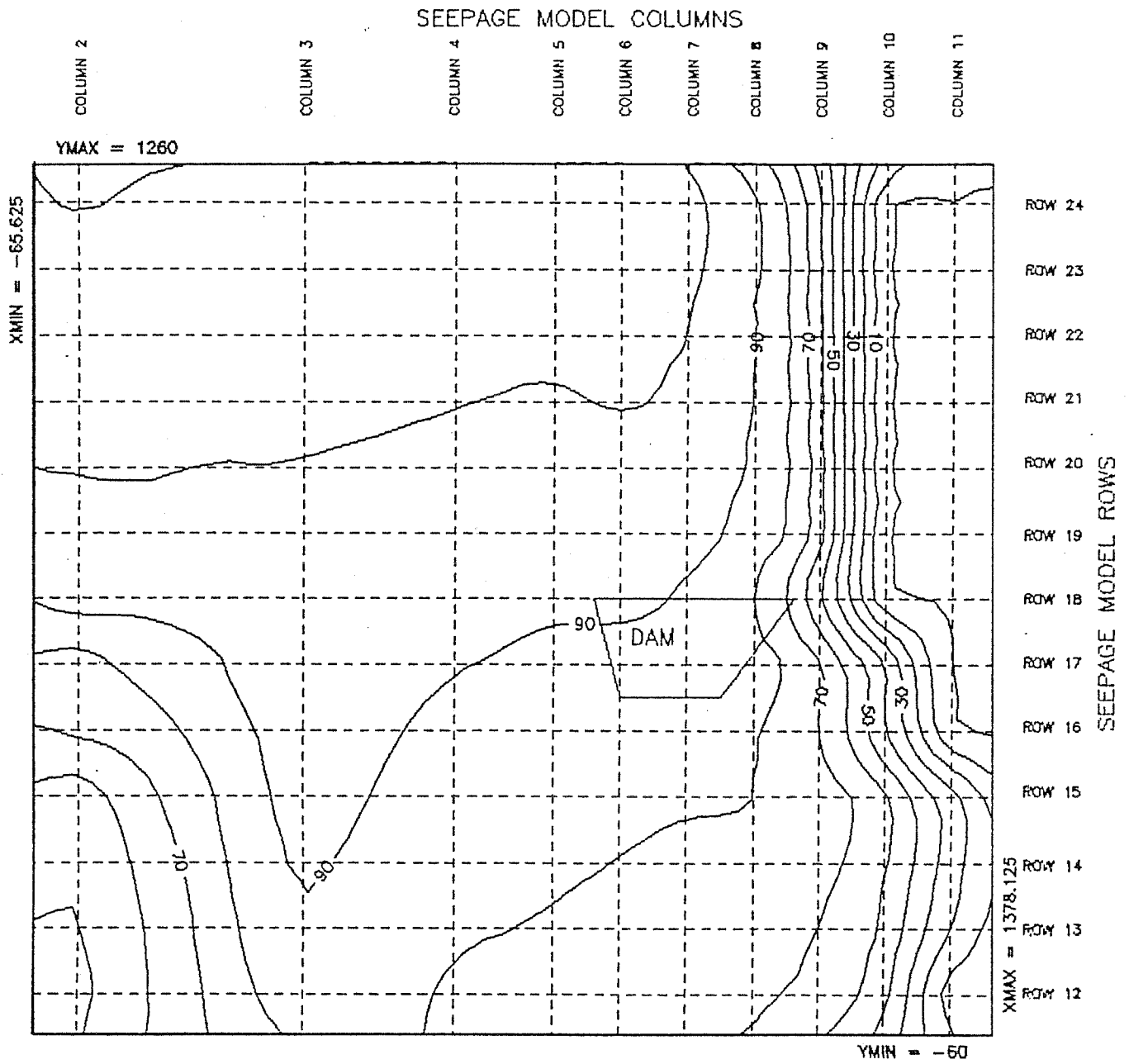


Fig. 11: Buried channel uplift pressure (psi) at 3 years.

Fig. 1-11: Uplift pressure distribution (psi) after three years.

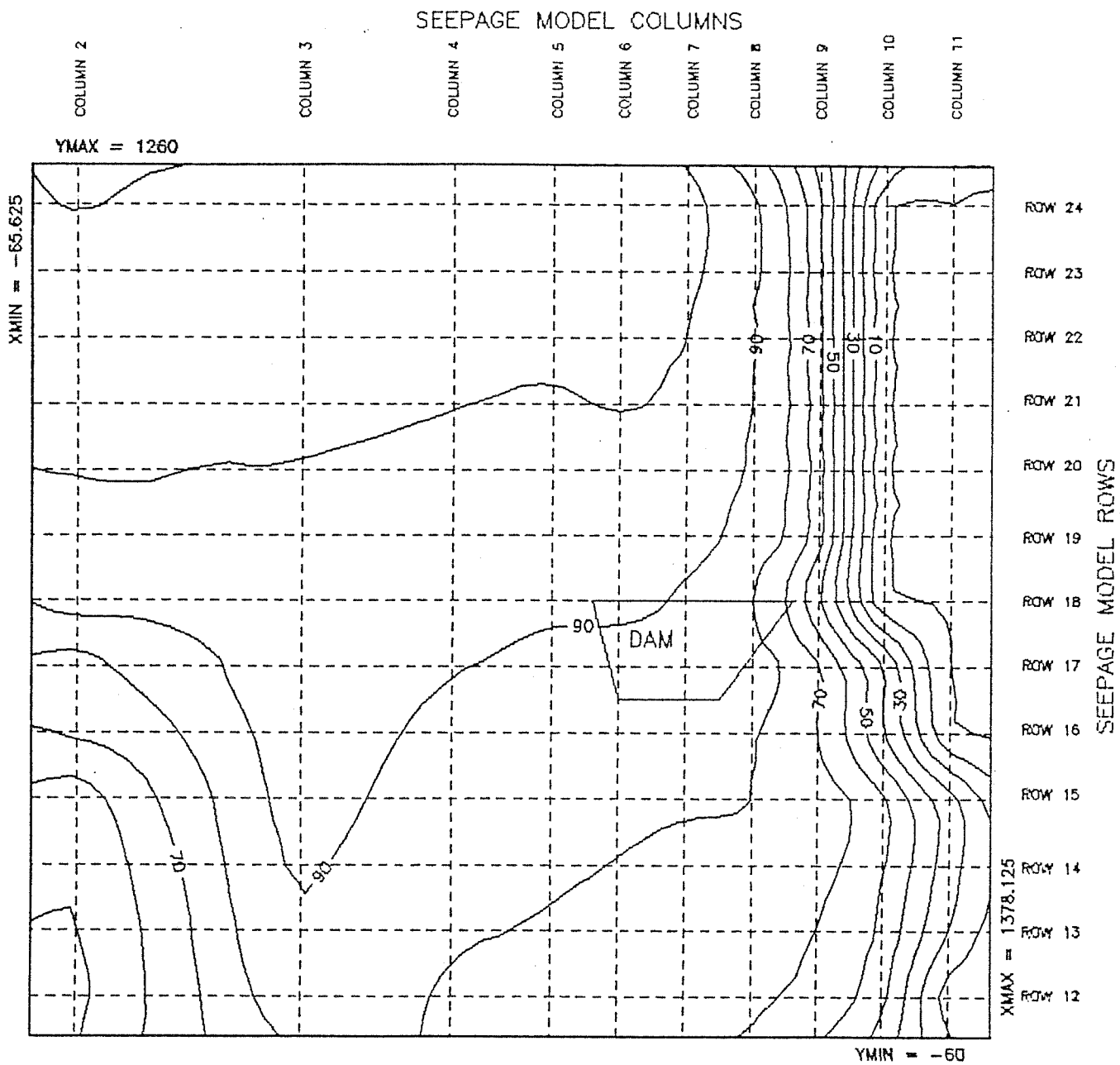


Fig. 12: Buried channel uplift pressure (psi) at 4 years.

Fig. 1-12: Uplift pressure distribution (psi) after four years.

at one, two, three, and four years of simulation of continuous seepage flow, respectively. Computer generated maps on Figures 1-9 through 1-12 show the distribution of uplift pressures in the buried channel as calculated from the elevation difference between the top of the buried channel (base of the overlying basalt) and the pore pressure head (potentiometric surface).

The uplift pressures indicated by the buried channel seepage model were compared to structural pressure by looking at specific nodes in the model that fall within the area of the foundation of the dam. Uplift pressure under the basalt in the floor of the river channel downstream from the dam was also compared to rock overburden pressure exerted by the basalt underlying the river channel at the downstream toe of the dam. The comparison of uplift pressure from the buried paleoalluvial channel and the associated paleocolluvium to the pressure load of the proposed concrete gravity dam and the basalt overlying the buried seepage paths is shown on Table 1-1. A net pressure profile from the upstream face of the dam to the downstream river channel is shown on Figure 1-13.

The data presented on Table 1-1 are from model nodes that lie either under the dam or in the river channel downstream from the dam. Node (7,18) is located at the upstream face of the dam as are all of the foundation area nodes on model row 18. Several nodes are presented as fractional locations between nodes in the seepage model in order to conform to the locations of calculated structural pressures for the concrete gravity dam. Pore pressure data for the fractional locations are extrapolated from adjacent nodes in the model. The node at (7,16) is defined on Table 1-1 as being in the "apron" of the dam. The apron as used on Table 1-1 is an area of rock excavation in the basalt at the toe of the

MINER FLAT DAM FOUNDATION AND DOWNSTREAM RIVER CHANNEL

ROCK DENSITY = 200 PCF
 WATER DENSITY = 62.4 PCF

| DAM NODES (X,Y) | FOUNDATIONAL | | ROCK OVERBURDEN THICKNESS (FEET) | PNEUMATIC SURFACE ELEVATION (FEET) | STRUCTURAL BEARING PRESSURE (PSI) | ROCK OVERBURDEN PRESSURE (FEET) | TOTAL LOAD (PSI) |
|-----------------------|------------------------------------------|--------------------------------------|-------------------------------------------|---------------------------------------------|--------------------------------------------|------------------------------------------|------------------------|
| | CONFINING BASE ELEVATION (FEET) | OR CHANNEL ELEVATION (FEET) | | | | | |
| DAM (7,18) | 5812.00 | 5907 | 95.00 | 6017.84 | 100.7 | 131.9 | 232.6 |
| DAM (7,17.28) | 5805.72 | 5907 | 101.28 | 6009.63 | 92.3 | 140.7 | 233.0 |
| DAM (7,17.22) | 5805.20 | 5895 | 89.80 | 6008.95 | 96.7 | 124.7 | 221.4 |
| DAM (7,16.80) | 5802.93 | 5885 | 82.07 | 6004.41 | 62.8 | 114.0 | 176.8 |
| TOE (7,16.375) | 5802.20 | 5885 | 82.80 | 6000.10 | 130.3 | 115.0 | 245.3 |
| AFROM (7,16) | 5801.55 | 5895 | 93.45 | 5996.29 | .0 | 129.8 | 129.8 |
| CHANNEL (7,15) | 5800.84 | 5909 | 108.16 | 5987.24 | .0 | 150.2 | 150.2 |
| CHANNEL (7,14) | 5799.11 | 5907 | 107.89 | 5979.21 | .0 | 149.8 | 149.8 |

| DAM NODES (X,Y) | SEEPAGE PRESSURE UPLIFT (PSI) | TOTAL LOAD (PSI) | NET UPLIFT | |
|-----------------------|----------------------------------------|------------------------|--------------------|---------------------|
| | | | "-" = LIFT LOAD | "+" = LOAD (PSI) |
| DAM (7,18) | -89.2 | 232.6 | 143.4 | |
| DAM (7,17.28) | -88.4 | 233.0 | 144.6 | |
| DAM (7,17.22) | -88.3 | 221.4 | 133.1 | |
| DAM (7,16.80) | -87.3 | 176.8 | 89.5 | |
| TOE (7,16.375) | -85.8 | 245.3 | 159.5 | |
| AFROM (7,16) | -84.4 | 129.8 | 45.4 | |
| CHANNEL (7,15) | -80.8 | 150.2 | 69.4 | |
| CHANNEL (7,14) | -78.0 | 149.8 | 71.8 | |

Table 1-1: Net pressure distribution at 200 PCF basalt density.

dam and does not include a concrete structure to provide structural load or pressure. Structural pressure at the toe of the dam is greater than at other locations under the dam due to the rotational forces exerted on the dam under full hydrostatic and hydrodynamic load. The structural pressures are based on an assumed water elevation of 6,062 feet, no tailwater, and ice at the crest of the dam and are the minimum structural pressures for a full reservoir condition.

The rock density used on Table 1-1 represents the upper limit of a range of rock density initially assumed for the lower basalt layer at the dam site which forms the foundation of the dam and provides the confining layer over the buried seepage path and to which the seepage pressures are theoretically transmitted. The assumed rock density of 200 pounds per cubic foot (PCF) used on Table 1-1 was based on the office estimate of the density of a solid core of hard, non-vesicular basalt from the foundation area. The actual result of the approximate density measurement of the core was 204.5 PCF. Subsequent laboratory analysis of 21 samples of the lower basalt indicated a range of rock density of 173 to 181 PCF and an average rock density of 177 PCF for the 21 samples. The samples analysed in the laboratory included discontinuities in the rocks due to fractures and vesicles. The core hole logs from the foundation of the dam as presented in the series of geotechnical reports by Mineral Systems, Inc. indicate that the basalt at and below the foundation elevation is relatively massive and dense with no significant zones of vesicularity, contact scoria, or flow breccia to significantly decrease the density of the rock mass or provide significant discontinuities in the structural and hydraulic integrity of the mass. Accordingly, the average rock density of 177 PCF for the lower basalt

is a reasonable representation of the foundation rock density.

A separate analysis of the net pressure distribution at the foundation area and in the downstream river channel is shown on Table 1-2 and Figure 1-14. The purpose of the analysis shown on Table 1-2 and Figure 1-14 is to determine the hypothetical basalt density in the foundation area at which the combined basalt rock overburden load and structural pressure would equal the seepage uplift pressure at some location in the foundation area. As shown on Table 1-2 and Figure 1-14, the hypothetical density of the basalt in the foundation area must be reduced to 130 PCF before the combined weight of the structure and underlying basalt is diminished to the extent that the structural and overburden pressures are decreased to equal the seepage uplift pressure.

The hypothetical basalt density of 130 PCF, as compared to the measured density of 177 PCF, is required to decrease theoretical load pressure enough to equal the uplift pressure shown by the seepage model. This requires that the basalt density in the foundation be reduced to 73 percent of the density of the measured core, that is, a 27 percent reduction in basalt density. Inspection of the various core logs, inspection of the core, and evaluation of the geologic and geotechnical information regarding the massive basalt strata constituting the foundation rock at the dam site indicates that it is totally improbable and unreasonable to anticipate that discontinuities of any kind might exist in the foundation basalt to the extent that the rock density might be reduced by 27 percent. Accordingly, the conclusion that 177 PCF is a reasonable rock density for the foundation area includes a large factor of safety in regards to seepage uplift pressures in that the rock density of 177 PCF would have to be reduced to something less than 130 PCF before seepage uplift pressure would

MINER FLAT DAM FOUNDATION AND DOWNSTREAM RIVER CHANNEL

ROCK DENSITY = 130 PCF
 WATER DENSITY = 62.4 PCF

| DAM NODES (X, Y) | CONFINING BASE ELEVATION (FEET) | FOUNDATION OR CHANNEL ELEVATION (FEET) | ROCK OVERBURDEN THICKNESS (FEET) | PHREATIC SURFACE ELEVATION (FEET) | STRUCTURAL BEARING PRESSURE (PSI) | ROCK OVERBURDEN PRESSURE (FEET) | TOTAL LOAD (PSI) | SEEPAGE PRESSURE UPLIFT (PSI) | NET UPLIFT "-" = LIFT "+" = LOAD (PSI) |
|------------------------|------------------------------------------|----------------------------------------------------|-------------------------------------------|--------------------------------------------|--------------------------------------------|------------------------------------------|------------------------|----------------------------------------|-------------------------------------------------|
| | | | | | | | | | |
| DAM (7,18) | 5812.00 | 5907 | 95.00 | 6017.84 | 100.7 | 85.8 | 186.5 | -89.2 | 186.5 |
| DAM (7,17.28) | 5805.72 | 5907 | 101.28 | 6009.63 | 92.3 | 91.4 | 183.7 | -88.4 | 183.7 |
| DAM (7,17.22) | 5805.20 | 5895 | 89.80 | 6008.95 | 96.7 | 81.1 | 177.8 | -88.3 | 177.8 |
| TOE (7,16.80) | 5802.93 | 5885 | 82.07 | 6004.41 | 62.8 | 74.1 | 136.9 | -87.3 | 136.9 |
| APRON (7,16.375) | 5801.55 | 5895 | 82.80 | 6000.10 | 130.3 | 74.8 | 205.1 | -85.8 | 205.1 |
| CHANNEL (7,15) | 5800.84 | 5909 | 93.45 | 5996.29 | .0 | 84.4 | 84.4 | -84.4 | 84.4 |
| CHANNEL (7,14) | 5799.11 | 5907 | 108.16 | 5987.24 | .0 | 97.6 | 97.6 | -80.6 | 97.6 |
| | | | 107.89 | 5979.21 | .0 | 97.4 | 97.4 | -78.0 | 97.4 |

Table 1-2: Net pressure distribution at 130 PCF basalt density

MINER FLAT DAM PRESSURE PROFILE

Basalt Density = 130 pcf

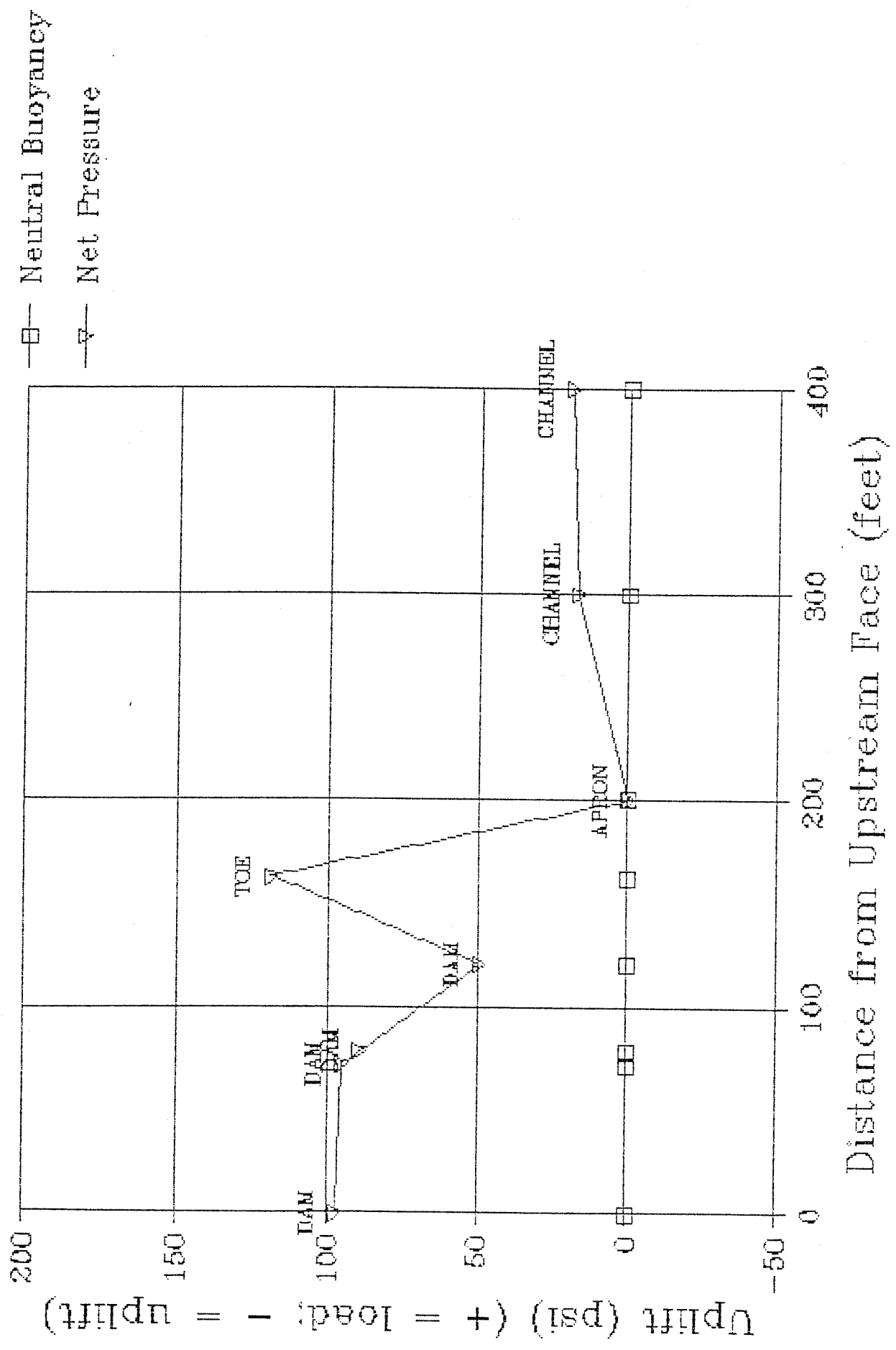


Fig. 1-14: Net pressure distribution profile at 130 PCF basalt density

exceed the load pressure exerted by the combination of the structure and the confining basalt.

A worst case assumption is shown on Table 1-3 and Figure 1-15 where it is assumed that the confined seepage pressure is transmitted directly to the base of the impermeable concrete gravity dam without exerting any pressure against the basalt overlying the buried paleoalluvium and paleocolluvium. This is, of course, a very unrealistic assumption in that it reduces the effective density of the rock in the foundation to zero pounds per cubic foot. The only way this could occur physically would be for the basalt permeability to be such that it was not confining the seepage in the buried pre-basalt channel. If this were the case, the pore pressures profile in the foundation would have a steeper gradient and decrease more rapidly from the upstream face to the toe of the dam than in the present model.

Accordingly, the worst case assumption presented on Table 1-3 and Figure 1-15 represents unrealistically high seepage uplift pressure conditions. Even so, when all of the seepage uplift pressure is transmitted to the concrete gravity dam with no rock overburden pressure, there is only a portion of the upstream to downstream cross section of the dam where seepage pressures from the model exceed the structural pressure of the dam. In other words, the mass of the dam taken as a whole and expressed as structural pressure, continues to exceed the seepage uplift pressure even when the foundation rock density is equated to zero density.

MINER FLAT DAM FOUNDATION AND DOWNSTREAM RIVER CHANNEL

ROCK DENSITY = 200 PCF
 WATER DENSITY = 62.4 PCF

| FOUNDATION | | CONFINING OR CHANNEL ELEVATION (FEET) | ROCK OVERBURDEN THICKNESS (FEET) | PHREATIC SURFACE ELEVATION (FEET) | STRUCTURAL BEARING PRESSURE (PSI) | ROCK OVERBURDEN PRESSURE (FEET) | TOTAL LOAD (PSI) |
|------------|-------------|---------------------------------------|----------------------------------|-----------------------------------|-----------------------------------|---------------------------------|------------------|
| DAM | (7, 18) | 5812.00 | 95.00 | 6017.84 | 100.7 | 131.9 | 232.6 |
| DAM | (7, 17.28) | 5805.72 | 101.28 | 6009.63 | 92.3 | 140.7 | 233.0 |
| DAM | (7, 17.22) | 5805.20 | 89.80 | 6008.95 | 96.7 | 124.7 | 221.4 |
| DAM | (7, 16.80) | 5802.93 | 82.07 | 6004.41 | 62.8 | 114.0 | 176.8 |
| TOE | (7, 16.375) | 5802.20 | 82.80 | 6000.10 | 130.3 | 115.0 | 245.3 |
| APRON | (7, 16) | 5801.55 | 93.45 | 5996.29 | .0 | 129.8 | 129.8 |
| CHANNEL | (7, 15) | 5800.84 | 108.16 | 5987.24 | .0 | 150.2 | 150.2 |
| CHANNEL | (7, 14) | 5799.11 | 107.89 | 5979.21 | .0 | 149.8 | 149.8 |

| SEEPAGE | | NET UPLIFT | STRUCTURAL BEARING PRESSURE (PSI) | NET UPLIFT |
|------------------|-----------------------|--------------------------------|-----------------------------------|--------------------------------|
| DAM NODES (X, Y) | PRESSURE UPLIFT (PSI) | "-" = LIFT "+" = LOAD (PSI) | BEARING PRESSURE (PSI) | "-" = LIFT "+" = LOAD (PSI) |
| DAM (7, 18) | -89.2 | 143.4 | 100.7 | 11.5 |
| DAM (7, 17.28) | -88.4 | 144.6 | 92.3 | 3.9 |
| DAM (7, 17.22) | -88.3 | 133.1 | 96.7 | 8.4 |
| DAM (7, 16.80) | -87.3 | 89.5 | 62.8 | -24.5 |
| TOE (7, 16.375) | -85.8 | 159.5 | 130.3 | 44.5 |
| APRON (7, 16) | -84.4 | 45.4 | .0 | (N/A) |
| CHANNEL (7, 15) | -80.8 | 69.4 | .0 | (N/A) |
| CHANNEL (7, 14) | -78.0 | 71.8 | .0 | (N/A) |

Table 1-3: Net pressure distribution at zero PCF basalt density.

MINER FLAT DAM PRESSURE PROFILE

All Pressure Transmitted to Structure

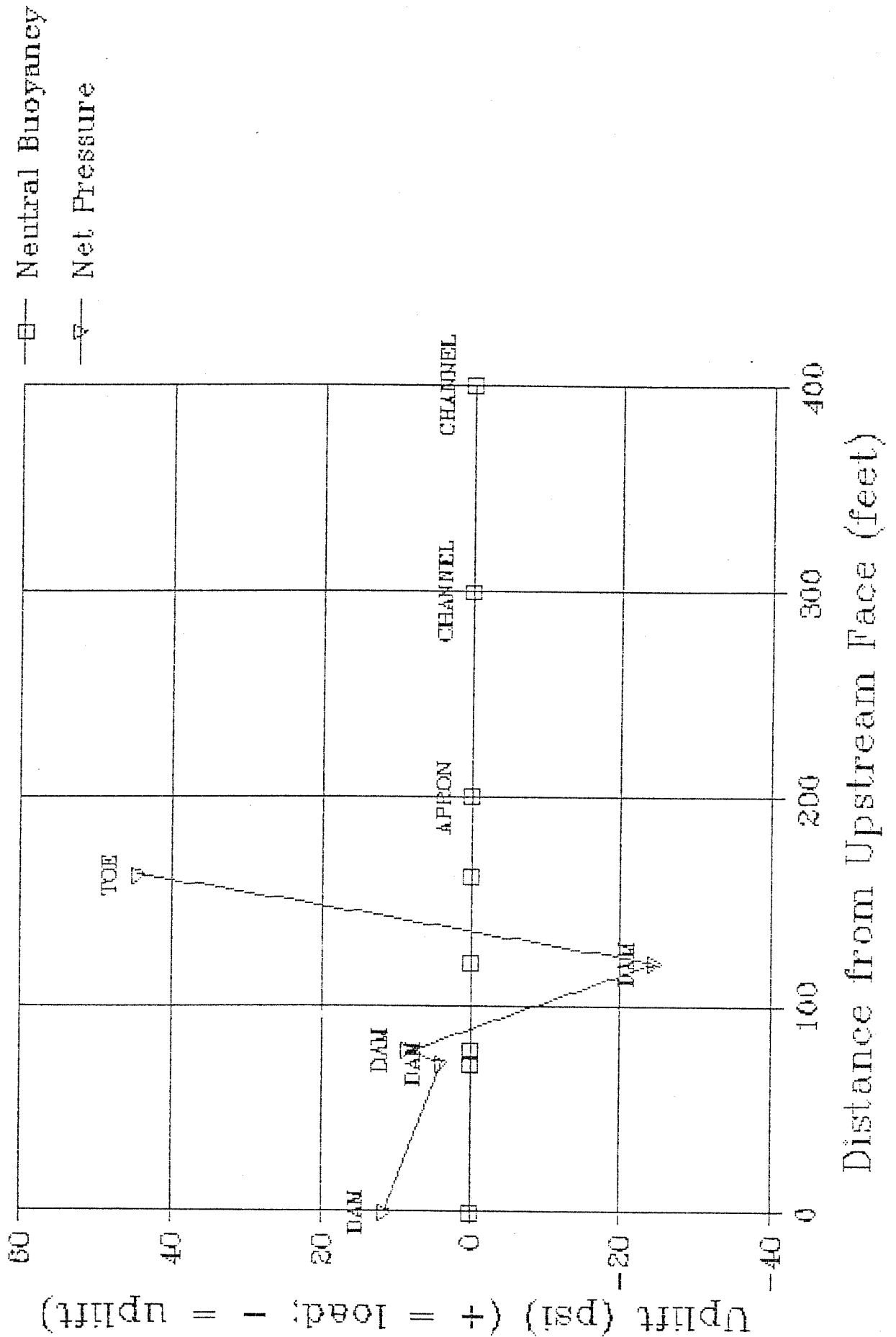


Fig. 1-15: Net pressure distribution profile at zero PCF basalt density.

1.3.5. Conclusions

The 288 node finite difference model used to simulate seepage quantities and pore pressure in the buried pre-basalt paleoalluvial channel at the proposed Miner Flat Dam site indicates that seepage losses through a confined seepage path of the geometry indicated by the geotechnical field investigations would be less than seven gallons per minute or 11.3 acre-feet per year at the measured hydraulic conductivity of a magnitude of 1.00×10^{-4} cm/sec.

Seepage losses calculated by the model are directly proportional to the hydraulic conductivity measured in the field. If the values of hydraulic conductivity measured in the field were erroneously low due to core hole wall damage, plugging of the paleoalluvial interstices by core hole fluid invasion, or other factors adversely affecting the field tests, the seepage quantity calculated by the seepage model would be reduced accordingly. Simulation of seepage flow quantities using a presumed value of hydraulic conductivity 100 times greater than the values measured in the field results in seepage quantities approaching 700 gpm or 1,129 acre-feet per year.

The finite difference seepage model is essentially a three-dimensional flow net analysis and provides the same type of information as a conventional flow net analysis, i.e., distribution of uplift pressure and seepage flow quantity based on differences in head (net head) from one location to another. Seepage uplift pressures determined by flow net analysis, whether it be by conventional two-dimensional flow net construction along a line of section or by finite difference digital modeling, are dependent only upon the shape of the flow net and the distribution of equipotential lines. The permeability assigned to a flow

net or digital model affects only the quantity of seepage flowing through the model but does not affect the shape of the flow net or the distribution of the pressures within the flow net.

Therefore, the uplift pressures generated by the seepage flow model using the field measurements of hydraulic conductivity at 1.00×10^{-4} cm/sec are identical to those using a presumed hydraulic conductivity of any reasonable range of values desired. The generation of calculated uplift pressures in the model is not influenced by the selection of a value of hydraulic conductivity.

Uplift pressures due to seepage in the buried pre-basalt paleoalluvial and paleocolluvial deposits as determined by application of the seepage flow model do not exceed the reasonable range of foundation overburden and structural pressures calculated for the foundation area and downstream river channel. The analysis shows that if the overburden pressure of foundation rock confining the buried pre-basalt seepage path is reduced to zero, there would be a localized zone of buoyancy under part of the concrete gravity dam structure at full reservoir with no tailwater, but that the overall mass of the structure would still exert a positive net downward force in excess of the uplift pressures. The analysis supports the conclusion that potential seepage pressures in the buried pre-basalt materials do not adversely affect the feasibility of the proposed dam site.

1.4. ABUTMENTS SEEPAGE MODEL

Essentially the same finite difference modeling techniques were used to simulate seepage flows through the abutments of the Miner Flat Dam site as were used to simulate seepage flows through the buried paleoalluvial channel. The nonuniform grid delineating the node positions for the abutments seepage model is shown on Figure 1-16. Dimensions for the node array as shown on

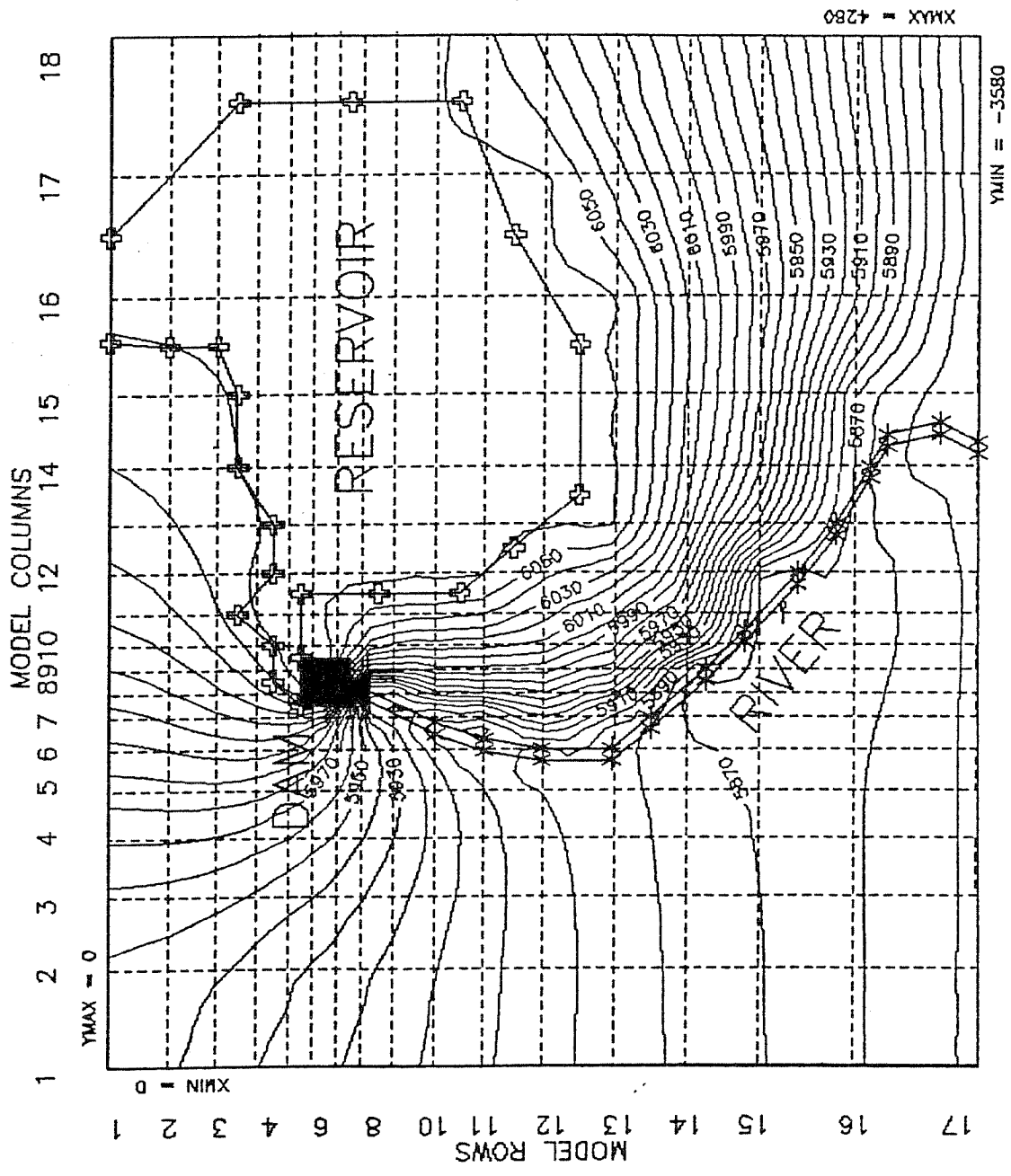


FIGURE 1-16: ABUTMENT SEEPAGE SURFACE

Figure 1-16 are as follows:

| <u>Coordinate Interval</u> | <u>X Coordinate Spacings (feet)</u> | <u>Y Coordinate Spacings (feet)</u> |
|----------------------------|-------------------------------------|-------------------------------------|
| 1 - 2 | 400 | 240 |
| 2 - 3 | 300 | 200 |
| 3 - 4 | 240 | 170 |
| 4 - 5 | 200 | 130 |
| 5 - 6 | 170 | 100 |
| 6 - 7 | 130 | 100 |
| 7 - 8 | 100 | 100 |
| 8 - 9 | 100 | 130 |
| 9 -10 | 100 | 170 |
| 10 -11 | 130 | 200 |
| 11 -12 | 170 | 240 |
| 12 -13 | 200 | 300 |
| 13 -14 | 240 | 300 |
| 14 -15 | 300 | 300 |
| 15 -16 | 400 | 400 |
| 16 -17 | 500 | 500 |
| 17 -18 | 600 | --- |
| Totals | <u>4,280</u> | <u>3,580</u> |

Initial water levels in the abutments seepage model were set at the elevation of the water surface of the White River where the river crossed each row of nodes except in the reservoir area where a water surface elevation of 6,062 feet was used. Aquifer bottom elevations were assumed to be 50 feet lower than the initial water level. Water levels in the sink nodes used to represent the river downstream from the dam were set two feet or more deeper than the river elevation at each row of nodes. Accordingly, flow in the model was always to the sinks representing the river.

No-flow boundary conditions were automatically established by the program code for all exterior boundaries of the model. Hydraulic conductivity values for the different geologic materials were the average values presented in the Mineral Systems Inc. report. Although the program code for the model was written to select confined or unconfined storativity values as appropriate, all of the seepage flow through the abutments took place under unconfined flow conditions with the top of the seepage zone

or aquifer being set equal to the land surface.

Values of hydraulic conductivity for the various types of geologic materials present in the abutments were obtained from the Mineral Systems Inc. report. Values of storativity for the unconfined conditions were assumed. Values of hydraulic conductivity and storativity used in the abutments seepage model are summarized on Table 1-4.

Table 1-4: Abutments seepage model aquifer parameters.

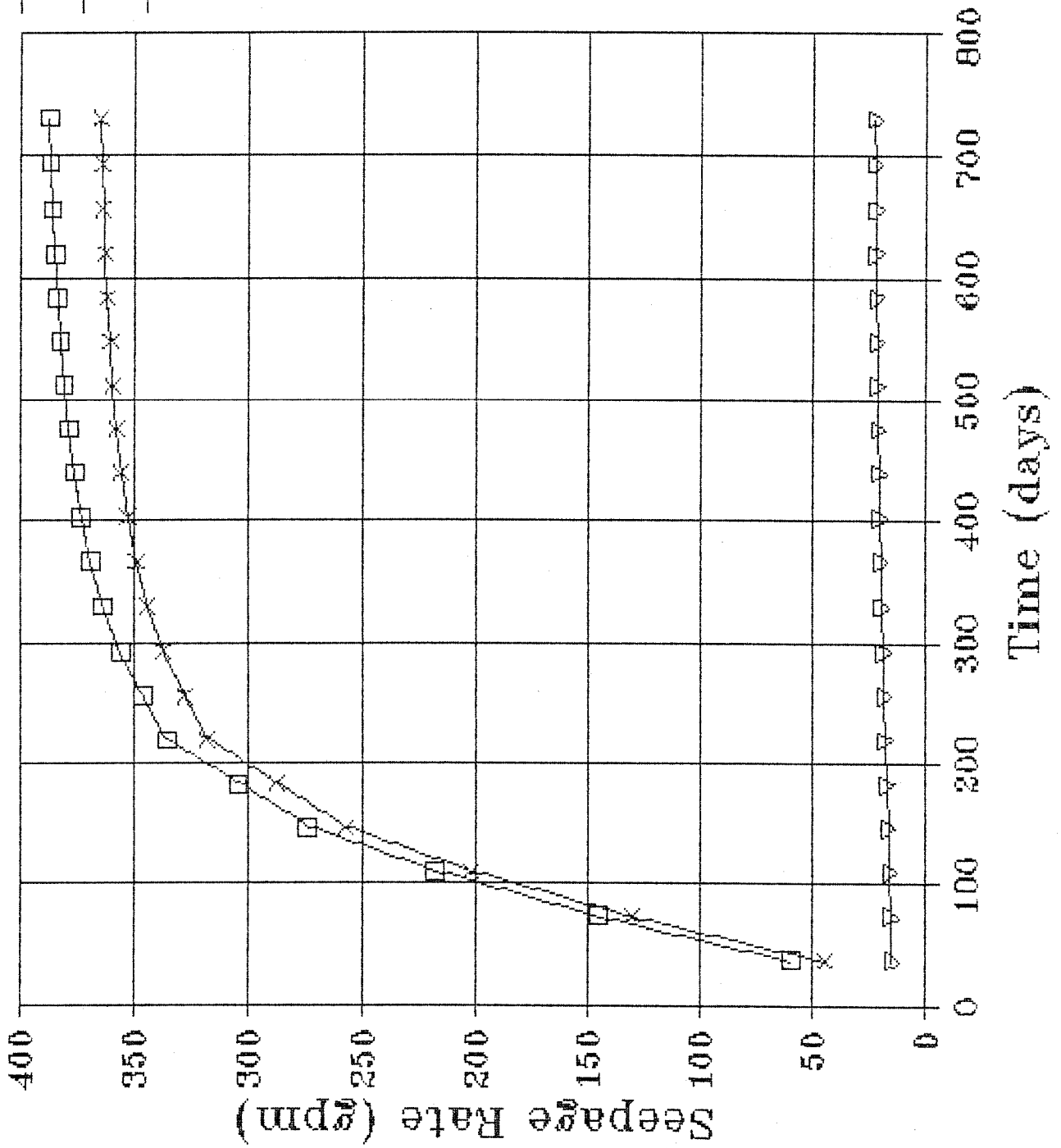
| <u>Geologic Material</u> | <u>Hydraulic Conductivity (gpd/ft²)</u> | <u>Coefficient of Storage</u> |
|--------------------------|----------------------------------------------------|-------------------------------|
| Paleoalluvium | 3.6050 | 0.15 |
| Supai Formation | 7.9734 | 0.10 |
| Basalt | 3.3930 | 0.05 |

Operation of the abutments seepage model from initial conditions consisted of instantaneous imposition of the full reservoir upon the steady state conditions prevailing during pre-Miner Flat Dam Conditions. The lessening of the rate of increase in the seepage flows from the reservoir through the right abutment shown on Figure 1-17 indicates that essentially steady state seepage flows were in effect through the left abutment after 438 days of a two-year long flow simulation of seepage from full reservoir conditions. In view of the fact that it is not anticipated that the reservoir will remain at full storage for continuous periods of one year or more, a duration of 365 days of continuously full storage in the reservoir was selected for modeling seepage through the abutments.

FIG. 1-17: SEEPAGE RATE

Miner Flat Dam Abutments

- Total Seepage
- × Left Abutment
- ▽ Right Abutment



The rate of seepage for the right and left abutments is shown on Table 1-5 in terms of 36.5-day increments. The increasing rates of seepage shown on Table 1-5 correspond to the seepage rate curves shown on Figure 1-17 and reflect the buildup of seepage from the time of instantaneous imposition of the reservoir onto the unsaturated reservoir site to seepage conditions at the end of 365 days of continuously full reservoir conditions.

Table 1-5: Abutment seepage rates.

| Elapsed Time (days) | Right Abutment Seepage Rate (gpm) | Left Abutment Seepage Rate (gpm) | Combined Abutment Seepage Rate (gpm) |
|---------------------|-----------------------------------|----------------------------------|--------------------------------------|
| 36.5 | 14.83 | 44.73 | 59.56 |
| 73.0 | 15.12 | 130.50 | 145.62 |
| 109.5 | 15.69 | 202.38 | 218.07 |
| 146.0 | 16.38 | 257.64 | 274.02 |
| 182.5 | 17.07 | 287.31 | 304.38 |
| 219.0 | 17.72 | 317.78 | 335.50 |
| 255.5 | 18.32 | 327.45 | 345.78 |
| 292.0 | 18.87 | 337.07 | 355.94 |
| 328.5 | 19.36 | 344.03 | 363.39 |
| 365.0 | 19.81 | 349.02 | 368.83 |

As shown on Table 1-5, the combined seepage rate from the left and right abutments of the dam site at the end of one year is about 369 gpm or about 4,450 acre-feet per year, assuming a full reservoir for the entire year. In view of the predicted annual spills of 50,000 to 60,000 acre-feet over the spillway, the simulated seepage loss of 4,450 acre-feet per year is negligible.

A number of factors cause the simulation of seepage flows in the abutments of the dam site to be conservatively large. One factor is the fact that it was assumed that the reservoir was full to the maximum storage elevation of 6,062 feet for the entire year of seepage simulation. In reality, the storage pool will be below an elevation of 6,062 feet much of the time. A

second factor is the no-flow external boundary conditions in the model. For example, seepage flowing from the reservoir towards column 18 in the model (Figure 1-16) encounters a barrier to flow before an equilibrium gradient is established. This forces the water to flow towards row 17 in the model, thus creating higher seepage surface elevations and more seepage discharge to the river than would occur without the presence of the no-flow boundary adjacent to column 18. Similar increases in seepage surface elevations and seepage flow occur in the right abutment due to the presence of no-flow boundaries at the top and left side of the seepage model.

A final factor increasing the rate of seepage flow to the river downstream from the dam is that the sink nodes representing the river in the model are set at elevations much lower than the actual river elevation in a number of instances to equalize initial heads in the sinks and prevent internodal transfers of water between sink nodes. Consequently, the differential head between the sink nodes and the adjacent abutment nodes is greater in the model than the actual differential head would be between the river and the abutment rocks in reality. The greater differential head in the model results in greater seepage flows to the sinks representing the river. Accordingly, the rates of simulated seepage flows through the abutments of the dam site are conservatively large due to several factors.

1.5. SUMMARY

The seepage models demonstrate that uplift pressures predicted in the buried paleoalluvial channel under the basalt rock foundation of the dam will not exceed the overall structural and rock overburden pressures exerted by the dam and basalt overlying the channel. If it is conservatively assumed that all

of the uplift pressure from the buried channel is transmitted directly to the dam without any confining pressure being exerted by the rock overburden in the foundation, a small area is identified in the footprint area of the dam where uplift pressures exceed the structural pressure; however, the overall or net structural pressure of the dam is still in excess of the net uplift pressure, even when the weight of the rock in the dam foundation is ignored.

Seepage flow losses through the buried paleoalluvial channel were approximately 11.3 acre-feet per year in a four-year simulation of seepage flow assuming full reservoir conditions. Four-years of seepage simulation were required to obtain steady-state flow conditions in the buried channel starting from initial steady state flow conditions related to the river elevation without the reservoir. Accordingly, the assumption of a continuously full reservoir for a period of four years provides a conservatively high estimate of potential seepage losses in the buried channel within the order of magnitude of hydraulic conductivities measured in the paleoalluvial materials in the field.

Field measured values of hydraulic conductivity in the buried channel materials were arbitrarily assumed to be 100 times more permeable than indicated by the field measurements. The result of this assumption was to increase the annual seepage losses simulated by the model to 1,129 acre-feet per year. Seepage uplift pressures in the buried channel did not change as a result of the assumed increase in hydraulic conductivity.

Flow simulations of seepage through the rocks above river level elevation in the abutments of the dam site were likewise conservatively large and resulted in prediction of about 369 gpm or 4,450 acre-feet per year of total seepage loss through the

right and left abutments. Combined seepage losses predicted for the buried channel and the abutments totaled 5,579 acre-feet per year under the worst case assumptions used in the seepage simulations. In comparison, surface water hydrologic analysis of the dam and reservoir site predicts that annual spills at the site will average in the range of 50,000 to 60,000 acre-feet per year. This means that the excess surface water supply which the dam and reservoir do not have enough capacity to regulate will far exceed the conservatively worst case seepage losses indicated by the models.

REFERENCES

Prickett, T.A., and Lonquist, C.G., 1971, Selected digital computer techniques for groundwater resource evaluation: Illinois State Water Survey Bulletin 55, 62 p.

DESIGN MEMORANDUM

SECTION E

E.1 CONCRETE AGGREGATE

Adequate quantities of suitable concrete aggregate are available at the dam site for the construction of the envisioned concrete gravity dam. The potential aggregate sources are:

- * Approximately 200,000 cubic yards of gravel deposits immediately upstream from the dam
- * Approximately 135,000 cubic yards of basalt excavated from the dam foundation.

These quantities far exceed the total concrete volumes of 141,040 cubic yards for the conventional concrete dam and 127,645 cubic yards for the rolled concrete dam. As indicated in Section J.4 for the roller compacted concrete option, 50-70% of the aggregate will come from the basalt foundation excavation and 30-50% from the gravel source.

The source area for the gravel is a river terrace deposit located immediately upstream of the dam on the west bank of the river and is accessed by the existing drill access road from State Highway 73 as shown on the "General Map B", Sheet A2. The basalt available from the foundation excavation is accessed from upstream and will be processed, stockpiled and excess disposed in the gravel borrow area indicated above.

Photographs of the gravel borrow and rock disposal area are included in Section D, Figure D1.3. As visible in the photographs, the area is timbered and will require clearing prior to use.

Quantity assessment and preliminary material testing for the aggregate is included in the following attached report and memos:

- * "Preliminary Report, Engineering Geology, Miner Flat Dam Site, White Mountain Apache Reservation", Mineral Systems, Inc., November 1983
- * Memorandum, Aggregate Test Pit & Petrographic Analysis for E. Schrader, December 8, 1986.
- * Memorandum, Results of Alkali Reactivity & L.A. Abrasion Tests, MF-102, December 5, 1986.

At this point, because the decision between conventional mass concrete and roller compacted concrete (RCC) has yet to be made and the high degree of confidence in the adequacy of available

aggregate for either technique, detailed mix designs for both options have not been prepared. It is intended that the final mix designs be prepared early in the project as indicated in Section J.4.

E.2 COMMERCIAL CONCRETE PLANTS

The dam site is located in a rural setting. The availability of existing commercial concrete plants is limited to the "Ready Mix" variety used for residential and light commercial structures.

The four plants within a hauling distance of approximately 30 miles from the dam site were surveyed and the results are presented below:

| <u>OPERATOR</u> | <u>DIST (mi)</u> | <u>FIXED BATCH PLANT</u> | <u>PORT. BATCH PLANT</u> | <u>NO. TRUCKS</u> | <u>OWN AGG. SOURCE</u> | <u>AGG. CRUSH/ SCREEN PLANT</u> | <u>AGG. WASH PLANT</u> |
|---------------------------------|------------------|--------------------------|--------------------------|-------------------|------------------------|---------------------------------|------------------------|
| Fort Apache Mat. Whiteriver, AZ | 8 | 1 | 0 | 4 | yes* | yes* | yes* |
| Show Low Rd. Mx. Show Low, AZ | 30 | 2 | 1 | 9 | no | no | no |
| A&A Ready Mix Show Low, AZ | 30 | 1 | 1 | 5 | no | no | no |
| Pierce Const. Show Low, AZ | 30 | 1 | 0 | 2 | no | yes | no |

* Located 20 miles from batch plant & 12 miles from dam site.

Figure E.2.1 "Summary of Commercial Concrete Plants"

E.3 ACCESS ROADS

Site access is presently difficult with the existing exploration drill roads affording the only vehicle and equipment access. These roads are indicated on the "General Map B", Sheet A2. Good access is available to the right abutment rim from the adjacent State Highway 73. Access to the aggregate source area, upstream diversion area and left abutment will require upgrading the existing drill road from the right abutment and constructing at least one work bridge over the river.

Upgrading the access road from the right abutment rim to the aggregate source area will require both alignment and width alterations. The present road alignment is suitable for exploration equipment and light vehicles but a tight, steep corner included in the road at the top the first section above the aggregate source area must be removed.

The bridge will access the existing drill road from river grade upstream of the dam to the rim of the left abutment. This road, constructed primarily through Supai Formation sandstone, is currently subject to sloughing of both cut and fill slopes and must be upgraded for construction use. The alignment is suitable for construction equipment but widening, drainage improvements and slope stabilization will be required. Surfacing may be required for all weather use.

Other crossings may be required to access the base of the abutments from the upstream direction. At present, river fords are used to cross to the left abutment rim access road, the base of the left abutment and from the base of the left abutment to the base of the right abutment.

There is no current access from downstream of the dam site to either abutment rim or river grade. A permanent downstream access road for daily use is designed as shown on "Access Road Plan & Profile", Sheet J5. This road will be useful for construction. A permanent service road intended for intermittent use is designed to access the left abutment rim and is shown on "East Side Access Road To Top Of Dam", Sheets J6 & J7. This road is for post-reservoir use and will not be directly useful during construction.

The right abutment rim and the pasture area immediately to the west across the highway are covered with a layer of soft clayey soil. Drill access roads crossing these areas required repeated applications of locally available cinder surfacing in order to remain passable during wet weather. A drill access road was successfully constructed across the pasture area through the use of road stabilization fabric overlaid with 6 inches of cinder surfacing. The road was subsequently reclaimed with the removal of the cinders and stabilization fabric.

As these areas are designated as construction staging sites their use under all weather conditions will require surfacing. A source of volcanic cinder surfacing is located adjacent to State Highway 73 approximately 8 miles north of the dam site.

E.4 TIMBER PRODUCT AVAILABILITY

The area supports a softwood timber industry producing yard and structural lumber. Plywood and stress-graded lumber are not locally produced. The timber products required for the construction of the envisioned dam are available either from local producers or suppliers.



MORRISON-MAIERLE, INC.

MEMO

TO: FILE: MINER FLAT DAM, JOB #1740-14-02-03(30)
FROM: DALE ORTMAN
SUBJECT: AGGREGATE TEST PIT & PETROGRAPHIC ANALYSIS FOR E. SCHRADER
DATE: DECEMBER 8, 1986

As requested by Ernie Schrader a single test pit was dug and logged on November 7, 1986 at the proposed aggregate source site. The purpose of the pit was to obtain a sample of material for preliminary petrographic testing in order to supply Mr. Schrader with data necessary to his initial concrete mix estimate for the rolled concrete dam alternative.

The test pit was dug to the depth limit of the Case 580 back hoe contracted for the work (Approximately 11 feet) and encountered groundwater at approximately 10 feet. The materials encountered are similar to those indicated in the previous test pits done by Mineral Systems Inc. (Mineral Systems Inc, 1983). The test pit was located adjacent to the earlier test pits as indicated on the attached map.

An approximately 500 pound bulk sample of 6 inch minus material was collected from the test pit. The sample was sieved at a testing laboratory in Tucson and representative samples of the 1 1/2 minus fractions were shipped to the following laboratory for petrographic analysis.

Construction Technology Laboratories
5420 Old Orchard Road
Skokie, IL 60077

Attn: Don Campbell

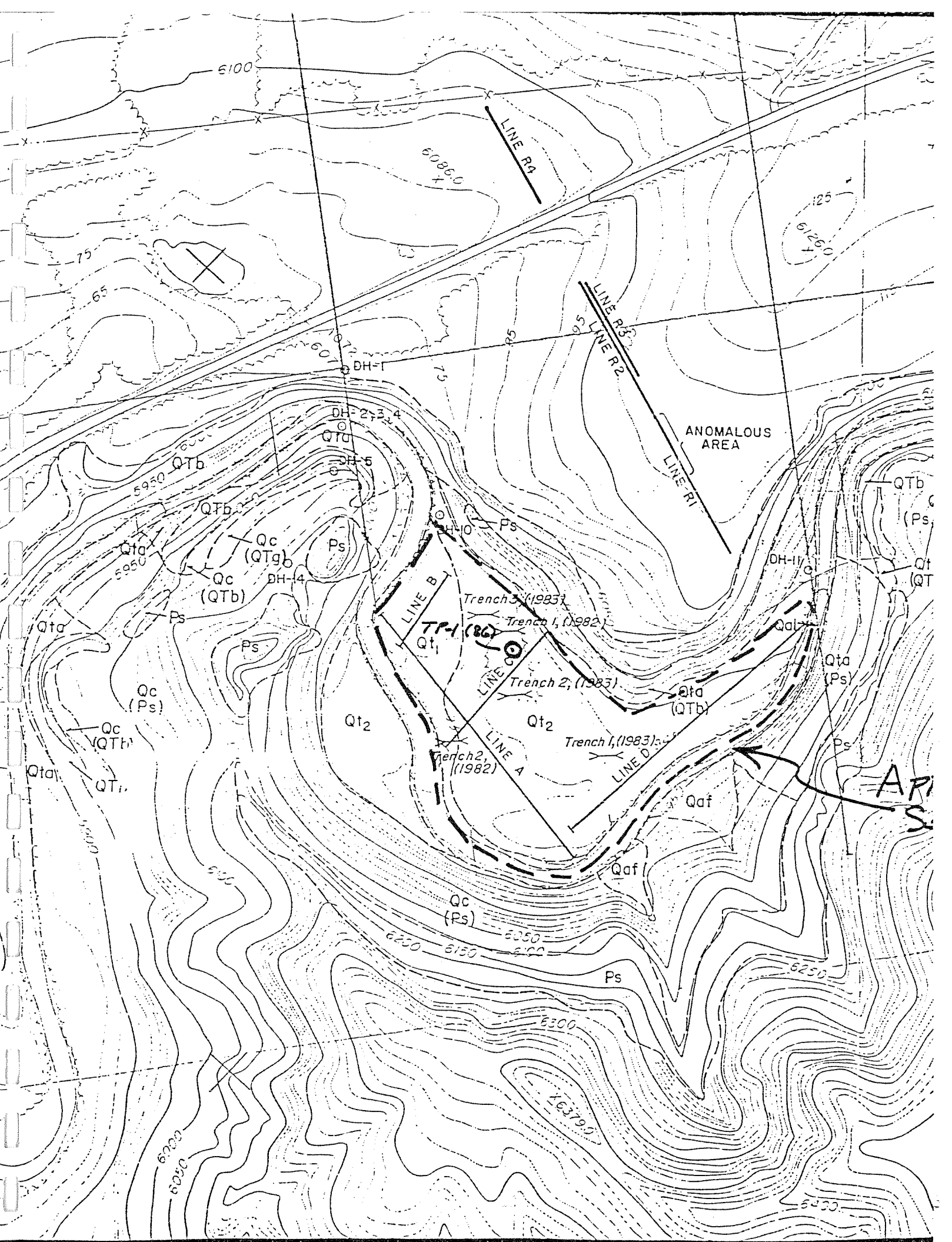
The results of the gradation and petrographic analyses are attached. It should be noted that material larger than 6 inch was excluded from the sample.

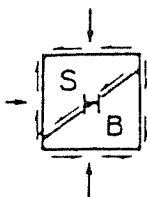
TEST PIT LOG

Location: Miner Flat Dam
Material: Aggregate
Equip: Case 580

Test Pit No: TP-1(86)
Date: 11/7/86
Logged by: Dale Ortman

| <u>Depth Interval</u> | <u>Description</u> |
|--------------------------|------------------------------------------------------------------------------------------------------------------------|
| 0 - 0.5 feet | Topsoil, Dk. Brown, Fine Sand some Silt, Roots & Organic material, moist |
| 0.5 - 3.0 | Sand trace Silt, med-fine, Lt. Brown, trace roots, moist |
| 3.0 - 11.0 | Sand & Gravel, approx. 20% cobbles & boulders 6"-2', damp (3-6 ft), moist (6-10 ft), groundwater encountered at 10 ft. |
| ----- E.O.H. 11.0 ft. | |





SERGEANT, HAUSKINS & BECKWITH

CONSULTING GEOTECHNICAL ENGINEERS

APPLIED SOIL MECHANICS • ENGINEERING GEOLOGY • MATERIALS ENGINEERING • HYDROLOGY

B. DWAIN SERGENT, P.E.
LAWRENCE A. HANSEN, PH.D., P.E.
RALPH E. WEEKS, P.G.
DARRELL L. BUFFINGTON, P.E.
DONALD VAN BUSKIRK, P.G.

JOHN B. HAUSKINS, P.E.
DALE V. BEDENKOP, P.E.
DONALD L. CURRAN, P.E.
J. DAVID DEATHERAGE, P.E.
MICHAEL R. RUCKER, P.E.

GEORGE H. BECKWITH, P.E.
ROBERT W. CROSSLEY, P.E.
DONALD G. METZGER, P.G.
JONATHAN A. CRYSTAL, P.E.
PAUL V. SMITH, P.G.

ROBERT D. BOOTH, P.E.
NORMAN H. WETZ, P.E.
ROBERT L. FREW
ALLON C. OWEN, JR., P.E.

November 11, 1986

Morrison-Maierle, Inc.
910 Helena Avenue
P.O. Box 6147
Helena, Montana 59604

SHB Job No. C86-6504

Project: Miner Flat Dam

Lab No. 1009 Bulk sample delivered to SHB on 11/10/86, by Mr. Dale Ortman, P.E.

SIEVE ANALYSIS

| <u>Sieve Size</u> | <u>Percent Passing</u> |
|-------------------|------------------------|
| 6.0 inch | 100 |
| 3.0 inch | 84 |
| 2.0 inch | 79 |
| 1.5 inch | 71 |
| 1.0 inch | 61 |
| 3/4 inch | 54 |
| 1/2 inch | 46 |
| 3/8 inch | 41 |
| No. 4 | 32 |
| No. 8 | 29 |
| No. 10 | 28 |
| No. 16 | 26 |
| No. 30 | 23 |
| No. 40 | 19 |
| No. 50 | 14 |
| No. 100 | 7 |
| No. 200 | 3.2 |

Tom L. Romero
Lab & Field Supervisor

REPLY TO: 1687 W. GRANT ROAD, SUITE 104B, TUCSON, ARIZONA 85745

PHOENIX
(602) 272-6848

TUCSON
(602) 792-2779

ALBUQUERQUE
(505) 884-0950

SANTA FE
(505) 471-7836

SALT LAKE CITY
(801) 266-0720

EL PASO
(915) 778-3369

Technical Services Report

to

MORRISON-MAIERLE, INC.

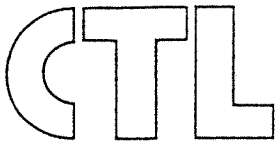
EXAMINATION OF AGGREGATE SAMPLES FROM
MINER FLAT DAM PROJECT

Submitted

by

CONSTRUCTION TECHNOLOGY LABORATORIES
5420 Old Orchard Road
Skokie, Illinois 60077

DECEMBER 10, 1986



a Division of the PORTLAND CEMENT ASSOCIATION

construction technology laboratories

5420 Old Orchard Road, Skokie, Illinois 60077-4321 • Phone 312/965-7500

TECHNICAL SERVICES REPORT

Project No.: CR-M318

Date: December 10, 1986

Re: Petrographic Examination of Fine and Coarse Aggregate Samples, Miner Flat Dam Project

One sieved sample of coarse aggregate and one unsieved sample of fine aggregate were received November 13, 1986, from Mr. D. Ortman, Morrison-Maierle, Inc., Helena, Montana. The coarse aggregate sample was comprised of five sieved fractions identified, respectively, as 1"-retained, 3/4"-retained, 1/2"-retained, 3/8"-retained, and No. 4-retained. The fine aggregate sand sample was identified as minus No. 4. Mr. Schrader, Consultant, Wallawalla, Washington, requested petrographic examination of both samples to determine the aggregate constituents. Results of the examination were reported by telephone to Mr. Schrader.

FINDINGS AND CONCLUSIONS

1. The coarse aggregate sample is a natural gravel comprised mainly of basalt, orthoquartzite, and metaquartzite. Minor amounts of sandstone, graywacke, siltstone, chert, limestone, and mud lumps are evident. The fine aggregate sample is a natural sand comprised mainly of basalt, feldspar, quartz, and mud lumps. The minor constituents

include orthoquartzite, metaquartzite, sandstone, graywacke, siltstone, chert, and magnetite. Mud lumps and free particles of rock-forming minerals are more abundant in the fine aggregate compared to the coarse aggregate. Tables 1 and 2 list aggregate constituents by number and weight percent.

2. Mud lumps are soft, friable, poorly consolidated mixtures of sand, silt and clay. Mud lumps are estimated to comprise 5.0% by weight of the coarse aggregate sample and 9.1% by weight of the fine aggregate sample. Friable coatings of similar material occur on some of the non-friable constituents of the aggregates.
3. Aggregate particles are rounded to subangular. The majority of particles are hard to moderately hard and dense. Particles of weathered rocks and minerals are concentrated in the finest sieve fractions, passing the No. 100 sieve.
4. Material passing the No. 200 sieve (finer than 0.075 mm diameter) consists mainly of feldspar at various stages of weathering, weathered rock fragments, quartz, mud lumps, iron oxides (magnetite, hematite, and limonite), and calcite.

DISCUSSION

Constituents of the aggregate samples are described in the ensuing discussion. Basalt is dark gray, brown to reddish brown, hard volcanic rock of fine grained plagioclase,

construction technology laboratories

pyroxene, and variable amounts of magnetite, brown glass and olivine. In addition, basalt contains variable amounts of secondary alteration minerals of hematite, limonite and iddingsite. Massive, trachytic, vesicular, tuffaceous and porphyritic varieties of basalt were observed. Dacite is a light gray, hard volcanic rock of mainly fine-grained feldspar, and comprises less than 5% by weight of the fine and coarse aggregate samples.

Orthoquartzite and metaquartzite are light gray tan to red rocks comprised of quartz and small amounts of feldspar, magnetite, hematite, calcite and chert. Particles of these rocks are generally hard and dense; however, approximately 10 to 20% of orthoquartzite and metaquartzite particles are moderately soft and porous. Orthoquartzite generally has rounded to subangular, sand-sized quartz grains in an interstitial matrix of fine grained quartz or quartz plus iron oxides. In contrast, metaquartzite generally has a mosaic of interlocking irregular grains of quartz.

Chert is a hard, dense rock with a waxy luster and ranges from gray, tan, brown, blue to red. Chert is comprised of microcrystalline quartz, chalcedony and minor amounts of other minerals, namely hematite, magnetite and calcite. Veining, laminations, and concretionary or concentric structures are evident in many chert particles.

Sandstone and graywacke are gray, tan, brown to red sedimentary rocks comprised of angular to rounded, mainly sand-sized grains of minerals and rocks. The most common

grains are quartz, feldspar, chert and iron oxides (magnetite and hematite). Siltstone consists of similar grains which are mainly silt-sized. Sandstone, graywacke and siltstone are hard to moderately hard, dense rocks and component grains are set in a fine-grained matrix comprised of various combinations of quartz, iron oxides, calcite and clayey minerals.

Limestone is a light gray, moderately hard rock comprised of fine- to coarse-grained calcite. Minor amounts of quartz, chert and clayey minerals were observed with calcite.

Mud lumps are soft, friable, brown to tan mixtures of sand, silt and clay-sized grains of feldspar, quartz, chert, volcanic rocks and other rock and mineral types. Mud lumps are poorly consolidated and readily disintegrate upon exposure to water or when rubbed between fingers.

The fine aggregate sample also contains free particles of the following minerals: quartz, feldspar at various stages of weathering, calcite, magnetite and hematite. Small accessory amounts of granitic rocks (granite and granodiorite) and metamorphic rocks (schist, phyllite and hornfels) were observed in the aggregate samples.

METHODS OF TESTS

The fine aggregate sample was sieved and weighed in accordance with ASTM C 136-84a, "Standard Method for Sieve Analysis of Fine and Coarse Aggregates."

The sieved fine and coarse aggregate samples were examined in accordance with ASTM C 295-85, "Standard Practice for

Petrographic Examination of Aggregates for Concrete." Over 150 particles were examined and identified in each sieve fraction. However, the 1-inch sieve fraction of the coarse aggregate was also examined and identified even though it contained less than 150 particles. Particles from the No. 8 and coarser sieves were examined using a stereomicroscope at magnifications up to 45X. Particles from the No. 16 and finer sieves, as well as representative rock-types of aggregates, were examined by thin-section methods using a polarized-light microscope at magnifications up to 250X. Material retained in the pan fraction (passing the No. 200 sieve) was too fine to be counted, and constituents by relative abundance were estimated.

P. A. Studemeister

P. A. Studemeister
Research Petrographer
Concrete Materials/
Technical Services Department

PAS/mv

CR-M318

Attachments

Copy to--
D. C. Sikes
A. A. Alonzo

TABLE 1 - RESULTS OF PARTICLE COUNTS FOR COARSE AGGREGATE SAMPLE, MINER FLAT DAM PROJECT

| Constituents | Composition of Fractions Retained on Sieves | | | | | Weight % in Coarse Aggregate |
|----------------------------------|----------------------------------------------------|-----------------------------------------------------|-----------------------------------------------------|----------------------------------------------------|--------------------------------------------------|------------------------------------|
| | 1 inch(a) (25 mm) Number of particles (%) | 3/4 inch (19.0 mm) Number of particles (%) | 1/2 inch (12.5 mm) Number of particles (%) | 3/8 inch (9.5 mm) Number of particles (%) | No. 4 (4.75 mm) Number of particles (%) | |
| Basalt | 46 (54.0) | 136 (48.0) | 184 (46.7) | 256 (54.6) | 214 (53.9) | 51.5 |
| Orthoquartzite and Metaquartzite | 13 (15.3) | 45 (15.9) | 76 (19.3) | 67 (14.3) | 54 (13.6) | 15.7 |
| Sandstone and Graywacke | 5 (5.9) | 18 (6.4) | 33 (8.4) | 25 (5.3) | 10 (2.5) | 5.7 |
| Siltstone | 2 (2.4) | 40 (14.1) | 18 (4.6) | 25 (5.3) | 23 (5.8) | 6.1 |
| Chert | 3 (3.5) | 18 (6.4) | 23 (5.8) | 37 (7.9) | 44 (11.1) | 6.8 |
| Limestone | 10 (11.8) | 15 (5.3) | 18 (4.6) | 13 (2.8) | 6 (1.5) | 5.6 |
| Mud Lumps | 2 (2.4) | 7 (2.5) | 27 (6.8) | 25 (5.3) | 33 (8.3) | 5.0 |
| Miscellaneous (b) | 4 (4.7) | 4 (1.4) | 15 (3.8) | 21 (4.5) | 13 (3.3) | 3.6 |
| TOTAL: | 85 (100.0) | 283 (100.0) | 394 (100.0) | 469 (100.0) | 397 (100.0) | 100.0 |

Weight % retained on sieve
(excluding pan fraction)

25.6 18.2 20.7 12.9 22.6 100.0

NOTES:

(a) Insufficient number of particles (less than 150) was present to perform a complete examination of this sieve fraction in accordance with ASTM C 295-85.

(b) Miscellaneous constituents include granitic rocks (granite and granodiorite), dacite, ironstone, hornfels, and quartz.

TABLE 2 - RESULTS OF PARTICLE COUNTS FOR FINE AGGREGATE SAMPLE, MINER FLAT DAM PROJECT

| Constituents | Composition of Fractions Retained on Sieves | | | | | | Weight % in Fine Aggregate |
|-----------------------------------------------------------|--------------------------------------------------|---------------------------------------------------|--------------------------------------------------|--------------------------------------------------|----------------------------------------------------|-----------------------------------------------------|----------------------------------|
| | No. 8 (2.36 mm) Number of particles (%) | No. 16 (1.18 mm) Number of particles (%) | No. 30 (0.6 mm) Number of particles (%) | No. 50 (0.3 mm) Number of particles (%) | No. 100 (0.15 mm) Number of particles (%) | No. 200 (0.075 mm) Number of particles (%) | |
| Basalt | 90 (34.5) | 109 (59.1) | 65 (26.5) | 41 (15.6) | 16 (8.3) | 12 (5.9) | 20.9 |
| Dacite | 10 (3.8) | 3 (1.6) | 6 (2.5) | 14 (5.3) | 6 (3.1) | 0 (0) | 3.3 |
| Orthoquartzite and Metaquartzite | 21 (8.1) | 8 (4.4) | 14 (5.7) | 8 (3.1) | 3 (1.5) | 0 (0) | 3.6 |
| Sandstone and Graywacke | 15 (5.8) | 8 (4.4) | 20 (8.2) | 8 (3.1) | 1 (0.5) | 0 (0) | 3.3 |
| Siltstone | 22 (8.4) | 2 (1.1) | 12 (4.9) | 9 (3.4) | 7 (3.6) | 5 (2.4) | 4.0 |
| Chert | 27 (10.3) | 19 (10.3) | 12 (4.9) | 17 (6.5) | 9 (4.7) | 5 (2.4) | 6.3 |
| Limestone and Calcite | 4 (1.5) | 0 (0) | 2 (0.8) | 3 (1.2) | 3 (1.5) | 7 (3.4) | 1.4 |
| Ironstone | 3 (1.1) | 0 (0) | 5 (2.0) | 4 (1.5) | 4 (2.1) | 6 (3.0) | 1.7 |
| Quartz | 7 (2.7) | 2 (1.1) | 13 (5.3) | 44 (16.8) | 18 (9.3) | 3 (1.5) | 8.6 |
| Feldspar | 16 (6.1) | 7 (3.8) | 58 (23.7) | 80 (30.5) | 80 (41.5) | 95 (46.3) | 28.0 |
| Magnetite | 0 (0) | 0 (0) | 0 (0) | 3 (1.2) | 15 (7.8) | 21 (10.2) | 3.3 |
| Mud Lumps | 38 (14.6) | 18 (9.8) | 27 (11.0) | 11 (4.2) | 16 (8.3) | 31 (15.1) | 9.1 |
| Miscellaneous (a) | 8 (3.1) | 8 (4.4) | 11 (4.5) | 20 (7.6) | 15 (7.8) | 20 (9.8) | 6.5 |
| TOTAL: | 261 (100.0) | 184 (100.0) | 245 (100.0) | 262 (100.0) | 193 (100.0) | 205 (100.0) | 100.0 |
| Weight % retained on sieve (excluding pan fraction) | 14.4 | 9.0 | 12.5 | 30.1 | 23.8 | 10.2 | 100.0 |

NOTES:

(a) Miscellaneous constituents include schist, phyllite, hornfels, granitic rocks (granite and granodiorite), claystone, hematite and other minerals.



MORRISON-MAIERLE, INC.

MEMO

TO: FILE: MINER FLAT DAM, JOB # 1740-14-02-03(30)

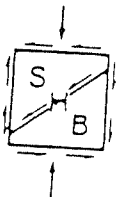
FROM: DALE ORTMAN

SUBJECT: RESULTS OF BASALT ALKALI REACTIVITY & L.A. ABRASION TESTS, MF-102

DATE: DECEMBER 5, 1986

In order to assess the preliminary suitability of basalt excavated from the dam foundation for use as concrete aggregate a sample has been submitted to a testing laboratory for Alkali Reactivity testing (ASTM C-289) and L.A. Abrasion testing (ASTM C-131). The attached results indicate the basalt is potentially as good as the upstream gravel source and is considered suitable as a source of concrete aggregate.

The sample is a composite of NX basalt core from drill hole MF 102 in the left abutment. The drill hole is directly adjacent to the proposed excavation and the sample was taken from the hole interval corresponding to the foundation excavation.



SERGEANT, HAUSKINS & BECKWITH

CONSULTING GEOTECHNICAL ENGINEERS

APPLIED SOIL MECHANICS • ENGINEERING GEOLOGY • MATERIALS ENGINEERING • HYDROLOGY

| | | | |
|---------------------------|------------------------|--------------------------|---------------------|
| B DWAIN SERGENT P E | JOHN B HAUSKINS P E | GEORGE H. BECKWITH, P.E. | ROBERT D BOOTH P E |
| LAWRENCE A HANSEN P-D P E | DALE V. BEDEKOP P E | ROBERT W CROSSLEY, P.E. | NORMAN H WETZ, P.E. |
| RALPH E WEEKS P G | DONALD L CURRAN P E | DONALD G METZGER, P.G. | ROBERT L FREW |
| DARRELL BUFFINGTON P E | J DAVID DEATHERAGE P E | JONATHAN A CRYSTAL, P.E. | ALLON C OWEN JR P E |
| DONALD VAN BUSKIRK P G | | | |

December 4, 1986

Morrison-Maierle, Inc.
 P. O. Box 6147
 Helena, Montana 59604

SHB Job No. LT86-3447
 Report No. 1

Attention: Dale Ortman, P.E.

Re: Miner Flat Dam/Hole MF 102

Gentlemen,

Transmitted herewith are the results of a potential reactivity test performed by Arizona Testing Laboratories on sample submitted. Results of L. A. Abrasion test performed in our laboratory is also attached.

Should any questions arise concerning this report, please do not hesitate to call.

Respectfully submitted,
 Sergeant, Hauskins & Beckwith Engineers

By 
 Dale V. Bedenkop, P.E.

Copies: Addressee (2)

REPLY TO: 3940 W. CLARENDON, PHOENIX, ARIZONA 85019

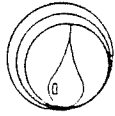
PHOENIX

ALBUQUERQUE

SANTA FE

SALT LAKE CITY

EL PASO



Arizona Testing Laboratories

817 West Madison Street □ Phoenix, Arizona 85007 □ 602/254-6181

For: Sergeant, Hauskins & Beckwith
3940 West Clarendon
Phoenix, Arizona 85019

Date: November 19, 1986

Lab. No.: 0412

Sample: Aggregate

Marked: LT 86-3447
W/O #1, Lab. #1
Your P.O. #L-4745

Received: 11/12/86

Submitted by: Same

REPORT OF LABORATORY TESTS

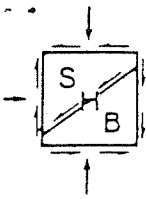
Potential Reactivity C 289:

| | |
|-------------------------------|----|
| Dissolved Silica, mm/L | 49 |
| Reduction in Alkalinity, mm/L | 35 |

Note: This material is not potentially reactive.

Respectfully submitted,
ARIZONA TESTING LABORATORIES


Claude E. McLean, Jr.



SERGEANT, HAUSKINS & BECKWITH

CONSULTING GEOTECHNICAL ENGINEERS

ENGINEERING ANALYSIS

PHYSICAL TESTING

QUALITY CONTROL

FIELD EXPLORATION

REPORT ON LABORATORY TESTS

DATE _____

PROJECT Miner Flat Dam JOB NO. LT86-3447

LOCATION - LAB NO. 6-3447-1

CLIENT Morrison-Maierle, Inc. ADDRESS P. O. Box 6147
Helena, MT 59604

SOURCE OF SAMPLE Hole MF 102

MATERIAL Vesicular Basalt

ASTM C-131
LOS ANGELES ABRASION

Grading A

Rev. 500

Loss 27.6%